NASA Contractor Report 3159

Actively Cooled Plate Fin Sandwich Structural Panels for Hypersonic Aircraft

L. M. Smith and C. S. Beuyukian

CONTRACT NAS1-13382
AUGUST 1979

NASA

NASA Contractor Report 3159

Actively Cooled Plate Fin Sandwich Structural Panels for Hypersonic Aircraft

L. M. Smith and C. S. Beuyukian
Rockwell International
Seal Beach, California

Prepared for
Langley Research Center
under Contract NAS1-13382

National Aeronautics
and Space Administration

**Scientific and Technical
Information Branch**

1979

FOREWORD

This is a final report covering results of a program on the design of a full-scale actively cooled structural panel for a hypersonic transport vehicle; and the fabrication of small-scale specimens, fatigue specimens, and a test panel for thermal and structural testing by NASA/LaRC. The program was conducted in accordance with the requirements and instructions of Contract NAS1-13382. Customary units were used for the principal measurements and calculations. Results were converted to the international system of units (SI) for this report.

L. M. Smith was the project engineer responsible for all design and analysis effort and C. S. Beuyukian was the project engineer responsible for all fabrication effort. J. I. Simonian was responsible for design, D. L. Pankopf for structural analysis, and C. S. Shuford and T. W. Tysor for thermal analysis.

CONTENTS

ILLUSTRATIONS

TABLES

SUMMARY

This program consisted of (1) the design of a full-scale 0.61 m by 6.1 m (2 by 20 ft) actively cooled panel based on a stringer-stiffened plate-fin sandwich concept, (2) fabrication of eight small-scale fatigue test specimens representative of the plate-fin sandwich, (3) design and fabrication of three fatigue specimens representative of critical areas of the full-scale design, and (4) the design and fabrication of a 0.61-m by 1.22-m (2- by 4-ft) test panel which is representative of the first or last 0.61 m (2 ft) of the full-scale design.

The full scale actively cooled panel was designed to sustain 20,000 cycles (5,000 times a scatter factor of 4) of cyclic (full tension and compression, R = -1) in-plane limit loads equal to ± 210 kN/m (± 1,200 lbf/in.) combined with a uniform panel pressure of 6.89 kPa (± 1.0 psi) and exposure to a uniform heat flux of 136 kW/m^2 (12 Btu/ft^2-sec).

The actively cooled panel configuration is a 4.17 mm (0.164 in.) thick brazed sandwich stiffened by bonded and mechanically fastened stringers. The sandwich consists of 0.81 mm (0.032 in.) thick inner and outer braze sheets fluxless brazed to a 2.54 mm (0.1 in.) high corrugated core fabricated from 0.127 mm (0.005 in.) 6061 aluminum foil that results in fins that run the length of the panel. Located at either end of the panel are inlet/outlet manifolds which distribute a 60/40 solution of ethylene glycol/water coolant across the panel width and into the longitudinal fins via access holes in the inboard face sheet of the brazed sandwich. The selected coolant inlet temperature, pressure and flow rate are 289 K (60°F), 827.4 kPa (120 psi) and 13,636 kg/hr (30,000 lb/hr), respectively. The manifold base is a machined 6061 fitting and is an integral part of the brazed sandwich. The manifold dome or top is welded to the base following sandwich heat treat quenching but prior to aging.

The stiffening is provided by five stringers. The two-edge stringers are extruded 7075-T7351 I-sections to which the brazed sandwich edges are mechanically fastened with Taper-Loc fasteners. The interior stringers are 7075-T6

brake formed channel sections bonded and periodically mechanically fastened to the brazed sandwich. The bonding is accomplished with an epoxy based, scrim reinforced adhesive system that is cured at 411 K (280 °F).

The structural dry mass of the panel is 9.66 kg/m^2 (1.98 lbm/ft^2), and the coolant inventory mass plus the auxiliary power system (APS) mass required to circulate the coolant through the panel is 2.76 kg/m^2 (0.56 lbm/ft^2). This results in a total panel mass of 46.18 kg (101.6 lbm) or 12.42 kg/m^2 (2.54 lbm/ft^2).

Eight small scale test specimens were fabricated and tested prior to the initiation of the full scale design process. These specimens were approximately 0.4 m (15.5 in.) in length, including load adapters, and 0.13 m (5.1 in.) wide. Four specimens were fabricated using straight corrugated core to form the fins and the remaining four were fabricated using lanced offset core. Room temperature fatigue tests were conducted at LaRC. Test results showed that even with intentionally placed surface flaws, the 20,000 cycle life requirement was exceeded and that through cracks, placed in the skins, slowly progressed, with increasing coolant leakage, to failure after more than 1,400 fatigue cycles. Hence, the fabrication processes and basic concept operational reliability were deemed adequate and full scale panel design was authorized.

Following panel design, three fatigue specimens of critical areas were designed and fabricated by Rockwell and tested at room temperature by NASA. The specimens ranged in size (including load adapters) from 0.67 m by 0.15 m (26.4 by 5.9 in.) to 0.77 m by 0.25 m (30.3 by 9.85 in.). Testing revealed design deficiencies dealing mainly with the end panel/transverse frame flange fastener system. A new fastener system was selected based on a test program conducted by Rockwell. The fatigue specimens were reworked or replaced incorporating the new fasteners and successfully tested by NASA to 20,000 cycles with no structural failures.

Following successful fatigue testing, the 0.61 m by 1.22 m (2 by 4 ft) test panel was designed and fabricated. The test panel incorporates all the design features of the final full scale panel configuration resulting from the preliminary design and analysis and as modified by the fatigue test program results. The panel was delivered to NASA for testing to determine the combined thermal/mechanical performance and structural integrity of the system.

INTRODUCTION

The skin structure of hydrogen fueled hypersonic transport vehicles traveling at mach 6 and above must be designed to withstand, for relatively long periods of time, the aerodynamic heating effects which are far more severe than those encountered by the subsonic and even supersonic aircraft of today. Three basic design options are available which will accommodate the aerodynamic heating. First, the use of radiative metallic heat shields which radiate the aerodynamic heat flux to the atmosphere, second, the use of conventional aircraft materials such as aluminum in combination with forced convection active cooling and third, a combination of radiation shields and active cooling. The purpose of this study is to advance active cooling technology (second option) beyond the theoretical stage proposed in References 1, 2 and 3 by dealing with the practical, real-life problems associated with the design and fabrication of the particular actively cooled structure concept depicted in Figure 1.

This concept was provided by NASA and is a stringer-stiffened plate-fin sandwich structure. A coolant circulates in a closed loop through the core, under pressure, and absorbs the aerodynamic heat via forced convection. The heated coolant is then transferred through a heat exchanger where the heat is absorbed by hydrogen fuel enroute to the vehicle engines. The result is that the actively cooled panel structure operates at a maximum temperature of less than 422 K (300°F). Below this temperature, conventional aluminum alloys can withstand the operational loads and maintain structural integrity over the life time proposed for hypersonic cruise vehicles.

The objectives of this program were: (1) the fabrication of small scale test specimens for basic concept fatigue testing by NASA, (2) the design of a mass sensitive full scale 0.61 by 6.1 m (2 by 20 ft) stringer stiffened plate-fin sandwich actively cooled panel, (3) the design and fabrication of fatigue specimens representing critical areas of the full scale panel for testing by NASA, and (4) the design and fabrication of a 0.61 by 1.22 m (2 by 4 ft) test panel for thermal and structural performance testing by NASA. All the above objectives were met.

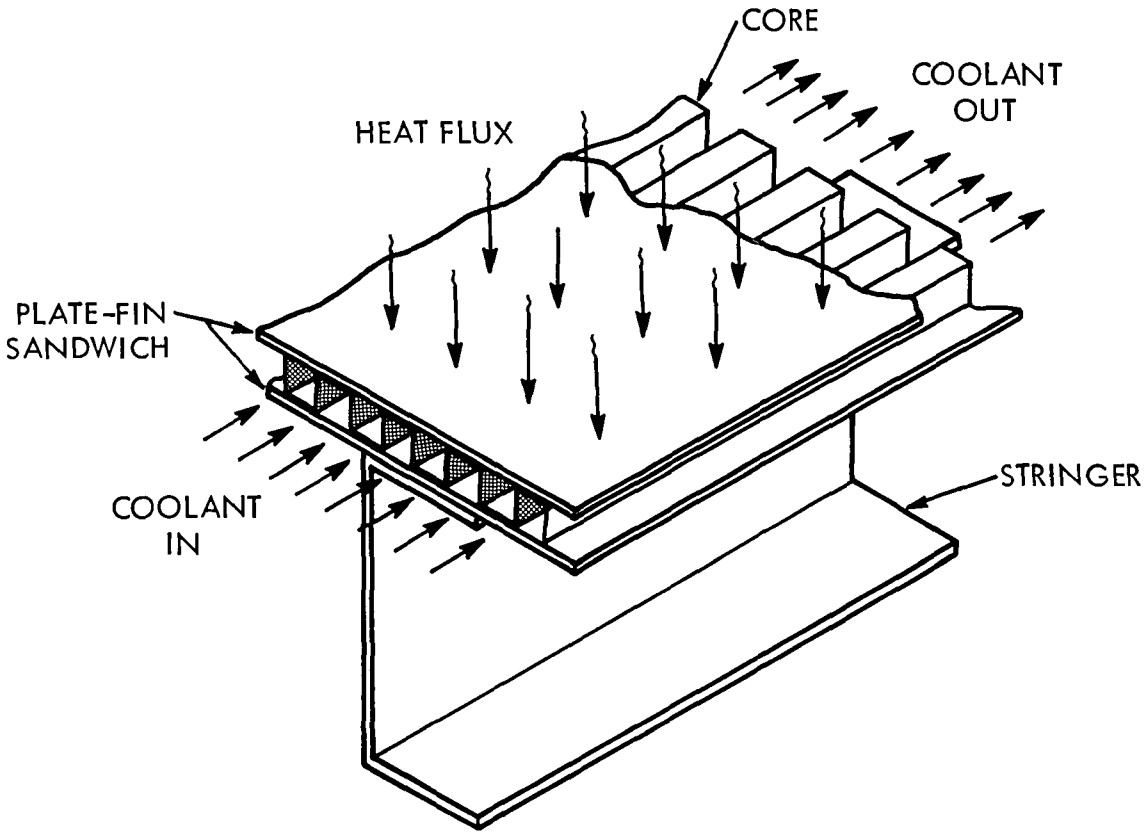

Figure 1. Basic Plate-Fin Stringer-Stiffened Active Cooling Concept

The main body of this report presents: (1) the design criteria, (2) the final full scale panel configuration, (3) the design process including analysis techniques and results and the impact of small test specimen and fatigue specimen testing on the design, (4) a test panel description, (5) fabrication techniques and (6) concluding remarks. Supporting details are presented in appendices.

Use of commercial products or names of manufacturers in this report does not constitute official endorsement of such products or manufacturers, either expressed or implied, by the National Aeronautics and Space Administration.

SYMBOLS AND PARAMETERS

A_c	Coolant passage cross-sectional area, m^2 ($in.^2$)
APS	Auxiliary power system
b	Core width, mm (in.)
B-PCS	Boilerplate panel corner specimen
BTU	British thermal unit
c	One-half of crack length, mm (in.)
Cp	Specific heat, J/kg • K (BTU/lbm • °F)
D	Coolant tube hydraulic diameter
e/D	Fastener hole edge distance to diameter ratio m/m (in./in.)
e_v	Pressure loss coefficient
E	Tensile modulus of elasticity, Pa (psi)
E_c	Compressive modulus of elasticity, Pa (psi)
EPISTS	End panel/internal stringer termination specimen
f	Friction factor
ft	Feet
°F	Temperature, degrees fahrenheit
F_{bru}	Ultimate bearing strength, Pa (psi)
F_{bry}	Bearing yield strength, Pa (psi)
F_{cy}	Compressive yield strength, Pa (psi)
F_{su}	Ultimate shear strength, Pa (psi)
F_{tu}	Ultimate tensile strength, Pa (psi)
F_{ty}	Tensile yield strength, Pa (psi)

SYMBOLS AND PARAMETERS (Continued)

g	Acceleration, m/sec^2 (ft/sec^2) or gram
g_c	Force - mass conversion factor
G	MODULUS OF RIGIDITY, Pa (psi); or auxiliary power system conversion factor
h	Heat transfer coefficient; film conductance, $W/m^2 \cdot K$ ($BTU/_{hr \cdot ft \cdot °F}$): core height, mm (in.)
hr	Time, hours
Hz	Cycles per second
in	Inch
K	Thermal conductivity, $W/_{m \cdot K}$ ($BTU/_{hr \cdot ft \cdot °F}$)
ksi	Thousand pound force per square inch
K_T	Stress concentration factor
l	Length, m (in.)
lbm	Pounds mass
lbf	Pounds force
L_e	Equivalent length, m (in.)
N_x	Axial load per unit length N/m (lbf/in.)
P	Pressure, Pa (lbf/in^2)
PCS	Panel corner specimen
Pr	Prandtl number
psi	Pounds force per square inch
r	Crack root radius, mm (in.)
R	Stress ratio - minimum stress divided by maximum stress
Re	Reynolds number

SYMBOLS AND PARAMETERS (Continued)

SIHS	Skin interior hardspot specimen
SSTS	Small scale test specimen
t	Thickness, mm (in.)
TA	Test article
THAP	Thermal hydraulic analyzer program
$\dot{w}$	Flow rate, kg/hr (lbm/hr)
α	Coefficient of thermal expansion, m/m•K (in/in•°F)
Δ	Delta; Difference
ϵ	Coolant passage relative roughness factor
μ	Viscosity, N • sec/m^2 (lbm/ft-hr)
ρ	Density, Kg/m^3 (lbm/ft^3)
σ_{ULT}	Ultimate applied stress, Pa (psi)
θ	Time, hour

SI UNITS

g	Gram (mass)
J	Joule (work)
K	Kelvin (temperature)
m	meter (length)
N	Newton (force)
Pa	Pascal (pressure and stress)
s	Second (time)
W	Watt (power)

SYMBOLS AND PARAMETERS (Continued)

SI PREFIXES

c	Centi	(10^{-2})
G	Giga	(10^{9})
k	Kilo	(10^{3})
m	Milli	(10^{-3})
M	Mega	(10^{6})

SUBSCRIPTS

B	Bulk flow conditions
c	Compression
L	Laminar
s	Surface flow conditions
T	Turbulant
TR	Transitional

1.0 DESIGN REQUIREMENTS AND CRITERIA

Design requirements and criteria for the actively cooled structural panel were obtained from NASA specifications, Federal Aviation Regulations (Reference 4) and practical considerations based on aircraft design and fabrication experience. These requirements and criteria fall into two categories - general and specific - and are described below.

1.1 GENERAL REQUIREMENTS AND CRITERIA

The general requirements and criteria for the design of a full-scale actively cooled panel are as follows:

1. The panel shall be designed to avoid catastrophic failure. Thus, the panel shall be designed such that the coolant is compatible with all materials that are used, and failure due to cracks including surface flaws and fatigue is avoided.

2. The panel shall be structurally sound. Thus, failure due to buckling or excessive stress, including thermal stress, shall be avoided. Eccentrically applied loads, interaction of in-plane loads with lateral pressure, and imperfect fabrication shall be considered.

3. The panel shall be designed for minimum mass. The panel mass shall include (a) all dry structure mass excluding end and intermediate transverse frames, (b) Auxiliary Power System (APS) mass penalty for one hour flight time, and (c) coolant inventory in the core and manifolds.

4. The full scale panel design shall include provisions along all four edges for joining other panels of similar design. The joining methods shall be compatible with a complete aircraft assembly. The manifolds shall terminate at the panels edge, that is, they shall be considered as isolated units which are fed and bled by supply lines (which are not part of the design).

1.2 SPECIFIC DESIGN REQUIREMENTS

The specific design requirements are tabulated in Table 1 indicating their source and are more explicitly defined, where possible, in Figure 2.

The thermal factor of safety = 1.0 is consistant with Rockwell requirements dictated for Aerospace and Aircraft programs such as Apollo, Shuttle and B-1. The structure temperature limitation of 422 K (300°F) is consistent with an approximate 20 percent mechanical properties degradation (when compared with room temperature) of structural aluminums as indicated by MIL-HDBK-5B (Reference 5 This temperature (422 K) is generally considered to be the maximum temperature at which structural performance of aluminum alloys can be predicted accurately. The coolant temperature maximum of 366 K (200°F) is conservative and provides considerable margin before elevated temperature corrosion mechanisms become a serious consideration.

Table 1. Specific Design Requirements and Criteria

ITEM NO.	PARAMETER	REQUIREMENT/CRITERIA	SOURCE
1	SIZE	.61 m BY 6.1 m	NASA
2	CONSTRUCTION TYPE	STRINGER STIFFENED SANDWICH	NASA
3	PANEL MATERIAL	ALUMINUM	NASA
4	CORE TYPE	STRAIGHT OR LANCED OFFSET	NASA
5	CORE SIZE	2.54 mm BY 2.54 mm (.1 x .1 inch)	NASA
6	TRANSVERSE FRAME SPACING	.61 m	NASA
7	COOLANT	ETHYLENE GLYCOL/WATER OR METHANOL/WATER	NASA
8	COOLANT OUTLET PRESSURE	344.75 kPa (50 psi) MINIMUM	NASA
9	HEAT FLUX	136.19 kW/m^2 (12 $Btu/ft^2 \cdot s$)	NASA
10	APPLIED LIMIT AXIAL LOAD	±210.15 kN/m (±1,200 lbs/in.)	NASA
11	APPLIED LIMIT LATERAL LOAD	±6.895 kPa (±1 psi)	NASA
12	LOAD CYCLES	5,000 WITH SCATTER FACTOR = 4 (e.g. 20,000)	NASA
13	FLIGHT LIFE	10,000 hrs	NASA
14	FACTOR OF SAFETY		
	PHYSICAL LOADS	1.5	REF 4
	THERMAL LOADS	1.0	ROCKWELL
15	STRUCTURE TEMP	422 K MAX (300°F)	ROCKWELL
16	COOLANT TEMP	366 K MAX (200°F)	ROCKWELL

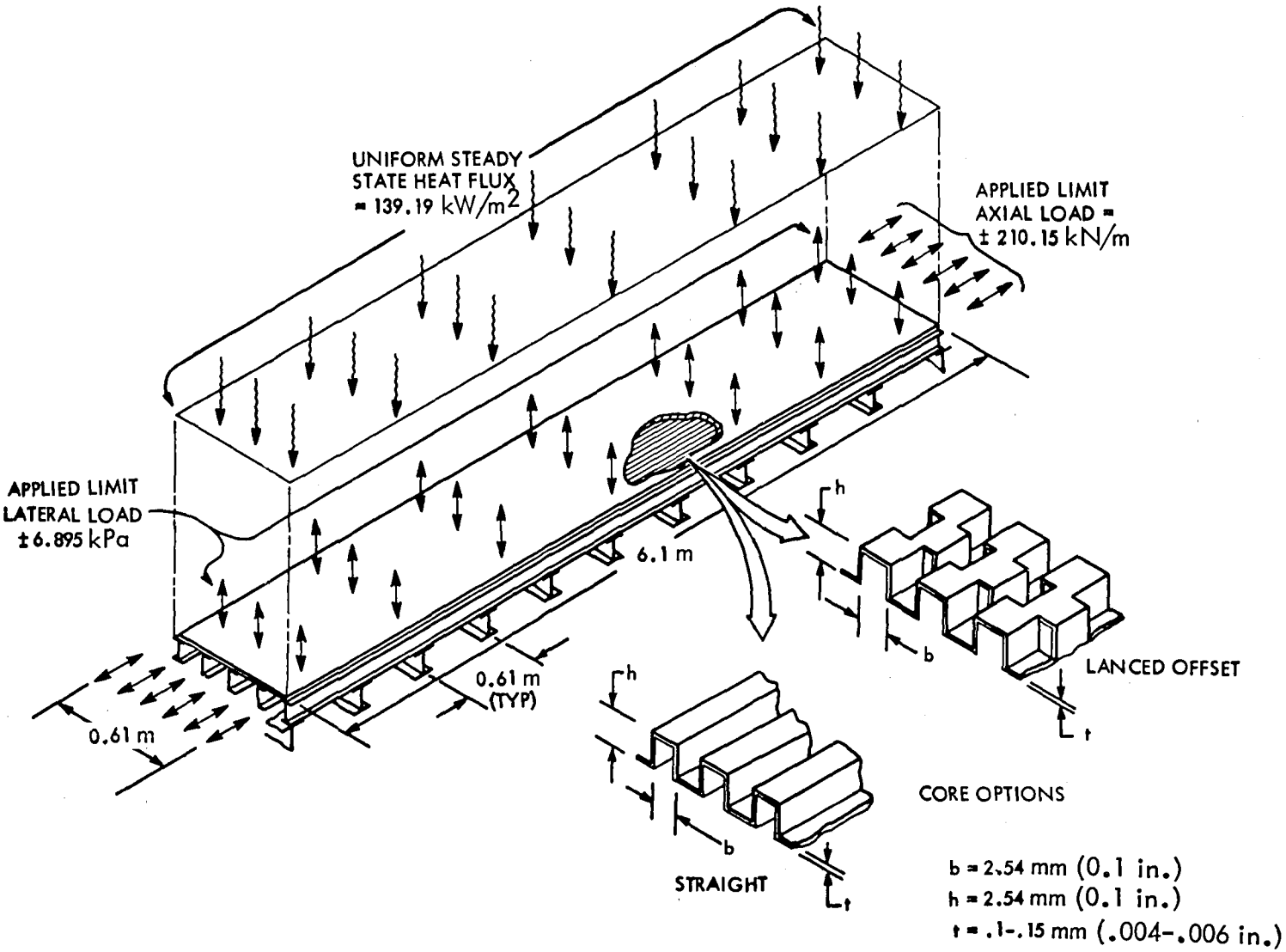

Figure 2. Specific Design Requirements

2.0 FINAL FULL-SCALE PANEL CONFIGURATION

The basic concept of a stringer-stiffened plate-fin sandwich actively cooled panel was provided by NASA. The final full-scale panel configuration reflects results of a design, analysis and component fabrication and test activity. This activity was aimed at developing the basic concept into a realistic design considering physical, functional and operational requirements and constraints dictated by its application to a hypersonic cruise vehicle. The full scale panel final design is illustrated in Figure 3. It is a 0.61 by 6.1 m (2 by 20 ft) fluxless brazed aluminum sandwich assembly that is longitudinally stiffened by three internal stringers and two edge stringers and has inlet and outlet manifolds at either end for the 60/40 ethylene glycol/water mixture selected as the coolant. Transverse support frames are spaced every 0.61 m (2 ft) down the length of the panel.

2.1 BRAZED ASSEMBLY

The brazed assembly shown in Figure 4 consists of two face sheets, a corrugated interior plain core, filler bars, hardspots, edge and end filler plates, edge conduction plates and the bases of the inlet and outlet manifolds. All elements are brazed together in a single braze operation which is discussed in Section 5.0 and Appendix E.

The face sheets are 0.81 mm (0.032 in.) thick No. 23F braze sheets composed of 6951 aluminum alloy clad with 4045 aluminum/silicon braze alloy. Material properties are presented in Appendix A. The core or fin material is made from 0.127 mm (0.005 in.) 6061 aluminum alloy which is run through a corrugating process by the supplier to form 2.54 mm (0.10 in.) high fin stock with a pitch of 393.7 fins per meter (10 per inch) of width. To prevent cavitation or "suck in" of the face sheets and attendant core crushing during the braze process, the design incorporates solid aluminum filler bars which run the length of the panel and are machined to fill in one flow passage every 0.076 meters (3 inches) across the width of the panel. In addition, hardspots are located at each of 27 internal stringer/transverse frame intersections to allow the panel/stringer to be attached to the transverse frame via MD111-3001

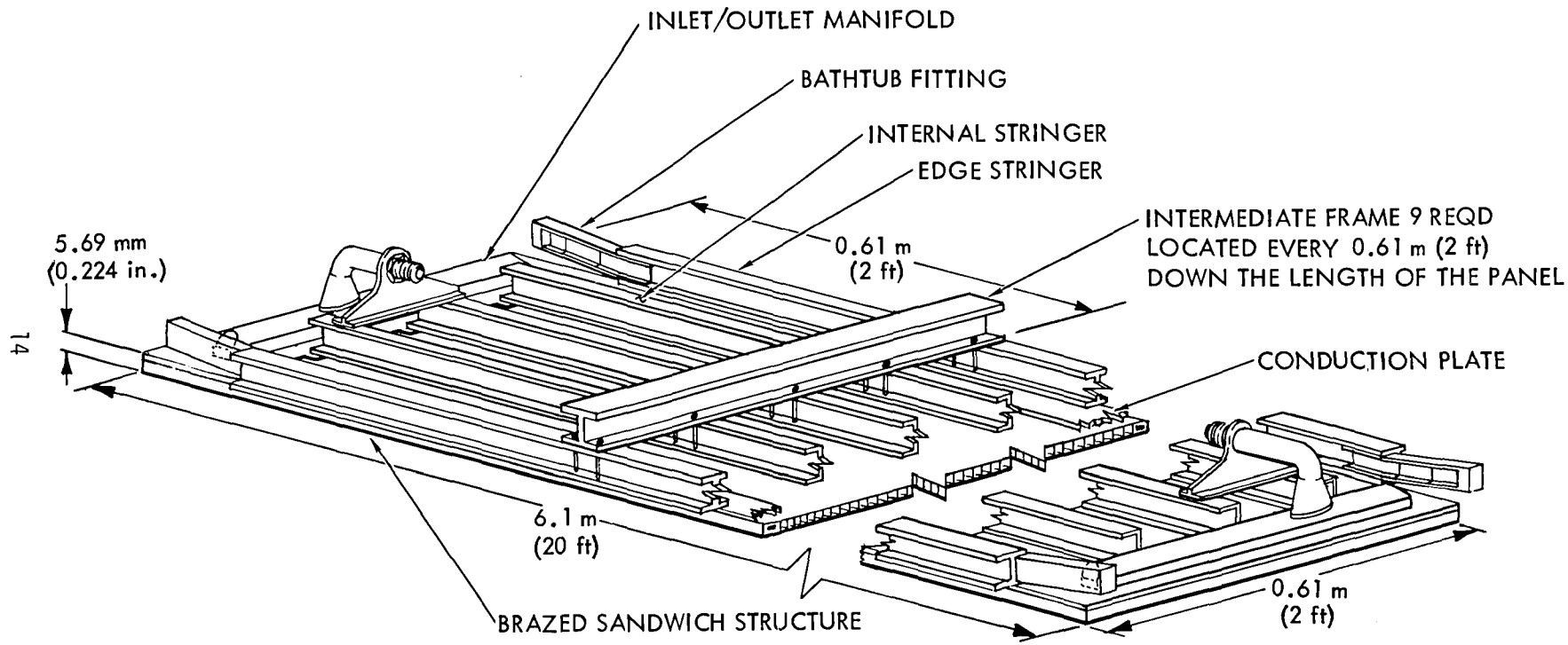

Figure 3. Final Full-Scale Panel Configuration

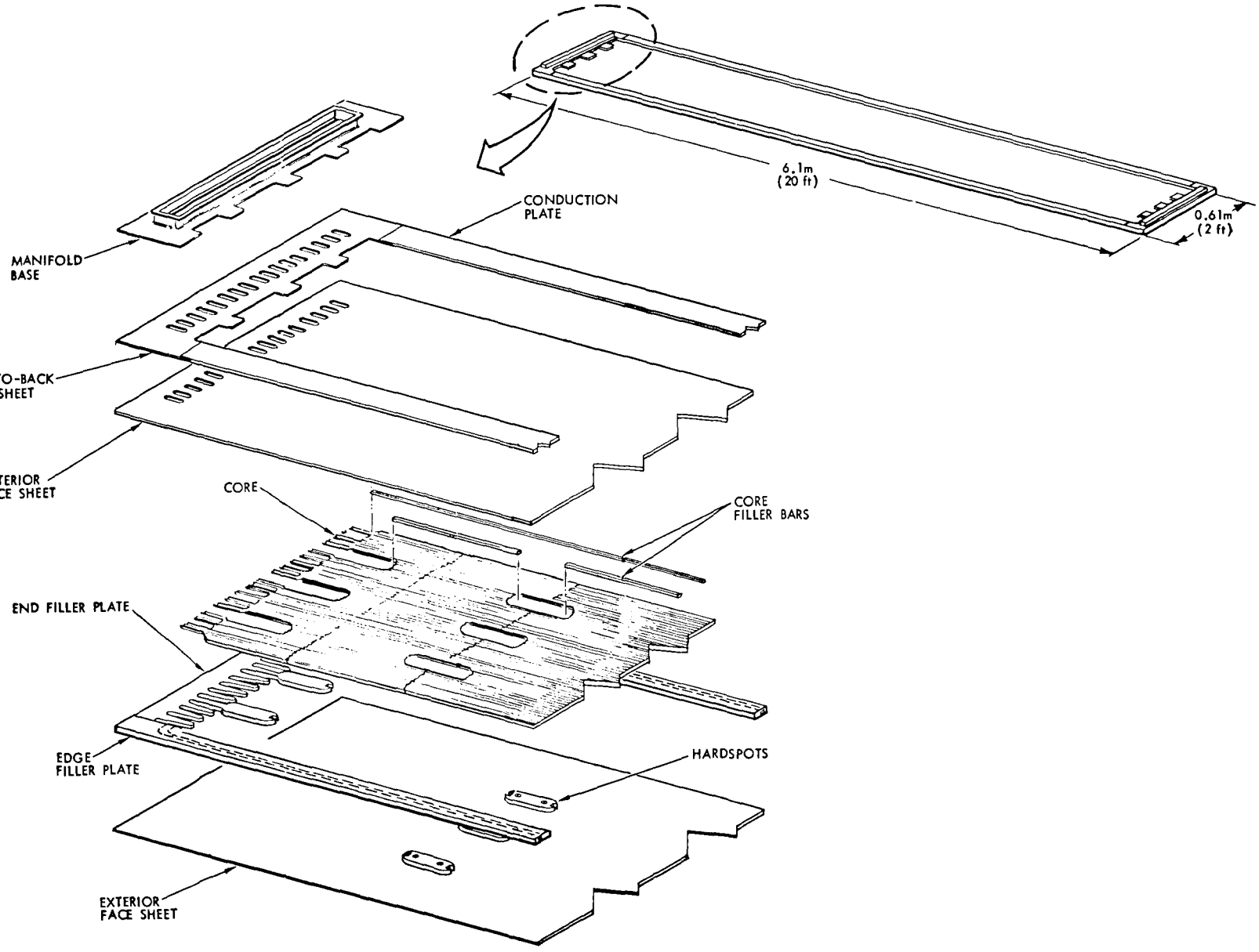

Figure 4. Actively Cooled Brazed Sandwich Structure

6.3 mm (1/4 in.) diameter flush head bolts. The core adjacent to the hardspots is cut away so that coolant flows around the hardspots with a minimum amount of restriction.

The perimeter of the sandwich consists of two edge filler plates along the 6.1 meter (20 ft) length and two end filler plates across the 0.61 meter width, all machined from 6061 aluminum alloy. The edge filler plates shown in Figure 5 are slightly thinner (2.38 mm versus 2.54 mm) than the core. This difference in thickness assures intimate face sheet to core contact during the braze cycle. The edge filler plates perform four functions in the design. First, they closeout and seal the 6.1 m length of the sandwich; second, they provide a rigid base for the application of mechanical pressure during the braze cycle; third, they provide a solid mass through which 4.76 mm diameter (3/16 inch) Taper-Loc fasteners are installed to attach the panel to the edge stringer; and, fourth, they incorporate a coolant flow passage external to the line of fasteners to provide forced convection cooling to the outer edges of the panel.

The end filler plates, best illustrated in Figure 4, resemble very deep toothed saw blades which are the same thickness (2.38 mm) as the edge filler plates and also perform a number of functions in the design. They closeout and seal the ends of the sandwich. They provide a solid mass through which 6.35 mm (1/4 inch) diameter Taper-Loc fasteners are installed to attach the panel to the main transverse frame of the aircraft. The fingers of end filler plates more than compensate structurally for the material removed from the inner face sheets in the form of oblong holes, 12.7 mm by 5.6 mm (0.5 by 0.22 in.). These holes function as coolant entrance and exit ports between the inlet and outlet manifolds and the sandwich cavity. The filler plates have three hardspots which protrude beyond the fingers. These hardspots provide the localized solid panel mass for the installation of long 6.35 mm (.25 in.) diameter bolts which mechanically attach the ends of the internal stringers to; (1) the panel, locally reinforcing the stringer/panel bond and (2) the brackets which are part of the transverse frame. Finally, the fingers provide a hardback or rigid support behind the inner face sheet to assure intimate contact of the inner face sheet and the manifold bases during the brazing process. Without this backup support there would be no way to be

certain that intimate contact exists between the inner face sheet and the manifold base during brazing. The edge and end filler plates are butt welded together in the four corners of the panel.

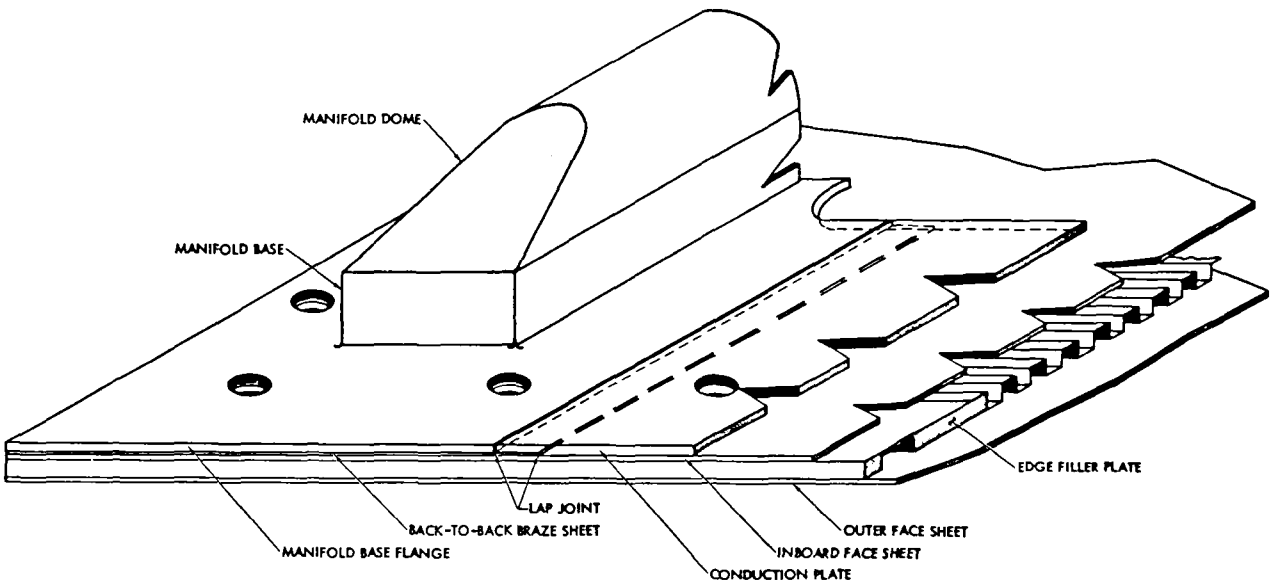

Figure 5. Closeup of Brazed Panel Details

The manifold bases are machined from 6061 aluminum alloy bar stock. These bases are brazed to the inboard face sheets with a 0.51 mm (0.020 in.) thick braze sheet with braze alloy on both sides. The manifold base flanges which are 1.02 mm (0.040 in.) thick extend to the edge and end of the panel and add to the solid thickness through which the perimeter Taper-Loc fasteners are installed.

The final parts of the brazed assembly are the conduction plates which are lap joined to the edges of the manifold base flange as illustrated in Figure 5 and extended the length of the panel. These conduction plates are 60.45 mm (2.38 in.) wide from the coolant outlet end of the panel to the mid-span. From midspan to the coolant inlet end of the panel, they are only 26.92 mm (1.06 in.) wide which is the width of one-half of the edge stringer flange. The purpose of the conduction plates is to conduct heat from the panel edge filler plates to the coolant media. This is necessary, in combination with the external coolant loop built into the edge filler plate, to keep the structure temperature along the fastener line within acceptable limits [i.e., less than 394 K (249°F)].

This complete assembly is fluxless brazed in one operation and then heat-treated to the T6 condition in accordance with the procedures outlined in Section 5.0.

2.2 MANIFOLDS

The inlet and outlet manifolds are made from 6061 aluminum alloy and consist of the base (described in Section 2.1), a manifold dome which is welded to the base following brazed assembly heat-treating, and welded inlet and outlet elbows which terminate in MS24386-12, Style E, male fittings. The inlet and outlet elbows are located off-center on either end of the panel. The off-center requirement is necessitated by the internal stringer terminations. The elbows are supported from the internal stringers by a tee bracket. The complete manifold configuration is illustrated in Figure 6.

2.3 STIFFENERS

The panel design incorporates five stringers of two different configurations. There are three 38.61 mm (1.52 in.) deep internal stringers which are brake formed channel sections made from 1.27 mm (0.050 in.) 7075-T73 aluminum alloy sheet stock. The stringer flanges are nominally 15.75 mm (0.61 in.) in width with localized increases to 19 mm (0.75 in.) to provide sufficient edge distance for panel attachment via long screws to the intermediate transverse frames of the aircraft which are spaced at 0.61 m intervals. These stringers are adhesively bonded to the inner face sheet of the sandwich structure with an epoxy-based scrim reinforced high temperature adhesive system. The adhesive is cured under vacuum at 416 K (290°F) for 180 minutes. The stringers are evenly spaced across the width of the panel. The stringers joggle and terminate at the inner edge of the manifolds and are bolted to a bracket protruding from the web of the transverse main frame as shown in Figure 6.

The edge stringer configuration is an extruded 7075-T73 I-section with dimensions as shown in Figure 6. In the actual application, this stringer would join two actively cooled panels along their length. The stringer is attached to the panel sandwich with 4.76 mm (3/16 in.) diameter Taper-Loc fasteners and to the intermediate frames by 6.3 mm diameter (1/4 in.) flush head bolts.

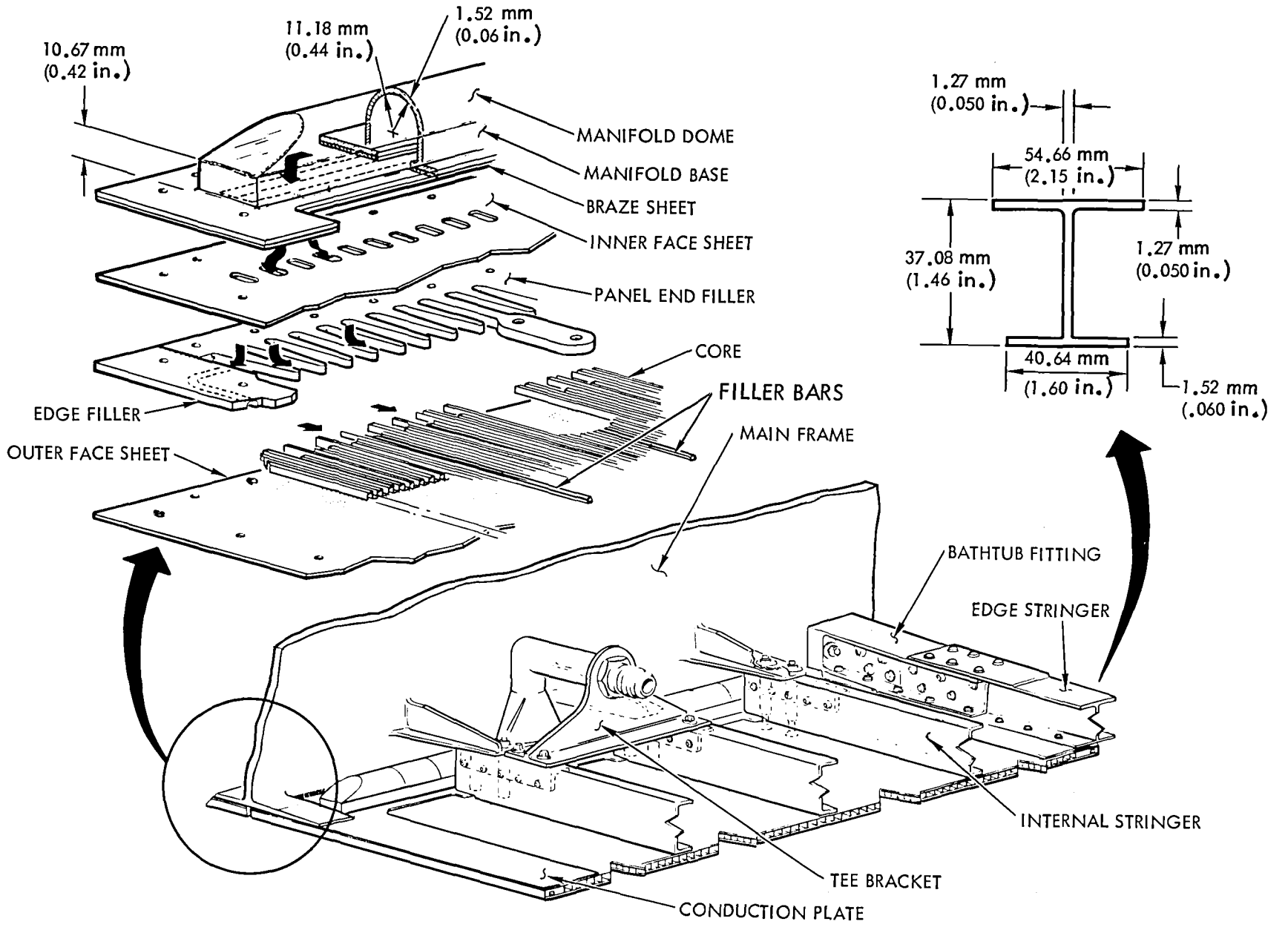

Figure 6. End Panel Details

2.4 PANEL MASS ESTIMATES

The panel mass is estimated to be 45.95 kilograms (101.1 lbs) or 12.36 kg/m^2 (2.53 lb/ft^2). This includes 35.69 kilograms (78.52 lbs) of dry structure mass, 8.27 kg (18.19 lbs) of ethylene glycol/water coolant inventory and an Auxiliary Power System (APS) penalty mass of 1.99 kg (4.38 lbs). A detailed mass breakdown is presented in Table 2.

2.5 PERFORMANCE CHARACTERISTICS

Predicted performance characteristics of the final full-scale actively cooled design are presented in Table 3. These predictions are based on results of thermal, fluid flow and structural analyses conducted to support the design activity. The selected coolant inlet conditions results in a minimum APS mass penalty.

Table 2. Panel Mass Breakdown

COMPONENT	MASS kg	UNIT MASS	
		kg/m^2	lb_m/ft^2
DRY STRUCTURE			
BRAZED SANDWICH	(24.32)	(6.54)	1.34
FACE SHEETS	16.25		
CORE	2.31		
HARDSPOTS	0.24		
FILLER BARS	0.61		
EDGE FILLER PLATES	1.99		
END FILLER PLATES	0.33		
MANIFOLD BASES	0.42		
CONDUCTION PLATES	2.17		
MANIFOLD TOP	(0.63)	(0.17)	0.03
DOMES	0.17		
TRANSITIONS	0.03		
END FITTINGS	0.20		
BRACKETS	0.23		
INTERNAL STIFFENING	(5.08)	(1.37)	0.28
STRINGERS	4.16		
BRACKETS	0.6		
SHIMS	0.02		
ADHESIVE	0.3		
EDGE STIFFENING	(3.36)	(0.90)	0.18
STRINGERS	2.86		
BATHTUB FITTINGS	0.5		
ATTACHMENT HARDWARE	(2.3)	(0.62)	0.13
DRY STRUCTURE TOTAL	35.69	9.60	1.96
RESIDUAL COOLANT	8.27	2.22	0.45
* AUXILIARY POWER SYS PENALTY	1.99	0.54	0.11
TOTAL PANEL MASS	45.95	12.36	2.52

* Based on an APS mass penalty conversion factor (G) equal to 0.34 g/kW·s (2 lb_m/hp· hr)

Table 3. Full-Scale Panel Performance Summary

● COOLANT INLET CONDITIONS	
FLOW RATE	13,608 kg/hr (30,000 lbm/hr)
TEMPERATURE	289 K (60°F)
PRESSURE	827.4 kPa (120 psi)
● MAXIMUM TEMPERATURES	
COOLANT	361 K (191°F)
STRUCTURE	414 K (286°F)
● OUTLET PRESSURE	362.7 kPa (52.6 psi)
● MINIMUM STRUCTURAL MARGIN OF SAFETY	.18

3.0 DESIGN PROCESS

The final full scale panel configuration reflects results of a design process which was conducted in accordance with the sequence shown on the flow diagram, Figure 7. Successful completion of each major phase was required prior to the start of the following phase. This was done to assure a high degree of confidence in the fabrication techniques and the structural integrity of the panel design when applied to the major piece of test hardware, the 0.61 m by 1.22 m (2 by 4 ft) test panel.

3.1 SMALL TEST SPECIMENS

The initial phase of the program was fabrication by Rockwell (Ref. 6) and test by NASA of eight small test specimens of the plate-fin sandwich active cooling concept selected by NASA for evaluation during this program. The objectives of this phase of the program were (1) to verify that acceptable fabrication results could be obtained from the Rockwell developed fluxless brazing process and a post braze heat-treat to the -T6 condition, and (2) to determine, by test, if the concept, as fabricated, could survive the 20,000 cycle fatigue life requirement both with and without intentionally placed cracks or flaws in the face sheets. Both objectives were met successfully.

The eight specimens were identical except for the core configuration. Four specimens contained plain fin core material and four specimens contained lanced offset core material as shown in Figure 8. Two specimens of each core configuration contained pin-fin supports. The pin-fin supports, which are essentially localized hardspots, were placed in the core to minimize face sheets cavitation or "suck-in" and attendant core crushing during the braze process when the core cavity is pulled to a vacuum. Modifications to the braze process discussed in Section 5.0 and the incorporation of longitudinal filler bars into the final design eliminated the need for these pin-fin supports. Both the plain and lanced offset core is 6061 aluminum alloy foil 0.127 mm (0.005 in.) thick. The core was preprocessed by the supplier to form a 2.54 mm (0.10 in.) high core with fins spaced on a pitch of 393.7/m (10/in.). The lanced offset core results in staggered fins one pitch in length.

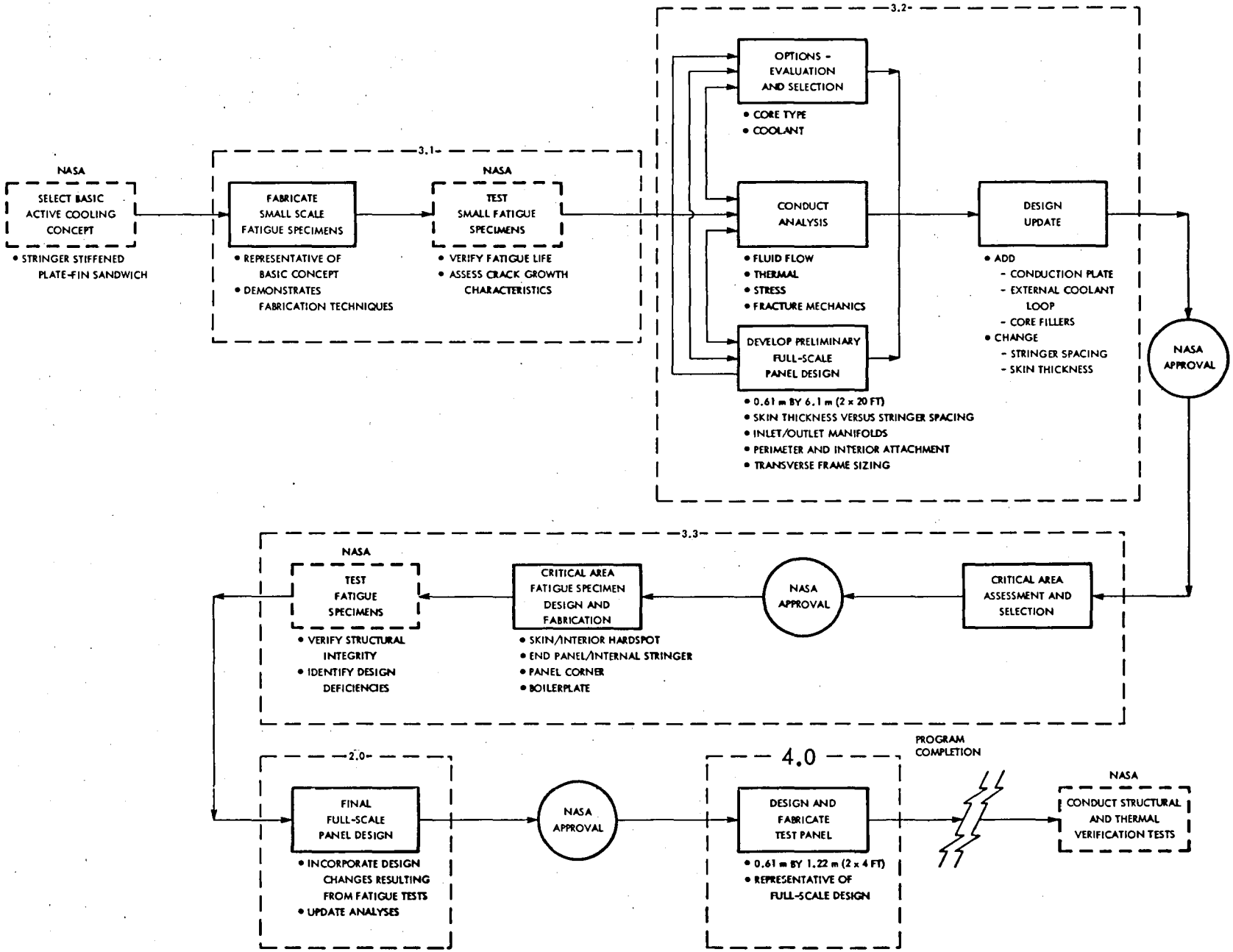

Figure 7. Full-Scale Actively Cooled Panel Design Process

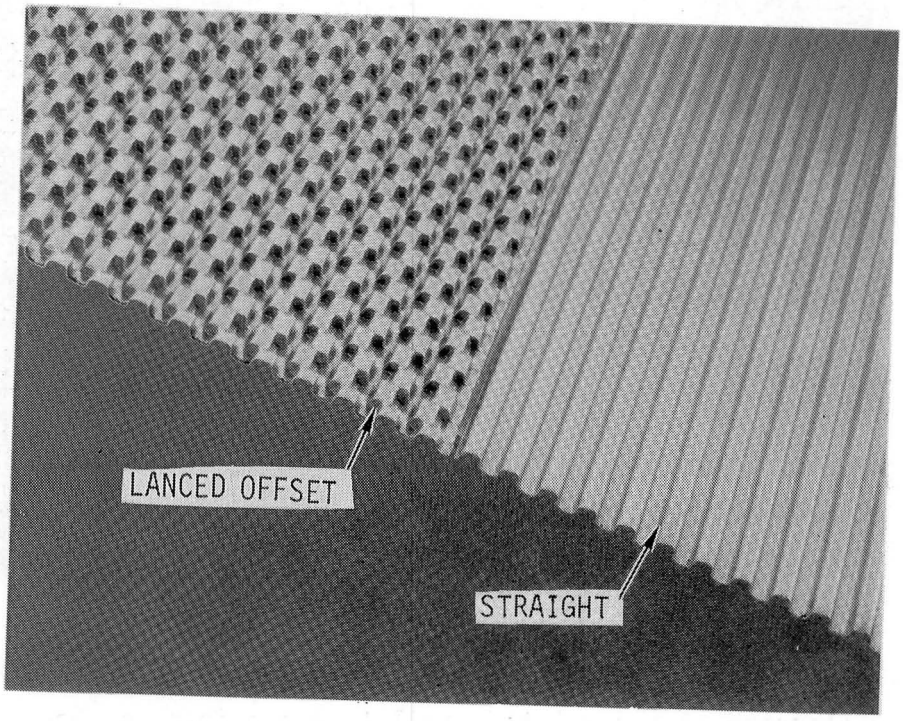

Figure 8. Straight and Lanced Offset Core Configurations.

The face sheets were 0.51 mm (0.020 in.) thick ALCOA No. 21F braze sheets of 6951 aluminum alloy clad on one side with 4045 braze alloy. Note that the final full scale design and all other test hardware fabricated for this program used 0.81 mm (0.032 in.) thick braze sheets.

The load adapters on either end of the test section consist of solid 6061 2.54 mm (0.10 in.) thick filler plates (in place of the core) that were brazed to the face sheets and four (two on either end) doublers made from 1.57 mm (0.062 in.) thick braze sheets that were brazed to the exterior of the face sheets. The finished test specimens, including load adaptors, were 0.39 m (15.5 in.) long and 0.13 m (5.12 in.) wide. Four specimens with a common load adapter section were brazed at one time as shown in Figure 9, cut apart, heat-treated, and finish machined to the above dimensions. Note that Figure 9 also shows the two core configurations and the core cutouts for the pin-fin supports. The finished specimens incorporated four access ports (two at either end of the core section) to provide pressurization capability during NASA fatigue

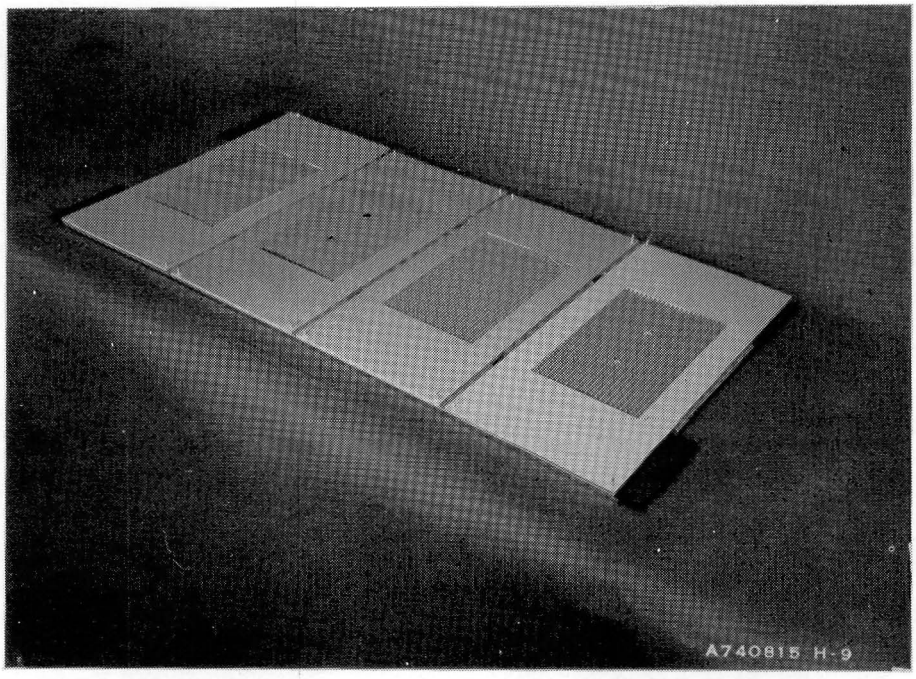

Figure 9. Small Test Specimen Braze Configuration

testing. A photograph of a completed small test specimen is shown in Figure 10.

The specimens were tested at ambient temperature with an internal pressure of 689.5 kPa (100 psi) at a tension stress level of approximately 124 MPa (18,000 psi). Results showed that (1) both core configurations can meet the 20,000 cycle design requirement, (2) the plain core has a longer fatigue life than the lanced offset core, (3) even with surface flaws intentionally placed in the external skins, the design 20,000 cycle life was exceeded, and (4) once a flaw became a through crack, as evidenced by fluid leakage, at least 1,400 additional cycles were required to produce a structural failure.

In summary, this phase of the program did verify that the planned fabrication processes were adequate and that the basic sandwich concept could survive the structural design environment.

3.2 DESIGN AND ANALYSIS

Following completion of the small test specimen phase of the program, design of a full scale 0.61 m by 6.1 m (2 by 20 ft) actively cooled panel was initiated. The objective was to develop the basic stringer-stiffened plate-fin sandwich concept into an all aluminum panel design configuration, supported by structural,

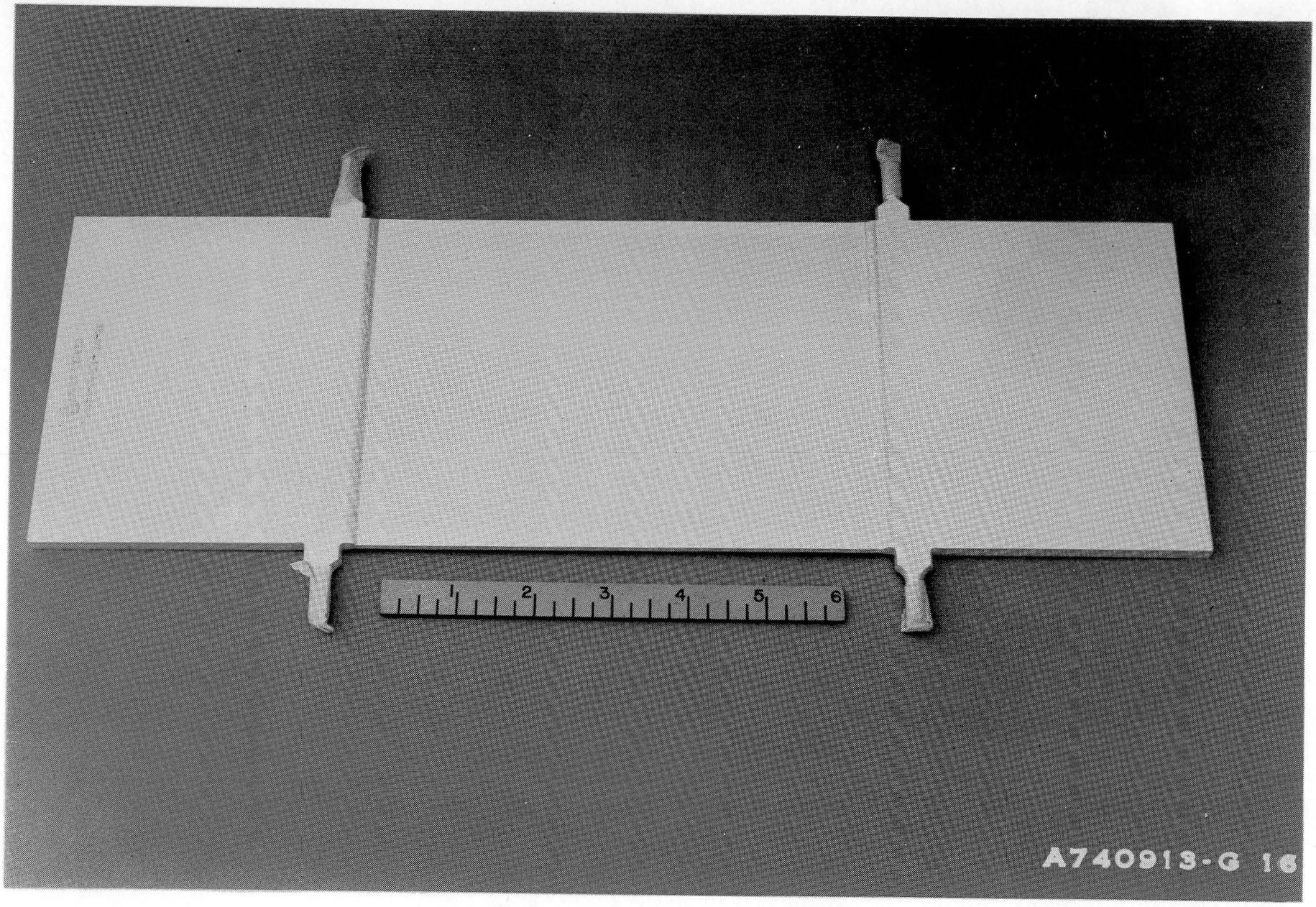

Figure 10. Completed Small Test Specimen

thermal and fluid flow analyses and fracture mechanics considerations that would meet the physical, functional and operational requirements of a hypersonic vehicle.

The baseline concept definition included the selection of a coolant system and core type. A 60/40 mixture of ethylene glycol/water was selected over a similar methanol/water mixture mainly because of safety considerations. The ethylene glycol/water mixture is less toxic and has much higher flash point and autoignition temperatures. Properties for the coolant are presented in Appendix A.

The plain or straight core was selected over the lanced offset core for the following reasons:

1. The straight core exhibited superior fatigue life in the small specimen test conducted by NASA.
2. The lanced offset core forming process produces very sharp edges between sheared surfaces which would act as local discontinuities and produce stress concentration points.
3. The offset core, by virtue of its multitude of edges, would significantly increase the system pressure drop and produce a corresponding increase in APS mass penalty.

With the baseline concept defined, preliminary design details were developed and iterated upon based on the dictates of the analysis results.

3.2.1 Thermal and Fluid Flow Analysis

The primary objectives of the thermal and fluid flow analysis were:

1. To select a coolant inlet condition (flow rate, pressure and temperature) that results in a minimum APS mass penalty considering structure and coolant temperature limitations and outlet pressure requirements.
2. To predict panel structure and coolant temperature distributions.
3. To size the inlet/outlet manifolds for minimum mass considering structure, residual coolant and APS penalties.

These analyses results are summarized here and discussed in detail in Appendix B.

The coolant inlet conditions and panel temperature distributions were determined using the Rockwell developed Thermal Hydraulic Analyzer Program (THAP), (Reference 7). This digital computer program allows the user to solve combined thermal/hydraulic transient and steady state problems. Initially, a model of a single core tube was developed and a parametric study conducted to determine the influence of variable coolant inlet conditions on longitudinal coolant and structure temperature distributions, pressure drops, and APS mass penalties. Results of this study provided a range of inlet flow rates from 9,072 kg/hr (20,000 lbm/hr) to 18,144 kg/hr (40,000 lbm/hr) and inlet temperature of 283 K (50°F) to 311 K (100°F) which were used as input data to more complex thermal models built to represent and determine the acceptability of the panel design detail concepts discussed below. Note that although the maximum allowable structure temperature is 422 K (300°F), a temperature, as determined by thermal analysis, across the width of the panel (excluding manifold and panel end conditions) above 394 K (250°F) was considered unacceptable. This condition was set to allow some margin for analysis uncertainties and for anticipated higher temperatures at the panel ends which were determined based on results of this main panel analysis.

3.2.1.1 Panel Edge Thermal Analysis

The two edge filler plates which run the length (6.1 m) of the panel were initially designed to meet only two objectives. One, to closeout or seal the brazed sandwich, and two, to provide solid material for the installation of flush head fasteners which attach the brazed sandwich to the edge stringer. In the preliminary design, the edge fillers were simple 2.38 mm (0.094 in.) thick by 19.0 mm (0.75 in.) wide 6061 aluminum plates. However, thermal analysis results indicated that edge panel structure temperatures would exceed the established thermal analysis allowable of 394 K (250°F) near the outlet end of the panel. The panel edge was modified to incorporate a conduction plate which would draw heat from the panel edge and feed it to the coolant in the adjacent flow passages. The temperature decreased but still did not fall within the established allowables. A final design configuration was established which added a coolant passage to the filler plate external to the fastener line. This panel edge design evolution is depicted in Figure 11. This final design configuration was then modeled and subjected to a reiteration of the initial parametric thermal and fluid flow analysis to select core coolant

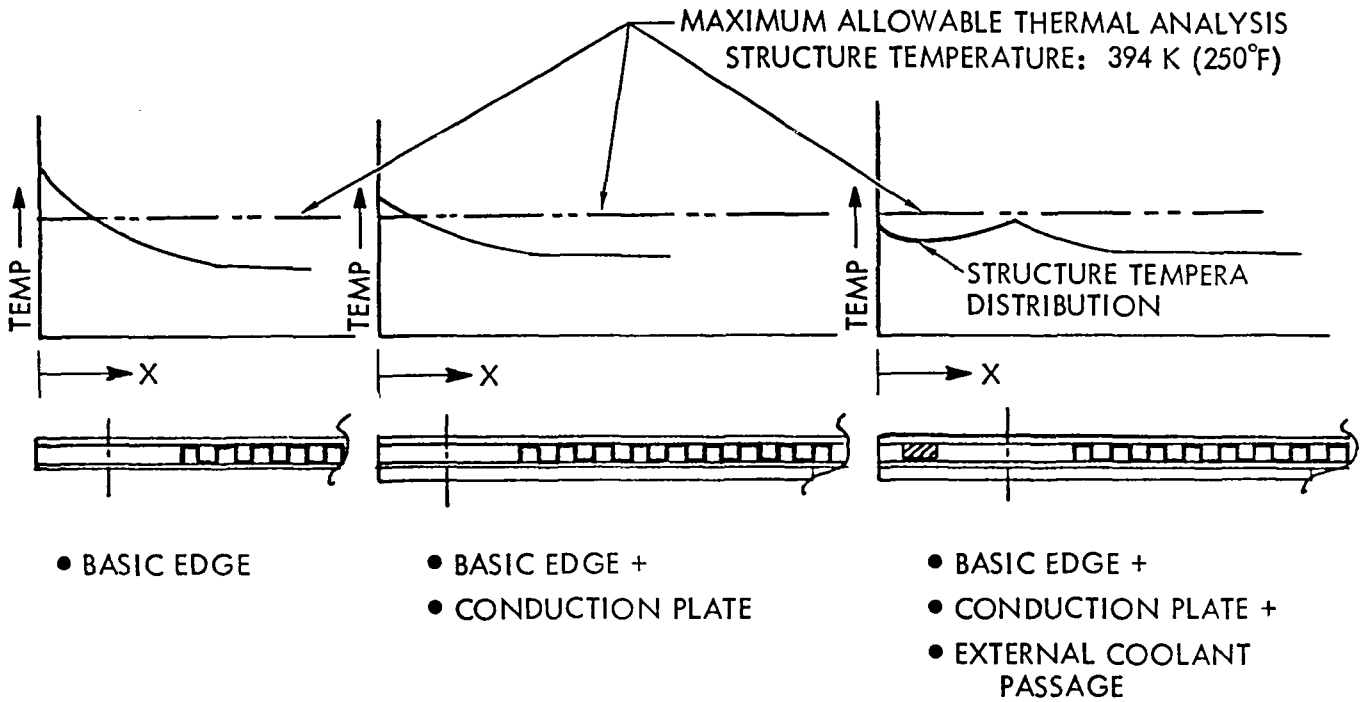

Figure 11. Panel Edge Design Evolution

inlet conditions and predict panel temperature distributions (exclusive of the panel end/manifold region). The selected coolant inlet conditions of 13,608 kg/hr (30,000 lbm/hr) flow rate and 289 K (60°F) inlet temperature resulted in predicted temperature distributions across the panel width from core inlet to outlet as shown in Figure 12. The sudden decreases in structure temperatures near the panel midpoint are caused by a large change in coolant heat transfer coefficient which takes place as the coolant regime changes from laminar to transitional flow. This is discussed in Appendix B.

3.2.1.2 End Panel Thermal Analysis

The panel end and manifold area temperature distributions were calculated using the Rockwell developed Aerodynamic and Structural Heat Transfer Thermal Analyzer Program No. YF0012 (Reference 8). The results are shown in Figure 13. The maximum predicted structure temperature for the entire panel is 414 K (286°F) and occurs at the corners on the outlet end of the panel.

The results of the manifold sizing analysis are presented in Figure 14. The selected diameter of the manifold for the final design is 2.24 cm (0.88 in.).

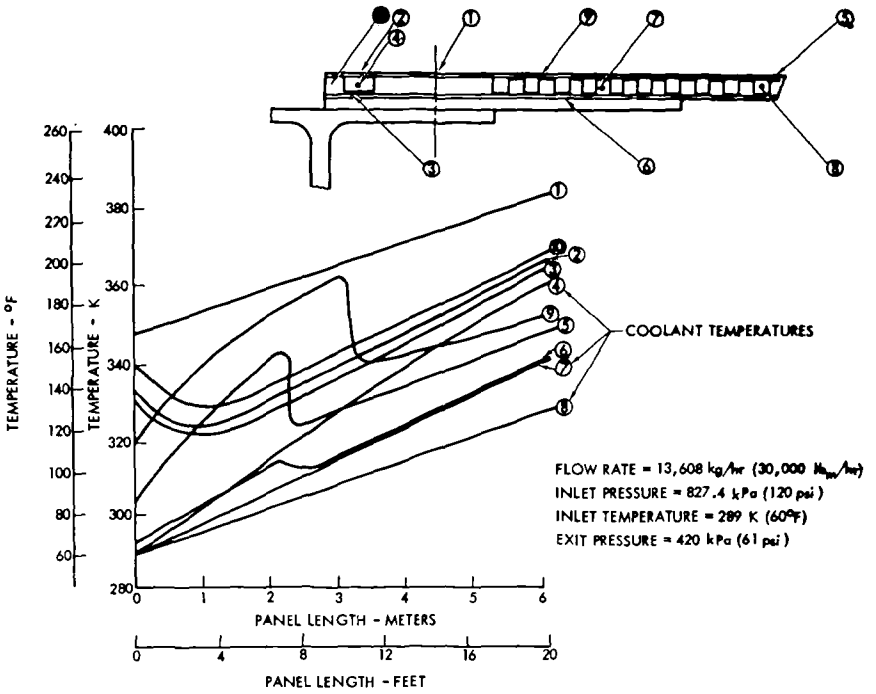

Figure 12. Panel Edge and Core Area Temperature Distribution

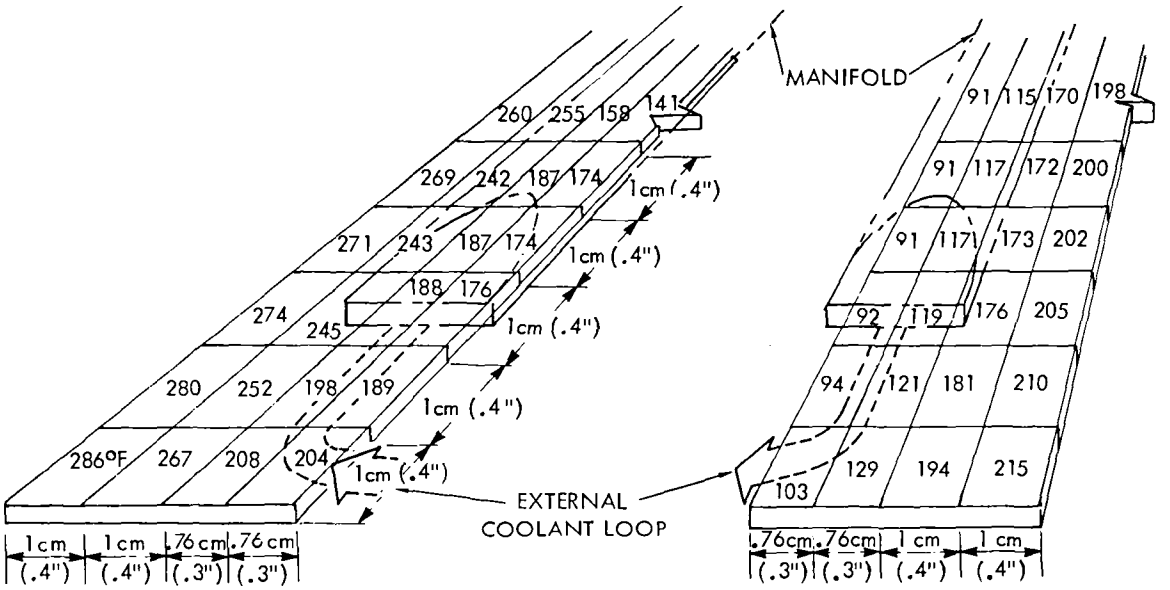

NOTE: TEMPERATURES IN °F

Figure 13. Panel End and Manifold Temperature Distribution

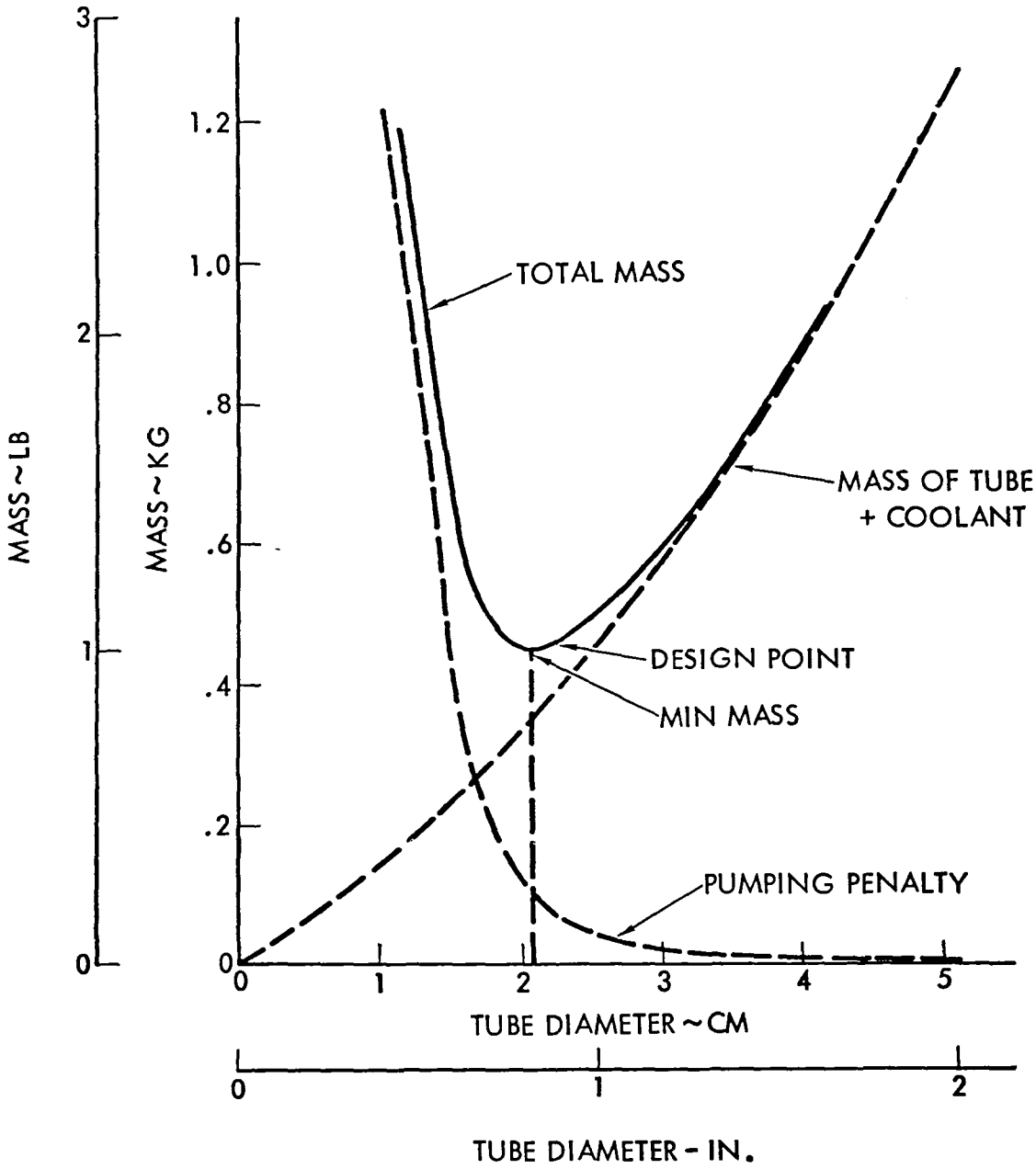

Figure 14. Manifold Sizing Results

This is slightly larger than the optimum of 2.1 mm (0.83 in.) but as indicated in the figure the mass penalty is insignificant.

3.2.2 Structural Analysis

A structural analysis of the panel was conducted using computer aids where beneficial. The Rockwell developed NARFEM computer program (Reference 10) was used for structural modeling and the NASA developed NASTRAN[1] computer program (Reference 11) was used for structural analysis. The structural analyses effort was directed toward the following:

1. Panel local and general stability analysis including the effects of imperfect fabrication using analysis techniques developed by NASA in Reference 9.
2. Inter-fastener buckling analysis near the inlet and outlet manifolds.
3. Sizing of main and intermediate transverse frames. (The frames are not part of the panel, but their stiffness is considered in the panel stability analysis.)
4. Calculations of maximum stress due to stress concentration around fastener holes.
5. An assessment of flaw growth from either part-through or through cracks in face sheets and/or those emanating from fastener holes.
6. Panel thermal stress predictions.
7. Panel local and general deflection predictions.
8. The effect of kick loads and local bending at the panel end to transverse frame attachment.

Analysis results predict positive margins of safety for all areas of the final panel configuration. The analysis techniques and results are presented in Appendix B. Two critical design features dictated by structural analysis considerations are discussed below.

3.2.2.1 Brazed Sandwich Face Sheets

The brazed sandwich face sheets are the largest single contributor to overall panel dry structure mass and hence should be as thin as possible. The preliminary design featured 0.51 mm (0.020 in.) thick face sheets. This

[1] NASTRAN: Registered trademark of the National Aeronautics and Space Administration.

thickness is readily available in No. 23F braze sheet and had performed satisfactorily in the small test specimen phase discussed in Section 3.1. The face sheet thickness is dictated not only by the overall panel/stringer section properties required to satisfy general and local stability constraints, but also by their ability to withstand maximum cavity inlet pressure without exceeding the tensile yield strength (F_{TY}) of the material. Face sheet yielding would result in a rippled external surface which is contrary to the basic design requirements. As long as the face sheet is supported every 2.54 mm (0.10 in.) by core webs, 0.51 mm (0.020 in.) thick face sheets are adequate. However, stress analysis of face sheets which span core cutouts around attachment hardspots required an increase in face sheet thickness. The next standard thickness available is 0.812 mm (0.032 in.) which was selected for the final design configuration. This thickness results in a relatively high margin of safety of 28 percent and should be subjected to a mass optimization analysis prior to detailed hypersonic vehicle design.

3.2.2.2 Internal Stringers

The internal stringers are the second largest contributor to panel mass and must also be selected with care. The preliminary design contained six channel section internal stringers spaced on 0.135 m (3.43 in.) centers. This spacing was based on the assumption that panel expansion in the transverse direction due to the elevated operational temperature would be restricted. In that case, transverse thermal stresses would require the close stringer spacing to prevent panel buckling in the transverse direction between stringers. Since the actual hypersonic vehicle application of the full scale actively cooled panel is unknown, the analysis assumption was modified to allow transverse panel growth with temperature, and hence eliminated gross transverse thermal stress considerations. The stringer quantity and spacing was then selected based on longitudinal bending stiffness requirements between the intermediate transverse frames. The final panel configuration with three internal stringers on 0.152 m (6 in.) centers met these requirements.

3.3 FATIGUE SPECIMENS

Based on the full scale panel design as supported by analysis, critical areas of the panel were identified and served, as the basis for the design and fabrication by Rockwell of an initial set of three fatigue specimens. These

specimens were tested by NASA to evaluate structural integrity of the panel and to identify any design deficiencies. The three critical areas selected and the resulting specimen configurations, including load adaptors, are shown in Figure 15.

A skin/interior hardspot specimen was selected to evaluate the effect of gaps between the core and the hardspot or solid insert and the hardspot sharp terminations on the face sheets. The overall length of the specimen, including load adapters, is 0.667 m (26.25 in.). The test section is 0.387 m (15.24 in.) long and 0.152 m (6.00 in.) wide and incorporates a brazed, heat-treated sandwich consisting of face sheets, core (with a core splice), hardspot, perimeter frame, a section of an internal stringer and associated attachment hardware.

An end panel/internal stringer termination specimen was selected. This area of the panel was considered critical because the load path from panel to panel joggles and kick loads and local bending exists. In addition, the fastener spacing between the panel to interior stringer attachment and the panel/interior stringer to main frame attachment is critical in an inter-fastener buckling mode. The overall length of the specimen, including load adapters, is 0.747 m (29.42 in.). The test section is 0.247 m (9.75 in.) long and 0.16 m (6.276 in.) wide and incorporates a brazed heat-treated sandwich, the end section of the internal stringer, a section of manifold and associated attachment hardware.

The third specimen simulates the corner of two adjacent panels. This area was considered critical because of (1) complexity of the panel/edge stringer termination and attachment to the main transverse frame, (2) load path from panel to panel uncertainty, and (3) the fact that the corner fasteners are the highest loaded fasteners in the panel based on the results of the stress analysis. The overall length of the specimen, including load adapters, is 0.77 m (30.55 in.). The test section is 0.246 m (9.70 in.) long and 0.22 m (8.66 in.) wide. It consists of two brazed sandwich corner sections, two manifold sections, a section of the end of an edge stringer, back-to-back bathtub fittings that attach the edge stringer to the main transverse frame and associated attachment hardware.

All three fatigue specimens incorporated pressurization access ports machined into the load adapters at the load adapter/test section interface. The load adapters for each end of each specimen were designed to simulate the

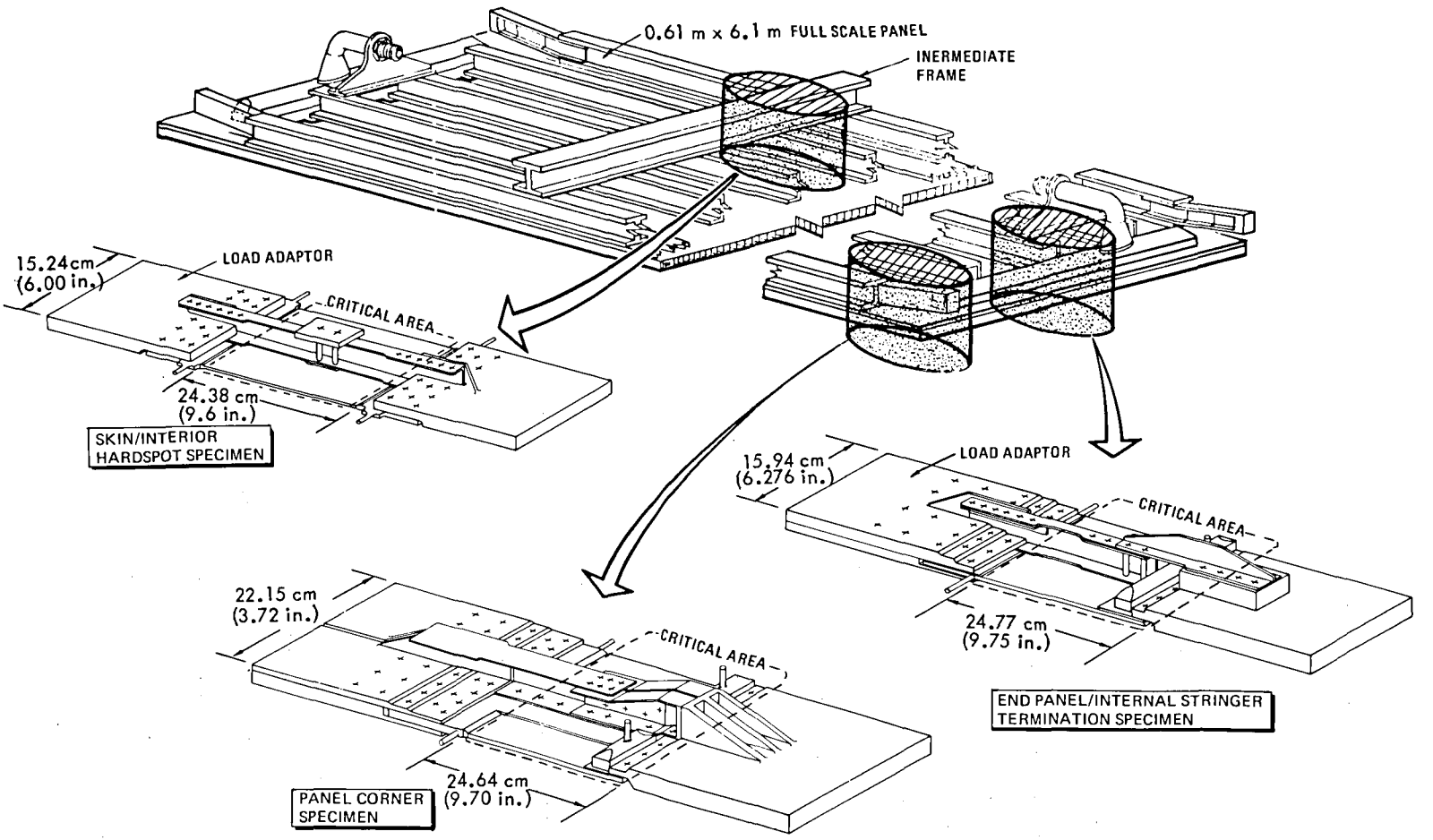

Figure 15. Full-Scale Panel Critical Area Locations

transverse neutral axis across the end of the test section and hence simulate the load path that would be present in adjacent areas of the full scale panel. This eliminates test peculiar kick loads. The fabricated fatigue specimens are shown in Figures 16, 17, and 18.

All specimens were tested at room temperature to fully reversed (R = -1) axial tension-compression loadings indicated in Figure 19. These load levels were adjusted from the basic design requirement of ± 210.15 N/m (1,200 lb/in.) to compensate for the lack of an elevated temperature environment by comparing fatigue allowables at room temperature and elevated design temperatures for like materials. This technique is described in detail in Appendix D. The test objective was for each specimen to complete 20,000 fully reversed tension-compression cycles without evidence of failure or excessive joint motion.

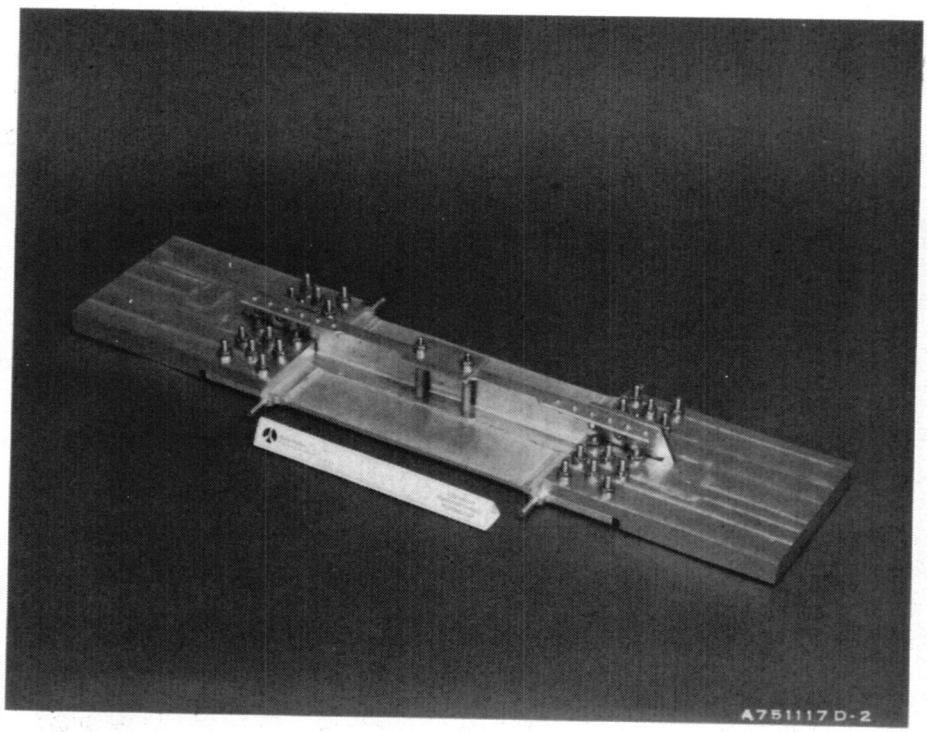

Figure 16. Skin/Interior Hardspot Fatigue Specimen

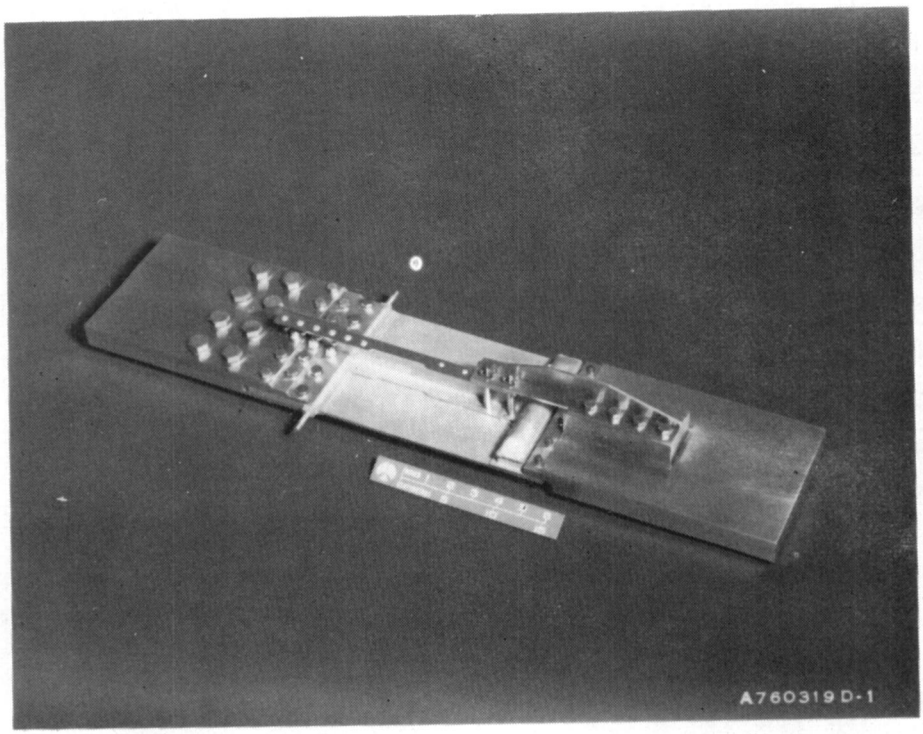

Figure 17. End Panel/Internal Stringer Termination Fatigue Specimen

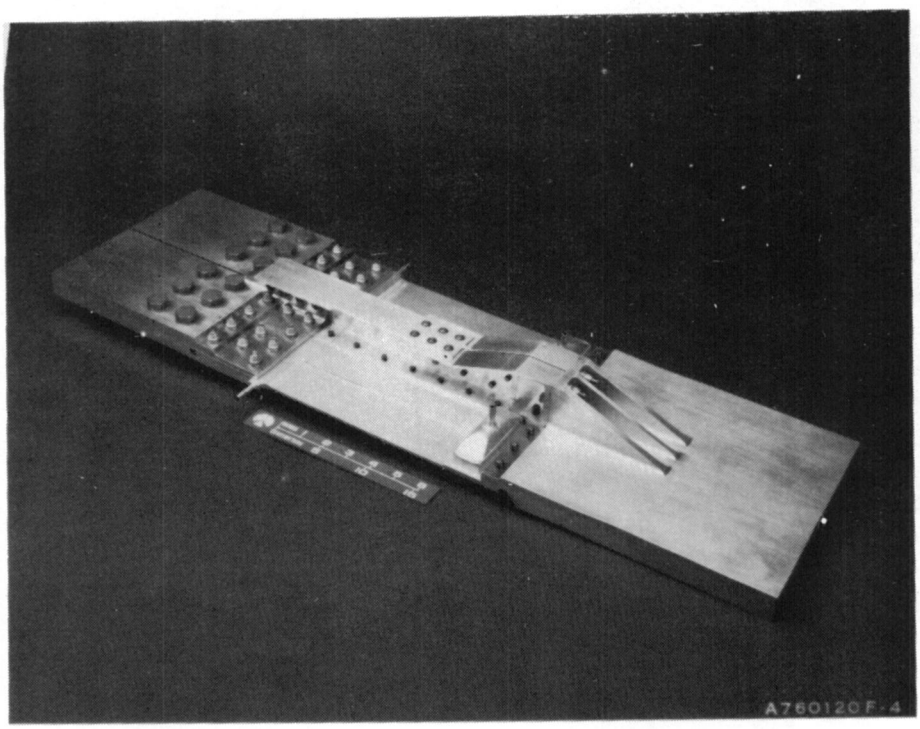

Figure 18. Panel Corner Fatigue Specimen

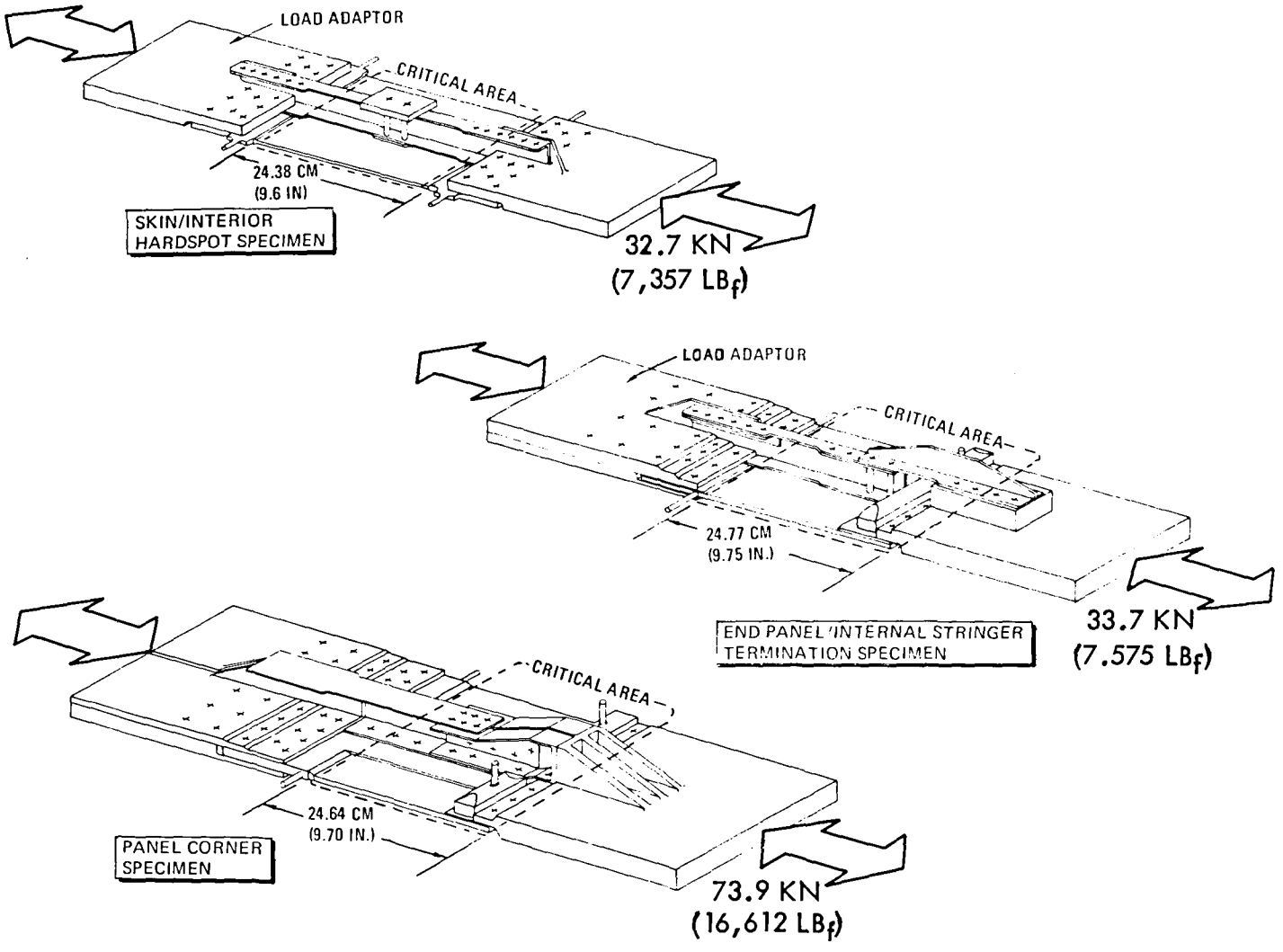

Figure 19. Fatigue Specimen Loadings

The fatigue test program conducted at NASA/LaRC was successful in that it did reveal design deficiencies which were corrected by (1) bathtub fitting redesign, (2) localized edge stringer inboard flange beef-up, and (3) a change in the panel to main frame and panel to edge stringer fastener system from Cherrylock blind rivets to Taper-Loc bolts. The bathtub fitting mentioned above was required to structurally attach the edge stringer termination to the panel end main frame. Figure 20 summarizes the fatigue test program. The events coded Ⓐ are described below.

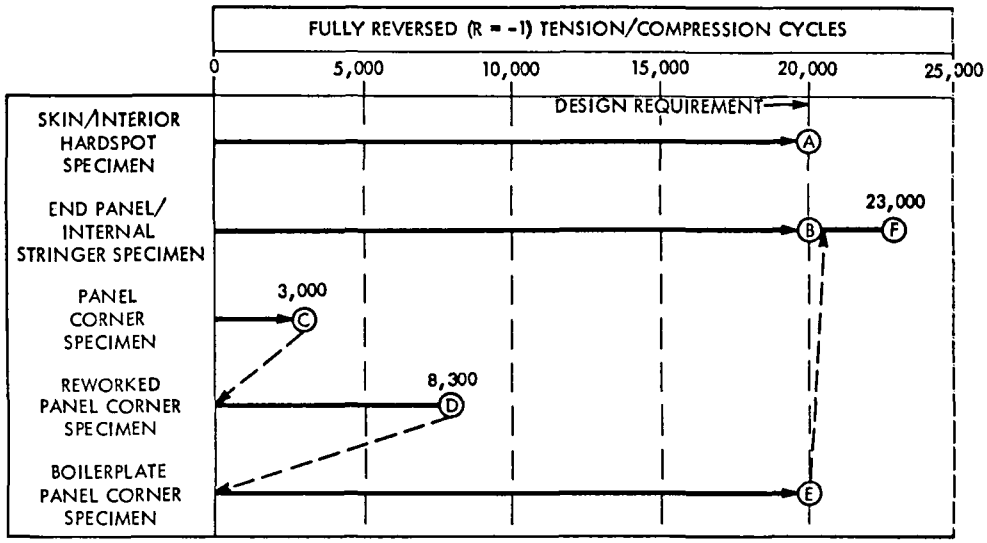

Figure 20. Fatigue Test Program Summary

Ⓐ The Skin/Interior Hardspot Specimen successfully completed the 20,000-cycle fatigue test.

Ⓑ The End Panel/Internal Stringer Specimen successfully completed 20,000 cycles without failure; however, some joint motion was observed at both the panel/main frame joint and the panel/ internal stringer/main frame flange attachment.

Ⓒ Failure of the inboard flange and part of the web of the bathtub fitting at the joggle termination point (Figure 21) occurred after 3000 cycles of test. The panel corner specimen was reworked incorporating redesigned bathtub fittings. The bathtub fitting redesign and the reworked specimen are shown in Figure 22.

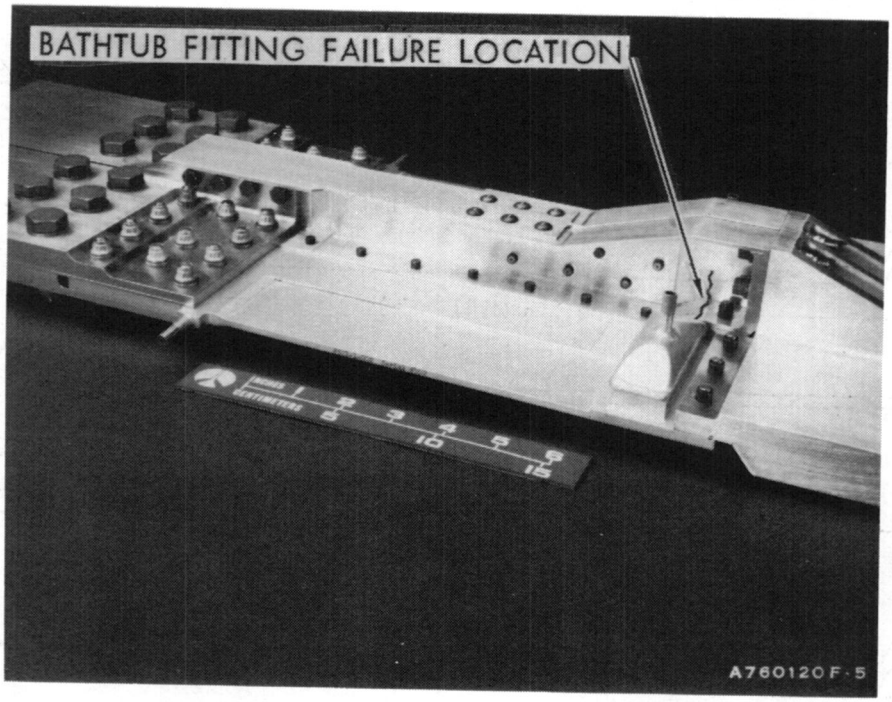

Figure 21. Panel Corner Specimen
Bathtub Fitting Failure

(D) Failure of the inboard flange of the edge stringer occurred across the stringer to bathtub fitting fastener line (Figure 23) after 8300 cycles of testing. Throughout the test, excessive motion at the panel/main frame Cherrylock riveted joint was noted. The specimen was scrapped. A boilerplate specimen (Figure 24) was fabricated which incorporated (1) a new fastener system based on results of an evaluation program conducted by Rockwell and discussed in Appendix C, (2) localized beef-up of the inboard flange of the edge stringer (2.03 mm versus 1.78 mm), and (3) a grooved plate to simulate the bending stiffness of the brazed assembly in the scrapped specimen.

(E) The Boilerplate Fatigue Specimen successfully completed 20,000 cycles of testing. No joint motion occurred.

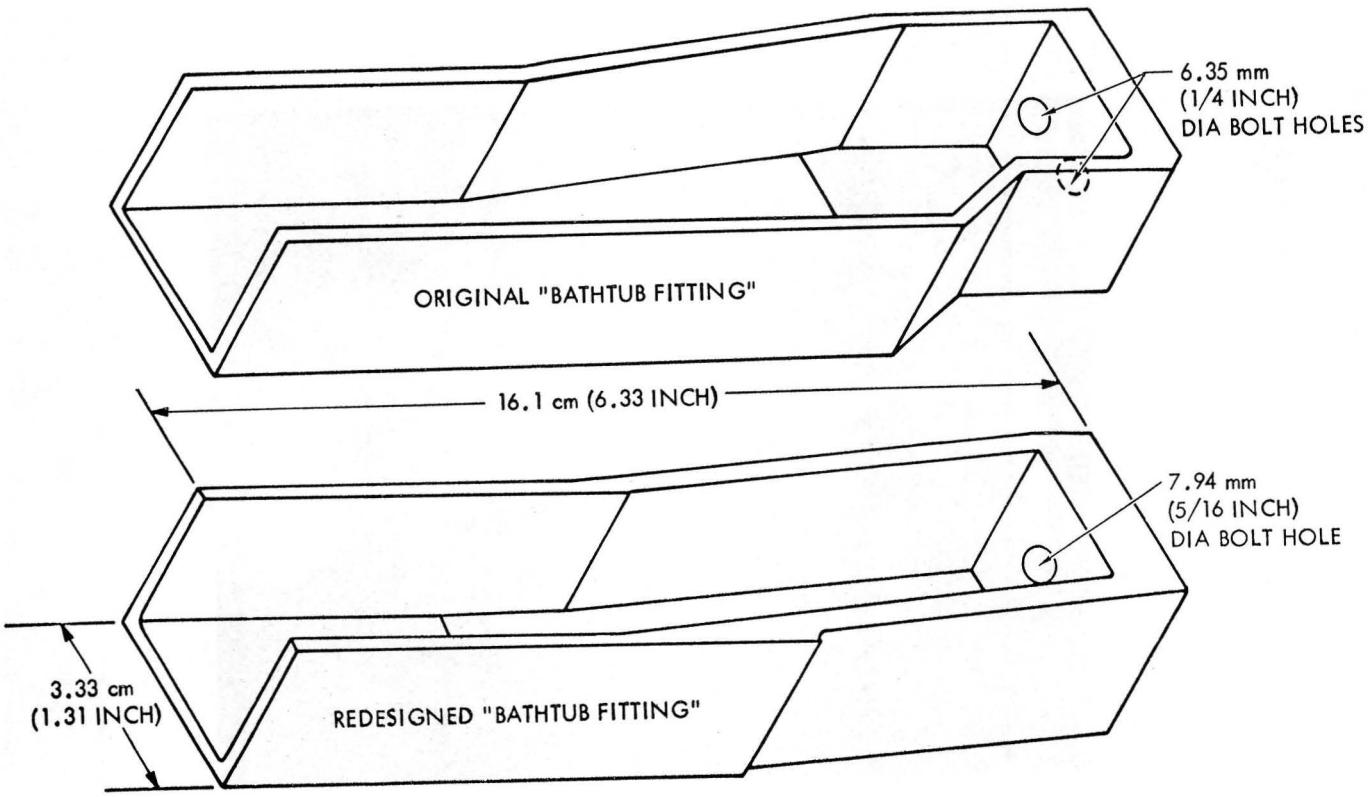

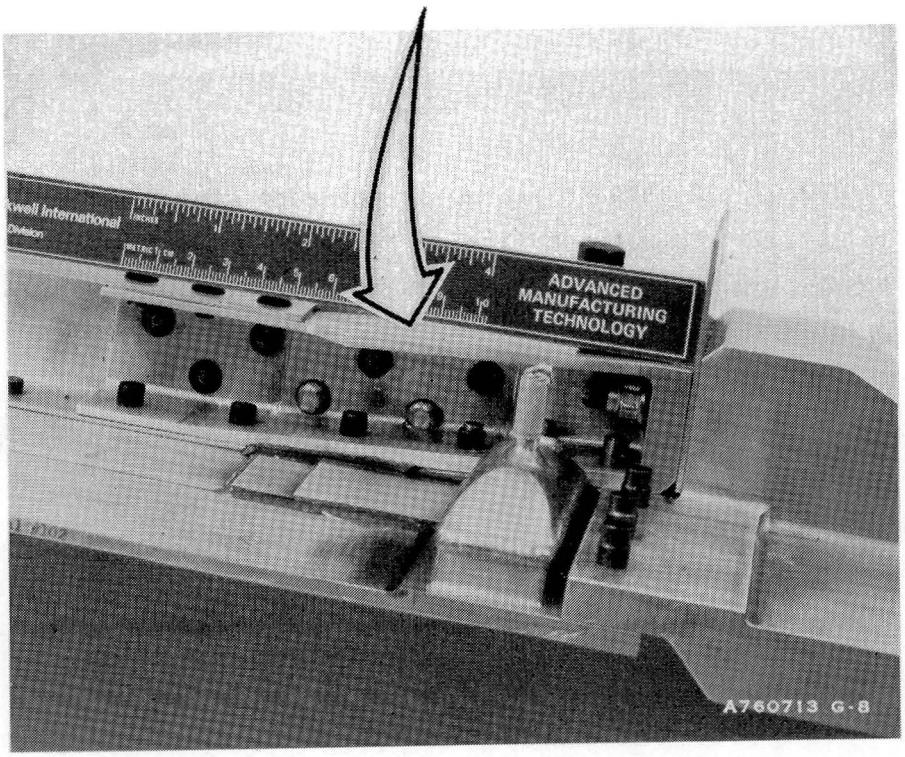

Figure 22. Edge Stringer Termination Bathtub Fitting Redesign and Reworked Panel Corner Specimen

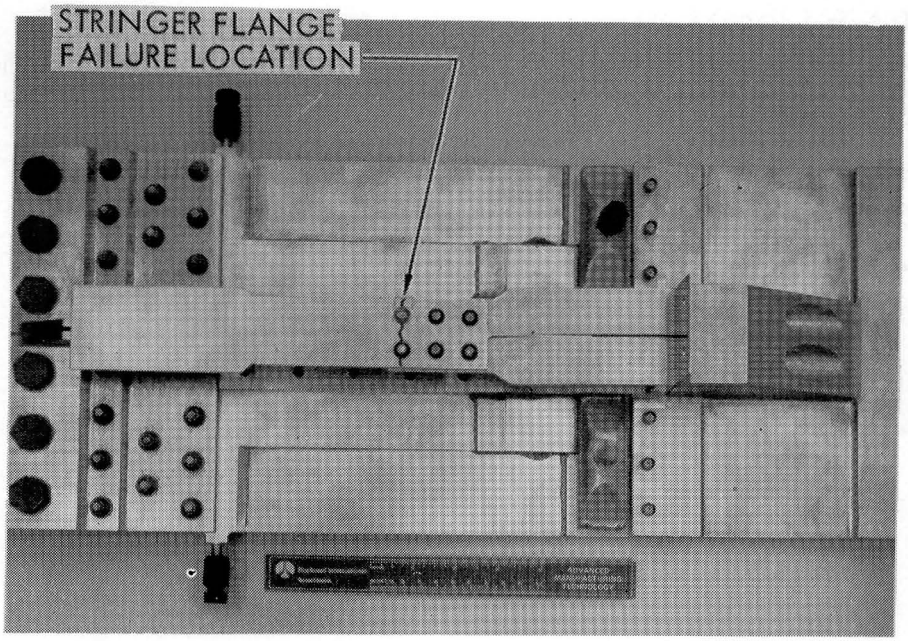

Figure 23. Reworked Panel Corner Specimen Edge Stringer Flange Failure Location

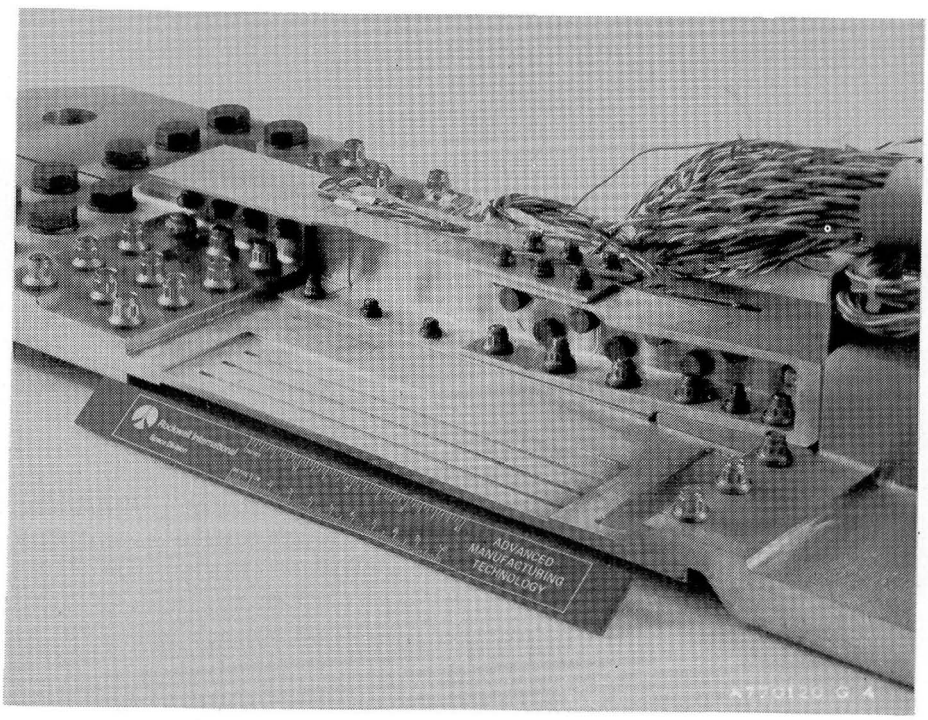

Figure 24. "Boilerplate" Panel Corner Fatigue Specimen

(F) The End Panel/Internal Stringer Specimen was reworked to incorporate the new Taper-Loc fastener system and to replace the 4.76 mm (3/16 in.) diameter bolt and nutplate attachment system at the panel/internal stringer/end panel flange location with a 6.35 mm (1/4 in.) diameter bolt and a tension nut. The specimen was then subjected to 3000 additional fatigue cycles. The joint motion noted in the earlier test (B) was eliminated.

Additional details related to the fatigue specimen program are presented in Appendix D.

4.0 TEST PANEL

Following successful completion of the fatigue test program, a test panel was designed and fabricated. A schematic of the test panel and load adapters is shown in Figure 25. The test panel is 0.61 m by 1.22 m (2 by 4 ft) with sculptured load adapters at either end. The overall length of panel and adapters is 1.98 m (78 in.). The test panel is essentially identical in configuration to the first 0.61 meters (2 ft) and the last 0.61 meters (2 ft) of the final full scale panel described in Section 2.0 of this report and incorporates all critical configuration features.

The load adapters are sculptured so that their neutral axis or load path follows the neutral axis of the end of the test panel across its width and they simulate the bending stiffness of a main transverse frame. This was done to assure that no test-peculiar local bending would occur during axial load application at the panel/adapter interface. In addition, each load adapter has two 1000-W, 8.7-ohm resistance heat strips bonded across its width close to the panel interface. These heat strips in conjunction with a thermal controller and sensing thermocouples on the panel and load adapter will be used during thermal testing to keep the load adapter, in the vicinity of its interface with the panel, at approximately the same temperature as the panel end. This will minimize heat leak from the panel to the load adapter and minimize, if not eliminate, transverse thermal stresses along the Taper-Loc fastener line at the load adapter/panel interface. This test-peculiar thermal stress would occur from differential transverse expansion at this interface. The load adapters are insulated with closed cell polyurethane foam to minimize heat leak to the environment. The test panel, as fabricated, deviates from the final full scale panel design discussed in Section 2.0 as follows:

1. The edge stringers are channel sections machined from bar stock. The full scale panel design calls for an extruded I-beam section. The I-beam section in the full scale design provides for attachment of two (2) adjacent panels.
2. Most of the Taper-Loc fasteners in the test panel are steel. The full scale panel design uses titanium fasteners as a mass savings.

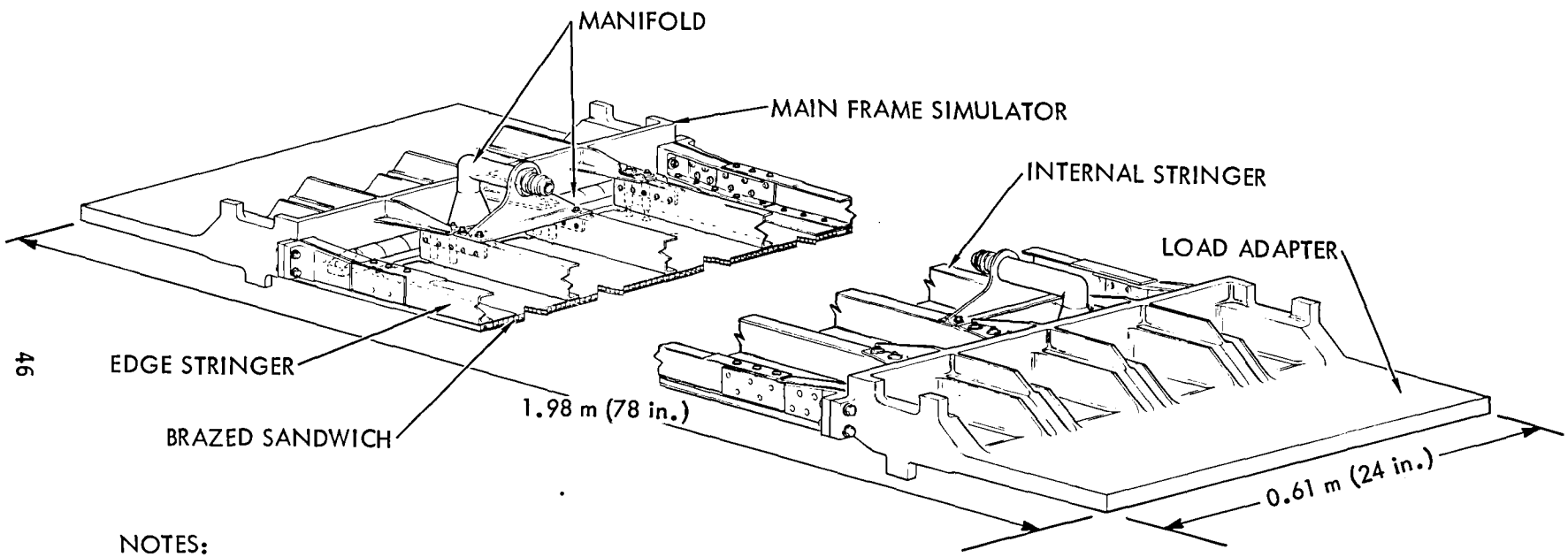

NOTES:

(1) INTERMEDIATE TRANSVERSE FRAME NOT SHOWN

(2) HEAT STRIPS ON REVERSE SIDE OF LOAD ADAPTERS

Figure 25. Test Panel Schematic

The substitution was necessary because of fastener availability problems.

3. The test panel coolant inlet and outlet elbows are welded assemblies. They would be formed parts in a full-scale panel.

4. The conduction plates are a continuous width of 60.45 mm (2.38 in.). In the full-scale design, they are 60.45 mm (2.28 in.) wide for the last 3.05 m (10 ft) at the hot or outlet end of the panel, and 26.92 mm (1.06 in.) wide for the first 3.05 m (10 ft) of the panel.

None of the above deviations are significant.

Structural analysis of the test panel and load adapter was conducted using the Rockwell developed NARFEM computer program (Reference 10) for modeling and the NASA developed NASTRAN program (Reference 11) for structural analysis. Comparing results of this analysis with that conducted for the full-scale panel design indicates that test panel and full-scale panel structural performance at temperature should be identical for the design load conditions.

Thermal analysis of both the test panel and the load adapters indicates that, with proper temperature control of the load adapter on the test panel inlet end, the temperature distribution for approximately the first 0.3 meter (2 ft) of test panel should closely approximate the predicted distribution for both the coolant and the structure in the full-scale panel. This assumes a coolant inlet temperature of 289 K (60°F), inlet pressure of 827.4 kPa (120 psi) and a coolant mass flow rate of 13,636 kg/hr (30,000 lb/hr). However, close approximation of the full-scale panel outlet temperature distribution will be more difficult to achieve. The test panel is one-fifth the length of the full-scale panel and the outlet or hot end transverse coolant temperature distribution is a function of the coolant flow regime at the outlet end of the core. This flow regime (i.e., laminar, transitional or turbulent) is a function of coolant temperature which is, in turn, a function of panel length. The predicted outlet distribution can be obtained by variation in coolant inlet conditions and outlet end load adapter temperatures during test conduct.

Details of the test panel thermal and structural analysis and fabrication procedures are presented in Appendix E. The fabricated test panel attached to the load adapters is shown in Figures 26 and 27.

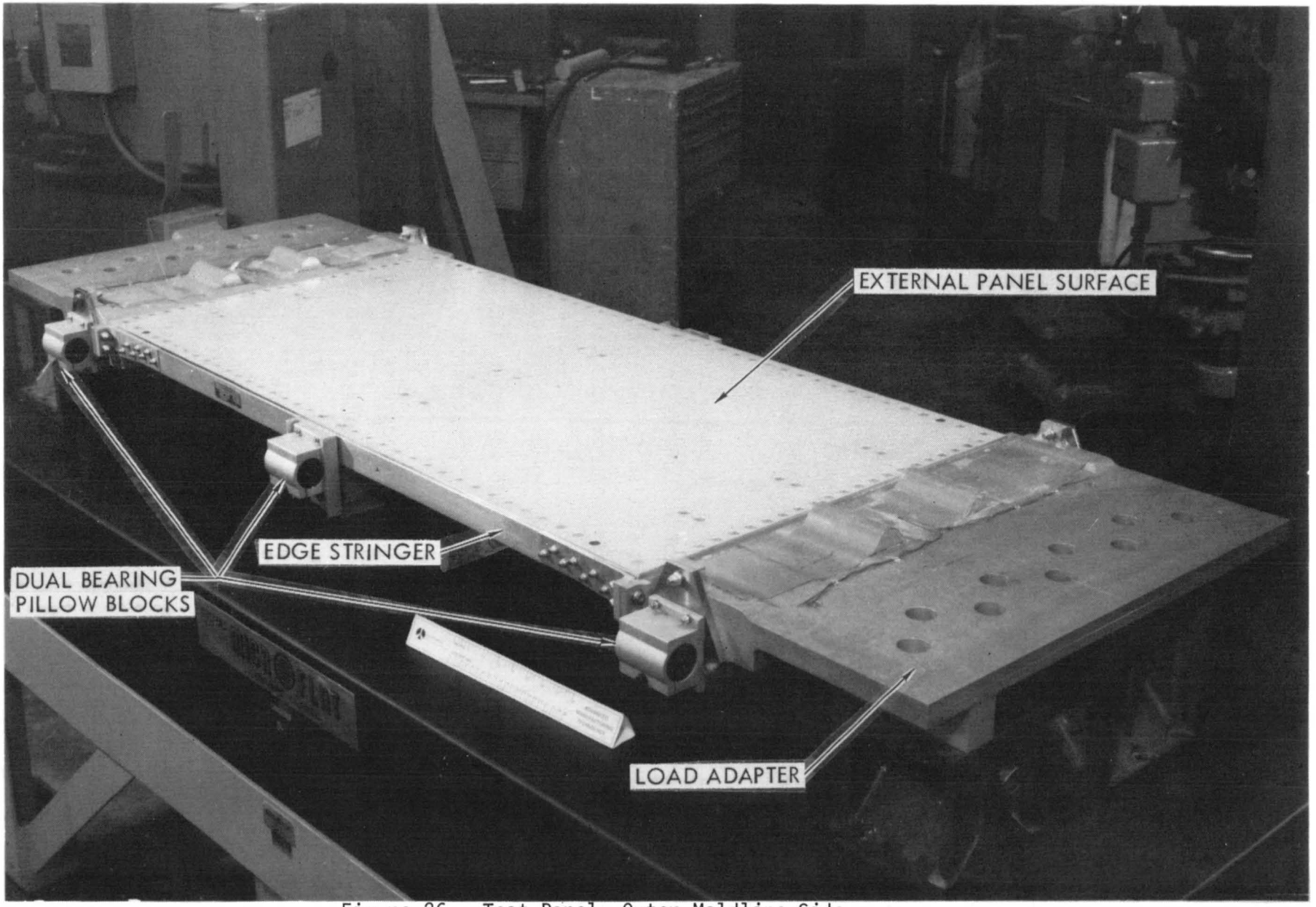

Figure 26. Test Panel—Outer Moldline Side

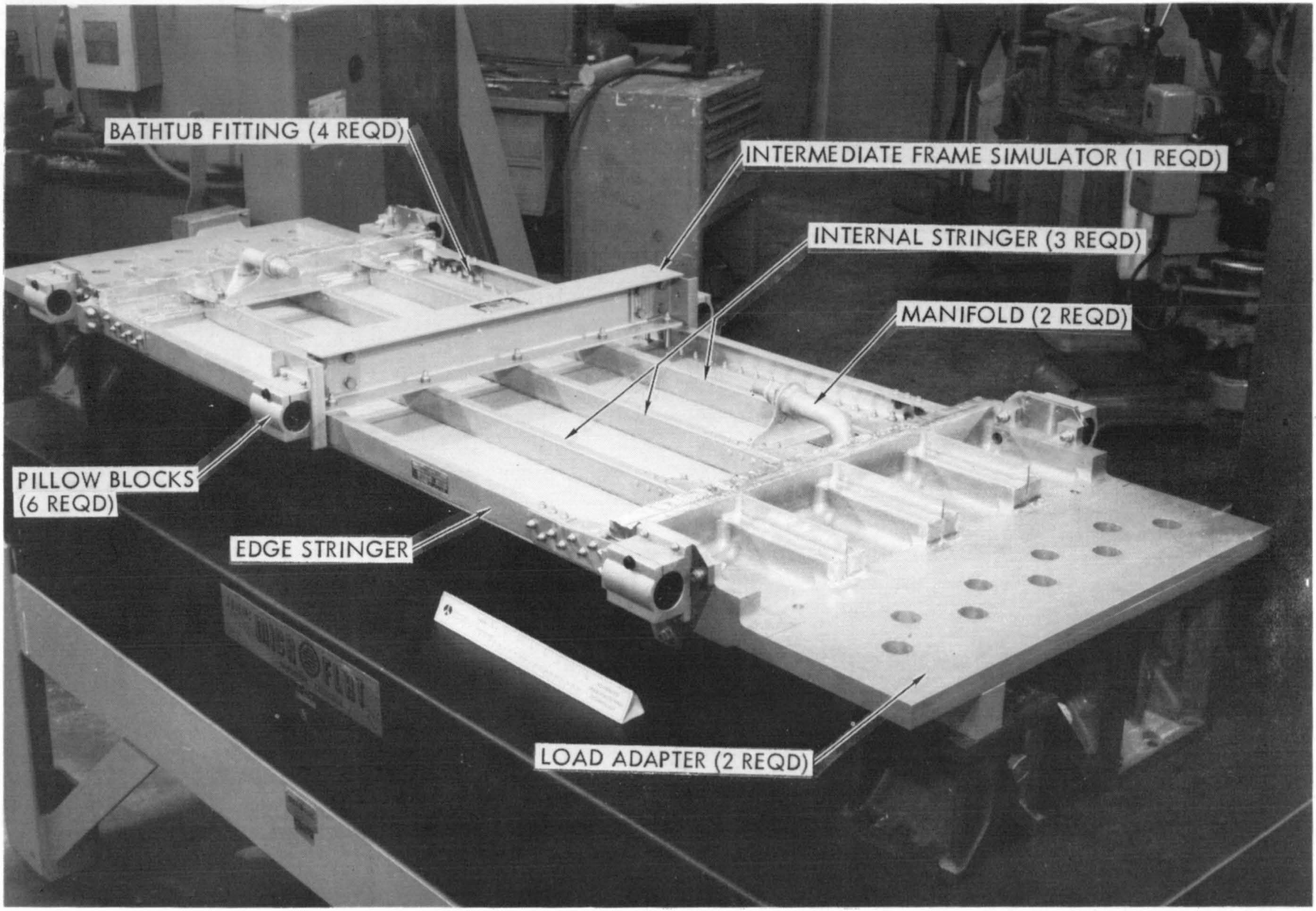

Figure 27. Test Panel—Inboard Side

5.0 FABRICATION

The stringer-stiffened plate-fin sandwich cooled panel concept is dependent on successful implementation of fabrication processes that will result in a leak-free sandwich structure with adequate strength to withstand the design environment over the service life of a hypersonic cruise aircraft.

During the fabrication phase of this program, two critical processes which have a major impact on the quality of resulting hardware were selected and tailored for this particular application. They were then assessed in terms of scale-up considerations for future fabrication of full-scale actively cooled panels. The two critical processes are brazing and post-braze heat treatments.

5.1 CRITICAL PROCESSES

The aluminum brazing process has a major influence in fabricating assemblies requiring multiple joints or large area joint coverage. Two brazing methods have been used successfully for the aluminum assemblies. The first method has been used in industry for many years and is referred to as salt bath brazing. As the name implies, the process utilizes a salt bath as the brazing media. However, this salt is highly corrosive to aluminum if even a minute amount is left on the assembly and, therefore, extensive care in post-braze cleaning is essential. The second aluminum brazing process having a major impact on high-quality aluminum assemblies is commonly referred to as fluxless brazing. Although several variations of the process exist, it generally consists of brazing aluminum assemblies without the use of corrosive fluxes. Thus, the use of a fluxless brazing process is best suited for assemblies whose in-service inspection is not possible and/or where corrosion could result in catastrophic failure.

Fluxless brazing is an ultra-high-quality fabrication process producing aluminum assemblies capable of being subjected to high internal pressure without evidencing corrosion problems. Over 2000 aluminum coldplates, a major subassembly of environmental control and life support systems for spacecraft, have been fluxless brazing in production with yields exceeding 99 percent. These coldplates

have been of the pin-fin core sandwich-type configuration. Other core types such as fin-on-plate, tube-on-plate, and honeycomb have been fluxless brazed on a developmental basis with equally high yields.

Based on this past history, it was determined that the fluxless brazing process was most applicable to this active cooling concept in that it lends itself to readily joining large areas and results in hardware which is corrosion-free and capable of long service life. Only the variation of the brazing process was necessary to determine. The two most common fluxless brazing techniques are vacuum and inert atmosphere brazing. The vacuum brazing process was used initially to braze the eight small-scale specimens. Subsequently, the three fatigue test specimens and the 0.61 m by 1.22 m (2 by 4 ft) test panel were brazed using the inert gas atmosphere brazing process. The inert gas atmosphere in the sandwich cavity minimizes sandwich thinning or core collapse during the brazing process.

All panels (eight small scale, three fatigue, and the test panel) were fluxless brazed in retorts. Retorts are welded stainless steel envelopes which contain the parts to be brazed. The brazing process basically consists of placing the aluminum details to be brazed in a retort, welding the retort, and then placing the retort in a press between heated ceramic platens. A vacuum system, attached to the retort, evacuates the retort of contaminants. The atmosphere in the retort is either vacuum or inert atmosphere, as desired. The temperature of the parts is monitored and controlled with thermocouples attached to the parts within the retort. During brazing, the sandwich is heated to a temperature range of 841 to 863 K (1055 to 1095°F). At this brazing temperature, the solid parts of the sandwich are subjected to a 1.03 to 1.38 MPa (150 to 200 psi) mechanical pressure to assure faying surface contact and to control final thickness of the specimens. The specimens are held at the brazing temperature for 10 minutes, then air-cooled to room temperature while maintaining the vacuum or inert atmosphere.

Heated platen press retort fluxless brazing of actively cooled sandwich structures containing thin foil core systems and the subsequent heat treatment posed several problems which had to be overcome. The major problems are core crushing, skin surface damage, core peeling, and overall flatness of panels. Three specific areas of processing were carefully reviewed,

controlled, and modified as necessary to overcome these problems. They were: (a) braze tooling, (b) braze tooling barriers, and (c) heat treat tooling and quenching. A brief summary of each area is discussed below:

(a) Braze Tooling - Heated platen press retort brazing of panels having essentially little or no internal support (only that provided by the core fins) requires critical tooling to minimize cavitation (thinning of overall thickness) of the panel. This is done by the judicial selection of tooling materials and a very tight control of tolerances. The braze tooling utilized in the fabrication of these panels provided sufficient support and dimensional accuracy to maintain the required panel configurations. The tooling used on the three fatigue specimens and the 0.61 m by 1.22 m (2 by 4 ft) test panel are good examples of the complex braze tooling necessary for successful heated platen press retort brazing. A lay-up of the braze tooling used on the test panel is shown in Appendix E.

(b) Braze Tooling Barriers - Tooling materials used in the heated platen press retort brazing process are fabricated from stainless steel or aluminum alloys. These materials are extremely difficult to remove or strip away from the aluminum brazed panels after being subjected to the heat and pressure necessary for the process. Coating the tooling materials with parting agents is not desirable due to possibility of contaminating the braze joints resulting in adverse effects on joint integrity. Adherence of the relatively thick tooling materials to the thin panel skins necessitates removal of the tooling by peeling. This peeling action can damage the panel skins, and worse yet, the thin foil core material in the cavity. This problem was overcome by utilizing thin oxidized stainless steel foil sheets at all contact areas of tooling-to-panel components. The foil was oxidized by heating it to a temperature range of 866 to 922 K (1,100 to 1,200 °F) in air. This temperature is low enough to prevent scaling, yet sufficiently high to form discolored oxide. Warpage or wrinkling of the foil is prevented by allowing free expansion and contraction during heating and cooling. The oxidized stainless steel foil is placed at the interface between the panel being brazed and its braze tooling. Use of this

oxidized foil eliminated the adhering problem without having to resort to use of parting agents with the attendant contamination concerns.

(c) Heat Treat Tooling and Quenching - It was expected that the major problem in the program would be encountered during thermal treatment of panels. Due to the internal construction of the panel, that is, it having little or no solid support in the core areas, it was felt that severe distortion and crushing would occur during the heat treating and quenching operation. During fabrication of the eight small scale test specimens, valuable information was gained regarding the use of fixtures and the quenching media. It was found that fairly severe distortion of panels occurred when quenching in water without use of a fixture. Quenching in water using an aluminum fixture also caused considerable distortion of both the panel and the fixture. Although the parts could be hand straightened, extensive effort was required to salvage the fixture. Quenching in water using a steel fixture was more successful. Distortion of the panel does occur but to a lesser degree. The steel fixture itself required minor rework and straightening after three or four quenching cycles.

Even though separator sheets were used between the panels and fixtures, some marking of the skins and, in a few cases, slight local crushing of the core occurred. It became obvious that these problems of distortion, core crushing, marking, and hand-straightening requirements must be minimized—especially when considering the larger and more complex configurations to be brazed and heat treated. As a result, a review of some other quenching concepts and quenching media was made. The revised concept selected was to solution-quench the panels without the use of heat treat fixtures, in a medium other than pure water, which would minimize the distortion problems and simplify straightening. Based on the recommendation of heat-treating firms in the Southern California area, a quenching solution of 76% water and 24% "UCON-A" was selected for solution quenching the remaining, more complex panels. "UCON-A" is a polymer or synthetic quenching medium whose properties are reported to result in more uniform heat transfer for the control of residual stresses and distortion. This material is manufactured by Union Carbide Corporation.

Quenching in a "UCON-A"/water solution proved to be successful. The final two fatigue specimen sandwiches were produced with considerably less distortion than obtained with water quenching. In addition, the amount of hand work necessary to straighten the panels was minor. No direct comparison exists with the two quenching media for the 2- by 4-foot test panel since only one quenching medium, the "UCON-A," was used. However, considering the size, shape, and overall structural configuration, the distortion obtained when quenched in "UCON-A" was considerably less than would be expected if quenched in water.

5.2 SCALE-UP CONSIDERATIONS

No major problems were encountered during the fabrication effort on this program. However, several processing procedures are involved which should be reviewed before scaling up to fabricate larger actively cooled panels with similar core configurations. These are discussed below.

Assembly of Corrugated Core. Assembly of the corrugated cores in the smaller panels was relatively simple. However, some difficulty was encountered holding the core in place during fabrication of the 0.61-m by 1.22-m (2- by 4-ft) test panel. The core is presently available in a maximum length of only 30.5 cm (12 in.) in the direction of the corrugations. Hence, for test panel sized assemblies, core pieces must be layed in place like a jigsaw puzzle in preparation for brazing. Several unsuccessful attempts were made to capacitor discharge weld the corrugated core to the face sheet (containing the clad braze alloy). This difficulty may be associated with the particular alloy combination, power capability, type of welding equipment, thickness combinations, or a combination of these factors. Assembly of the core components was accomplished without benefit of weld tacking. With considerable difficulty, the four core sections were carefully aligned, core filler bars located in their respective core convolutions, and the inner face sheet installed. Fabrication of larger panels will certainly compound this assembly problem. Cementing and other similar techniques might be viable solutions; however, contamination effects must be considered. In any case, availability of a simple method of locating the core and attaching to the face sheet without contamination of the brazed joints is highly desirable. Two advantages exist when the core is "locked" to the contacting face sheet. First, assembly of the core sections is simplified

such that all convolutions at adjoining sections would be easily aligned during lay-up, and concern for convolution mismatch while locating the final face sheet over the core would be minimized. Secondly, experience has shown that the core convolutions shift or relax from time of assembly to brazing. This shift is evidenced in the radiographs of the test panel and in radiographs of other panels previously brazed having this type of corrugated core. Thus, if some degree of mismatch of abutting core sections cannot be tolerated and must be controlled, a method of tacking or positively locating the core to the face sheet must be established.

Solution Heat Treatment and Quenching. The 0.61-m by 1.22-m (2- by 4-ft) test panel sandwich structure was solution heat treated and quenched in a free-standing state; that is, a heat treat fixture was not used. The results were very successful. It is believed that scaling up to larger panels would likewise dictate that fixtures not be used, especially considering the fact that the size and weight of the fixtures would be massive.

Quenching the panels in pure water without a fixture results in relatively severe distortion. Quenching the panel in a water/"UCON-A" quenching solution without a fixture did result in some distortion although far less than with pure water. In any case, hand straightening was necessary. Distortion of larger panels would in all probability be considerably magnified and the amount of hand straightening necessary to eliminate the distortion in panels would likewise be expected to increase considerably. Thus, it is believed that a study is required to determine the optimum "UCON-A" concentration for this particular combination of materials and thicknesses which would result in the least distortion while still yielding the required hardening characteristics and properties. Quenching in liquid nitrogen should also be reviewed.

Straightening. The amount of hand straightening necessary to straighten panels should be minimized principally to reduce the possibility of damage to the panel as a direct result of the hand straightening operation. Although hand straightening is the conventional and generally accepted method of straightening panels of this nature, other methods of straightening, such as stretcher leveling, should be reviewed for use on scaled-up panels. Of course, any straightening method reviewed should consider the time element after quenching to assure that the panel is still in the "soft" condition to facilitate the straightening operation.

Contoured Panels. In actual application, panels with single contours may be required. If the contour radius is large and the contour is in the transverse direction across the panel width, contouring can probably be accomplished after brazing, but before heat treatment. However, if the contour radius is small or the contour is in the longitudinal direction along the core, the fabrication complexity is greatly magnified. The contouring would have to be accomplished on the individual parts of the sandwich separately prior to brazing using an elevated temperature forming process. Brazing and heat treatment would probably require the use of fixtures, and resolutions to the fixture attributable problems discussed above would have to be obtained.

6.0 CONCLUDING REMARKS

This report presents results of a program in which a basic plate-fin stringer-stiffened active cooling concept was developed into a full-scale 0.61 m by 6.1 m (2 ft by 20 ft) actively cooled panel design for potential application to hypersonic vehicles. Fatigue specimens of critical areas of the full-scale panel design were fabricated by Rockwell and tested by NASA and a 0.61 m by 1.22 m (2 ft by 4 ft) test panel was fabricated and delivered to NASA for future testing. The design loading conditions, heat flux, and life cycle requirements were representative of those for skin panels on a Mach 6 to 8 hypersonic cruise transport aircraft. The final design consists of a brazed aluminum alloy corrugated sandwich structure with welded-on manifolds and adhesively bonded and/or mechanically fastened longitudinal stringers. The design heat flux is transferred via forced convection to an ethylene glycol/water coolant that circulates, under pressure, through the corrugated sandwich structure. The panel unit mass is 12.36 kg/m^2 (2.52 lbm/ft^2) and includes the structural dry mass, coolant inventory mass, and Auxiliary Power System (APS) mass.

Specific conclusions derived from this study are presented in the following paragraphs.

The largest contributors to panel system mass are the brazed sandwich face sheets. The full-scale panel defined in this report uses 0.81-mm (0.032-in.) thick face sheets because they are a standard size available from the aluminum industry. The next-thinner available size is 0.51 mm (0.020 in.) which is not acceptable structurally. However, if the thickness selected were based solely on structural requirements and a special mill run was deemed economically viable, a face sheet as thin as 0.6 mm (0.0236 in.) would be acceptable. The thickness depends on the end fixity condition assumed in the analysis of the unsupported face sheets in the vicinity of internal hardspots. This mass optimizing would result in an overall system mass reduction of up to 9 percent.

The critical design feature of a plate-fin stringer-stiffened actively cooled panel is the perimeter attachment requirements. The perimeter of the panel is solid metallic material to accommodate the fastener system which attaches the panel to the aircraft frame structure. The temperature this

solid material achieves in a design environment is a major factor in the selection of a coolant inlet condition. For instance, for the selected coolant inlet conditions, the maximum predicted panel perimeter temperature is 414 K (286°F), while the maximum temperature predicted for structure in close proximity to coolant passages is less than 366 K (200°F). Hence, the design inlet condition for the coolant is dictated by a relatively small percentage (approximately 10 percent) of the panel area. In addition, this solid metallic perimeter material is approximately three times as dense as the coolant it replaces and, hence, adds to the panel structure mass.

Adhesively bonding the actively cooled structural panel to the aircraft frame structure is feasible. This would eliminate most of the solid metallic material around the panel perimeter, reduce the panel structure mass, and reduce the APS mass penalty by requiring a lower coolant inlet flow rate. This approach is worthy of consideration for future actively cooled panel development.

If mechanical fasteners are required, selection of these fasteners is extremely critical. This is particularly true of fasteners attaching the ends of the panel to the main frame. Joint motion must be minimized. Thermal considerations dictate that the solid metallic uncooled ends of the panel be narrow to avoid exceeding allowable structure temperatures. Hence, there is width for only a single row of fasteners rather than staggered multiple rows traditionally designed for structural joints. In addition, the requirement for a smooth outer surface mold-line eliminates the option of adding an external doubler to the joint, which would put the fasteners in double shear. The selected fastener system must not only be "hole-filling" with high shear strength, it also must have high, predictable "clamp-up" capability. Rivet systems investigated during this program do not meet the latter requirement. Bolt and nut systems, in general, do meet the above requirements and drastically reduce the joint motion obtained with rivets. The Taper-Lok fastener system was selected for the full-scale design based on its superior performance in test.

Successful fabrication of brazed, actively cooled sandwich structures requires that tolerances of the braze tooling be closely controlled during tooling stack-up to assure an even application of mechanical pressure during

brazing. Failure to do this will result in localized core crushing and/or voids in brazed joints.

The selection of a heat treatment quenching solution is critical. Quenching media selection appears to be directly related to assembly distortion resulting from residual stresses. A quenching solution of 24%/76% UCON-A/water was used with great success in this program. Assembly distortion was much less than would be anticipated for a pure-water quench.

APPENDIX A

MATERIAL DATA

This appendix presents the selection rationale and the material properties data for the metals, coolants, and adhesives used in the actively cooled panel design.

Metals

The state of the art in fluxless brazing technology dictates the use of 6000 series aluminum alloys for all elements of the brazed sandwich structure. The 6000 series aluminum is the only heat treatable alloy that has been successfully fluxless brazed on a large scale. Within the 6000 series, only 6951 aluminum alloy is available in braze sheet, which is used for the sandwich skins. This braze sheet is designated as No. 23F brazing sheet. It consists of 6951 aluminum core alloy clad on one side with a 10-percent thickness of 4045 braze alloy containing 10-percent silicon. The 6951 core alloy, when heat-treated to the T6 condition has an ultimate tensile strength of 263.9 MPa (39,000 psi) and a tensile yield strength of 227.5 MPa (33,000 psi) at room temperature, per Reference 12. For stress analysis calculations, these allowables were further reduced by 10 percent to account for the relatively ineffective 4045 cladding material, resulting in a tensile ultimate of 242 MPa (35,000 psi) and a tensile yield of 207 MPa (30,000 psi) at room temperature. Reference 12 does not give the remaining material properties required for analysis. Therefore, the required properties were developed by comparing the selected room temperature tensile ultimate of 242 MPa (35,000 psi) with that contained in MIL-HDBK-5B (Reference 5) for 6061-T6 material [289.3 MPa (42,000 psi)] and developing a reduction ratio. The elastic moduli (E), physical properties, and reduction in strength due to elevated temperature are not considered affected by the braze cladding or the braze process. Although all elements of the brazed sandwich structure are 6061-T6 alloy except the braze sheets, the reduced allowables, consistent with the ratio reduction technique described above, and shown as a function of temperature in Figures 28 through 30, were used for all sandwich stress analysis. These properties are for exposures at temperature up to 10,000 hours. The thermal coefficient of expansion, thermal conductivity, and specific heat values are presented in Figures 31 and 32.

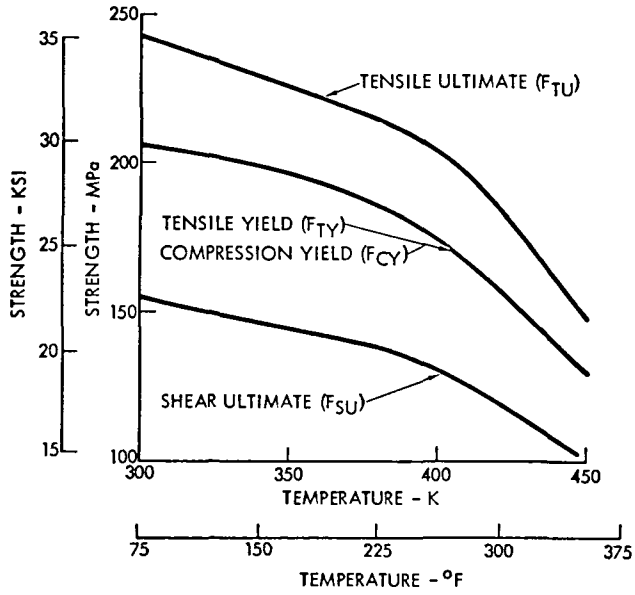

Figure 28. Tensile, Compressive and Shear Strengths of 6951 Aluminum Alloy

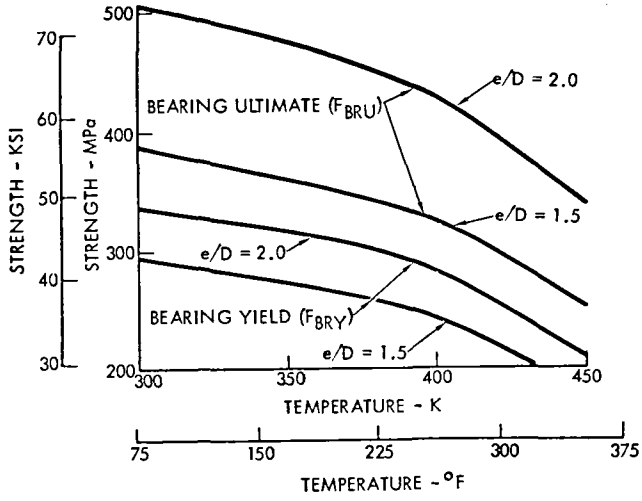

Figure 29. Bearing Strength of 6951 Aluminum Alloy

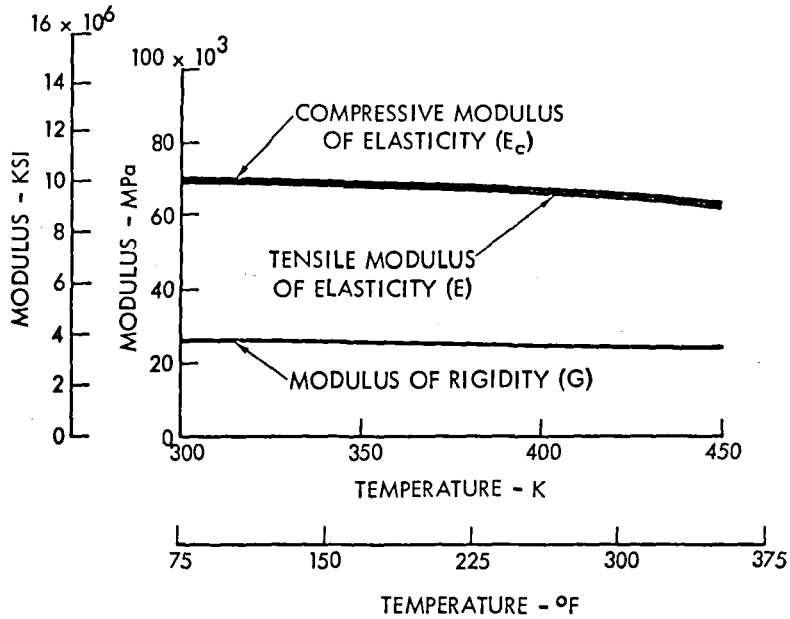

Figure 30. Modulus of Elasticity and Rigidity of 6951 Aluminum Alloy

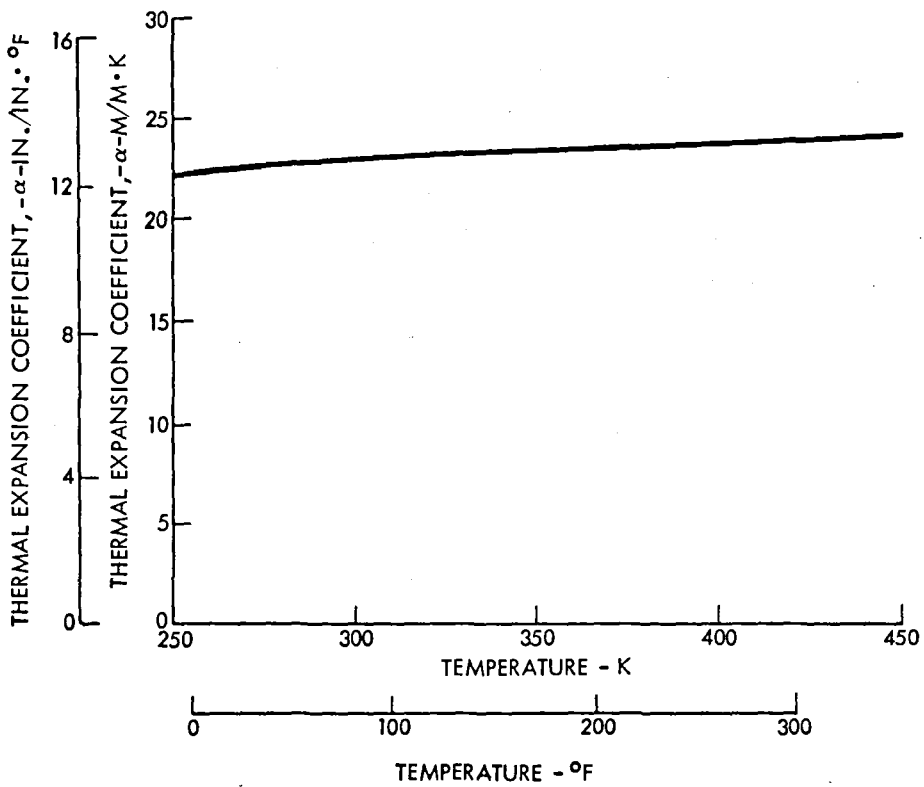

Figure 31. Thermal Coefficient of Expansion of 6951 Aluminum Alloy

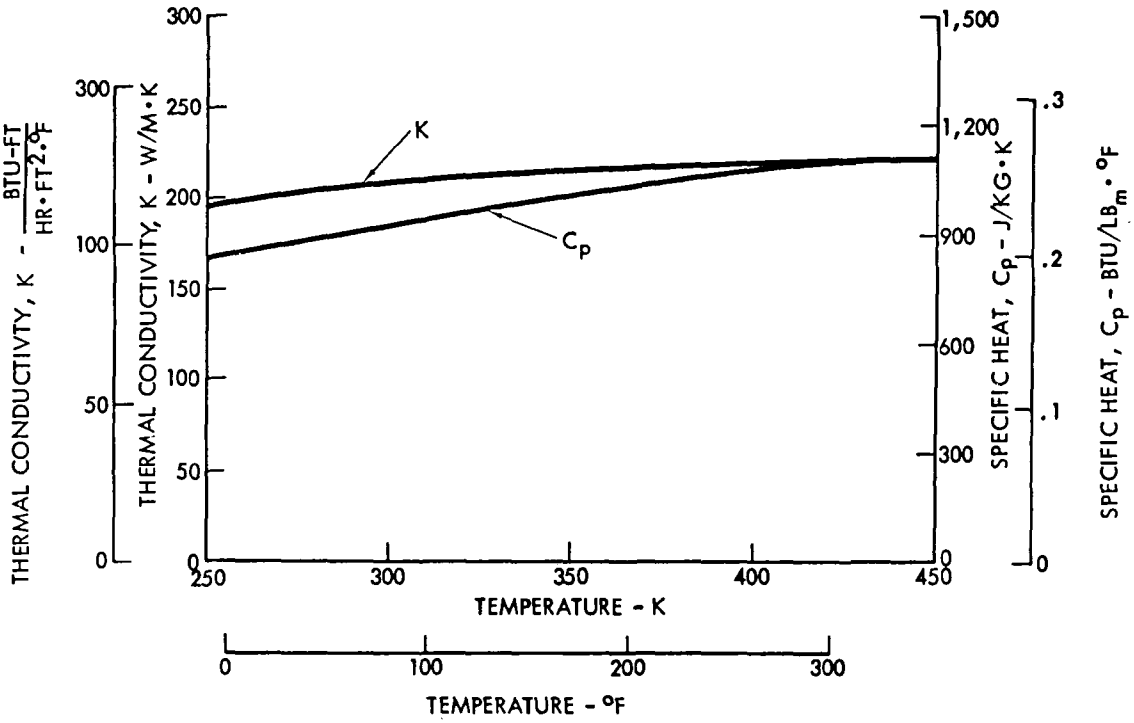

Figure 32. Thermal Conductivity and Specific Heat of 6951 Aluminum Alloy

The material of all metallic structural elements of the panel that are neither part of the brazed sandwich assembly nor welded to it following heat treatment (e.g., manifold domes) are 7075-T7351 aluminum alloy. The -T7351 heat-treat condition was selected on the basis of superior toughness and corrosion resistance when compared with -T6 and -T7651, although the latter heat treats result in higher strength. Since the 7075-T7351 structural elements must work in combination with the relatively weak 6000 series alloys in the brazed sandwich, strength was not the major driver in material selection for stringers and other nonbrazed structural elements. Material properties for the 7075-T7351 alloy were obtained from References 5 and 13.

Coolants

Two coolant candidates were evaluated for use as active coolants for the full-scale panel. They were 60/40 mixtures of Ethylene Glycol/water and Methanol/water. The Ethylene Glycol/water coolant was selected based on safety considerations for both ground handling of the coolant (storage, transfer, and

system maintenance) and flight operations. Characteristics of the candidate coolants are presented in Table 4. In addition, all testing to be conducted by NASA on the test panel will use the Ethylene Glycol/water coolant regardless of which coolant was selected for the full-scale design. Hence, performance in a test environment can be directly compared with analytical predictions without having to account for coolant property variations. The above selection was made realizing that data presented in Reference 14 predict a slight residual coolant and APS mass penalty increase when compared with use of a Methanol/water mixture. The 60/40 Ethylene Glycol/water properties used for panel thermal analysis are indicated in Figure 33. (These properties were provided by NASA from data generated by LTV.)

Table 4. Ethylene Glycol and Methanol Coolant Safety-Related Characteristics

CHARACTERISTIC	ETHYLENE GLYCOL	METHANOL
Toxicity	Low	High
Flash Point	389 K (240°F)	289 K (61°F)
Autoignition Temperature	736 K (867°F)	686 K (775°F)
Fire Hazard	Slight	Dangerous

Adhesive Systems

The interior stringers are bonded to the inboard face sheet of the brazed sandwich. A cryogenic and heat-resistant adhesive tape was selected for this application. This adhesive system is an epoxy-phenolic glass fabric-supported tape suitable for use from 20 K (-423°F) + 533 K (500°F). This system has a minimum lap shear strength of 13.70 MPa (2000 psi) at 422 K (300°F), which is more than adequate for this application. Additional properties for this adhesive are contained in Reference 15.

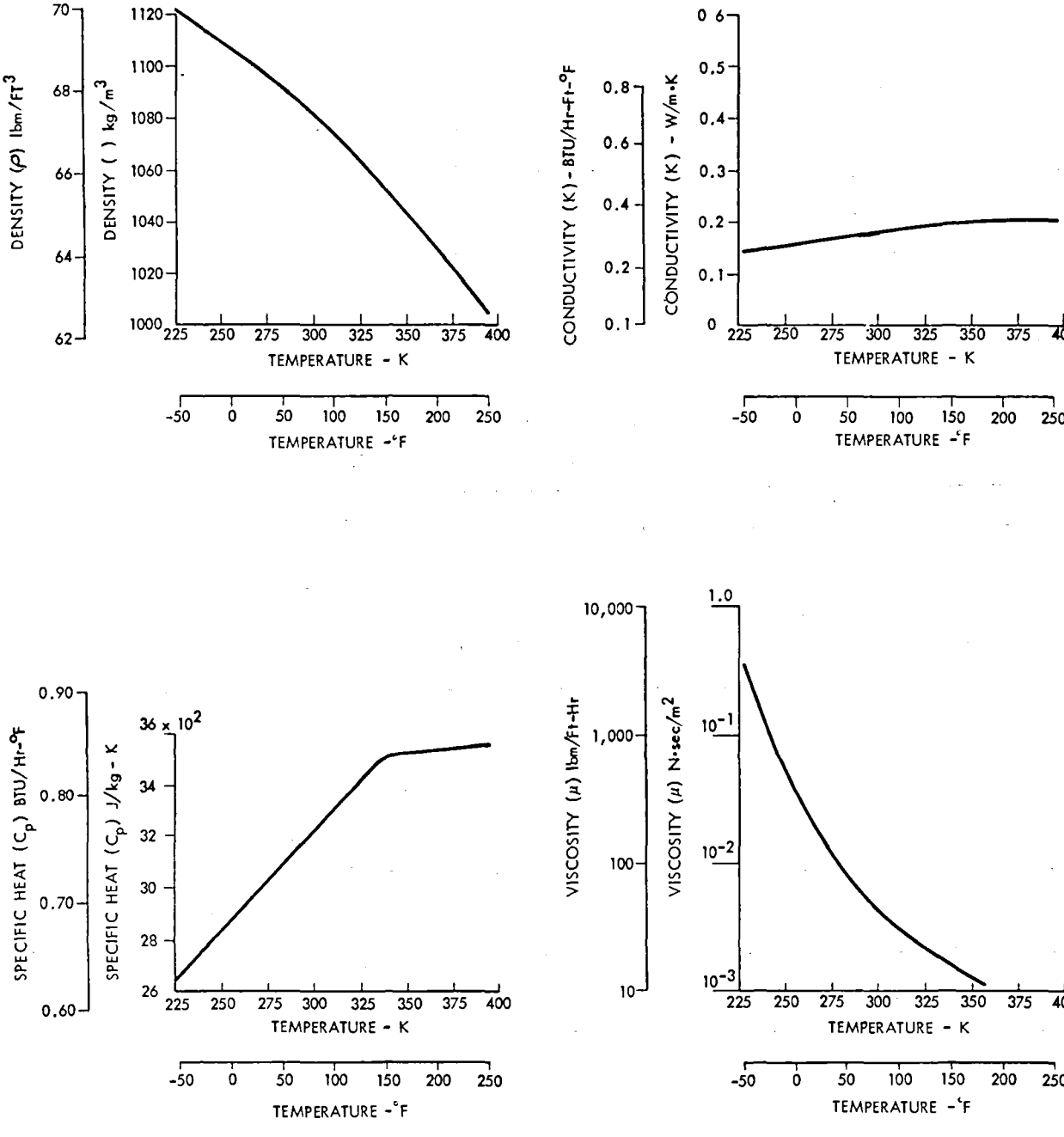

Figure 33. 60/40 Ethylene Glycol/Water Properties Versus Temperature

APPENDIX B

FULL-SCALE PANEL IN-DEPTH ANALYSIS

This appendix presents details of the thermal, fluid flow, structure, fracture mechanics, and fatigue analyses conducted in support of the full-scale actively cooled structural panel design definition.

Thermal and Fluid Flow Analysis

The primary factors influencing cooling system design for the actively cooled panel (ACP) are related to mass and size of components and the integration of the cooling system with the structure. Of prime importance was minimum mass, necessarily coupled with fabrication limitations. Panel size and the size and distribution of coolant channels within the panel were specified by NASA. No attempt was made to optimize this panel design feature. Attention was directed to panel edge and end configurations required for structural attachment, coolant supply manifold concepts, and connections to the cooling system.

The objective of the thermal and fluid flow analyses was to select coolant fluid inlet conditions that will allow panel operation consistent with the requirements and criteria established by NASA and Rockwell during the course of the study (reference Section 1.0). These requirements and criteria, as they apply to the thermal and fluid flow analyses, are summarized below.

- Coolant: 60% ethylene glycol/40% water
- Coolant temperature: 366.6 K (200°F) maximum
- Coolant outlet pressure: 345 kPa (50 psi) minimum
- Coolant flow rate: No restrictions
- Heat flux: 136.19 kW/m^2 (12 Btu/ft^2 sec) uniform and constant
- Structure temperature: 422 K (300°F) maximum
- Core: Straight through 90-deg corrugation
- Manifold: Single inlet and single outlet

The thermal and fluid flow analyses determined the following:

- Panel temperature distributions and temperature gradients for structural evaluation
- Coolant mass flow requirements and pressure drops
- Effect of heat shorts, such as the edge attachment and manifolds

Details related to the methods of analysis, the panel configurations considered, and the predicted results are discussed below.

Methods of Analysis

A three-dimensional finite difference computer program was used for the detailed thermal and fluid flow analyses. The working equations and operating procedures for this program, known as the Thermal Hydraulic Analyzer Program (THAP), are discussed in Reference 7. THAP performs heat balances for selected structure and fluid temperature nodes and mass balances for selected fluid pressure nodes with equal ease. Along with the physical dimensions, the thermal model defines materials, external heating and cooling conditions, and the modes of heat transfer between temperature nodes. The hydraulic model defines external pressure and flow conditions and the modes of flow resistance between pressure nodes. The variation in material properties with temperature is included since all thermal conductance and capacitance terms and all fluid resistance terms are recomputed for each iteration.

Coolant heat transfer coefficients were computed by three expressions depending upon the coolant flow Reynolds number (Re). For Re less than 2100, the flow is laminar. The heat transfer coefficient is given by:

$$h_L = 1.24 \frac{K_B}{D} \left(Re\ Pr \frac{D}{L} \right)^{1/3} \left(\frac{\mu_B}{\mu_S} \right)^{0.14} \qquad (1)$$

where L refers to the length of tube from the point where heating begins. For Re greater than 10,000, the flow is turbulent. The heat transfer coefficient is given by:

$$h_T = 0.026 \frac{K_B}{D} (Re)^{0.8} (Pr)^{1/3} \left(\frac{\mu_B}{\mu_S} \right)^{0.14} \qquad (2)$$

For Re greater than 2100 but less than 10,000, the flow is transitional. The heat transfer coefficient is given by:

$$\frac{h_{TR} - h_L}{h_T - h_L} = \left(\frac{Re - 2100}{10,000 - 2100}\right)^{1/4} \tag{3}$$

where h_L and h_T are evaluated at the local Reynolds number.

The constant aerodynamic heat flux of 136.19 kW/m^2 (12 Btu/sec-ft^2) was represented by an equivalent conductance of 50.45 W/m^2 (16 Btu/hr-ft^2) and an adiabatic wall temperature of 1922 K (3000°F). The use of this technique provides a more stable heat balance calculation at panel surface nodes than does the use of the heat flux directly. Because the surface temperatures are small compared to the adiabatic wall temperature, negligible error is introduced into the computations.

The pressure drop for each fluid element was computed by Equation (4) and summed to determine the total pressure drop in the panel.

$$\Delta P = \frac{\rho g}{g_c} \Delta h + 1/2 \left(e_v + f \frac{Le}{D}\right)\left(\frac{\dot{w}^2}{g_c \rho A_c^2}\right) \tag{4}$$

Friction factors (f) were computed by various expressions, depending upon the coolant flow Reynolds number. For laminar flow (Re <2000),

$$f_L = 64/Re \tag{5}$$

For turbulent flow (Re >3800),

$$f_T^{-1/2} = -0.86 \text{ Ln} \left(\frac{\varepsilon}{3.7} + \frac{2.51 f_T^{-1/2}}{Re}\right) \text{(Ref. 16)} \tag{6}$$

where ε is the tube wall relative roughness. This equation is solved by an iterative process described in Reference 7. For transitional flow (2000 < Re < 3800),

$$\frac{f_{TR} - f_L}{f_T - f_L} = \frac{Re - 2000}{3800 - 2000} \tag{7}$$

Panel Configurations and Thermal Models

Design considerations related to integration of the cooling system with the aircraft structure required that a baseline configuration and several modified configurations of the actively cooled panel be evaluated. Each configuration required that a thermal math model be constructed. In the following paragraphs, each configuration and its thermal model are described and pertinent information related to design evolution is presented.

Baseline Configuration. The baseline configuration of the actively cooled panel is a brazed sandwich structure consisting of aluminum alloy face sheets and corrugated core. The panel is 0.61 m (2 ft) wide by 6.1 m (20 ft) long. The face sheets are 0.81 mm (0.032 in.) thick. There are 215 coolant channels, 5.81 mm^2 (0.009 $in.^2$) with a 0.127 mm (0.005 in.) wall thickness running parallel to the panel length. A thermal model representative of one tube is adequate to determine longitudinal variations in fluid and panel temperature and to determine pressure drops. This configuration and its thermal model are illustrated in Figure 34.

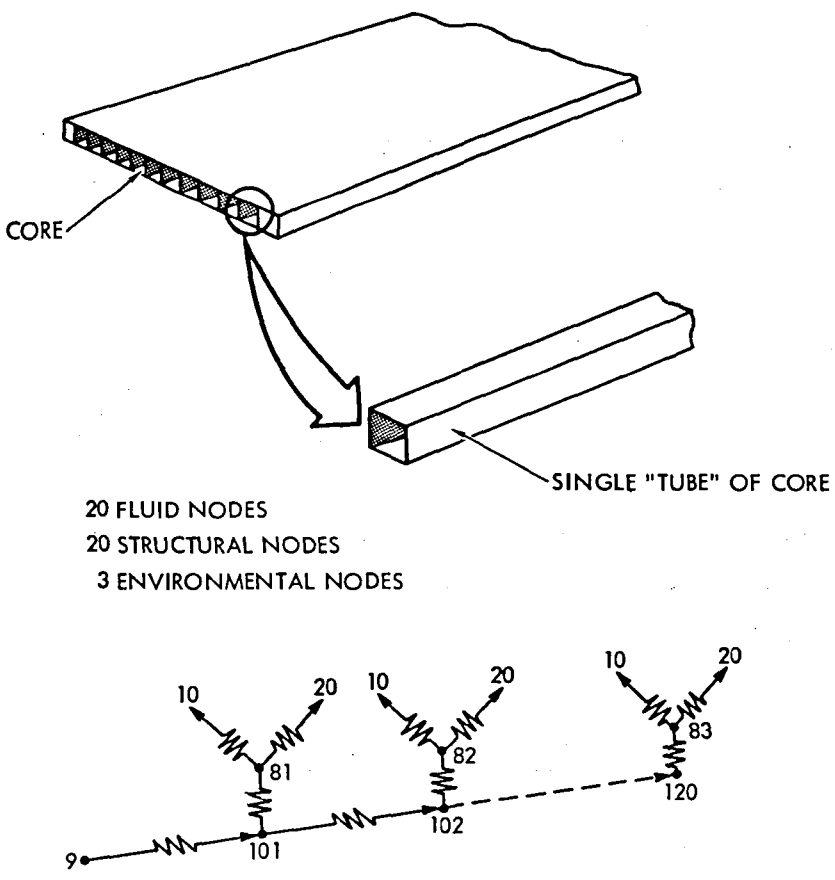

Figure 34. Baseline Thermal Model

The thermal model consists of 20 fluid nodes, 20 panel structure nodes, and 3 boundary nodes. The fluid nodes are 5.81 mm^2 (0.009 $in.^2$) by 30.5 cm (12 in.) long. The panel structure nodes are 2.5 mm (0.1 in.) wide, 30.5 cm (12 in.) long, and 0.81 mm (0.032 in.) thick aluminum alloy. The boundary nodes represent the specified inlet fluid temperature, the adiabatic wall temperature for aerodynamic heating, and a sink temperature radiation node. Adjacent fluid and panel structure nodes were connected by a convective conductance using the heat transfer coefficient discussed previously. Adjacent fluid nodes are connected by convective flow conductances. The structure nodes are connected to the environment by aerodynamic convection from the adiabatic wall temperature and by radiation to a sink temperature. Longitudinal conduction between structure nodes was neglected. This model was used for preliminary design thermal evaluation and for a special analysis to explain a panel temperature incompatibility that is discussed on page 77.

Modified Configurations. To provide for structural attachment of the panel to substructure frames, the baseline thermal configuration and model were modified to include an edge filler strip 19.05 mm (0.75 in.) wide on each side of the panel, as shown in Figure 35. For this modified configuration, the single tube of the baseline thermal model was replaced by a flow

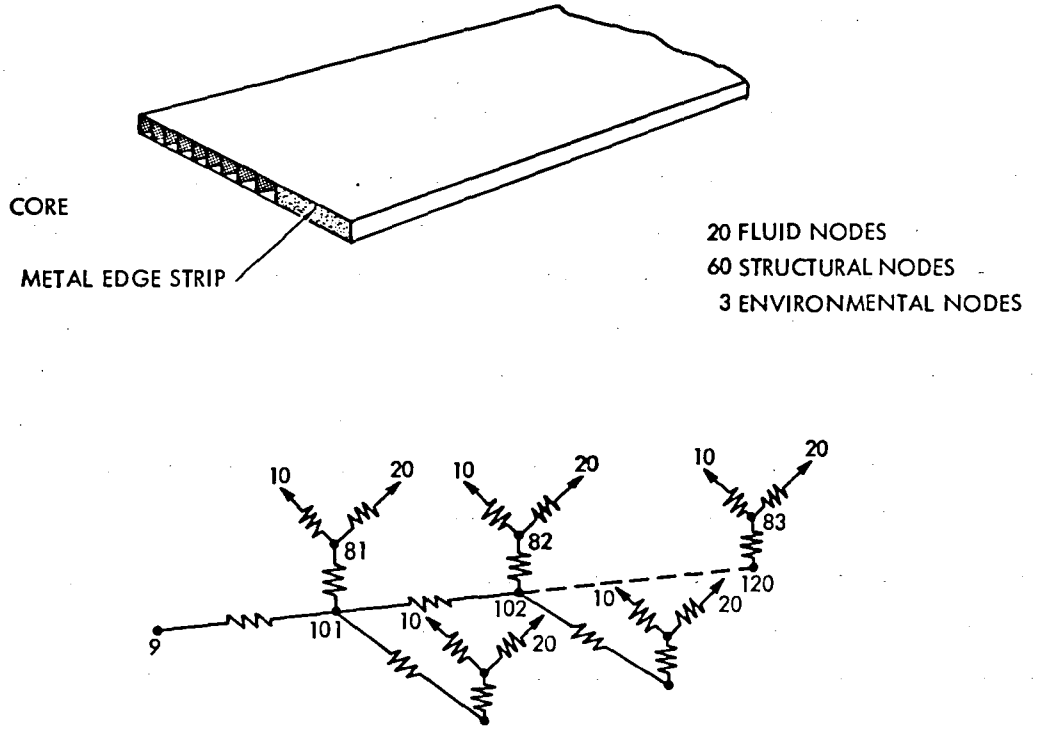

Figure 35. Initial Panel Edge Thermal Model

channel 16 tubes wide, and 40 structure nodes were added to account for edge heating effects. Twenty of the new nodes are located beneath the coolant channels at locations compatible with the fluid nodes. The other 20 nodes represent panel edge temperatures adjacent to the fluid nodes. The new structure nodes and the fluid nodes were connected by convective conductances. Adjacent panel and edge nodes were connected by conduction-type conductances. The edge nodes were connected to the environment by aerodynamic convection and by radiation. This uncooled strip is subject to the same aerodynamic heat flux as the main panel.

Analysis results for this model predicted panel edge structure temperatures above the 394 K (250°F) allowable for this area. Modifications were incorporated in the design to reduce the panel edge temperatures to acceptable levels. Initially, a conduction plate running the length of the panel, 6.04 cm (2.38 in.) wide and 1.52 mm (0.06 in.) thick, was added to the panel inboard face sheet. Its width extended from the panel edge beyond the first 16 coolant channels in the sandwich core. The purpose of this conduction plate was to draw heat from the solid panel edge and feed it via forced convection to the coolant in the core. The result was a reduction in panel edge temperature predictions but not below the maximum allowable value. The design was modified again by the addition of a coolant passage in the edge filler plate outside of the fastener line. This panel edge configuration and the resulting thermal model are shown in Figure 36.

The thermal model consists of two parallel flow channels and the uncooled strip between the flow channels. To facilitate conduction path modeling, nodes were defined for both the upper and lower panel surfaces adjacent to the flow channels. The panel upper surface nodes of both flow channels and the nodes representing the uncooled strip were connected to the environment by aerodynamic convection and by radiation. Both the upper and the lower surface nodes were connected to fluid nodes by convective conductances. The lower surface nodes were connected to the uncooled strip nodes by conduction-type conductances.

This thermal model was used to evaluate the edge cooling concept with and without the conduction plates discussed previously. Acceptable panel temperatures were obtained when the conduction plates were included.

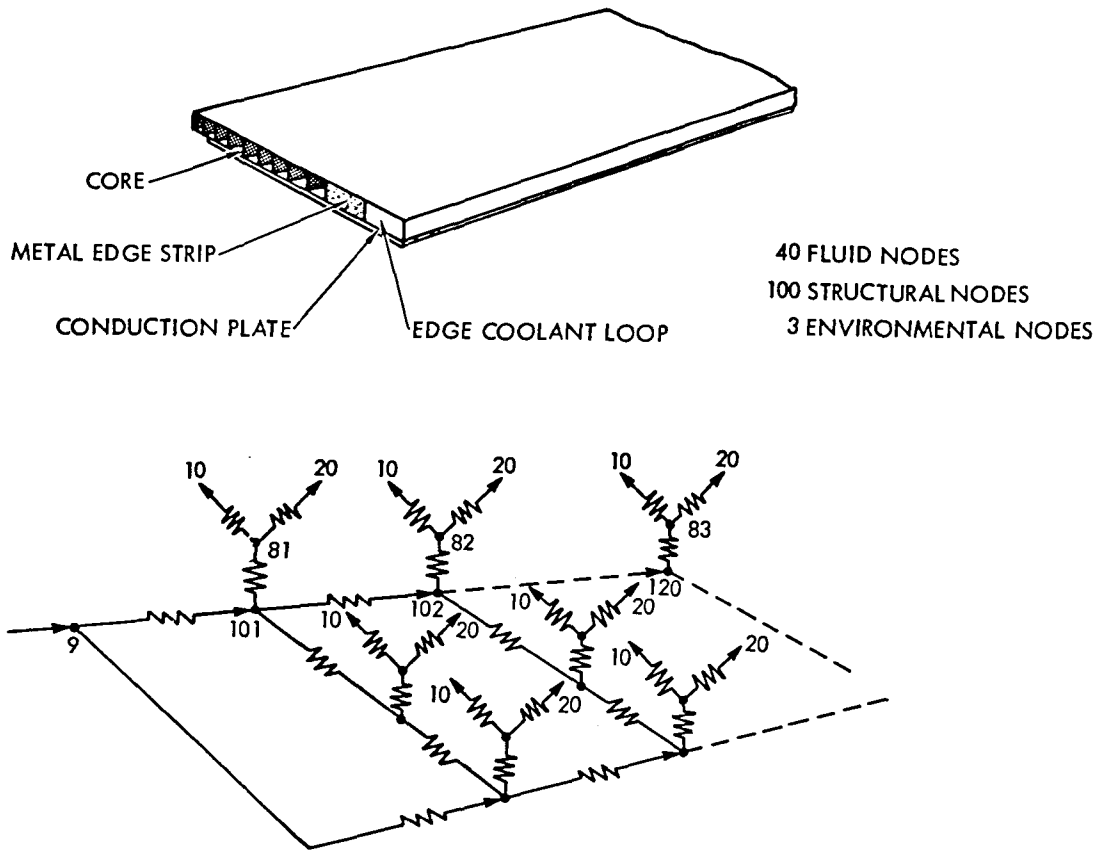

Figure 36. Modified Panel-Edge Thermal Model

Final Full-Scale Panel Thermal Model. The model described above and shown in Figure 36 was expanded so that it was representative of one-half the final full-scale panel width from core inlet to core outlet. A new set of fluid and panel surface nodes, together with the appropriate conductances, was added to represent the remaining width of the half-panel as shown in Figure 37. Three coolant channels in parallel were evaluated.

This model was used to perform parametric analysis for different inlet temperatures and flow rates, and provided the longitudinal and lateral temperature gradients used in the structural analyses.

Manifold Configuration. The thermal and fluid flow characteristics of the inlet and outlet manifold and of the panel in the vicinity of the end fastener attachment were determined separately from the main panel characteristics. The configuration of the end panel and its thermal model are illustrated in Figure 38. One half of the end panel is represented by 25 nodes together with appropriate conductive, convective, and radiative conductances.

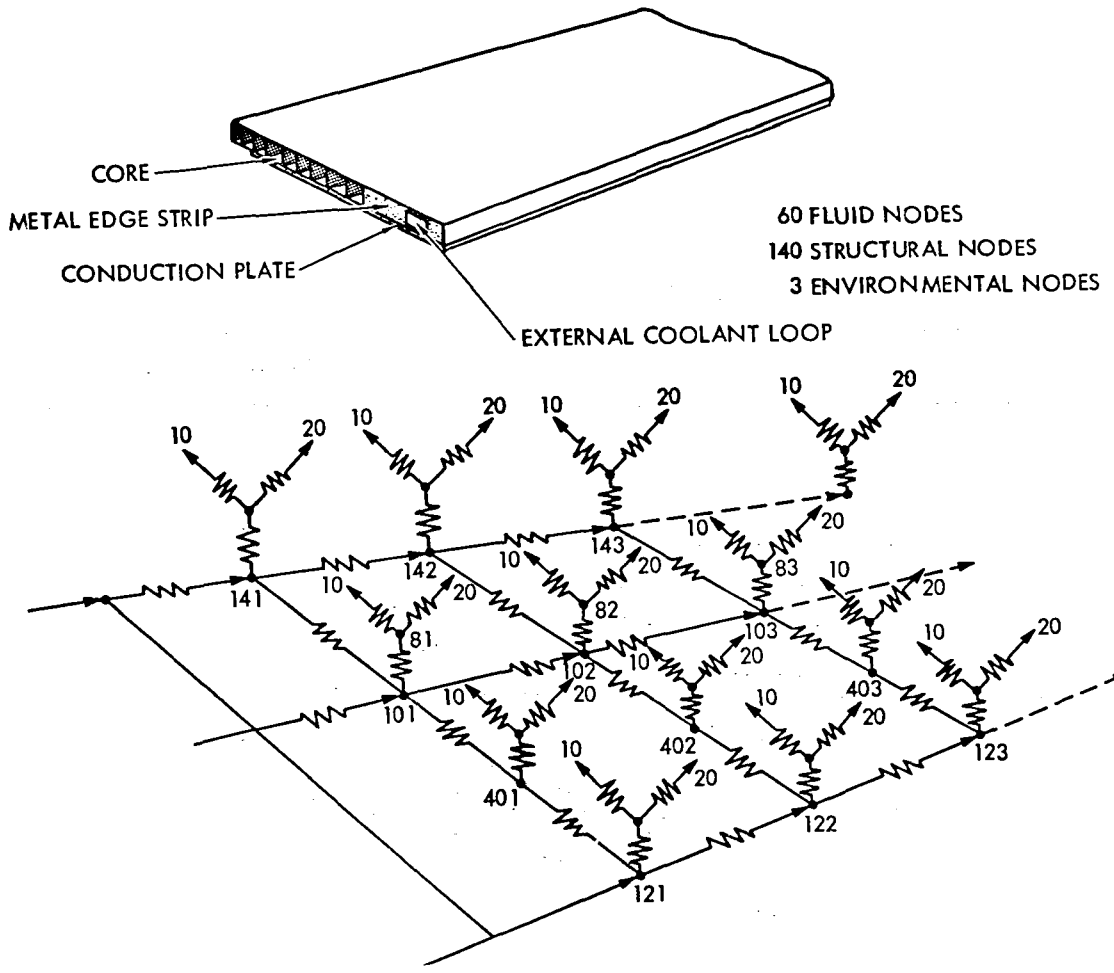

Figure 37. Final Full-Scale Panel Thermal Model

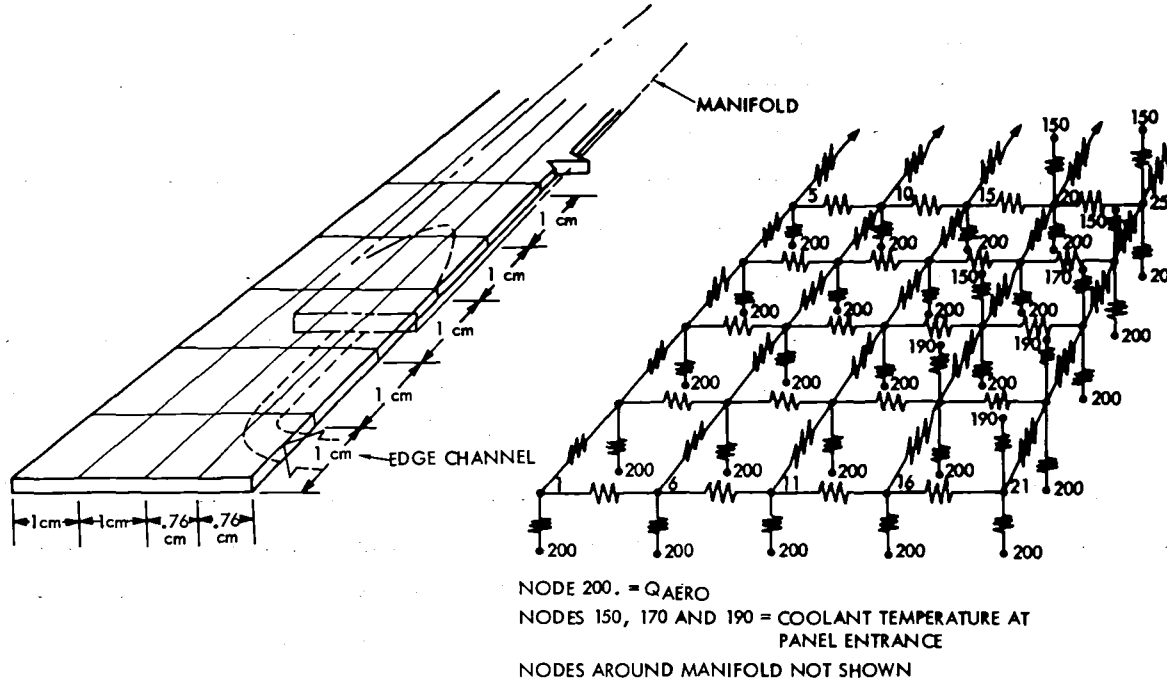

Figure 38. Panel End Thermal Model

Thermal and Fluid Flow Analysis Results

The following paragraphs present results of the analyses conducted on the pertinent thermal models described above.

Baseline Configuration. An example of predicted longitudinal temperature distributions for the baseline (single tube) configuration are presented in Figure 39. The results are for a coolant tube inlet temperature of 283.3 K (50°F) and a flow rate of 205 kg/hr (93 lbm/hr). As shown, a sharp change in structure temperature occurs near midpanel. This temperature rises from 338.9 K (150°F) near the inlet to a maximum of 466.6 K (380°F) approximately 372.2 K (210°F) and remains nearly constant over the remaining tube length. The coolant temperature, on the other hand, rises uniformly from inlet to exit. For the constant heat flux conditions imposed on the panel, a continuous temperature rise for both the coolant and structure was expected. Therefore, an investigation was undertaken to determine the cause of the sharp temperature drop and to determine if it could be eliminated by a proper combination of flow rate and inlet temperature.

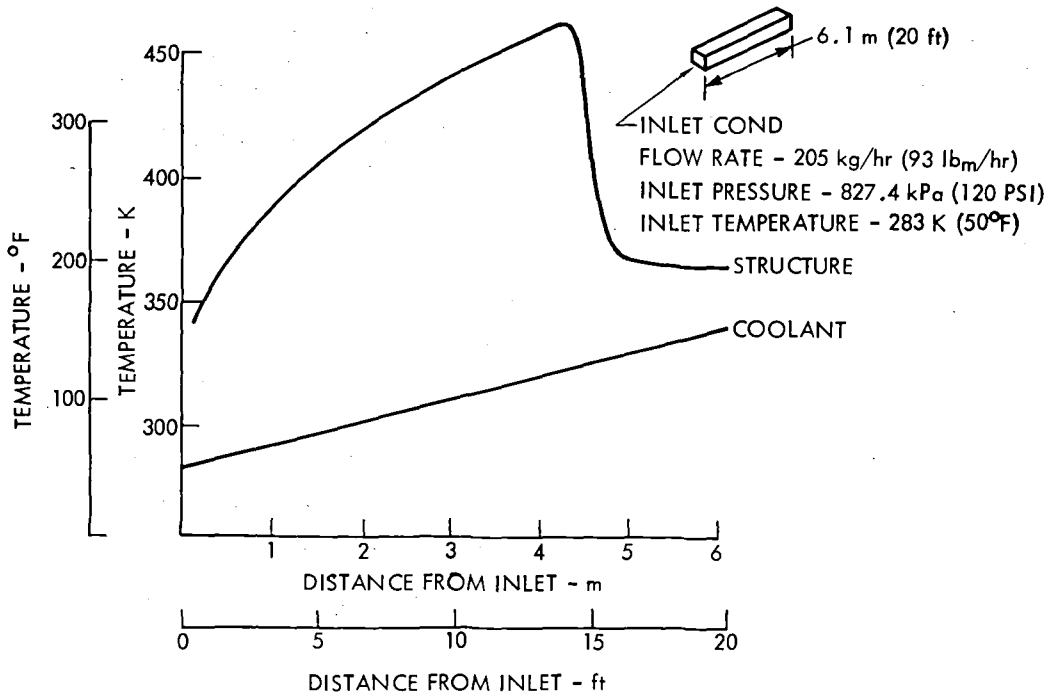

Figure 39. Baseline Model Typical Results

A review of coolant property data (reference Appendix A) shows that coolant viscosity decreases significantly over the temperature range of interest. For the inlet temperature of 283.3 K (50°F), the viscosity is 8.27×10^{-3} Pa•s (20 lbm/ft-hr), while it is 1.48×10^{-3} Pa•s (3.6 lbm/ft-hr) at the exit temperature of 338.5 K (150°F). As a result, the flow Reynolds number for the given flow rate increases from approximately 600 at the tube inlet to approximately 3100 at the tube exit. A change in tube flow regime from laminar to transitional occurs at a flow Reynolds number of 2100. Correspondingly, a significant change in film conductance occurs at this Reynolds number. Hence the panel structure temperature drop is due to a change from laminar to transitional flow within the coolant tubes. This point is illustrated in Figure 40.

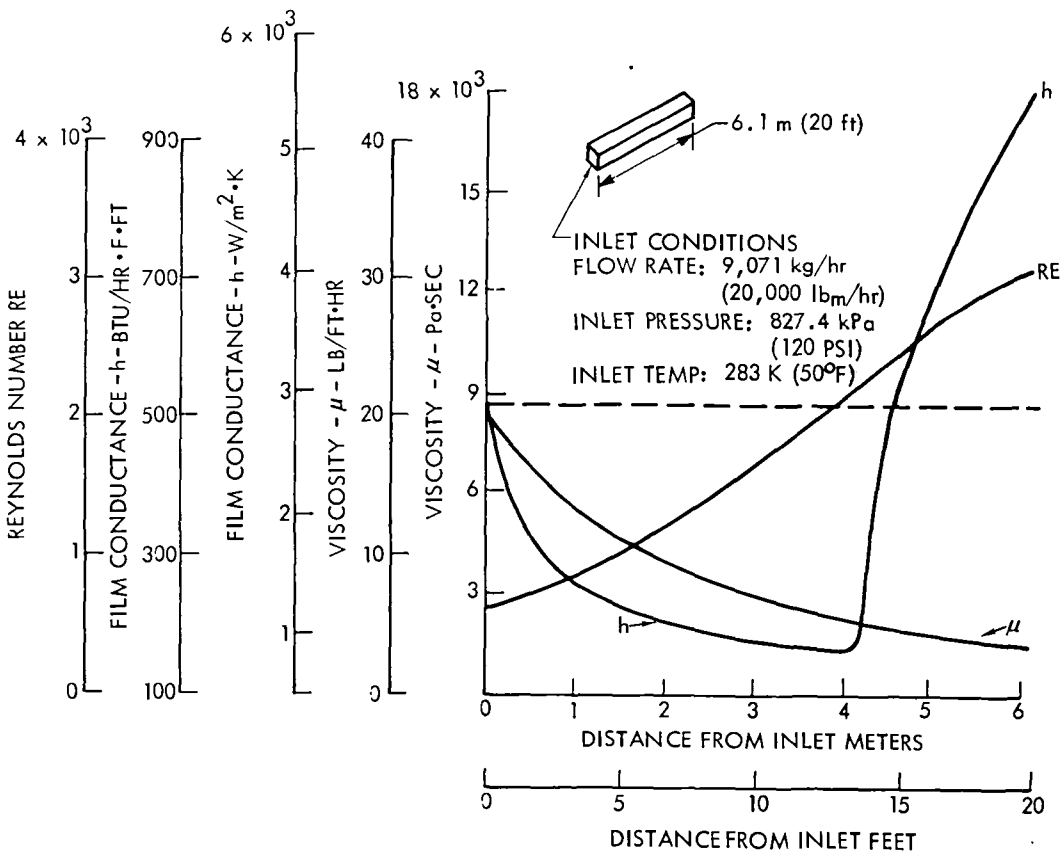

Figure 40. Viscosity, Film Conductance and Reynolds Number as a Function of Coolant Tube Length

As indicated in Figure 41, elimination of this radical structure temperature drop would require that the coolant remain in the laminar regime ($Re < 2100$) or in the turbulent regime ($Re > 10{,}000$) during its transfer from panel inlet to outlet. Laminar flow can be achieved only if the coolant outlet temperature is kept below approximately 320 K (117°F) in combination with a flow rate of less than 10,000 kg/hr (22,046 lbm/hr). This condition, however, is not achievable for a design heat flux of 136.10 kW/m^2 (12 Btu/ft·s) and a maximum structure temperature of 394 K (250°F). Either the flow rate must be increased or the allowable coolant outlet temperature set at a higher value. The all-turbulent condition requires extremely high flow rates, which results in unnecessarily high APS mass penalties. In summary, this analysis led to the conclusion that the structure temperature shift must be accepted if the panel design requirements were to be met and system mass kept to a reasonable minimum.

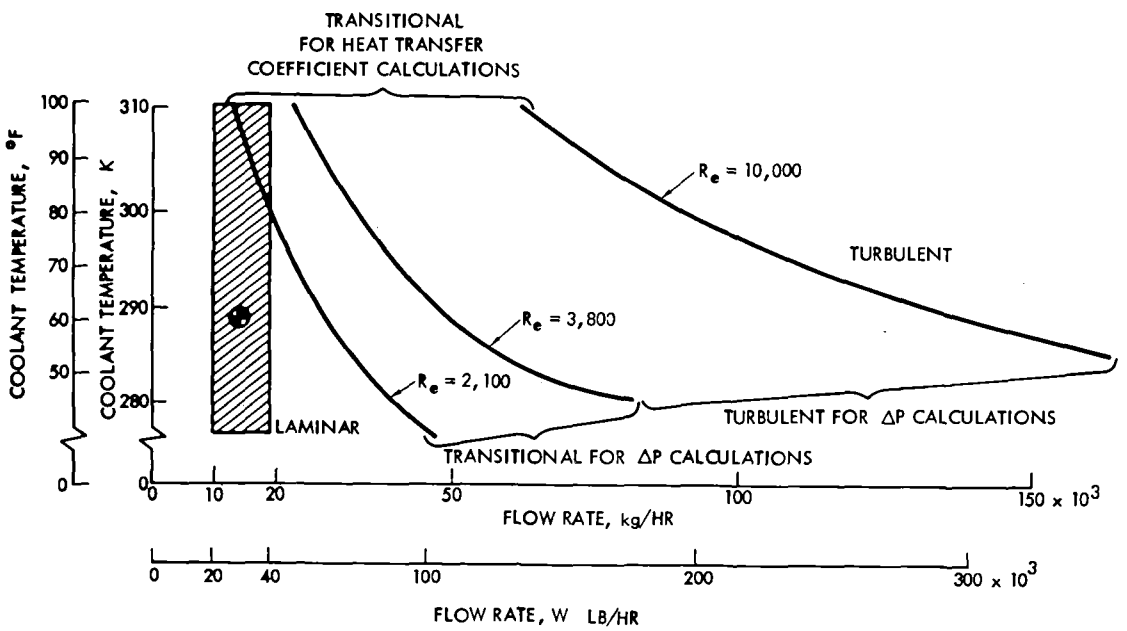

Figure 41. Flow Regime as a Function of Flow Rate and Coolant Temperature

Final Full-Scale Panel Configuration. Using the final panel configuration and its thermal model, parametric studies were run for a range of coolant inlet conditions. This was done to select a design inlet condition that would

meet the design requirements while being sensitive to the design goal of minimum mass. Coolant inlet conditions affect system mass in that they are directly related to APS mass penalties as follows:

$$APS = \frac{G \dot{W} \Delta P \theta}{\rho} \tag{8}$$

The range of coolant flow rates and inlet temperatures used in this study are indicated by the shaded portion of Figure 41. Parametric study results are tabulated in Table 5. From these data, a full-scale panel design coolant inlet

Table 5. Panel Temperature and Pressure Drop Results for Variable Coolant Inlet Conditions

INLET COOLANT TEMPERATURE K (°F)		MAXIMUM STRUCTURE TEMPERATURE K (°F)		MAXIMUM COOLANT TEMPERATURE K (°F)		PRESSURE DROP KPa (PSI)		APS PENALTY (1) Kg (LB)		
9,078 Kg/HR (20,000 LB/HR)										
277.8	(40)	402.2	(264)	373.9	(213)	283	(41)	0.92	(2.03)	
283.3	(50)	406.6	(272)	379.4	(223)	241	(35)	0.78	(1.73)	
288.9	(60)	411.1	(280)	386.1	(235)	214	(31)	0.70	(1.54)	
300.0	(80)	421.1	(298)	400.0	(260)	186	(27)	0.60	(1.34)	
311.1	(100)	430.5	(315)	411.1	(280)	172	(25)	0.56	(1.20)	
11,348 Kg/HR (25,000 LB/HR)										
277.8	(40)	390.5	(243)	365.0	(197)	400	(58)	1.63	(3.59)	
283.3	(50)	395.5	(252)	371.7	(209)	338	(49)	1.38	(3.04)	
288.9	(60)	399.4	(259)	376.6	(218)	297	(43)	1.20	(2.67)	
300.0	(80)	409.4	(277)	388.9	(240)	262	(38)	1.06	(2.35)	
311.1	(100)	417.2	(291)	397.2	(255)	255	(37)	1.04	(2.29)	
13,617 Kg/HR (30,000 LB/HR)										
277.8	(40)	378.3	(221)	350.5	(171)	538	(78)	2.64	(5.80)	
283.3	(50)	382.2	(228)	356.1	(181)	448	(65)	2.19	(4.83)	
288.9	(60)	386.1	(235)	361.6	(191)	407	(59)	1.99	(4.38)	(2)
300.0	(80)	394.4	(250)	371.7	(209)	228	(53)	1.78	(3.94)	
311.1	(100)	403.3	(266)	380.5	(225)	379	(55)	1.85	(4.08)	
15,886 Kg/HR (35,000 LB/HR)										
277.8	(40)	372.2	(210)	345.0	(161)	662	(96)	3.77	(8.32)	
283.3	(50)	375.5	(216)	348.9	(168)	572	(83)	3.26	(7.12)	
288.9	(60)	380.0	(224)	355.5	(180)	517	(75)	2.95	(6.25)	
300.0	(80)	388.9	(240)	366.1	(199)	497	(72)	2.83	(6.24)	
311.1	(100)	397.8	(256)	375.5	(216)	524	(76)	2.99	(6.58)	
18,156 Kg/HR (40,000 LB/HR)										
277.8	(40)	364.4	(196)	336.1	(145)	807	(117)	5.26	(11.59)	
283.3	(50)	370.0	(206)	343.9	(159)	711	(103)	4.63	(10.20)	
288.9	(60)	374.4	(214)	350.0	(170)	655	(95)	4.21	(9.41)	
300.0	(80)	381.6	(227)	191.6	(185)	676	(98)	4.41	(9.71)	
311.1	(100)	390.5	(243)	367.2	(201)	703	(102)	4.58	(10.10)	

(1) BASED ON AN APS MASS PENALTY CONVERSION FACTOR (G) EQUAL TO 0.34 G/kW•S (2 LBm/Hp-HR)
(2) SELECTED COOLANT INLET CONDITION

condition of 13,607 kg/hr (30,000 lbm/hr) flow rate and 288.5 K (60°F) inlet temperature was selected. The inlet pressure was set at 827.4 kPa (120 psi). This is consistent with: a predicted pressure drop from core inlet to core outlet of 406.8 kPa (59 psi); an inlet and outlet manifold total pressure drop of 57.92 kPa (8.4 psi) (refer to Table 5); and a minimum outlet pressure requirement of 344.7 kPa (50 psi). The APS mass penalty is 1.99 kg (4.38 lbm), which is among the lowest values obtained for inlet conditions that meet the maximum temperature criteria for both structure and coolant.

Predicted temperature distributions for the selected coolant inlet conditions as a function of panel length are presented in Figure 42. Location (1) represents the uncooled fastener strip. The predictions show a steady temperature rise from 347.2 K (165°F) at the panel inlet to a maximum of 386.1 K 235°F) at the core exit for this location. Locations (4), (7), and (8) reflect the coolant temperatures in the edge coolant channel, channels over

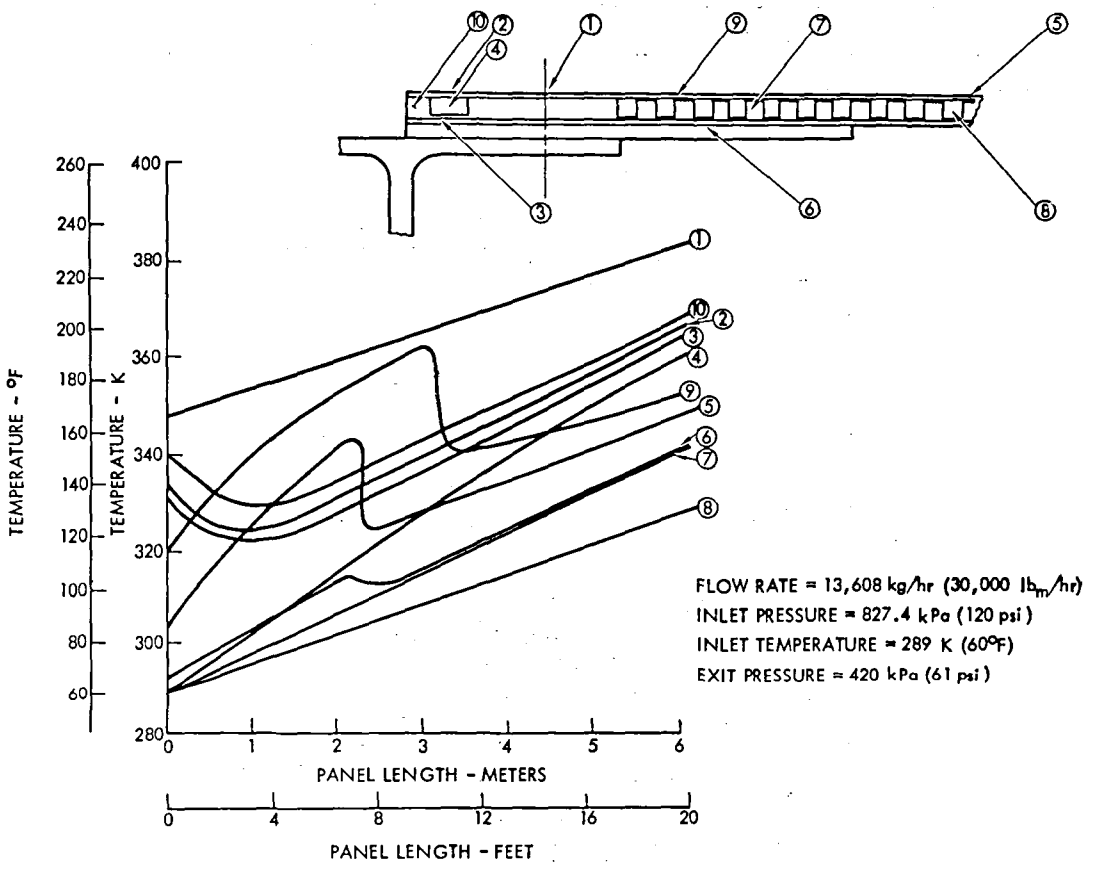

Figure 42. Predicted Panel Temperature Distribution for Selected Coolant Inlet Condition

the conduction plate, and center panel coolant channels, respectively. These temperatures show a uniform temperature rise from inlet to outlet. The coolant in the edge cooling channel experiences the largest temperature rise and the conduction plate flow channels have the next largest temperature rise, as would be expected due to their close proximity to the edge filler strip. Locations (2), (9), and (5) refer to panel structure temperatures adjacent to the coolant temperatures in locations (4), (7), and (8), respectively. Locations (3) and (6) refer to conduction plate temperatures. The temperature distributions for this design condition were used in the stress analysis discussed later in this appendix.

Figures 43, 44, and 45 are presented to show the impact that variations in coolant inlet temperatures between 233 K (50°F) and 311 K (100°F), at a constant flow rate, have on panel temperature distributions. Three inlet temperature-related effects can be noted. First, panel structure temperature level increases with increasing coolant inlet temperature. Second, the location of the flow transition from fully developed laminar flow to laminar/turbulent transition flow shifts with coolant inlet temperature. For the

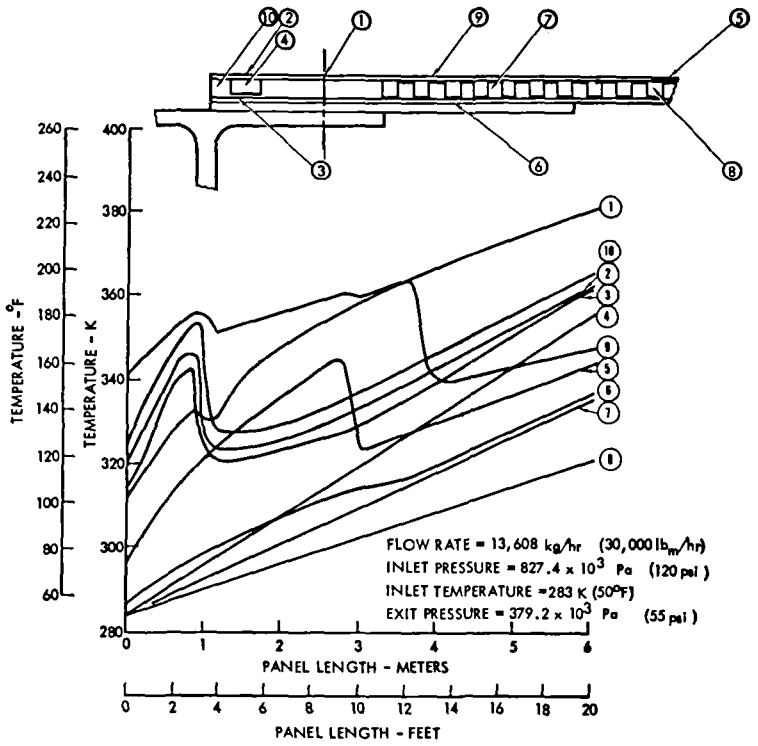

Figure 43. Panel Temperature Distribution for 283 K (50°F) Inlet Temperature and 13,608 kg/hr (30,000 lbm/hr) Flow Rate

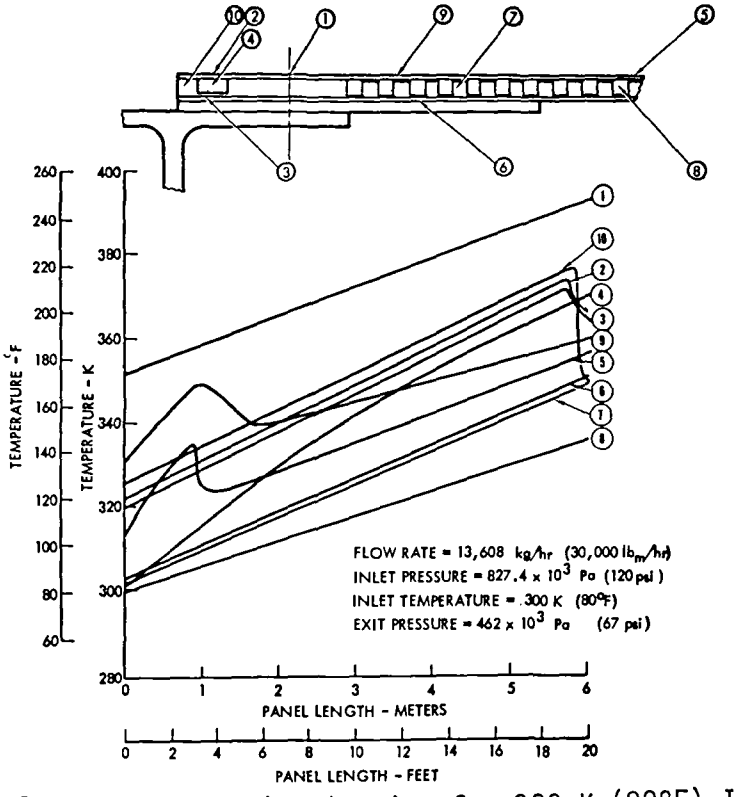

Figure 44. Panel Temperature Distribution for 300 K (80°F) Inlet Temperature and 13,608 kg/hr (30,000 lbm/hr) Flow Rate

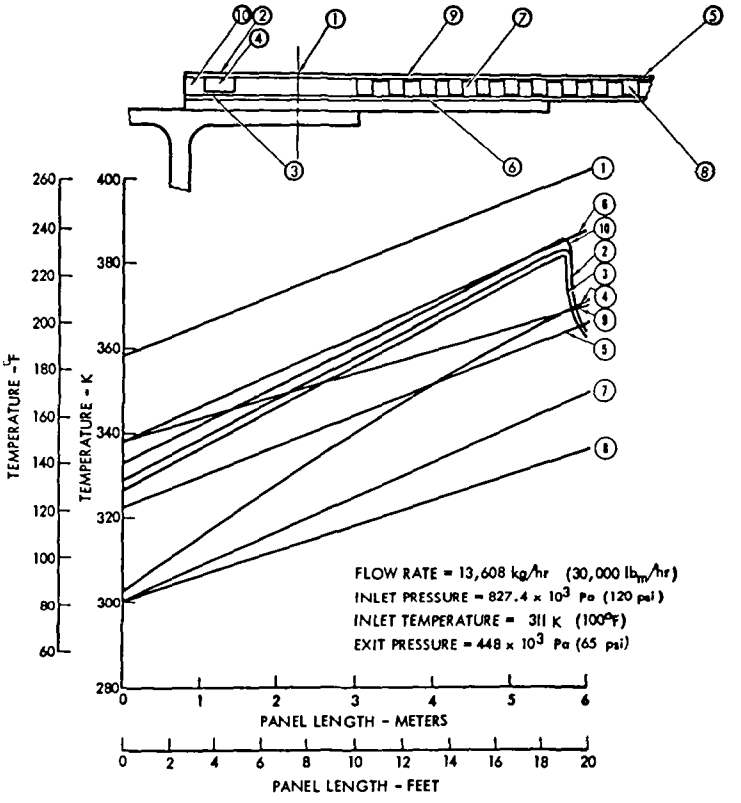

Figure 45. Panel Temperature Distribution for 311 K (100°F) Inlet Temperature and 13,608 kg/hr (30,000 lbm/hr) Flow Rate

design condition, the flow transition occurs approximately 2.25 m (7.5 ft) from the tube inlet. As coolant temperature is increased, the distance from inlet to transition decreases until no transition occurs for coolant temperatures greater than 311.1 K (100°F); and, finally, the peak structure temperature prior to transition decreases with increasing coolant inlet temperature. These trends may be useful when evaluating test data.

The effect of different coolant flow rates on panel temperature distributions for the design coolant inlet temperature can be observed by comparing Figure 46 with Figure 42. Figure 46 presents longitudinal temperature distributions for ten selected locations across the panel for design coolant temperature of 288.9 K (60°F) and for a coolant flow rate of 11,340 kg/hr (25,000 lb/hr). Three coolant flow rate effects should be noted. First, panel structure temperatures decrease with increasing coolant flow rate. For the examples shown, panel structure temperature, (5), near the panel exit is decreased from 358.3 K (185°F) to 347.2 K (165°F) as coolant flow rate is increased from 11,340 kg/hr (25,000 lb/hr) to 13,617 kg/hr (30,000 lb/hr). Second, the peak

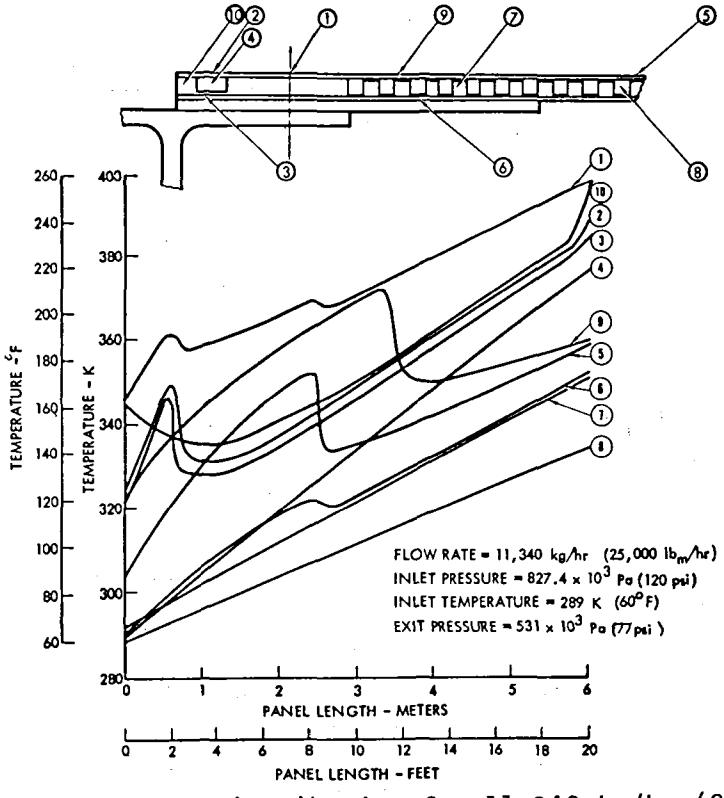

Figure 46. Panel Temperature Distribution for 11,340 kg/hr (25,000 lbm/hr) Flow Rate and 289 K (60°F) Inlet Temperature

panel structure temperature prior to flow transition from laminar to transitional is reduced as coolant flow rate is increased. Third, the distance from panel inlet to the transition point is reduced as flow rate is increased. These results are a natural consequence of the increased heat transfer capability of fluids as flow rate is increased. These trends also will be useful in evaluating test data.

Manifold Configuration. Predicted temperature distributions in the panel structure surrounding the entrance and exit manifolds are presented in Figure 47. A maximum panel structure temperature of 414.4 K (286°F) is predicted for the corners of the panel near the outlet manifold for the selected final design coolant inlet conditions.

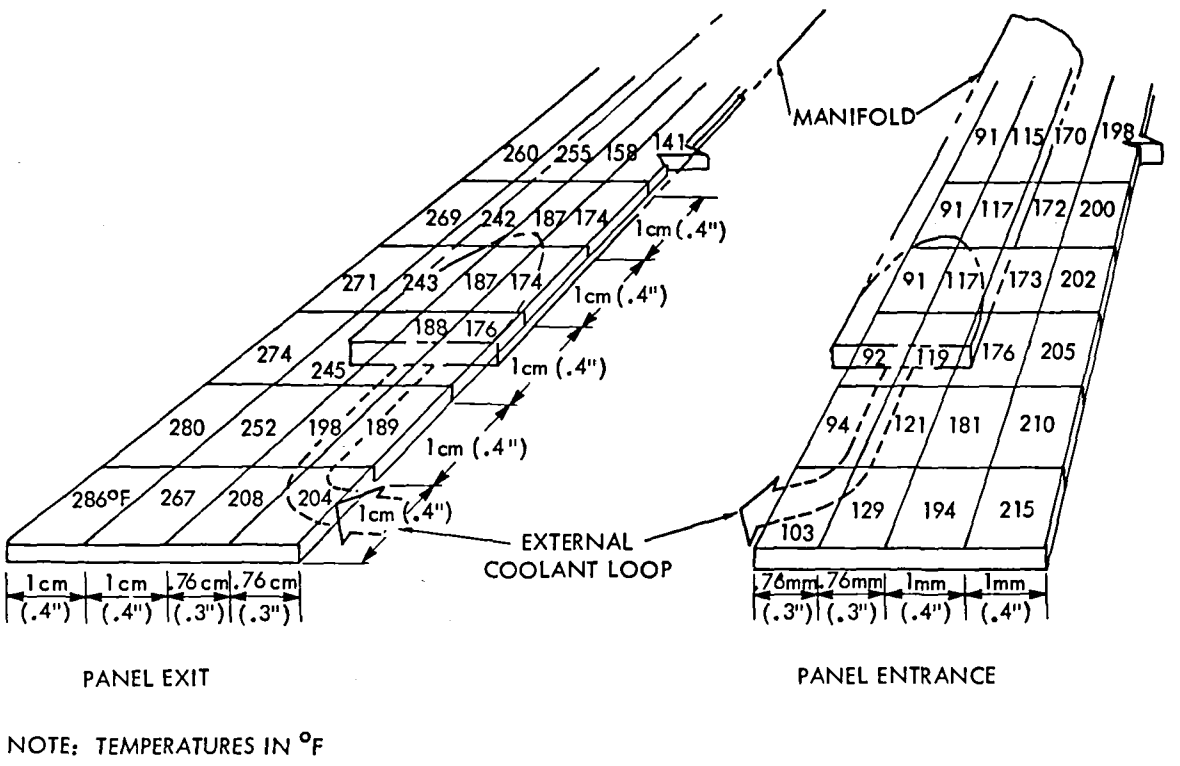

Figure 47. Panel End Temperature Distributions for Design Coolant Inlet Condition

The predicted pressure drop from the entrance of the manifold to the entrance of the coolant tubes is 28.96 kPa (4.2 psi) for the design case. The inlet/exit manifold component pressure losses were calculated using the following equation:

$$\Delta P = \rho_V \left(\frac{\rho V^2}{2\ g} \right) \qquad (9)$$

The component pressure losses are summarized in Table 6. The exit manifold will have a pressure loss similar to that of the entrance manifold. Hence, the anticipated total system pressure drop will be approximately 28.96 kPa (4.2 psi) (inlet) + 406 kPa (59 psi) (core) + 28.96 kPa (4.2 psi) (outlet) = 464.73 kPa (68.4 psi). The predicted outlet pressure is 356 kPa (51.6 psi).

Table 6. Inlet/Outlet Manifold Pressure Drop

Component	Loss Factor, ρ_V	Pressure Drop, ΔP	
		kPa	(psi)
90-degree bend	0.8	8.96	(1.3)
Flow expansion	0.3	2.76	(0.4)
Turn into manifold	0.8	4.14	(0.6)
Oval holes	3.2	2.76	(0.4)
90-degree turn into panel	0.9	3.45	(0.5)
Friction in manifold	Est.	3.45	(0.5)
Stagnation flow effects	Est.	3.45	(0.5)
Total/manifold		28.96	(4.2)

The results of a manifold sizing analysis for the design condition are presented in Figure 48. The total mass is the sum of the tube mass, coolant

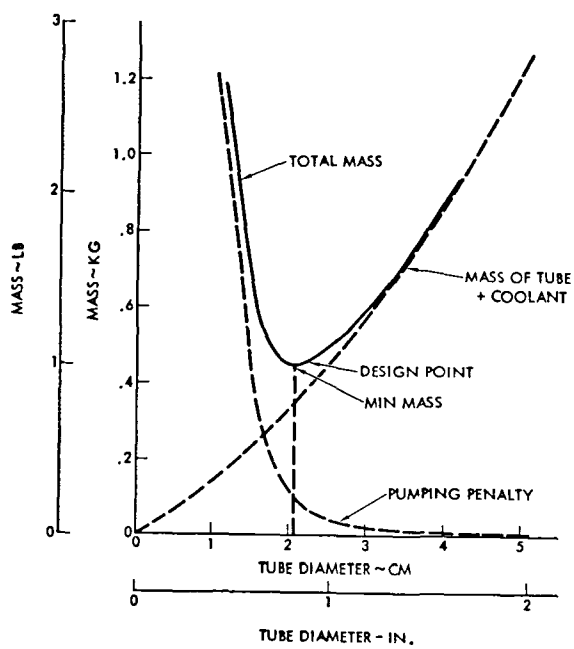

Figure 48. Manifold Sizing Results

mass, and additional mass due to APS mass penalties. The calculation of additional mass due to APS assumed a value of G = 0.84 g/kW•s (5 lbm/hp-hr) and turbulent flow in rough tubes. The minimum total mass of 0.45 kg (1.0 lb) is obtained for a tube diameter of 2.05 cm. A design point of 2.2 cm (0.88 in.) was selected. Note that after this design was completed, the value of G was reduced to 0.34 g/kW•s (2 lbm/hp-hr) at NASA's request. The manifold design was not updated to incorporate the new conversion factor. All other calculations of APS mass penalties do reflect use of the lower value [i.e., 0.34 g/kW•s 2 lbm/hp•hr)].

Structural Analysis

This section of Appendix B presents the structural analysis of the full-scale actively cooled structural panel configuration. The stress analysis calculates the minimum margins of safety of the structural panel for the design load conditions. It was the intent of this analysis to provide analytical substantiation that the panel design meets the specified structural design criteria, and is a minimum-weight design. The design load criteria which are representative of loads and environments of skin panel structure on hypersonic transport aircraft were provided by NASA.

The stress analysis was developed using a computer-programmed finite element technique. The program used for structural analysis was the NASA-developed NASTRAN program (Reference 11). A three-dimensional structural model with 2214 degrees of freedom was developed in NASTRAN, representing the entire 0.61-m (2.0-ft) by 6.1-m (20-ft) panel. The model includes the sandwich panel, stringers, and the intermediate and main frames to which the panel is attached. Because of the length of the panel, the model was divided into five equal sections for CRT output. Each section represents two frame bays along the length of the panel. A description of the model using a CRT plot showing the element numbering system is depicted in Figure 49. One of the individual sections (0.6096 m × 1.2192 m) is shown in Figure 50. In the model, the sandwich panel is divided into 15.24 cm (6 in.) long by 7.62 cm (3.0 in.) wide elements for which sandwich plate bending elements are used. Beam elements are used to represent the frames and stringers; these are connected to the appropriate panel node points. This model was used to determine the internal loads and stress distributions, nodal forces, and nodal deflections for all applied load

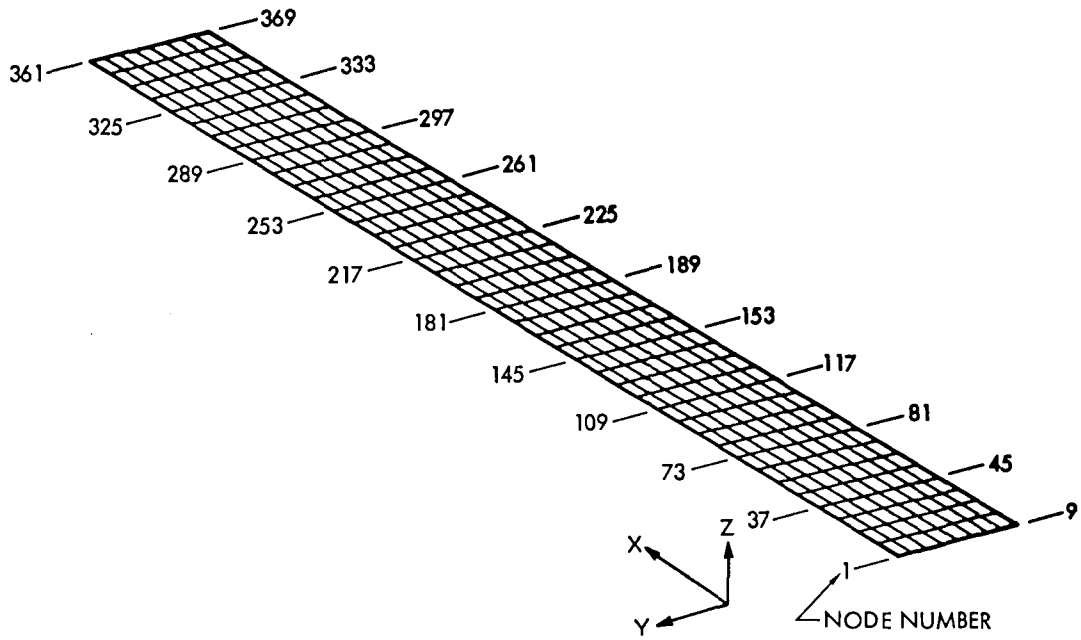

Figure 49. Structural Model—Actively Cooled Structural Panel

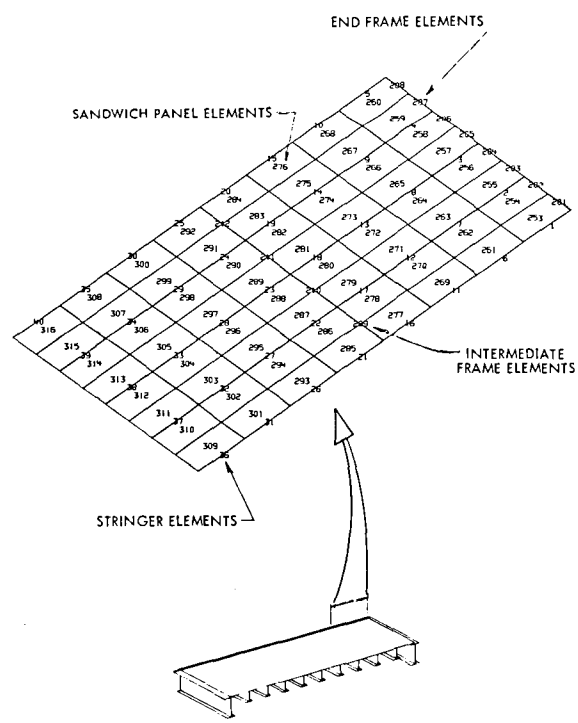

Figure 50. CRT Plot of a Section of the NASTRAN Structural Model

and thermal load conditions. The development of a model representing the entire panel and associated substructure was chosen in order to evaluate the thermal stresses resulting from the non-symmetrical temperature distributions.

Initial member sizing for the structural model was based on buckling criteria for the panel and stringers and general stability for the intermediate frames. The end frames are not part of the panel design, but must be included in the analysis. Therefore, they are sized to be typical of aircraft main frames. Point loads derived from the specified limit uniaxial in-plane distributed load of ±210K N/m (1200 lb/in.) and lateral pressure of ±6.9 kPa (1.0 psi), and the calculated structural temperature distributions presented earlier in this appendix (refer to Figure 42), were applied to the NASTRAN structural model (Figure 49), assuming statically determinate load paths. Member loads from this preliminary solution were used to make detailed stress and buckling calculations, resulting in revised member sizing. The resulting member sizes and stiffnesses were then used to revise the structural model. The load conditions were run on the revised model, using the NASTRAN program, to determine internal load distributions and element stresses which were used to verify that the panel design meets the strength, stability, fatigue, thermal life, and fracture control criteria.

Because of the main frame attachment at each end of the panel, the in-plane loads are applied eccentrically by 0.62 mm (0.024 in.) with respect to the panel/stringer assembly neutral axis. The interaction of this in-plane load eccentricity and the lateral pressure was included in the load conditions run for internal load distributions and stresses. Imperfect fabrication was not included for the following reasons: (1) precise definition of the as-fabricated flatness of 6.096-m-long brazed sandwich panels does not exist; and (2) a check of the equivalent-eccentricity parameter (Ø) from Reference 9 indicates that the effect of imperfect fabrication, based on a reasonably assumed flatness tolerance of 0.79 mm (0.31 in.), is small.

The resulting internal loads and stresses were then used to perform panel buckling and detail stress analyses. Panel buckling checks were made at three levels in order to assure the compressive load-carrying capability of the actively cooled panel. These levels were: (1) general instability with the entire panel assembly between frames acting as a stiffened plate; (2) panel/

stringer column stability with each stringer and the associated effective sandwich panel width acting as a Euler column between frames; and (3) local stability where stringers, flanges, and face sheet elements are checked for crippling, lateral stability, and inter-fastener buckling. In order to reinforce the panel general stability and the panel/stringer column analyses, the sandwich panel sections between stringers and frames were checked for buckling as composite plates. Section models for the panel stability and column analyses are shown in Figure 51. The panel stability and column

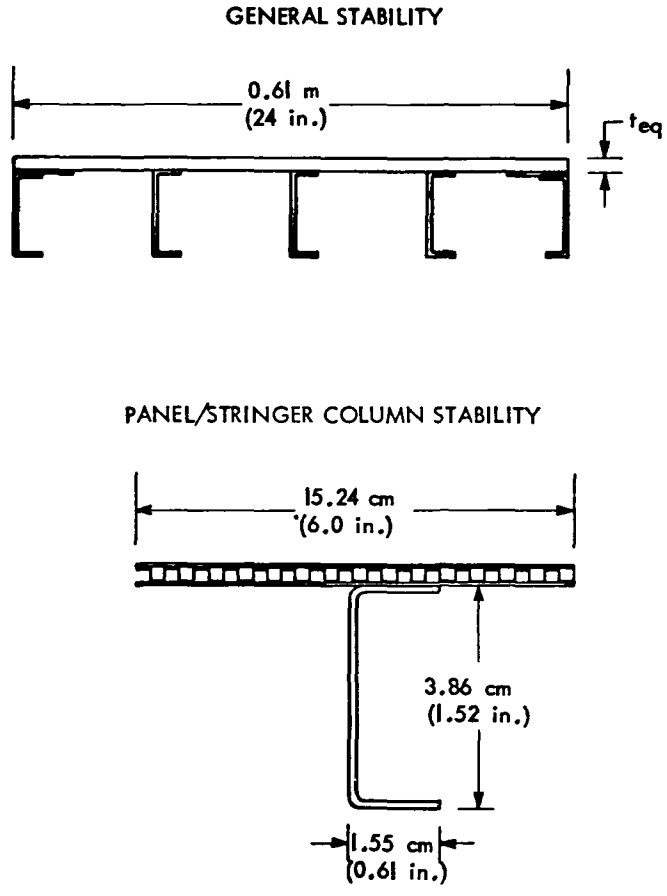

Figure 51. Section Models for Panel Stability and Column Analyses

analyses were conducted assuming simply supported panel edges and pinned column ends in order to be conservative. The resulting margins of safety are presented in Table 7.

Table 7. Full-Scale Panel Structural Margins of Safety

NUMBER	TYPE OF LOADING	ULTIMATE APPLIED LOAD OR STRESS	ULTIMATE FAILURE LOAD OR STRESS	M. S.
1	PANEL GENERAL ULTIMATE TENSILE STRESS	154.4 MPa (22,387 PSI)	207.5 MPa (30,100 PSI)	+0.344
2	ULTIMATE COMP LOAD (GENERAL BUCKLING)	318.7 KN/M (1,820 LB_f/IN.)	432 KN/M (2,467 LB_f/IN.)	+0.355
3	STRINGER PLUS EFF SKIN COLUMN BUCKLING	106.6 MPa (15,457 PSI)	159.8 MPa (23,178 PSI)	+0.50
4	LOCAL BUCKLING OF PANEL BETWEEN EDGE AND INTERMEDIATE STRINGERS	131.8 MPa (19,011 PSI)	155.9 MPa (22,612 PSI)	+0.189
5	LOCAL BUCKLING OF PANEL BETWEEN INTER-MEDIATE STRINGERS	106.6 MPa (15,457 PSI)	169.8 MPa (24,628 PSI)	+0.593
6	INTER-RIVET BUCKLING AT MANIFOLD	151.6 MPa (21,984 PSI)	177 MPa (25,673 PSI)	+0.168
7	MAXIMUM TENSION AT PANEL TO MAIN FRAME FASTENER HOLES	169.9 MPa (24,640 PSI)	207.5 MPa (30,000 PSI)	+0.22
8	BEARING - PANEL TO MAIN FRAME FASTENERS	280.2 MPa (40,636 PSI)	331.1 MPa (48,024 PSI)	+0.18

The critical panel area, with respect to inter-fastener buckling, is the span across the inlet and outlet manifolds at each end of the panel. This section is shown in Figure 52. The 5.33 cm (2.10 in.) fastener spacing is the

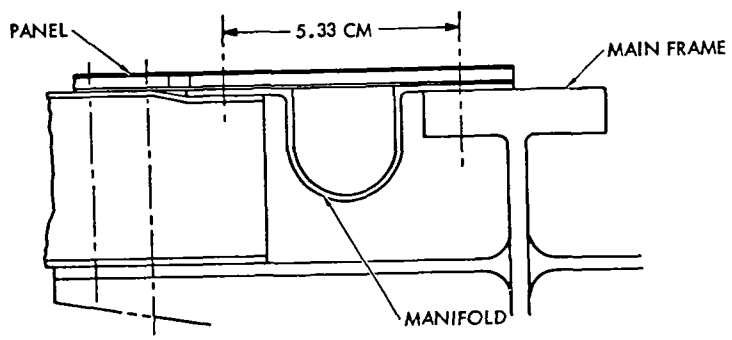

Figure 52. Fastener Spacing at Inlet/Outlet Manifolds

largest unsupported fastener spacing on the panel design. The sandwich panel was checked for inter-fastener buckling, using this dimension, and the resulting margin of safety also is given in Table 7.

The frame analysis was concerned with two types of frames—main frames at each end of the panel, and intermediate frames spaced along the length of the panel on 0.61-m centers. The main frames were sized to be typical of the lightest main frames of a large transport aircraft. They are not part of the panel design, but are included in the analysis to provide realistic boundary conditions. Loads and stresses in the main frames, resulting from the panel load conditions, are very small and would not represent critical frame design conditions in an actual aircraft by themselves. The intermediate frames are sized to have sufficient stiffness to force node points in the panel and thereby preclude failure of the entire panel by general instability. This sizing represents the minimum requirement for aircraft frames that are not subjected to significant externally applied loads. Also, the use of minimum-weight frames is a conservative assumption for the panel analysis. The resulting frame moment-of-inertia requirement is 1097 cm^4 (26.35 $in.^4$) which can be compared to the actual frame design moment of inertia of 1204 cm^4 (28.92 $in.^4$). Like the main frames, loads and stresses in the intermediate frames resulting from the panel load conditions are very small.

One particular area where detail stress analysis resulted in a design impact was in setting the thickness of the sandwich panel face sheets. Panel sizing based on buckling analyses indicated face sheet thickness of 0.51 mm (0.020 in.) was adequate and could support the coolant inlet pressure between core fins. However, when the final design incorporated core cut-outs around internal hardspots, it was determined that the 0.51-mm (0.020-in.) face sheets in these localized areas could not withstand the combination of axial and pressure loads without yielding. The critical area is at the attachment of the panel to the intermediate frames. This area along with a load/stress diagram is shown on Figure 53. The unsupported face sheet acts as a fixed ended beam column which must support the panel in-plane axial loads plus the coolant pressure as a distributed lateral load. After considering many options, the solution chosen was to increase the inner and outer face sheet thicknesses. The face sheets were increased to the next available thickness

of 0.81 mm (0.032 in.). Then, the stringer sizing was adjusted in order to minimize the attendant panel weight impact and to maintain relatively low margins of safety on panel buckling modes.

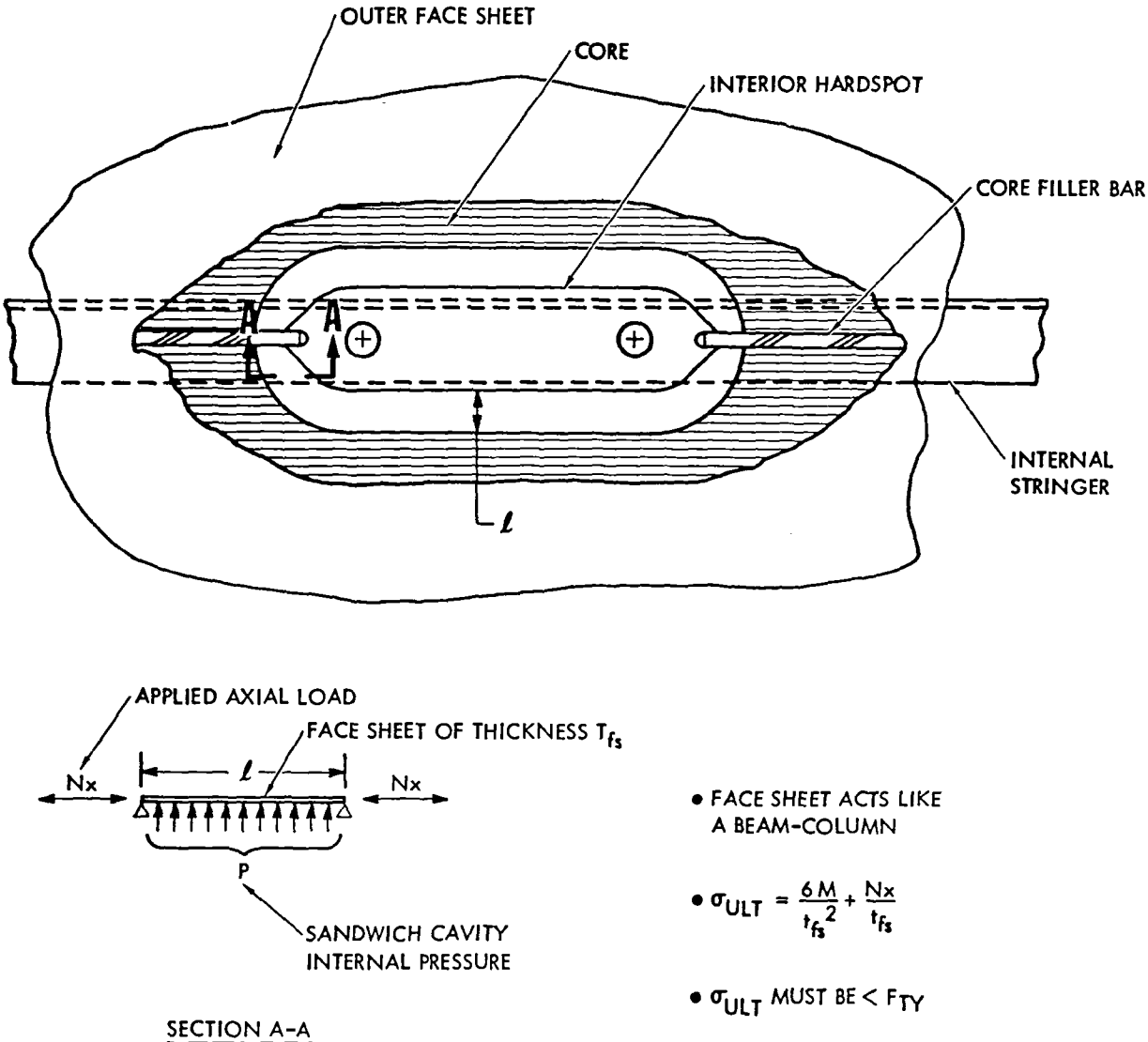

Figure 53. Core Cutouts around Hardspots Determine Face Sheet Thickness

An important output of the NASTRAN analysis is the stresses generated in the panel structural elements by the thermal environment. For this reason, the thermal environment cases were run as separate load conditions in addition to the combined mechanical load plus thermal environment load conditions. Typical results from these runs are shown in Figures 54 and 55. Figure 54

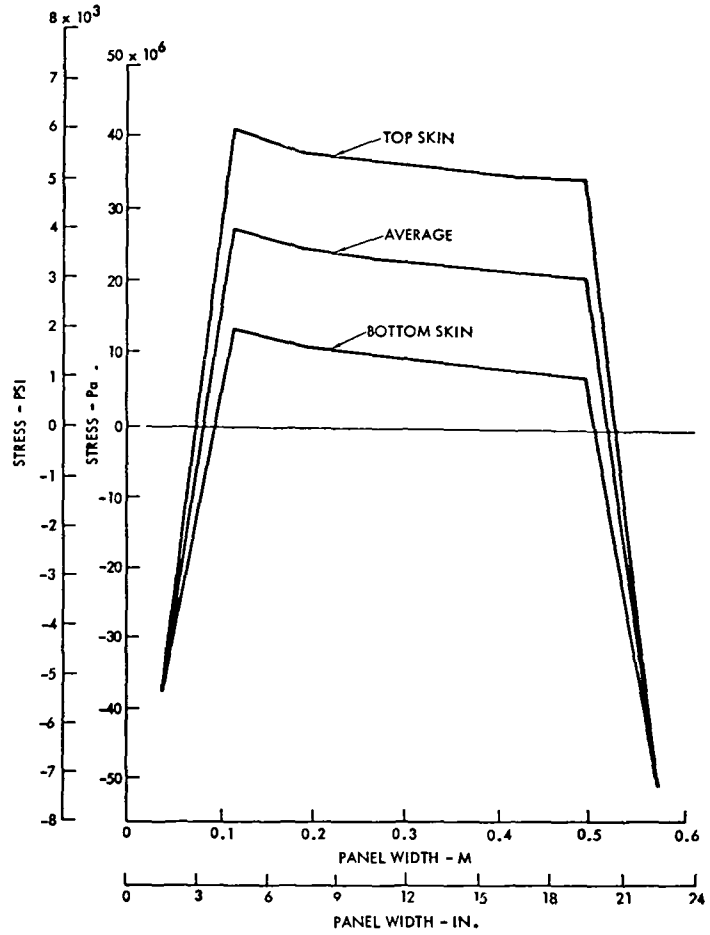

Figure 54. Thermal Stresses Across Panel Width at the Inlet End

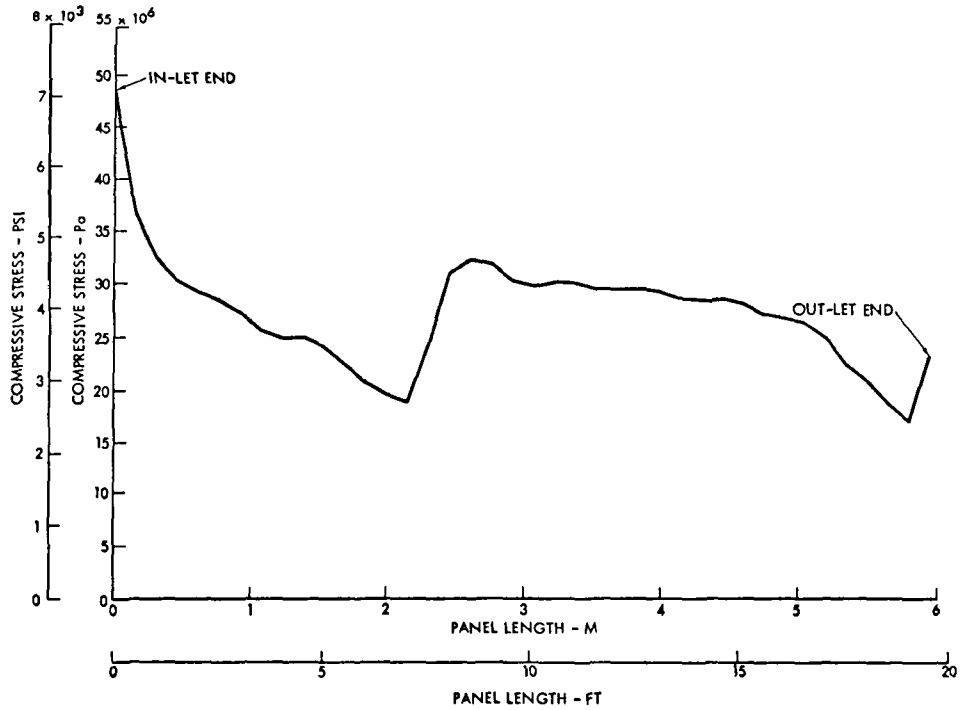

Figure 55. Thermal Stress Distribution Along One Edge of the Panel

presents the distribution of thermal stresses across the panel width at the coolant inlet end of the panel. Figure 55 presents the distribution of compressive thermal stresses along one longitudinal edge of the panel. These thermal stresses shown represent the maximum values obtained from the NASTRAN analyses.

In addition to the general panel stress analyses discussed above, numerous detail checks were conducted on local panel areas that might be subjected to maximum stress concentrations or exhibit unique failure modes. An example check of this type is the local maximum panel tensile stress at the holes for the fasteners attaching the panel to the main frames. This stress condition is critical at the hot end of the panel where a stress concentration factor (K_t), computed to be 2.3, magnifies the average tensile ultimate stress of 56.41 MPa (8181 psi) to a maximum tensile ultimate stress of 170 MPa (24,656 psi), resulting in a 22-percent margin of safety when compared to the material tensile ultimate allowable stress (F_{tu}) at 394 K (250°F) of 207.5 MPa (30,000 psi). This margin of safety, along with a summary of the minimum margins of safety resulting from the general panel stress analysis, are shown in Table 7.

Fatigue and Fracture Mechanism Analyses

The subject analyses were conducted on the full-scale panel design configuration. Consideration was given to flaws in the face sheet and flaws emanating from fastener holes. In addition, a fluid loss analysis was conducted assuming a thru-crack develops in the brazed sandwich face sheet.

Face Sheet Flaws. Past test experience at Rockwell indicates that a thin face sheet made from relatively soft 6000 series aluminum with a flaw or part-thru-crack is fatigue critical rather than flaw-growth critical for stress levels below 103.4 kPa (15,000 psi). This is true for the actively cooled panel unless fluid loss following flaw growth to full face sheet penetration (thru-crack) would result in a catastrophic failure of the panel.

Assume an undetected flaw or surface scratch exists that has a sharp root radius of 0.05 mm (0.002 in.) and penetrates through one-half of the 0.81-mm (0.032-in.) thick skin. From Figure 56 (reproduced from Rockwell Fatigue Manual), the stress concentration factor (k_t) is 2.5. The face sheets operate at a maximum limit tensile stress (combined mechanical and thermal) of

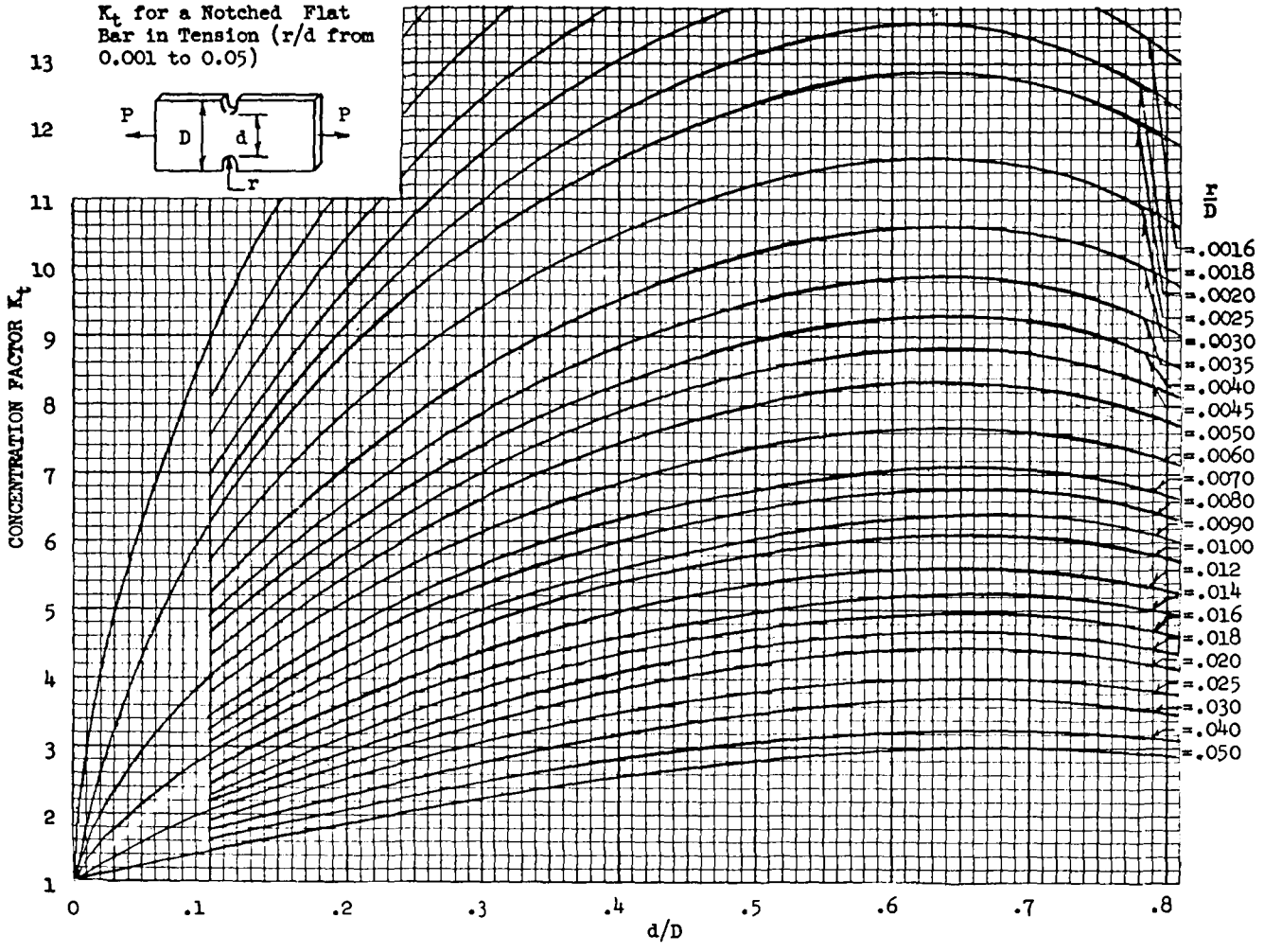

Figure 56. Stress Concentration Factor (k_t) as a Function of Flaw Depth-to-Thickness Ratios

102 MPa (14,790 psi) which is 49 percent of the tensile ultimate strength (f_{tu}) at 394 K (250°F). Using Figure 57 and interpolating, the fatigue life is greater than 30,000 cycles. Hence, it is reasonable to conclude that the 20,000-cycle life requirement will be exceeded by flawed skins in the final panel design.

The fluid loss analysis was conducted to provide some insight as to the magnitude of the problem in the event a thru-crack developed. Results of this very conservative analysis (the discharge coefficient was assumed equal to 1.0 which is true for nozzles—for cracks it would be much less) indicate that for crack lengths up to 2.54 cm (1.0 in.), which are certainly of a detectable size, coolant loss would be less than 0.28 m^3/hr (10 ft^3/hr). However, a coolant makeup capability should be considered for the overall system design.

Flaws emanating from fastener holes were also considered. The analysis indicates that dual flaws emanating from a single fastener hole located on the panel edge in the vicinity of the midspan would be most critical. The stress level in this area cycles between -42 MPa (6100 psi) and 102 MPa (14,790 psi). Initial dual flaws, each 1.27 mm (0.05 in.) long will survive 20,000 cycles. A flaw of this initial size can easily be detected by dye-penetrant, ultrasonic or eddy current inspection techniques during fabrication and installation. These flaws would have to grow to a length greater than 7.62 cm (3.0 in.) in service before failure would occur. In the event the initial flaws were not detected during fabrication, in-service maintenance and inspection would detect them prior to their reaching critical size.

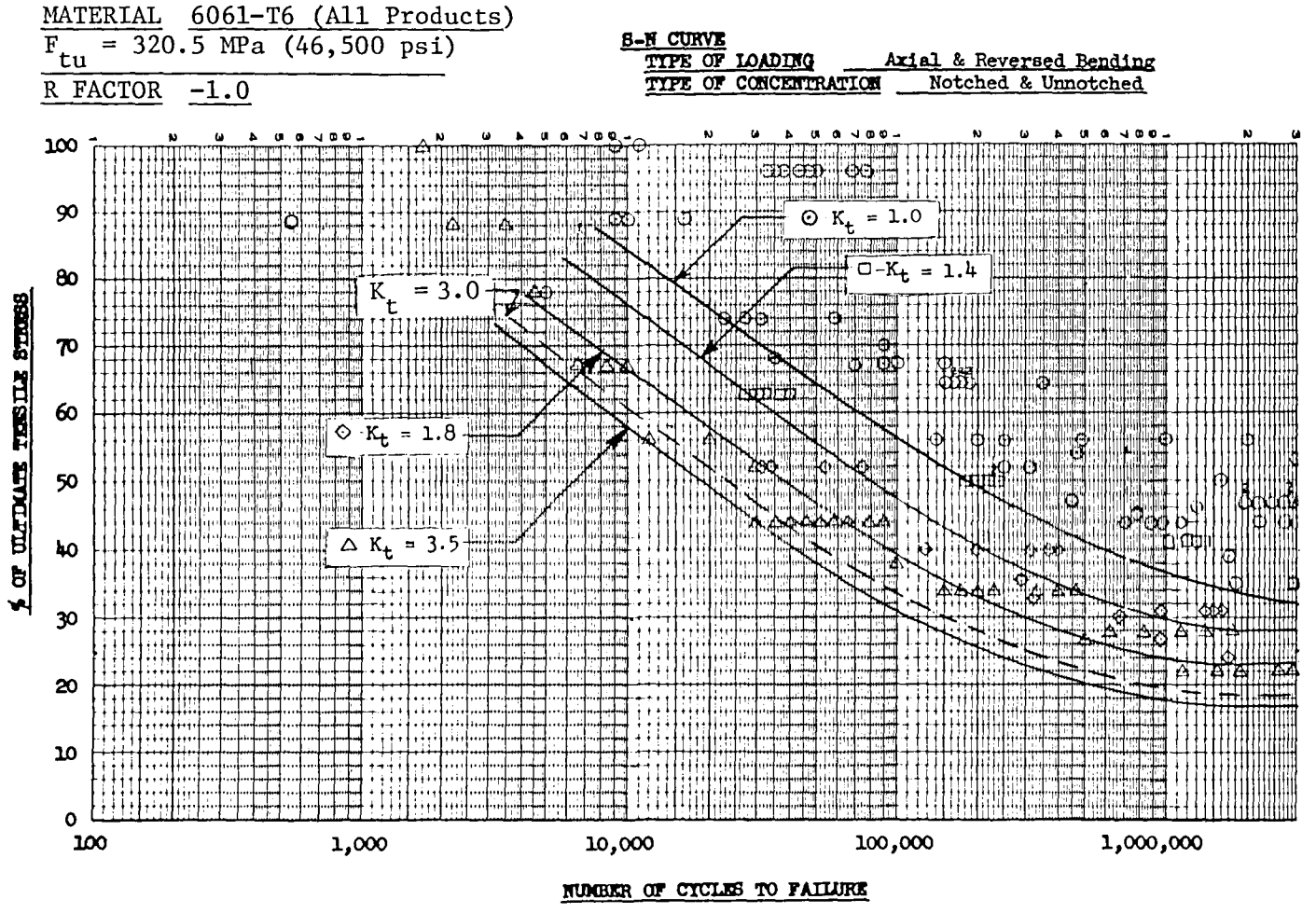

Figure 57. Cycle Life for Flawed Skin Panels

APPENDIX C

DESIGN PROCESS SUPPORTING TESTS

This appendix presents a discussion of two test programs conducted by Rockwell to support the design and analysis of the full-scale actively cooled panel. The first test program was conducted during the preliminary design and analysis phase to develop brazed joint lap-shear strength. The second test program was conducted following tests by NASA of the initial set of fatigue specimens and was aimed at selecting an alternate fastener system for panel-to-frame structure attachment.

Lap Shear Tests

The structural quality of the brazed joints is directly related to the braze process. Hence, it was necessary to test specimens fabricated by the Rockwell-developed fluxless brazing process proposed for the actively cooled panel sandwich structure rather than relying on published data from other sources.

Ten double lap-shear specimens were fabricated to the configuration shown in Figure 58. Five were brazed under 103.4 kPa (15 psi) pressure and five were brazed under 1379 kPa (200 psi). The vacuum pressure that is used to braze face sheets to core is 103.4 kPa (15 psi), and the mechanically applied pressure in the areas of panel interior hardspots and solid-edge and end filler plates is 1379 kPa (200 psi). The specimens were postbraze heat-treated to the -T6 condition. They were then pulled to failure, and the failure load and ultimate stress recorded (see Table 8). The resulting 3 σ design ultimate shear strength for 103.4 kPa (15-psi) joints is 99.15 MPa (14,380 psi), and 100.94 MPa (14,640 psi) for 1379 kPa (200-psi) joints. The ultimate tensile strength is 1.6 times the shear allowable, or 158.6 (23,000) and 161.3 MPa (23,400 psi), respectively. This ratio is consistent for 6000 series aluminum alloy brazed joints.

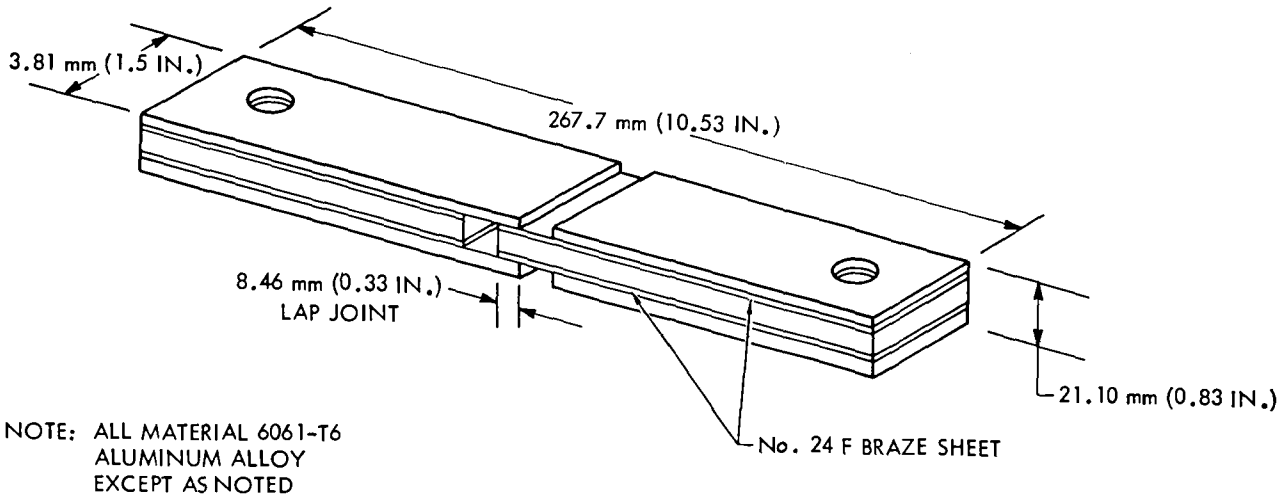

Figure 58. Lap Shear Test Specimen Configuration

Table 8. Lap Shear Specimen Test Results

Specimen Number	Thickness (mm)	Width (mm)	Area (mm^2)	Ultimate Load (N)	Ultimate Stress	
					MPa	ksi
15-1	8.89	38.125	678.10	70,726	104	15.1
15-1	8.89	38.5	681.94	72,506	106	15.4
15-3	8.89	38.227	680.00	74,285	106	15.4
15-4	8.89	38.113	677.42	72,172	107	15.5
15-5	8.89	36.322	645.8	67,722	102	14.8
200-1	8.89	38.252	680.00	82,515	121	17.6
200-2	8.89	38.227	680.00	83.404	123	17.8
200-3	8.89	38.227	680.00	78,956	116	16.8
200-4	8.89	36.227	680.00	76,287	112	16.3
200-5	8.89	36.322	645.8	71,616	111	16.1

Fastener Evaluation Tests

Background. Excessive motion of the joint at the panel end/load adapter (main transverse frame simulation) interface was noted during NASA fatigue tests of the end panel/internal stringer specimen and the panel corner specimen. The joint motion was reported by NASA to be approximately 0.76 mm (0.03 in.) through a complete tension/compression cycle. The inability of this joint to carry its share of the load causes excessive load to be carried by the inboard load path through the bathtub fitting and into the web and inboard flange of the edge stringer. This joint inefficiency is considered to be a major contributor to the original bathtub fitting failure and the subsequent edge stringer failure.

The original fastener system used at the panel end/load adapter (main) transverse frame) interface was a 6.35-mm (1/4-in.) diameter flush head rivet, part number NAS1399C8.

Teardown inspection of the panel corner fatigue specimen indicated that the rivet "rolled" back and forth elastically deforming the holes in the panel end and the transverse frame cap simulation on the load adapter. There was little evidence of plastic hole elongation, and the rivet pins and sleeves were not bent. This "rolling" is attributed to the lack of rivet bearing or clamping area on the formed head (inboard end) of the fastener.

Because of the above described deficiency of the NAS1399C8 rivet, a fastener evaluation test program was conducted by Rockwell, which resulted in the selection of a titanium Taper-Lok pin (part number TL 300-4) and washer nut (part number TLN 1001-4) system for the final full-scale panel configuration. Detailed information on the Taper-Lok fastener system can be found in Reference 17. Details of the test program are described below.

Selected Fastener Systems. Research into available fastener systems resulted in the five fastener types listed in Table 9 being selected for test. Each fastener has different characteristics and allowed evaluation of four basic parameters: (1) fastener configuration (straight or tapered shank);

(2) hole fit (interference or close tolerance); (3) clamp-up torque; and (4) installation access requirements (one side vs. two sides). All fasteners tested were nominal 6.35-mm (0.25-in.) diameter.

Table 9. Fastener Systems Selected for Test

Item No.	Nomenclature	Manufacturer's Part Number	Manufacturer
1	Taper-Lok Bolt	TL100-4-10	Deutsch Fastener Corporation
2	Shear Bolt	NAS1581-C4510	*
3	Tension Bolt	MD111-3001-0401	*
4	Jo-Bolt (Blind)	PLT110-8-10	VOI-Shan Corp.
5	Tapered Jo-Bolt (Blind)	VA212-8-10	VOI-Shan Corp.
6	Cherrylock Rivet	NAS1399C	Cherry Rivet**

*Many manufacturers make these bolts to the indicated NAS or MD (Rockwell) specifications.

**Tested to provide a baseline.

Test Specimen Configuration. Two (2) specimen designs were tested—one that would accept a single row of fasteners, and a second that would accept a double row of staggered fasteners (Figure 59). The second configuration (double-row) was provided as a backup in the event that no single-row fastener system would provide an acceptable result (significant reduction in joint motion).

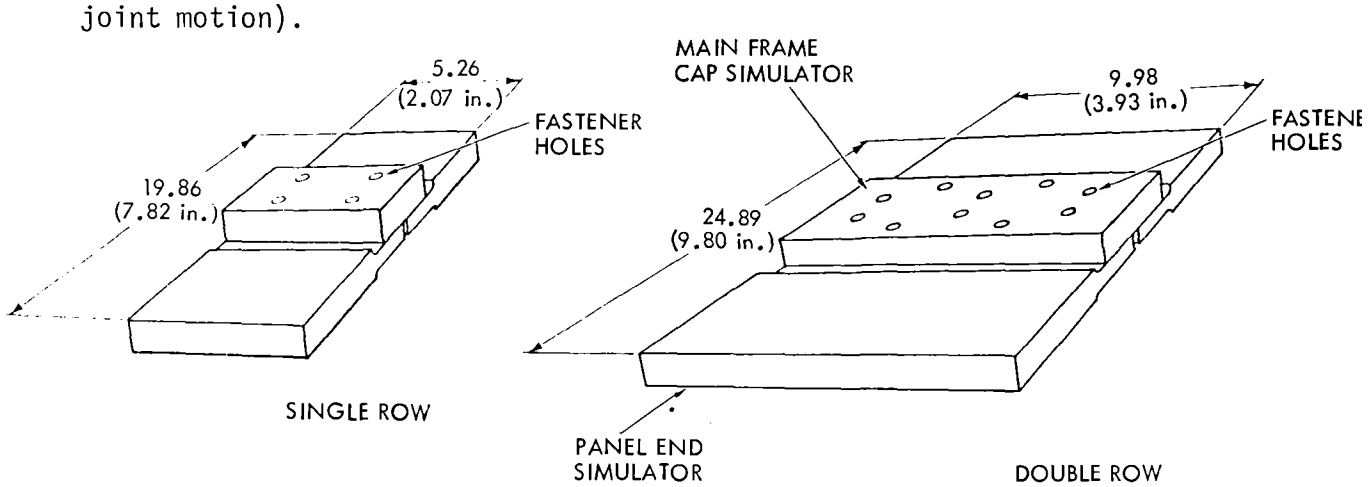

Figure 59. Fastener Evaluation Specimen Configurations

The test specimen blanks were fabricated by Rockwell's advanced manufacturing development organization. The specimen material was 6061-T6 aluminum. Care was taken to assure that the material longitudinal direction was parallel to the load direction. The fastener installation (including hole preparation) was accomplished by the fastener manufacturer for the Taper-Lok and Jo-Bolt fasteners. The shear and tension bolts were installed by Rockwell.

Eleven specimens were fabricated and tested. Detailed information on specimen configurations is presented in Table 10.

Table 10. Candidate Fastener Characteristics

TEST SPEC. NO.	FASTENER SYSTEM (NO. OF ROWS)	FASTENER MATERIAL	STRENGTH PROP. SHEAR MPa (KSI)	STRENGTH PROP. TENSION MPa (KSI)	HEAD DIAMETER mm (in.)	C'SINK DEPTH mm (in.)	HOLE PREP & FIT INFORM.	INSTALL TORQUE N-m (in.-lb$_f$)	FASTENER PRELOAD N (lb$_f$)
1	TAPER-LOC BOLT P/N TL-100-4-10 (SINGLE ROW)	ALLOY STEEL-4340 OR 8740	745 (108)	1,241 (180)	9.58 (.377)	1.6 (.063)	TAPER/REAM .076 TO .084 INTERFERENCE FIT	13.56 (120)	10,676 (2,400)
2	TAPER-LOC BOLT P/N TL110-4-10 (1ST REPAIR SIZE) (SINGLE ROW)	ALLOY STEEL -4340 OR 8740	745 (108)	1,241 (180)	9.58 (.377)	1.6 (.063)	TAPER/REAM .071/.084 INTERFERENCE FIT	13.56 (120)	10,676 (2,400)
3	SHEAR BOLT P/N NAS1581-C4T10 (SINGLE ROW)	A286 CRES	(96)	(160-180) (180)	8.89 (.350)	1.6 (.063)	REAMED HOLE .00761/.0127 CLEARANCE FIT	10.17 (90)	8,007 (1,800)
4	SHEAR BOLT P/N NAS1581-C4T10 (SINGLE ROW)	A286 CRES	662 (96)	1,241 (180)	8.89 (.350)	1.6 (.063)	REAMED HOLE .051/.089 CLEARANCE FIT	10.17 (90)	8,007 (1,800)
5	TENSION BOLT P/N MD111-3001-0410 SINGLE ROW	MP24N PER AMS 5758 CRES	910 (132)	1,655-1,896 (240-275)	11.35 (.447)	2.69 (.106)	REAMED HOLE .0076/.0127 CLEARANCE FIT	19.77 (175)	15,569 (3,500)
6	TENSION BOLT P/N MD111-3C01-0410 (DOUBLE ROW)	MP24N PER AMS 5758 CRES	910 (132)	1,655-1,896 (240-275)	11.35 (.447)	2.69 (.106)	REAMED HOLE .051/.089 INTERFERENCE FIT	19.77 (175)	15,569 (3,500)
7	TAPER-LOC BOLT P/N TL100-4-10 (SINGLE ROW)	ALLOY STEEL -4340 OR 8740	745 (108)	1,241 (180)	9.58 (.377)	1.6 (.063)	TAPERED/REAMED HOLE .081/.094 INTERFERENCE FIT	13.56 (120)	10,676 (2,400)
8	JO-BOLT P/N PLT110-8-10 (SINGLE ROW)	BOLT: 4130, 4140 OR 8740 NUT: 4130, 4140 OR 8740 SLEEVE: 304 CRES	745 (108)	1,241-1,379 (180-200)	11.76 (.463)	2.59 (.102)	REAMED HOLE .025/.038 CLEARANCE FIT	N/A	1,868 (420)
9	TAPERED JO-BOLT P/N VA212-8-10 (SINGLE ROW)	BOLT: 8740 STEEL ALLOY NUT: 8740 STEEL ALLOY SLEEVE: 304 CRES	745 (108)	1,241-1,379 (180-200)	10.03 (.395)	1.6 (.063)	TAPERED/REAMED HOLE .0635/.089 INTERFERENCE FIT	N/A	1,868 (420)
10	TAPERED JO-BOLT P/N VA212-8-10 (SINGLE ROW)	BOLT: 8740 STEEL ALLOY NUT: 8740 STEEL ALLOY SLEEVE: 304 CRES	745 (108)	1,241-1,379 (180-200)	10.03 (.395)	1.6 (.063)	TAPERED/REAMED HOLE .0635/.089 INTERFERENCE FIT	N/A	1,868 (420)
11	TAPERED JO-BOLT P/N VA212-8-10 (SINGLE ROW)	BOLT: 8740 STEEL ALLOY NUT: 8740 STEEL ALLOY SLEEVE: 304 CRES	745 (108)	1,241-1,379 (180-200)	10.03 (.395)	1.6 (.063)	TAPERED/REAMED HOLE .0635/.089 INTERFERENCE FIT	N/A	1,868 (420)

Test Set-Up. All tests were performed with an electro-hydraulic test machine. Each specimen was gripped with Amsler rigid-wedge grips capable of applying compression loads to the test specimen with zero backlash when going through zero load. Relative deflection of the fastener row centerlines was measured with a displacement transucer. The transducer was installed by

percussion-welding a 0.135-mm (0.053-in.) diameter wire to each of the rivet row centerlines, sliding a pre-drilled transducer mounting clip over each wire and peening the wire end to hold the clip in place. The displacement transducer was then installed between these clips. Figure 60 depicts the test set-up. The transducer is wired to a recorder that provides a real-time plot of load vs. deflection from rivet line to rivet line. Lateral motion

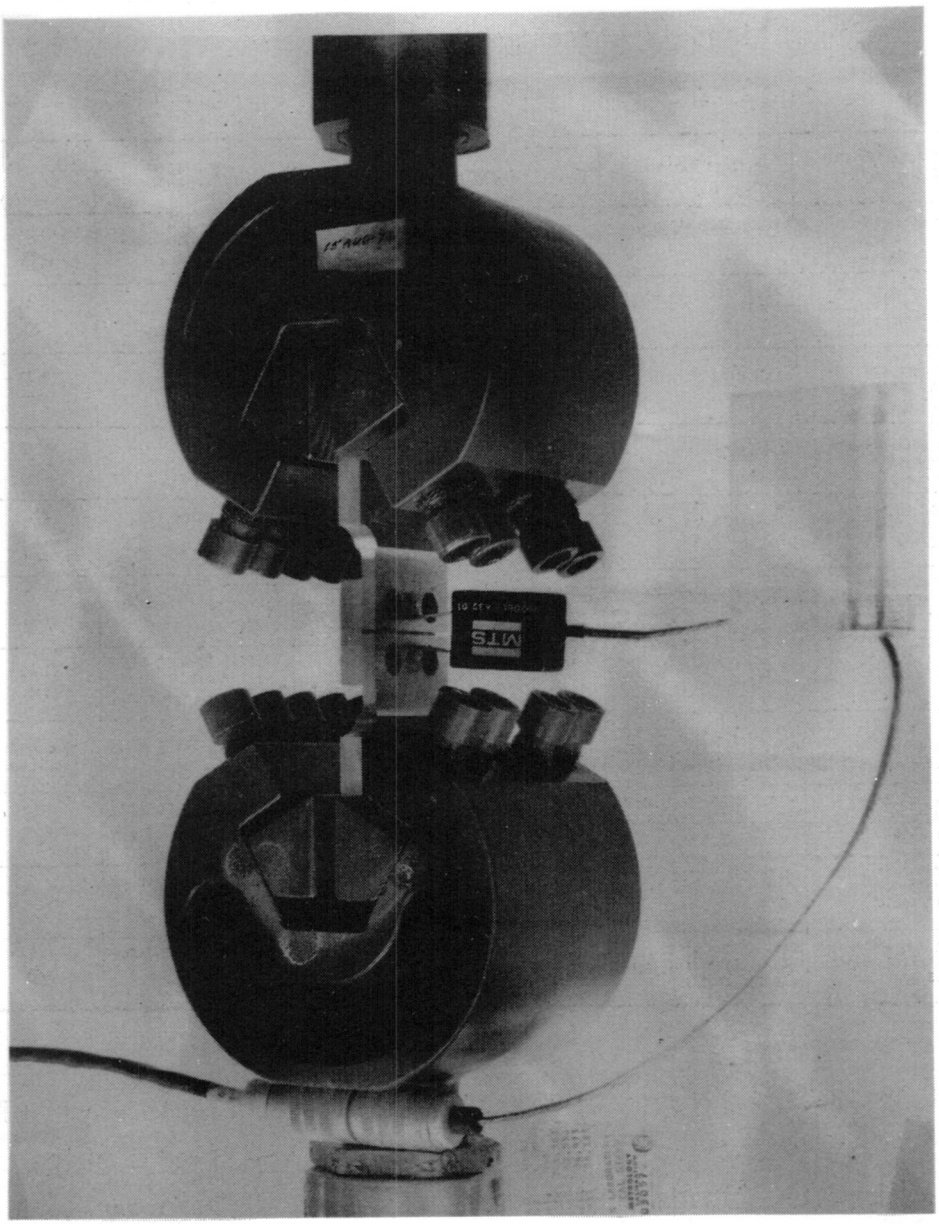

Figure 60. Joint Specimen Test Set-Up

in one direction is restricted by a Teflon-coated block (Figure 61) that simulated (in one direction at least) the lateral motion restriction that an aircraft main transverse frame would provide.

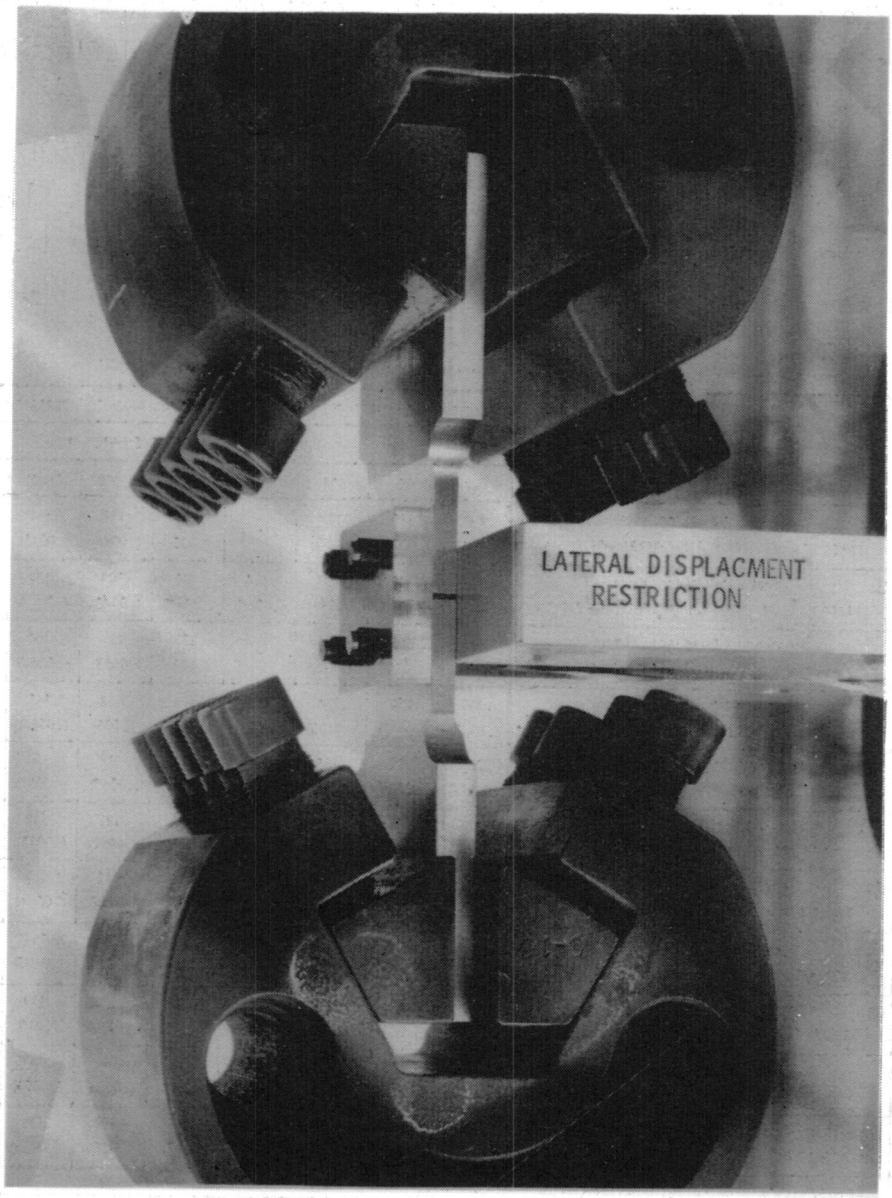

Figure 61. Test Set-Up with Lateral Displacement Restriction In Place

Test Procedure. The single-row fastener test specimens were cyclic loaded from 10.676 N (2400 lb) tension to 10,676 N (2400 lb) compression (R = -1) at 2 Hz for 20,000 cycles. The double-row fastener test specimens were cyclic loaded from 17,482 N (3930 lb) compression at 1 Hz for 20,000 cycles.

Deflection measurements were recorded as a function of load at various cycle totals up to 20,000 cycles for each specimen tested.

Test Results. Test results for all specimens tested are tabulated in Table 11. The deflections listed are total joint deflections experienced from maximum tension to maximum compression. Hence, the joint deflection attributed to a single fastener is one-half the listed deflection minus the deflection due to strain of the 9.52-mm (0.375-in.) thick frame flange simulator calculated to be 0.006 mm (0.00024 in.). Therefore, the one-direction joint slop for a Taper-Lok system is less than 0.054 mm (0.0022 in.) as opposed to 0.312 mm (0.012 in.) for the Cherrylock Rivet system. Actual deflection data for the

Table 11. Fastener Evaluation Test Results

TEST SEQ	TEST SPEC NO.	FASTENER SYSTEM	TOTAL MEASURED DISPLACEMENT (TENSION AND COMPRESSION) - mm (INCH)								
			NUMBER OF CYCLES (CYCLE RATE - 1 Hz)								
			1	10	100	500	1,000	5,000	10,000	15,000	20,000
1	1	TAPER-LOK (TL100-4-10) TAPER REAMED HOLE - INTERFERENCE FIT	.190 (.0075)	.190 (.0075)	.189 (.0072)	-	.127 (.005)	.117 (.0046)	.114 (.0045)	.114 (.0045)	.114 (.0045)
4	2	① TAPER-LOK (TL110-4-10) TAPER REAMED HOLE - INTERFERENCE FIT	.178 (.007)	.173 (.0068)	.130 (.0051)	.114 (.0045)	.109 (.0043)	.109 (.0043)	.109 (.0043)	.109 (.0043)	.109 (.0043)
2	3	SHEAR BOLT (NAS1581-CAT10) REAMED HOLE - INTERFERENCE FIT	.406 (.016)	.381 (.015)	.381 (.015)	-	.279 (.011)	.185 (.0073)	.160 (.0063)	.165 (.0065)	.147 (.0058)
6	4	SHEAR BOLT (NAS1581-CAT10) REAMED HOLE - INTERFERENCE FIT	.300 (.0018)	.297 (.0017)	.274 (.0108)	.227 (.009)	.191 (.0075)	.152 (.006)	.145 (.0057)	.145 (.0057)	.145 (.0057)
3	5	TENSION BOLT (MD111-3001-0410) REAMED HOLE - CLOSE TOL FIT	.287 (.0013)	.292 (.0115)	.185 (.0073)	.140 (.0055)	.137 (.0053)	.137 (.0053)	.130 (.0051)	.130 (.0051)	.130 (.0051)
5	6	TENSION BOLT (MD111-3001-0410) REAMED HOLE - INTERFERENCE FIT	.208 (.0082)	.216 (.0085)	.165 (.0065)	.147 (.0058)	.142 (.0056)	.132 (.0052)	.132 (.0052)	.127 (.0050)	.127 (.0050)
7	7	② TAPER-LOK (TL100-4-10) TAPER REAMED HOLE - INTERFERENCE FIT	.145 (.0057)	.145 (.0057)	.135 (.0053)	.127 (.005)	.122 (.0048)	.112 (.0044)	.112 (.0044)	.109 (.0043)	.109 (.0043)
8	8	JO-BOLT (PGT110-8-10) REAMED HOLE - STD STRUCT CLEARANCE	.648 (.0255)	.648 (.0255)	.508 (.020)	.373 (.0147)	.297 (.0117)	.300 (.0118)	.262 (.0103)	.259 (.0102)	.254 (.0100)
9	9	② TAPERED JO-BOLT (VA212-8-10) TAPER REAMED HOLE - INTERFERENCE FIT	.282 (.0111)	.279 (.011)	.267 (.0105)	.254 (.010)	.254 (.010)	.254 (.010)	.254 (.010)	.236 (.0093)	.237 (.0092)
10	10	SAME AS TEST SPEC NO. 9	.284 (.0112)	.279 (.011)	.292 (.0115)	.259 (.0102)	.262 (.0103)	.244 (.0096)	.241 (.0095)	.221 (.0087)	.203 (.008)
11	11	TAPERED JO-BOLT (VA212-8-10) DOUBLE ROW TAPERED REAMED HOLE - INTERFERENCE FIT	.211 (.0083)	.203 (.008)	.203 (.008)	-	.198 (.0078)	.198 (.0078)	.185 (.0073)	.185 (.0073)	.185 (.0073)
12	12	CHERRYLOCK BLIND RIVET (NAS1399C4-10) EXISTING DESIGN	.623/.732 (.0248/.030) 1 CYCLE →								.623/.762 (.0248/.030) 20,000 CYCLES

① REPAIR SIZE .396 mm (.0156 INCH) OVERSIZE
② DOUBLE ROW FASTENERS - STAGGERED

NOTES:
(A) ALL TEST SPEC SINGLE ROW EXCEPT AS NOTED
(B) ALL FASTENERS STRAIGHT SHANK, FLUSH HEAD, 6.35 mm (.25 INCH) NOMINAL DIAMETER EXCEPT AS NOTED

Cherrylock Rivet system and the Taper-Lok system are reproduced in Figures 62 and 63, respectively. The Taper-Lok system shown in Figure 64 consists of

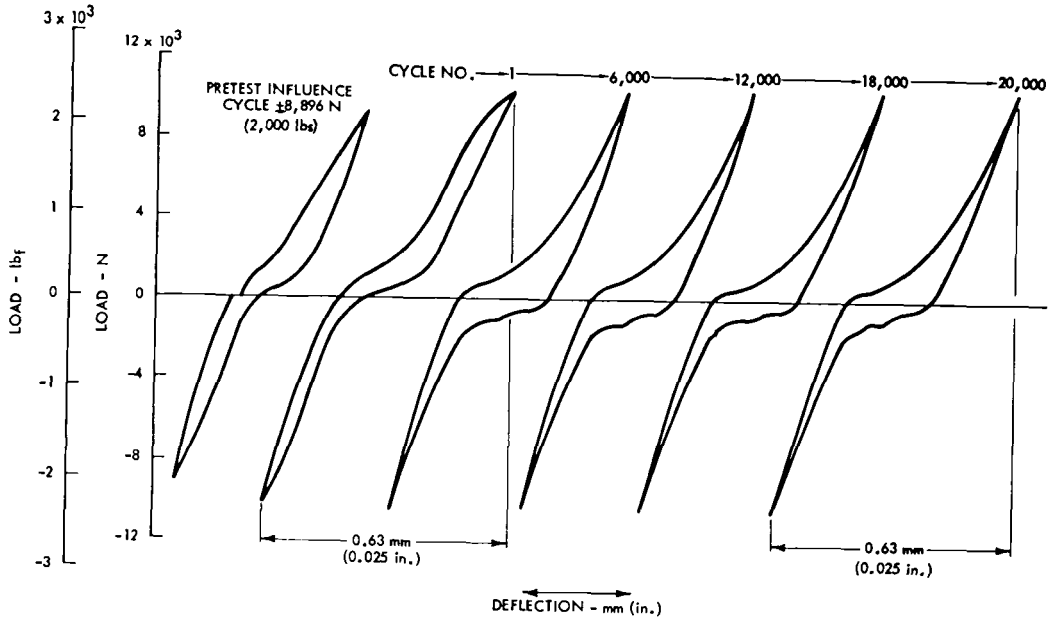

Figure 62. Cherrylock Rivet Test Results

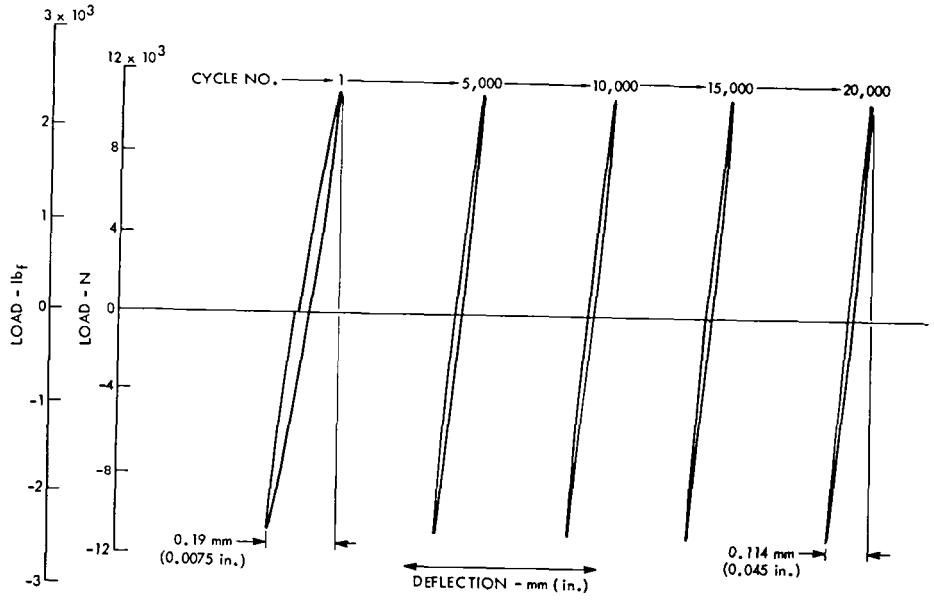

Figure 63. Taper-Lok Test Data

a tapered flush-head bolt and a nut with an integral washer. The fastener is drawn into the tapered hole as the nut is tightened, thus assuring an interference fit. The Taper-Lok was selected for the final full-scale panel design based on its superior performance over all candidate systems tested.

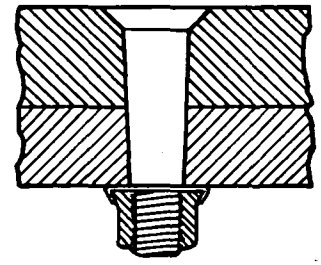

Figure 64. Taper-Lok Fastener

APPENDIX D

FATIGUE SPECIMENS

This appendix presents the rationale for the selection of the load correction factor used on the fatigue specimens to compensate for the room temperature test environment and a discussion of the fatigue specimen fabrication processes.

Fatigue Specimen Load Correction Factor

The fatigue specimens were tested at room temperature; yet, the objective of these tests was to verify structural integrity of critical areas of the full-scale panel in their elevated temperature operational environment over 20,000 fully reversed load cycles (R = -1). Therefore, it was necessary to develop a load input correction factor to compensate for the lack of elevated temperature during test. Two phenomena were considered—the reduction in mechanical properties due to elevated temperature, and the reduction in fatigue life due to elevated temperature. The reference temperature for the analysis was 394 K (250°F).

Strength data at elevated temperatures for the 6951-T6, 6061-T6, and 7075-T7351 aluminum alloys and tempers used in the panel design are readily available either from Appendix A in this report or from References 5 and 12. However, the corresponding elevated temperature fatigue data are not available. Therefore, the fatigue life temperature correction factor was based on estimations using data available for 6061-T6 aluminum at room temperature, and 2024-T3 and -T851 aluminum at room temperature and at 402 K (265°F). This estimation process, employing the best available fatigue life data, is considered appropriate and conservative because of the very close variation in physical properties and the almost insignificance of the creep phenomena for the subject aluminum alloys and tempers up to temperatures of 422 K (300°F).

Strength data for the subject aluminum alloys and tempers are shown in Table 12 for room temperature and 394 K (250°F). Also, the reduction in

strength at 394 K (250°F) is indicated as the percent of strength at room temperature. The minimum percentage shown is 86 percent, which would indicate a 16-percent increase in specimen loading as a temperature correction, considering only material strength properties.

Table 12. Degradation of Properties at Elevated Temperatures for Various Aluminum Alloys

ALLOY AND TEMPER	MECHANICAL PROPERTY	ROOM TEMPERATURE STRENGTH		STRENGTH AT 394 K (250 F)		% OF R.T. STRENGTH AT 394 K (250 F)
		MPa	(PSI)	MPa	(PSI)	
6061-T6	F_{TU}	289.6	(42,000)	248.2	(36,000)	86%
	F_{TY}	248.2	(36,000)	220.6	(32,000)	88%
	F_{CY}	241.3	(35,000)	213.7	(31,000)	88%
7075-T7351	F_{TU}	468.9	(68,000)	427.5	(62,000)	91%
	F_{TY}	399.9	(58,000)	358.5	(52,000)	90%
	F_{CY}	399.9	(58,000)	358.5	(52,000)	90%
6951-T6	F_{TU}	241.3	(35,000)	206.9	(30,000)	86%
	F_{TY}	206.9	(30,000)	179.3	(26,000)	88%
	F_{CY}	200.0	(29,000)	179.3	(26,000)	88%
2024-T851	F_{TU}	462.0	(67,000)	420.6	(61,000)	91%
	F_{TY}	406.8	(59,000)	351.6	(51,000)	86%
	F_{CY}	406.8	(59,000)	351.6	(51,000)	86%
2024-T3	F_{TU}	448.2	(65,000)	393.0	(57,000)	87%
	F_{TY}	324.0	(47,000)	303.4	(44,000)	94%
	F_{CY}	268.9	(39,000)	255.1	(37,000)	94%

To determine the temperature correction considering fatigue life, a constant life approach was used. Entering the room and elevated temperature 2024 alloy curves, corresponding to $R = -1.0$ and $K_T = 3.0$, at the test stress level a life reduction ratio was developed. This ratio was then applied to the 6061-T6 alloy room temperature data to determine the test stress level required to generate the same reduction in fatigue life. This procedure resulted in a 21.75-percent increase in specimen loading for the fatigue life temperature correction. Therefore, using the baseline panel loading of 210 kN/m (1200 lbf/in.), the area ratios between the panel and the

fatigue specimen cross-sections, and a 21.75-percent increase in loading for temperature correction, the resulting specimen loads were:

- Panel corner specimen ~73.9 kN (16,612 lb)
- End panel/internal stringer termination specimen ~33.7 kN (7,575 lb)
- Skin/interior hardspot specimen ~32.7 kN (7,357 lb)

These load levels were supplied to NASA prior to fatigue specimen test set-up.

Fatigue Specimen Fabrication Details

Fabrication of eight small-scale test specimens, which was a precursor to fatigue specimen fabrication, has been reported in SD 74-CE-0010 (Reference 6). That report describes in detail the fabrication, brazing, heat treatment, and inspection of the eight test specimens and includes detailed photographic coverage of all pertinent aspects of that activity. Figures 65 through 67 are shown herein merely for continuity. Figure 65 shows four specimen details being assembled for simultaneous brazing. The two cores on the left are straight fin, while the two on the right are the lanced off-set

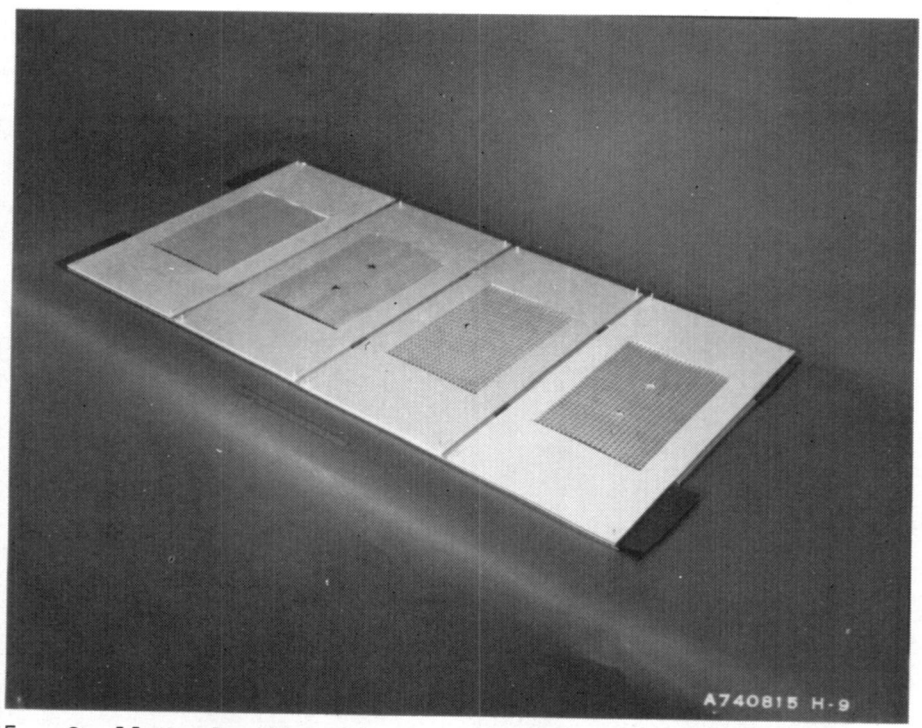

Figure 65. Small-Scale Test Specimen (SSTS)—Four Panel Details Being Assembled for Simultaneous Brazing

cores. Figure 66 shows the four simultaneously brazed specimens being removed from the brazing retort, and Figure 67 shows a straight fin core small-scale test specimen after final machining.

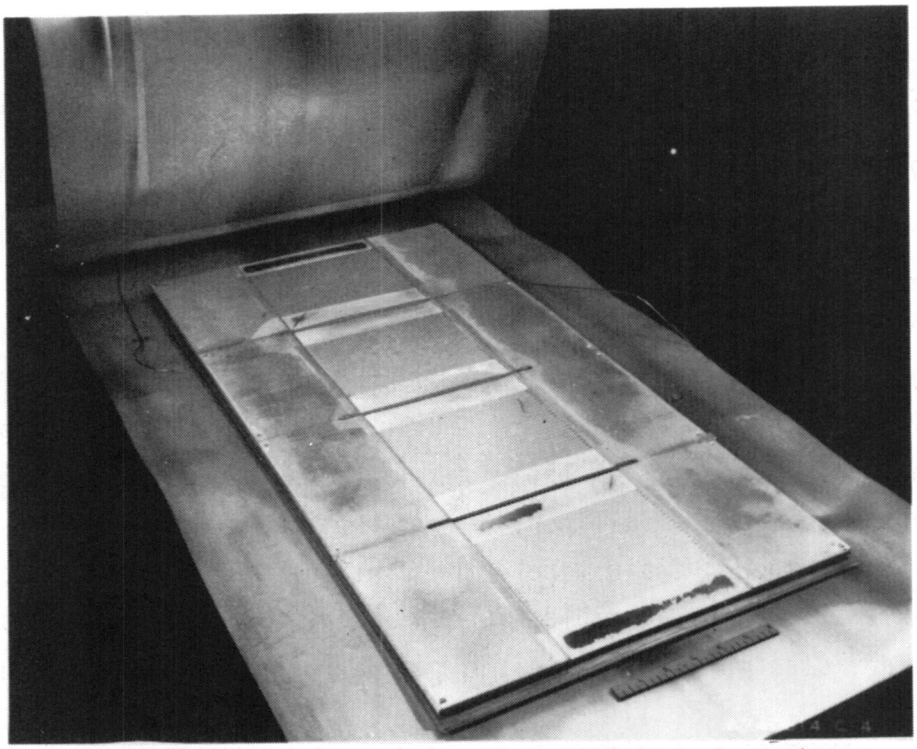

Figure 66. SSTS—Four Simultaneously Brazed Panels Being Removed from Retort

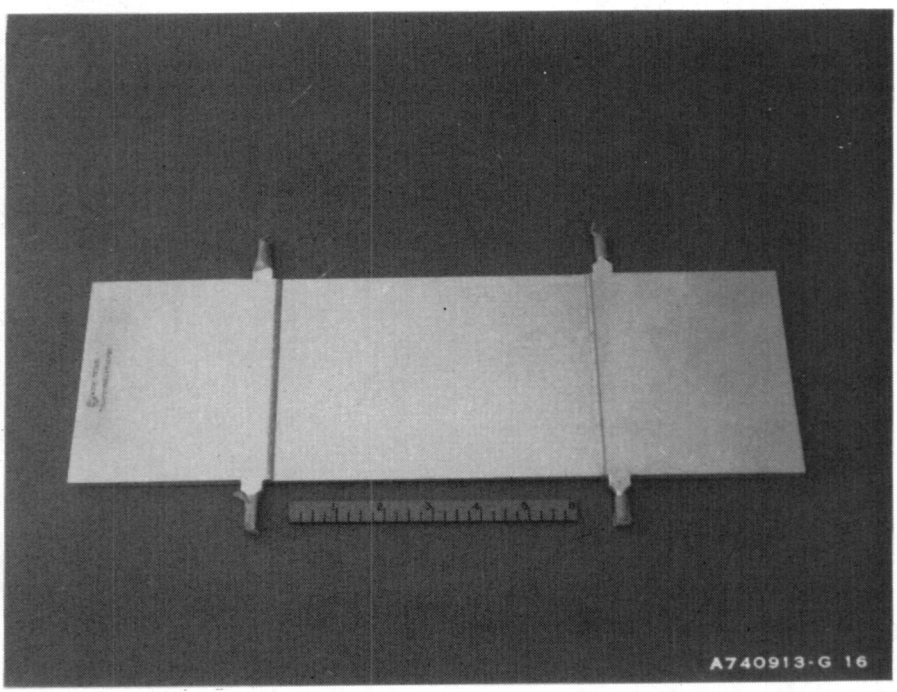

Figure 67. SSTS—Straight Fin Core Panel after Final Machining

The next manufacturing task was the fabrication of fatigue specimens representative of critical areas of the full-scale panel design. Initially, three fatigue specimens were fabricated. These were identified as (1) the skin/interior hardspot specimen, (2) the panel corner specimen, and (3) the end panel/internal stringer termination specimen. Each specimen was representative of a critical area of the full-scale (2- by 20-foot) panel. A fourth specimen was fabricated to replace the panel corner specimen following failures in test. This specimen was identified as the "boilerplate" panel corner specimen.

Skin/Interior Hardspot Specimen. The first specimen fabricated was the skin/interior hardspot specimen. This specimen was representative of the full-scale panel design in the vicinity of the hardspots for attachment to the intermediate frames. The specimen consisted of a flat frame containing two sections of the corrugated core with a cut-out in the center of the core for the hardspot. Two filler bars were inserted in a core convolution, both to provide support during brazing and to maintain alignment of the convolutions between the two abutting sections of core. Face sheets placed on each side of the frame formed a sandwich structure. Six doublers, located on the ends of the two face sheets, completed the components. Manifolding of this panel was accomplished by machining inlet and outlet ports into the panel components.

Brazing was performed using the inert gas atmosphere technique. With this technique, argon gas pressure is introduced into the retort during the brazing cycle. This part was solution-heat-treated with the use of a fixture and quenched in water. Several small surface indentations were introduced on the face sheets in the core area during the solution-heat-treating process and were determined to be caused by the fixture. The panel was subsequently aged to the T-6 temper. After final machining, the panel successfully passed the helium leak check and the pressure test to 1.724 MPa (250 psi). No leaks could be detected.

Mass of the completed panel itself was 605 grams (1.33 lbm). After bonding of stringers and channels, the panel weight was 773 grams (1.70 lbm). The finished specimen consisting of the panel, load adapters, and fasteners weighed 4131 grams (9.11 lbm) as delivered for testing.

Figures 68 through 71 show this fatigue specimen during various stages of fabrication. Figure 68 shows the two corrugated core sections, the insert or hardspot, and filler bars all contained within the frame cavity during pre-braze assembly. Figure 69 shows one side of the fatigue specimen immediately after brazing. Note the impression of the core and insert on the face sheet. Figure 70 shows the moldline side of the panel after attaching the two end-load adapters. Figure 71 shows the opposite (or inboard) side of the completed fatigue test specimen.

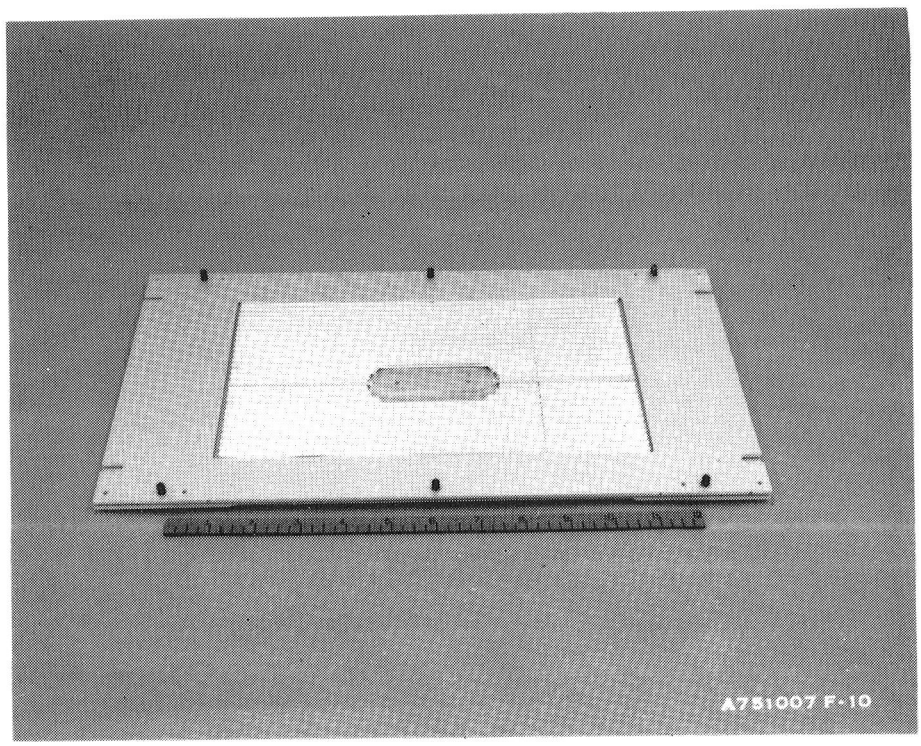

Figure 68. Skin Interior Hardspot Specimen (SIHS)—Internal Details of Panel during Pre-Braze Assembly

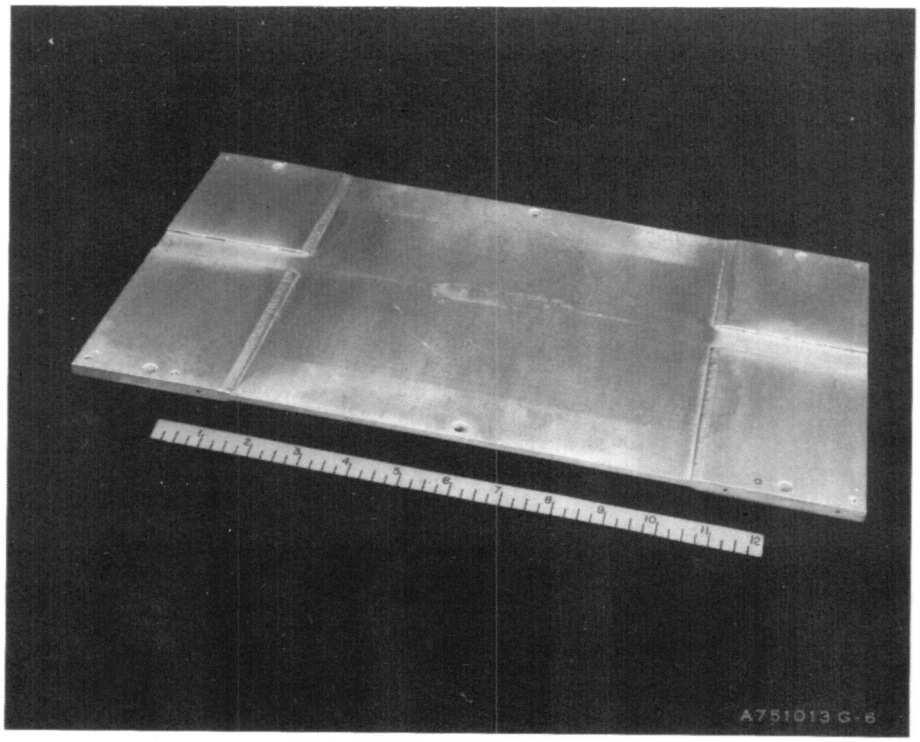

Figure 69. SIHS—Inboard Side of Fatigue Specimen after Brazing

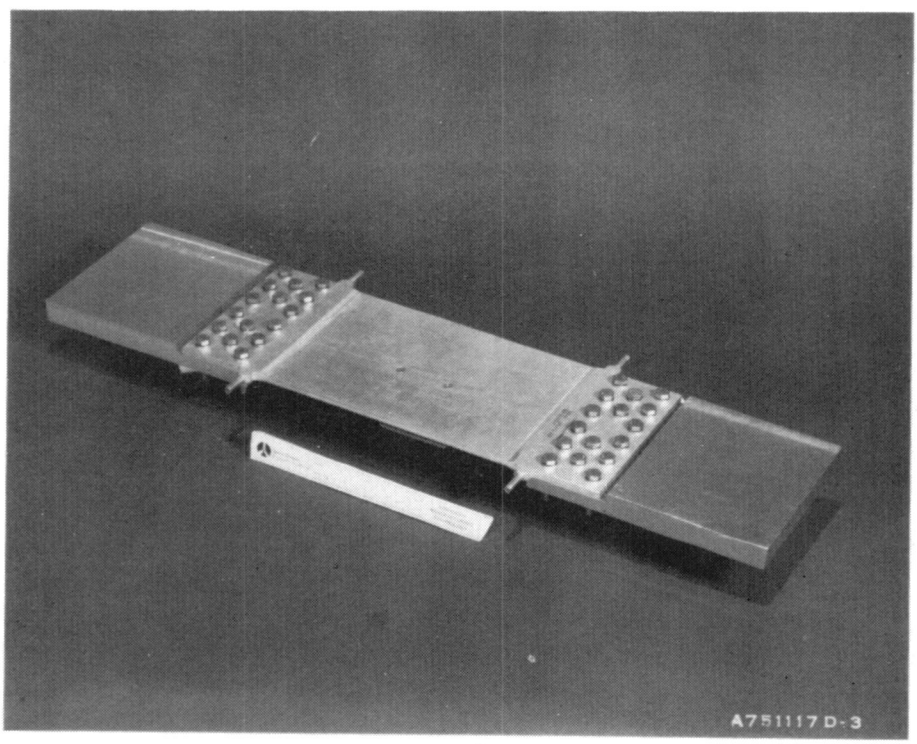

Figure 70. SIHS—Moldline Side of Panel with End-Load Adapters

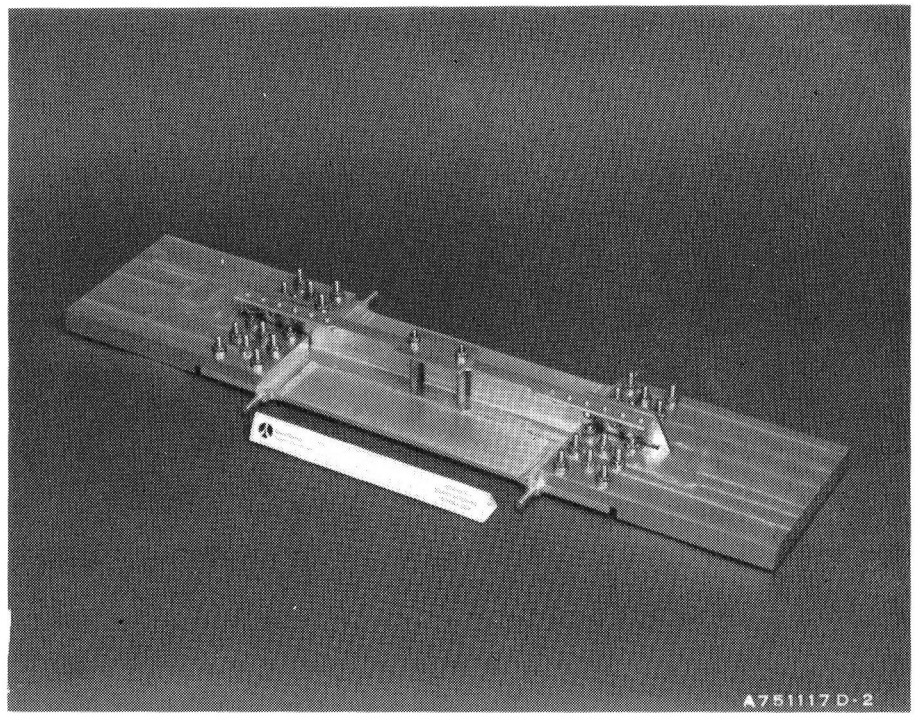

Figure 71. SIHS—Inboard Side of Completed Fatigue Test Specimen

Panel Corner Specimen. The second fatigue specimen fabricated was the panel corner specimen. This specimen is representative of adjacent corners of the full-scale panel design. The specimen generally can be described as consisting of two separate panels butted together along their length and attached to two end-load adapters. The manifolding of each panel was similar. The inlet manifolds are of the full-scale design configuration. The outlet ends of each panel were similar to those of the skin/interior hardspot specimen; that is, they were fabricated from integrally assembled panel details. These panels consisted of a flat frame containing two sections of corrugated core butted together. The perimeter frame consists of a portion of the end and edge filler plates, a 3.175-mm (0.12-in.) closeout strip, and a load adapter filler plate. Face sheets on each side of the frame formed the sandwich structure.

Brazing of these panels also was performed, using the inert gas pressure technique. Solution-heat-treating was performed without the use of a fixture and panels were quenched in the "UCON-A"/water solution. Only minor straightening of the panels was required. After straightening, the manifold caps

were fusion-welded to the inlet manifolds. During welding of the first unit, the panel edges bowed up toward the weld approximately 1.52 mm (0.060 in.) in the area of the manifold. During straightening, a small dent developed in the skin on the side opposite the weld. When the second panel manifold cap was welded, a reverse bow was pre-formed on the panel which compensated for weld shrinkage and straightening was not required. Both panels were then aged to the T-6 temper. After final machining, both panels successfully passed the pressure test of 1.724 kPa (250 psi) and the helium leak test. No leaks were detected.

The two panels weighed a total of 904 grams (1.99 lbm). The finished specimen which included the machined panels with welded manifold caps, all attach fittings, fasteners, and end-load adapters weighed a total of 10,140 grams (22.35 lbm) as delivered for testing.

Figures 72 through 76 show this fatigue specimen during fabrication stages. Figure 72 shows the two corrugated core sections located within the frame cavity during pre-braze assembly. The edge of the core nested into the manifold "fingers" of the frame are carefully machined for proper fit and location.

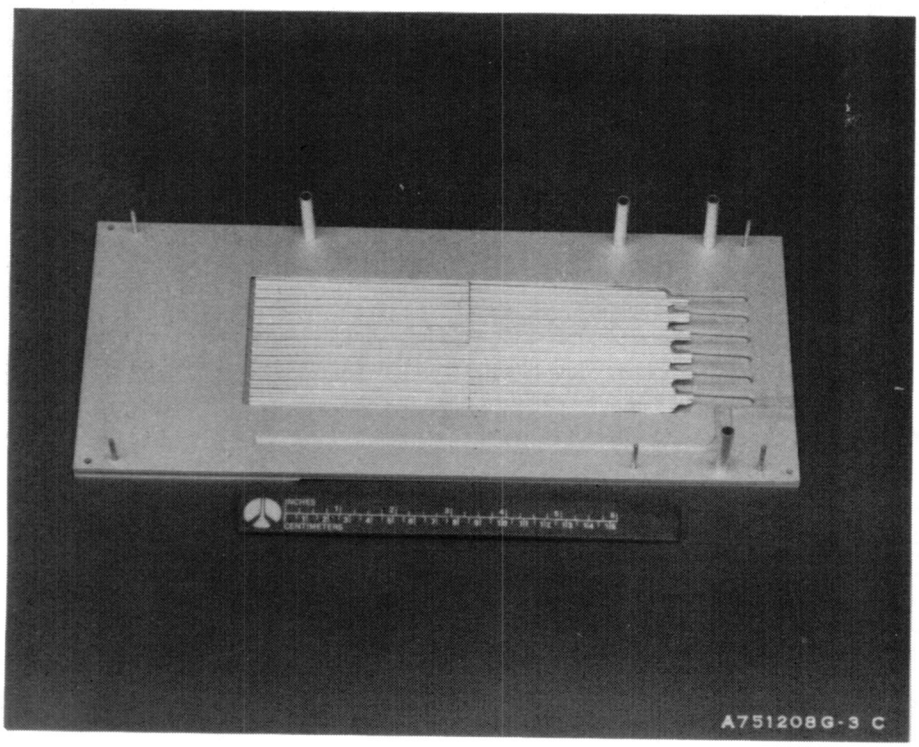

Figure 72. Panel Corner Specimen (PCS)—Specially Machined Core Sections Fit around "Fingers" of Frame

The edge cooling channel machined into the frame is visible. Figure 73 shows the inboard side of the panel immediately after brazing. The small hole in the edge of the panel will later become part of the outlet manifold tube. Figure 74 shows the inboard side of the two panels after solution heat treatment, welding of the manifold caps, aging, and final machining. The outlet manifold protrudes from each panel. Figures 75 and 76 are overall views of the completed specimen with load adapters and the edge stringer attached. Figure 75 shows the moldline side of the completed fatigue specimen. The edge fluid flow channels of the panel are along the abutting edges. The small dent which developed in the moldline side skin during straightening is visible in the far side panel. Figure 76 shows the inboard side of the completed specimen.

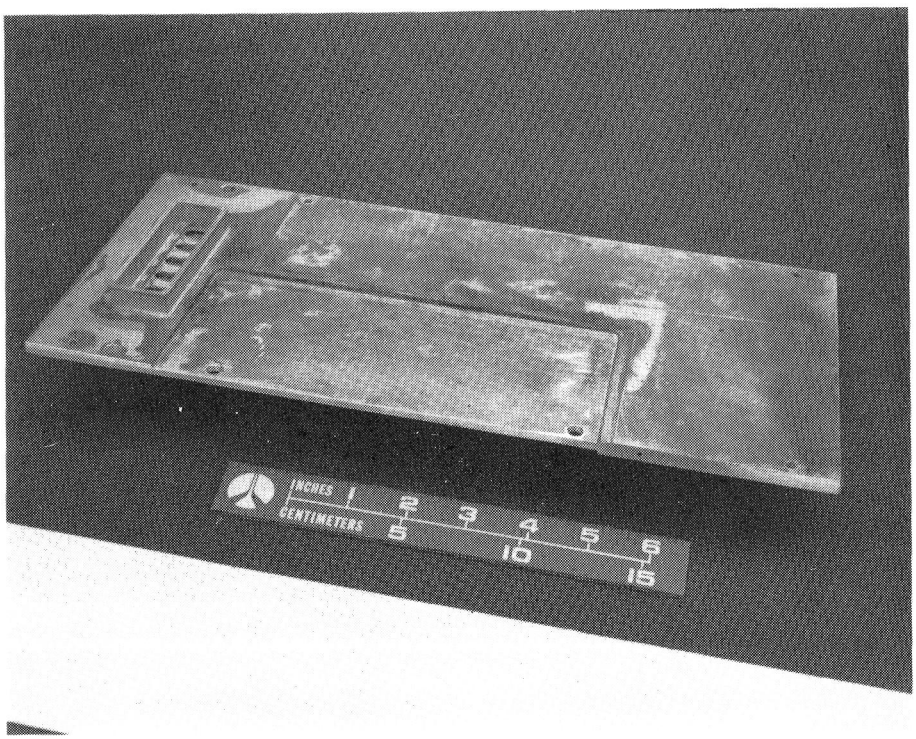

Figure 73. PCS Inboard Side of Panel After Brazing

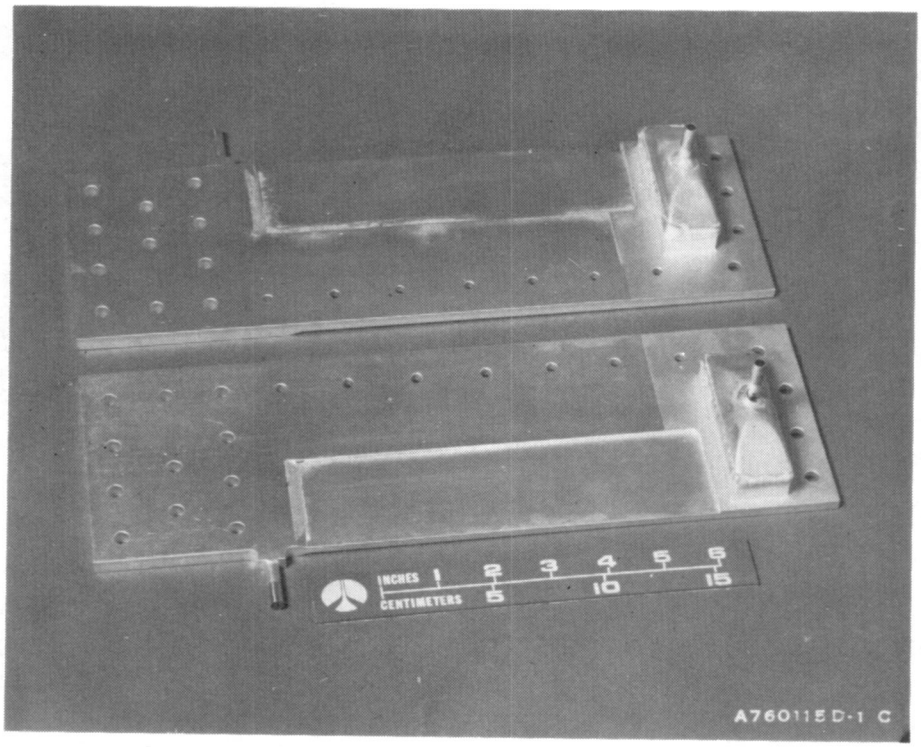

Figure 74. PCS Inboard Side of Two Panels after all Welding, Heat Treatment and Finish Machining. Integrally Fabricated Tubes Form Manifolds.

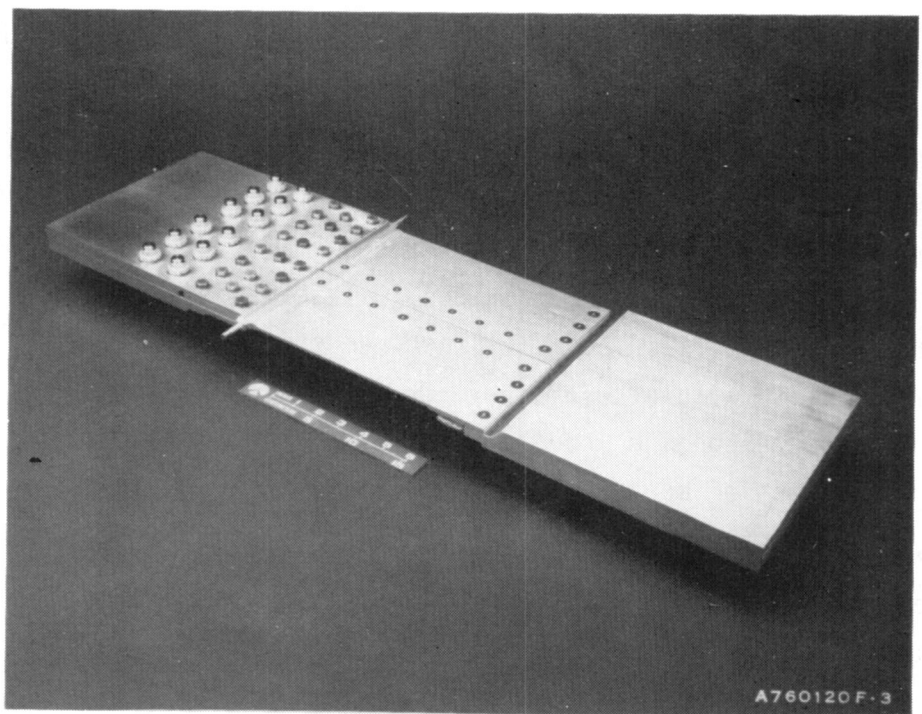

Figure 75. PCS Moldline Side of Completed Fatigue Specimen. Small Dent in Skin Developed during Straightening.

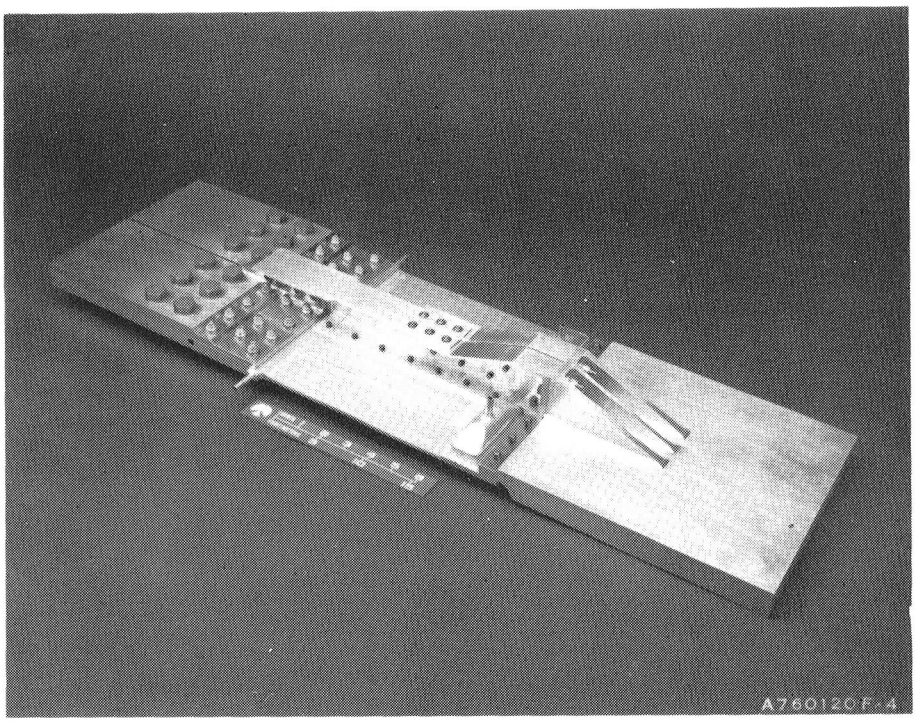

Figure 76. PCS Inboard Side of Completed Fatigue Specimen

End Panel/Interior Stringer Termination Specimen. The third fatigue specimen fabricated was the end panel/interior stringer termination specimen. This specimen is representative of the end of the panel in the vicinity of an internal stringer termination. This specimen was a single panel with two end-load adapters. The panel consists of a flat frame containing two sections of corrugated core and face sheets. The frame contained, in part, the appropriate section of end filler plate from the full-scale design. The core at the inlet end of the panel was specially machined to generally conform to the frame configuration with a sufficient gap for coolant passage. A single inlet manifold was located on the inboard side of the panel. Two outlet tubes were provided for egress of coolant from integrally fabricated parts of the panel.

Brazing of this panel also was performed using the inert gas pressure technique. Again, a fixture was not used during the solution-heat-treating process and "UCON-A" quenchant was used during the quenching operation. After minor hand-straightening of the panel, the inlet manifold cap was fusion-welded to the manifold. Prior to welding, a reverse bow was also pre-formed on this

panel to compensate for the expected weld shrinkage. Again, pre-bowing the panel resulted in an essentially flat panel with no straightening required after welding. The panel was subsequently heat-aged to the T-6 temper. After final machining, the panel successfully passed the helium leak check and the pressure test to 1.724 kPa (250 psi). No leaks were detected. The center stringer section was bonded to the panel before attaching the two end-load adapters.

The total mass of the brazed panel itself (after machining) was 549 grams (1.21 lbm). The finished specimen including the machined panel with welded manifold cap, bonded channel, fasteners, and end-loaded adapters was 7233 grams (15.95 lbm) as delivered for testing.

Figures 77 through 81 show the end panel/internal stringer termination specimen during assembly and fabrication. Figure 77 shows the two corrugated core sections set in proper location in the frame cavity. The hardspot (or insert) is fabricated as part of the fingers of the frame. Figure 78 shows the panel after brazing. The cut-outs visible in the manifold were previously machined in the inner face sheet. Figure 79 shows the panel after the manifold cap has been welded to the base, after heat treatment to the T-6 temper,

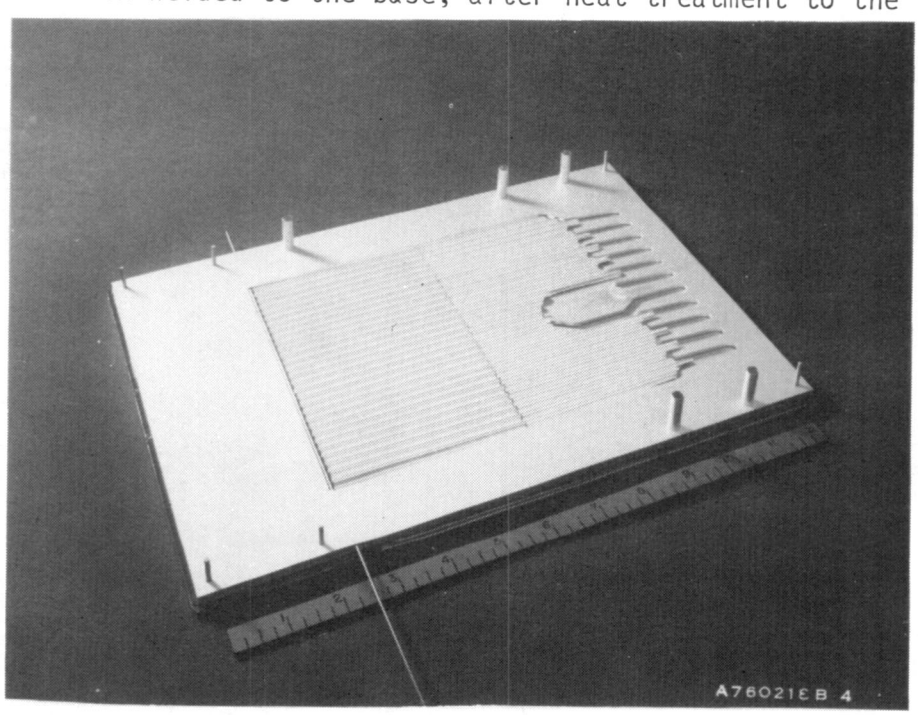

Figure 77. End Panel/Internal Stringer Termination Specimen (EPISTS)— Corrugated Core Sections set in Location in Frame Cavity

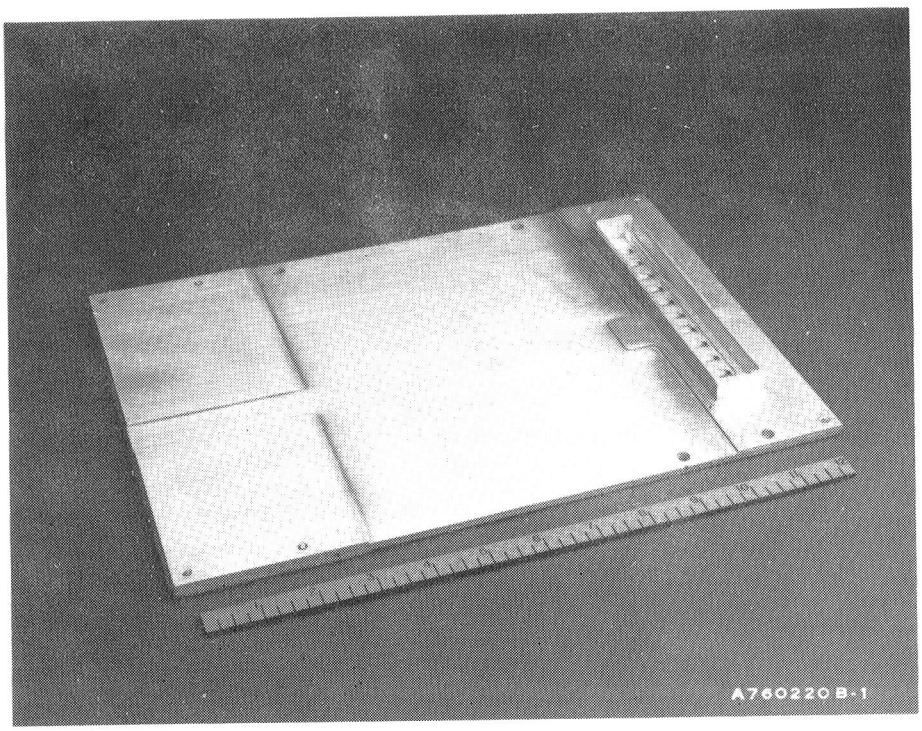

Figure 78. EPISTS Panel after Brazing. Inner Face Sheet Cut-Outs Visible beneath Manifold Base

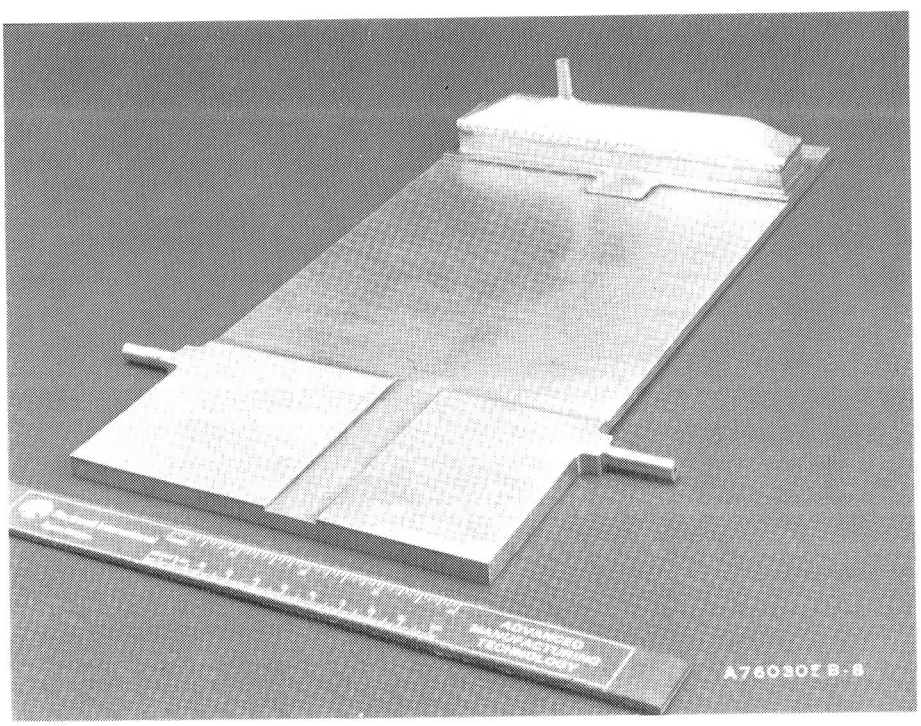

Figure 79. EPISTS Brazed Panel after all Welding, Heat Treatment, and Final Machining

and after peripheral machining to final configuration. Figure 80 shows the inboard side and Figure 81 shows the outer moldline of the completed panel assembly.

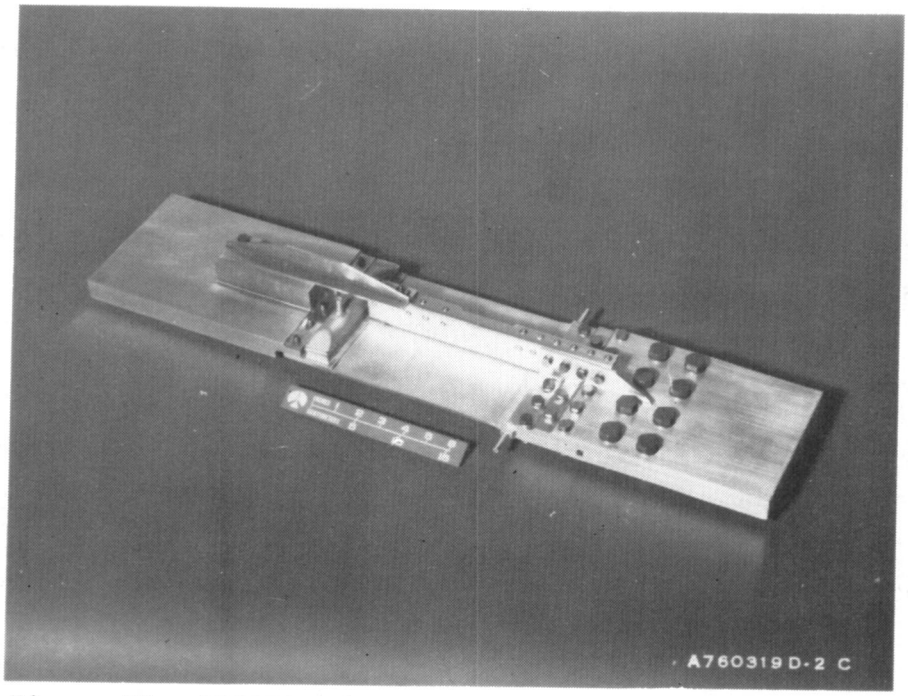

Figure 80. EPISTS Inboard Side of Completed Specimen

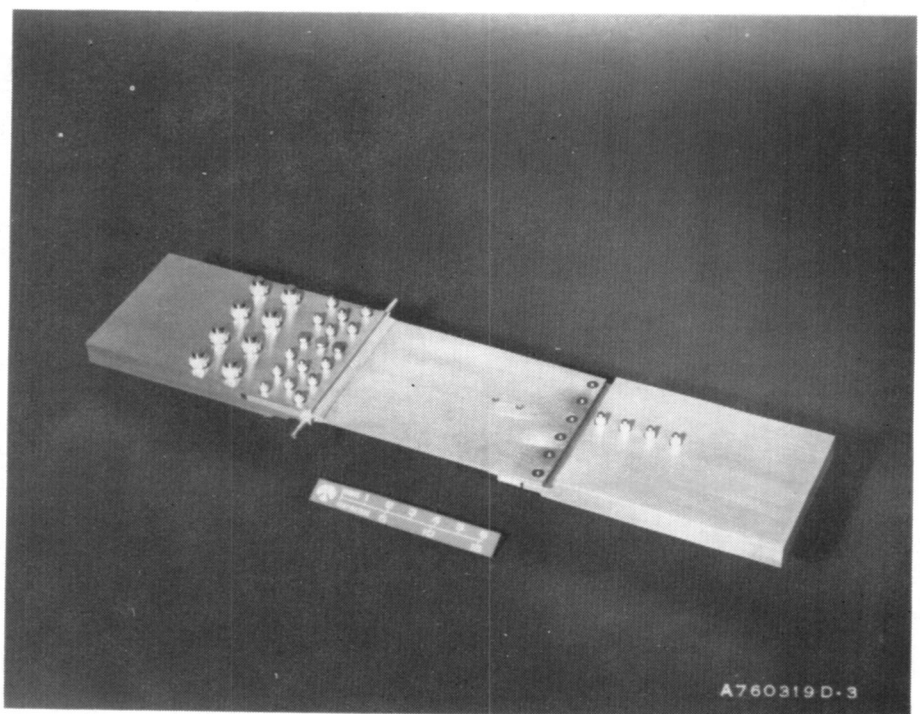

Figure 81. EPISTS Moldline Side of Completed Fatigue Specimen

"Boilerplate" Panel Corner Specimen. The boilerplate corner specimen was fabricated to replace the original panel corner specimen which suffered an edge stringer inboard flange failure during fatigue testing by NASA. This failure precipitated a change to the perimeter fastener system from Cherrylock rivets to Taper-Loc nuts and bolts. The boilerplate specimen incorporated the new fastener system, a localized "beef-up" of the edge stringer inboard flange, strain gauges for monitoring stress distribution during test, and grooved solid-aluminum plates in place of the brazed sandwich panels in the original specimen. The grooved plates have the same bending stiffness as the brazed panels.

Figures 82 and 83 show the completed boilerplate/panel corner specimen with strain gauges attached. Figure 82 is an overall view of the specimen showing the inboard side. The fasteners attaching the panels to the end-load adapters and the bathtub fittings to the center stringer are the new Taper-Loc fasteners. Figure 83 shows the outer surface of the boilerplate specimen.

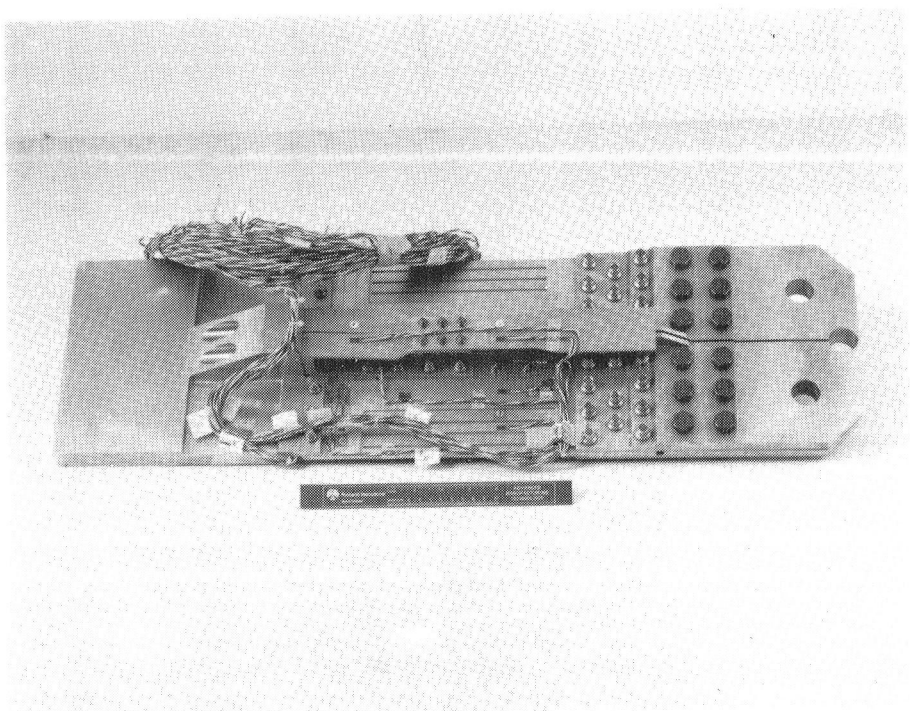

Figure 82. Boilerplate-Panel Corner Specimen (B-PCS)—Inboard Side of Completed Boilerplate Specimen with Strain Gauges Attached

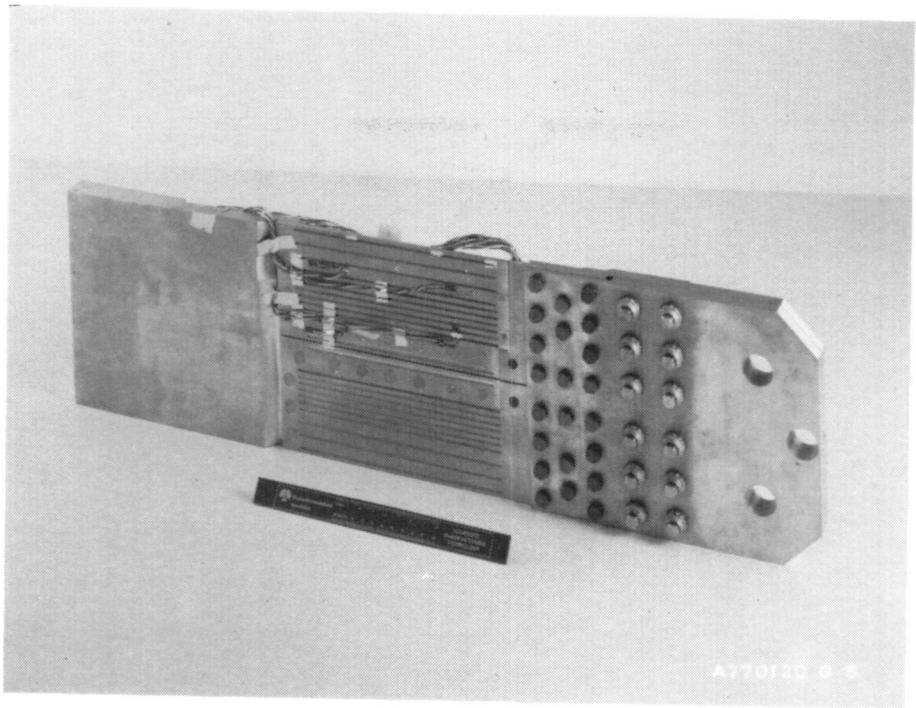

Figure 83. B-PCS Moldline Side of Boilerplate Specimen

APPENDIX E

TEST PANEL

This appendix presents design details that are test-panel-peculiar and a discussion of the thermal, fluid flow, and structural analyses conducted for the test panel and febrication procedure.

Test Panel Design Details

The test panel incorporates all the design features of the first 0.61 m (2 ft) and last 0.61 m (2 ft) of the full-scale panel. The only physical deviations are the edge stringers and conduction plate width. These stringers are channel sections in the test panel and I-sections in the full-scale design. They terminate, and are attached to, a full-scale design configuration bathtub fitting and a dummy bathtub fitting so that the stringer web/bathtub fitting attachment is in double shear as is the case for adjacent full-scale panels. See Figure 84.

The test panel system includes load adapters that attach to the test panel and to the facility load grips. These adapters were designed to simulate, as closely as possible, the structural and thermal interfaces a full-scale panel would encounter in a hypersonic vehicle application. The structural simulation was accomplished by sculpturing the load adapters (Figure 84) to (1) provide a simulation of a main transverse frame cap so that a "flight type" end panel attachment could be made, and (2) duplicate the end panel neutral axis shift (inboard/outboard) across its width so that no test-peculiar local bending occurs at the panel/adapter joint.

The thermal simulation assumed that adjacent full-scale panels would be installed inlet end to inlet end and outlet end to outlet end in order to minimize coolant plumbing mass and thermal stresses. Hence, the load adapter design should be such that during test, when the test panel is subjected to the design heat flux from a quartz lamp system, little or no heat should flow from the test panel to the load adapter and no transverse thermal stress should exist at the test panel/load adapter interface.

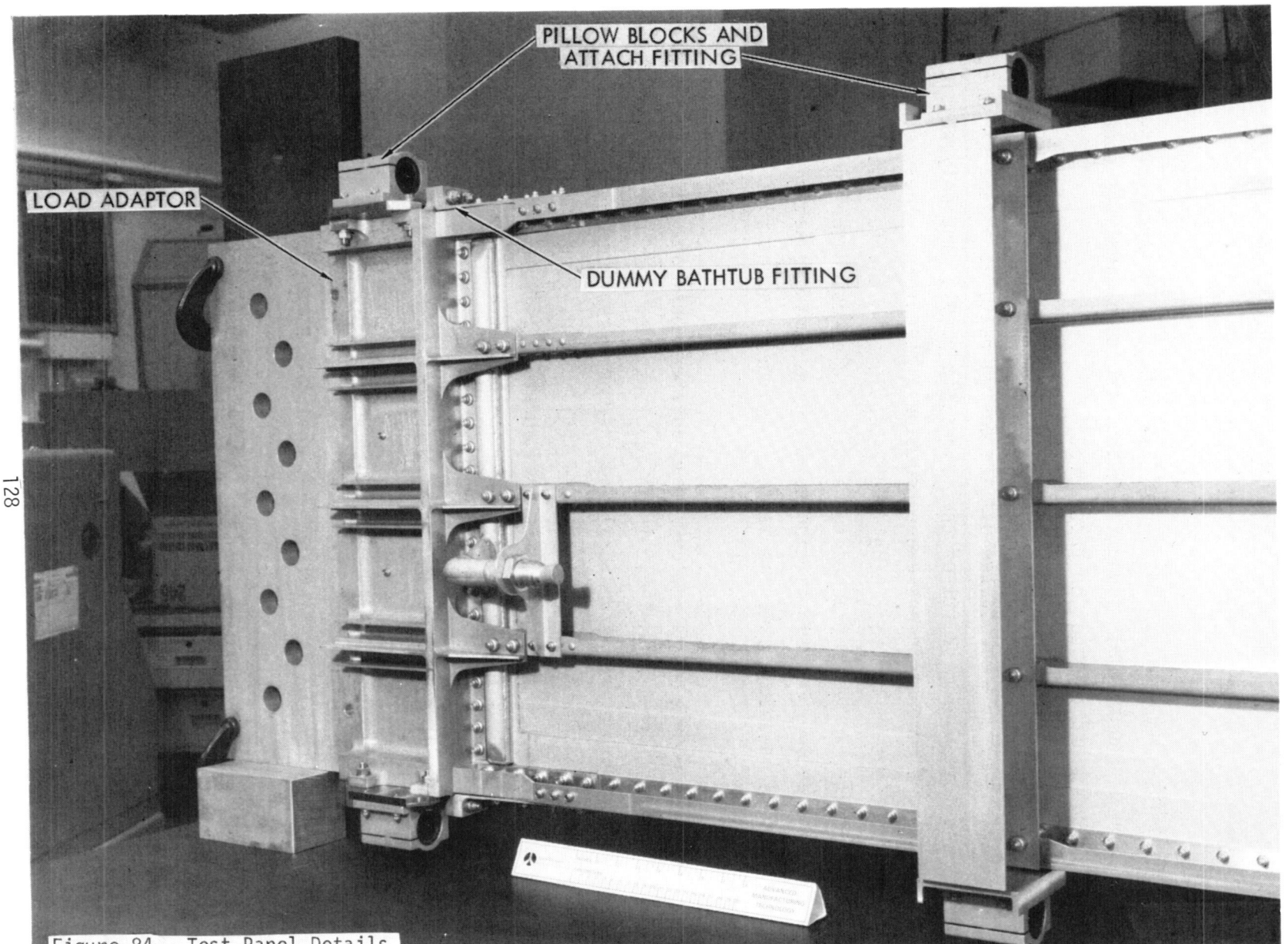

Figure 84. Test Panel Details

Three design options, shown in Figure 85, were considered to meet the above requirements:

1. Titanium links to tie the load adapter to the test panel
2. Elongated or slotted fastener holes
3. Heat strips bonded to the external surface of the load adapter, adjacent to the interface

The titanium link and elongated fastener hole concepts were evaluated and rejected for this application. The titanium links do provide structural continuity while thermally isolating the load adapter from the test panel. The links rotate as the test panel heats up and eliminate joint transverse thermal stress. This concept was dropped because of concern over joint stiffness during full tension/compression fatigue cycling. The elongated or slotted holes would theoretically provide a rigid attachment in the longitudinal direction while allowing unrestrained panel growth in the transverse direction. This concept was dropped because of the precision hole quality required and because of the friction restraint provided by joint clamp-up. In addition, neither concept allowed the structural simulation of the full-scale panel end/main frame joint.

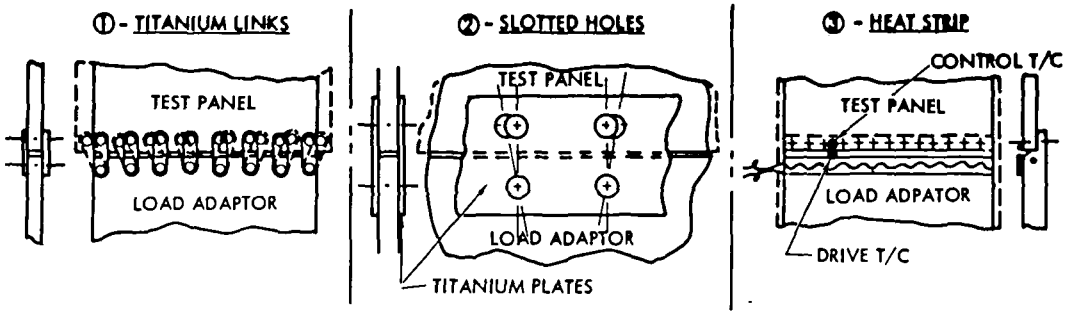

Figure 85. Test Panel/Load Adapter Thermal Interface Options

The heat strip concept was selected. Two 1000-watt, 8.7-ohm heat strips are located on each load adapter adjacent to its interface with the test panel. The heat strips, used in combination with a temperature controller and sensing thermocouples, maintain the temperature of the load adapter at or near the temperature of the test panel end during application of radiant heat to the test panel. This temperature-matching satisfies both design requirements. Heat flow from the test panel to the load adapter is eliminated since both are at approximately the same temperature. No transverse thermal

stresses develop along the fastener line as the load adapter will grow transversely with the test panel as joint temperature increases. The other unique feature of the test panel system is the incorporation of fittings for the attachment of six "pillow blocks" (part of the NASA test facility). These "pillow blocks" are mounted (via bearings) on hardened steel bars which are, in turn, mounted to the test facility structure as shown in Figure 86. This mounting system restricts test panel lateral motion while allowing longitudinal and transverse motion due to axial loads and thermal expansion during test.

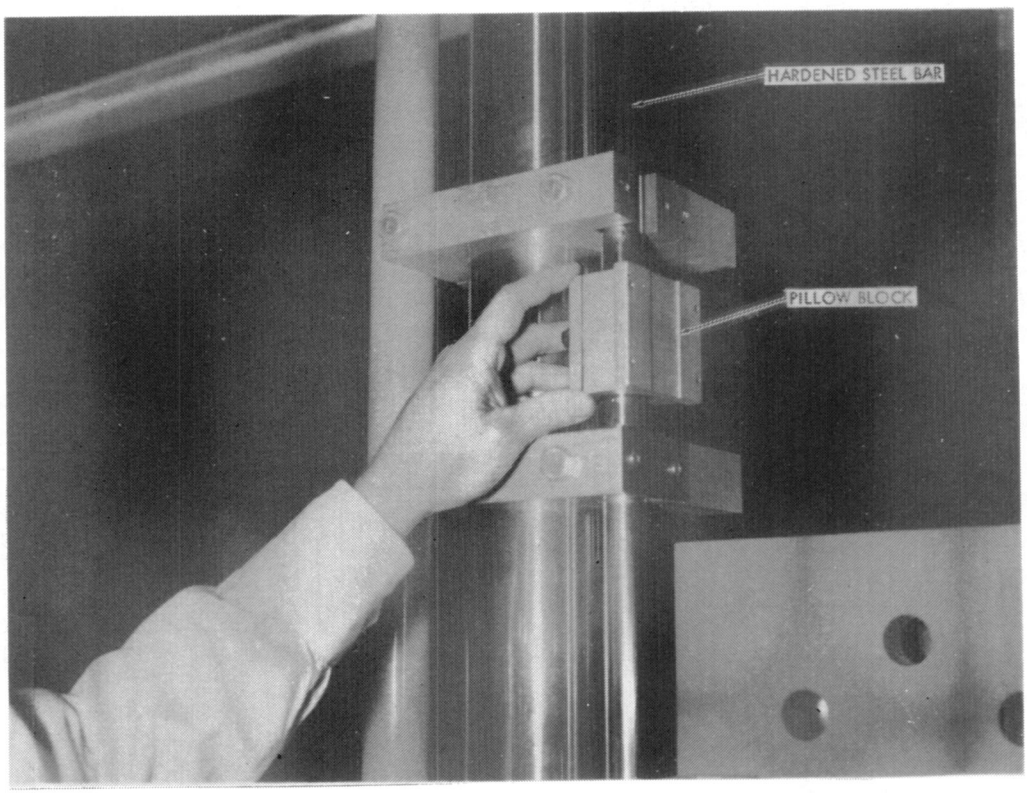

Figure 86. Test Facility "Pillow Blocks"

The channel edge stringer, dummy bathtub fittings, load adapters, and "pillow block" attach fittings of the intermediate transverse frame are shown in Figure 84.

Test Panel Thermal and Fluid Flow Analysis

The test panel is a small-scale version of the full-scale panel discussed in Appendix B. The test panel design uses the same manifold, panel core, edge coolant loop, and edge fastener strip concepts that are used in the full-scale panel. The only difference thermally is panel length. A thermal design objective of the test panel is to simulate 0.61 m (2 ft) of inlet panel core and manifold and final 0.61 m (2 ft)of exit panel core and manifold for testing purposes.

A detailed thermal/hydraulic model of the test panel was constructed as shown in Figure 87. In the model, the coolant flows through the test panel in eight parallel flow channels. The outermost flow channels are edge coolant

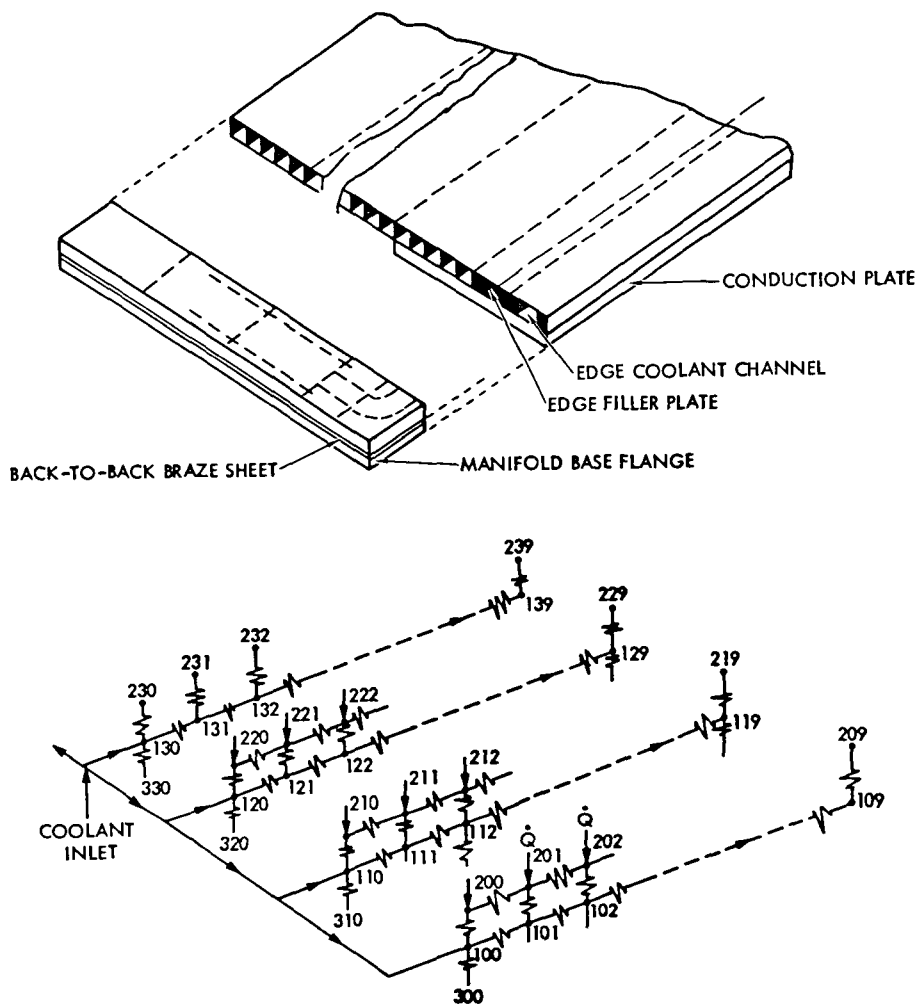

Figure 87. Test Panel Thermal Model

channels that are 0.477 cm (0.188 in.) wide by 0.198 cm (0.08 in.) deep. The solid portion of the edge filler strip is inboard and adjacent to each edge coolant channel. Immediately inboard of the solid filler strip is a coolant channel that is located directly over the conduction plate. The remaining panel surface is divided into four equally sized coolant channels. Due to symmetry, only four of the coolant channels are shown in the figure. The hydraulic circuits were completed by connecting each coolant channel to the inlet and outlet manifolds.

Each coolant channel is divided into eight equal-length sections to define nodes for the thermal model. The top and bottom surfaces of coolant channel sections are defined as structure nodes. Convective-type conductances connect the structure nodes with the coolant nodes. The coolant side heat transfer area is increased slightly to account for fin effects within the tubes. The structure nodes were interconnected with conduction-type conductances. The structure nodes also were connected to the induced and natural environments by aerodynamic heating and radiation conductances.

This thermal/hydraulic model was used with Rockwell's THAP computer program (Reference 7) to predict fluid and structure temperature distributions and pressure drops within the test panel. The calculations were made for an inlet coolant flow rate of 13,600 kg/hr (30,000 lbm/hr) and an inlet temperature of 289 K (60°F). This corresponds to the coolant inlet conditions selected for the full-scale panel. No attempt was made to select a test panel inlet condition, which would result in a test panel outlet temperature distribution similar to that predicted for the full-scale panel.

Predicted fluid and structure temperature distributions for the nine selected locations on the test panel are presented in Figure 88. Locations (4), (7), and (8) are coolant temperatures. The coolant temperature increases linearly with distance from the inlet manifold. The maximum coolant temperature of 310 K (98°F) occurs in the edge coolant channel (coded (4)) near the entrace to the exit manifold. Locations (2), (9), and (5) are for outboard moldline structure temperatures, and Location (1) represents the temperature along the fastener line. The maximum structure temperature of 393.9 K (240°F) occurs on the fastener strip (coded (1)) approximately 0.95 m (3.1 ft) down the panel from the inlet manifold. Beyond this point, the temperature drops

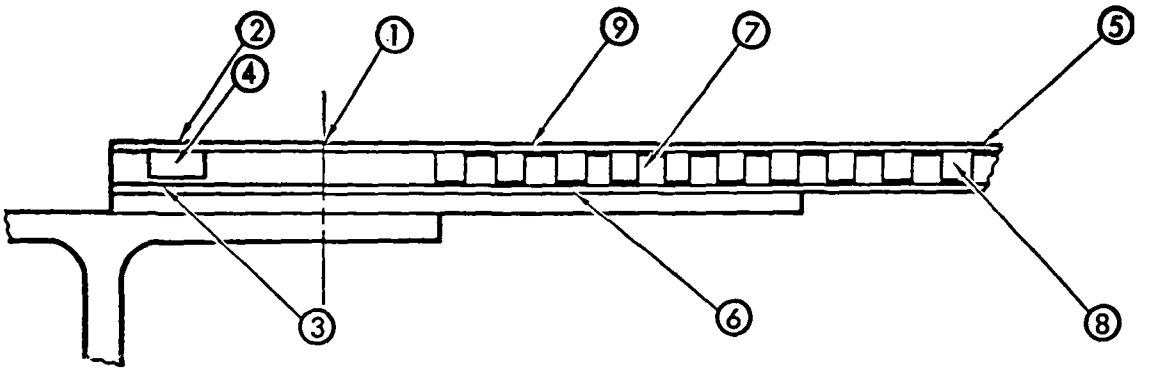

FLOW RATE = 13,608 KG/HR (30,000 LBm/HR)
INLET PRESSURE = 827.4 KPa (120 PSI)
INLET TEMPERATURE = 289°K (60°F)

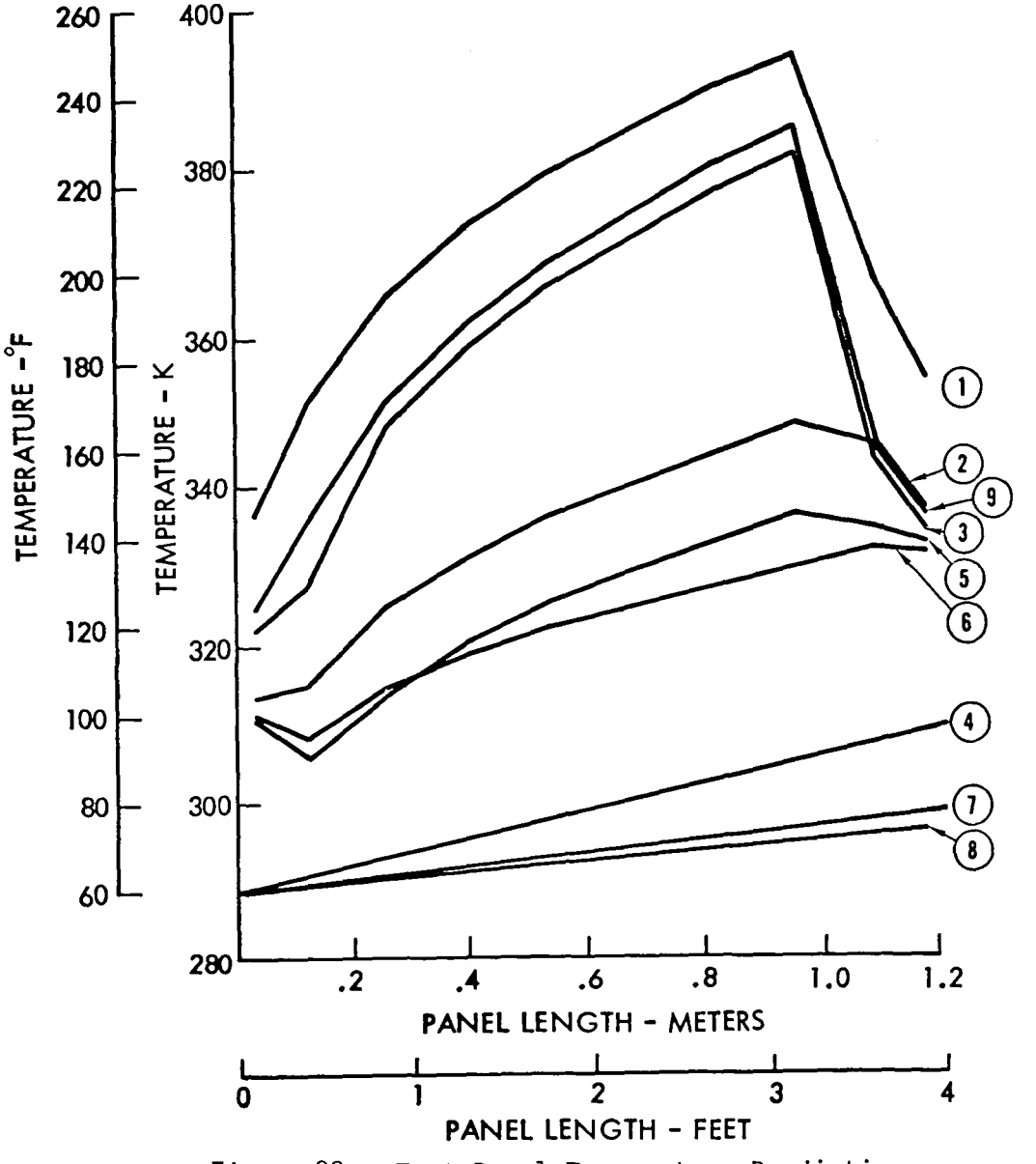

Figure 88. Test Panel Temperature Predictions

quickly to 353.9 K (177°F) near the outlet manifold. The other structure temperatures display a similar trend. A possible explanation is longitudinal conduction through the panel face sheets into the manifold. The relatively massive panel end/manifold structure provides a good conduction path to the coolant fluid in the manifold. Due to inlet and secondary flow effects, the value of coolant thermal conductance at the exit manifold is approximately double its value in the main panel coolant channels. The validity of the temperature predictions must be verified by test.

Temperature distributions for the structural support stringers were determined. Selected temperatures for the edge stringer adjacent to the edge fastener strip are summarized in Table 13.

Table 13. Test Panel Edge Stringer Temperature Predictions

Panel Location	Stringer Location					
	Outboard Flange		Web		Inboard Flange	
	K	(°F)	K	(°F)	K	(°F)
Panel inlet	326.5	(127.7)	325.1	(125.2)	324.9	(124.9)
Panel midpoint	355.0	(179.1)	350.2	(170.4)	349.3	(168.7)
Panel outlet	373.6	(212.5)	366.7	(200.1)	365.3	(197.6)

A pressure drop of 34.5 kPa (5 psi) is predicted for each inlet/outlet manifold for the design coolant inlet conditions of 13,600 kg/hr (30,000 lb/hr) and 288.9 K (60°F). This prediction includes the effects of 90-degree bends, flow expansion, fittings, and fluid friction within the manifold. The predicted coolant pressure drop through the 1.2-m (4-ft) long plate fin sandwich is 125.6 kPa (18.2 psi). Therefore, the expected coolant pressure drop for the entire test panel is 194.6 kPa (28.2 psi).

Load Adapter Thermal Analysis

A detailed thermal analysis of the load adapter with heat strips was conducted to determine:

1. Steady-state temperature distributions of the load adapter when the test panel end is at the full-scale design predicted maximum temperature of approximately 408.3 K (275°F); this assumes that this temperature can be achieved by varying coolant inlet conditions during test.

2. Transient response time to heat the load adapter with heat strips with different power ratings.

The axial load input system consists of an aluminum load adapter plate, carbon-steel load grips, and a load cell connector. A typical cross-section is shown in Figure 89 along with the nodes and conductances of the thermal model. Polyurethane foam 2.54 cm (1.0 in.) thick is installed around the load adapter and load grips to reduce heat loss to the environment. Two 1000-watt, 8.7-ohm electric strip heaters are mounted on the outboard side of the load adapter near the test panel to load adapter interface. An asbestos strip 0.32 cm (1/8 in.) thick separates the heaters from the foam insulation. Polyimide glass fabric 0.635 cm (1/4 in.) thick is installed between the load adapter and the load grips to reduce the heat transfer to the facility hydraulics.

The thermal model consists of 34 nodes and 51 conductances. Referring to Figure 89; Nodes 10, 20, and 30 represent the load adapter, Nodes 40, 50, and 60 represent the load grips, and Node 72 represents the load cell connector. Additional nodes are used to represent (1) the foam insulation at locations adjacent to the major component nodes, (2) the interface between the load adapter/load grips and the foam insulation, and (3) the external surface of the foam insulation. All of these nodes are connected to each other by conduction-type conductances using the appropriate dimensions and thermal conductivities. Node 1 represents the 294.4 K (70°F) room environment. Insulation external surfaces and other exposed surfaces are connected to Node 1 by convection-type conductances.

The temperature distributions within load adapter components were predicted using the model described above with Rockwell's General Thermal Analyzer Program. A detailed description of working equations and operating procedures is presented in Reference 18. This digital computer program solves diffusive processes by approximating the physical system with a lumped parameter representation and by using an electrical thermal analog network. The program is very similar to the Thermal Hydraulic Analyzer Program in many respects, but is more efficient to use when detailed hydraulic calculations are not required.

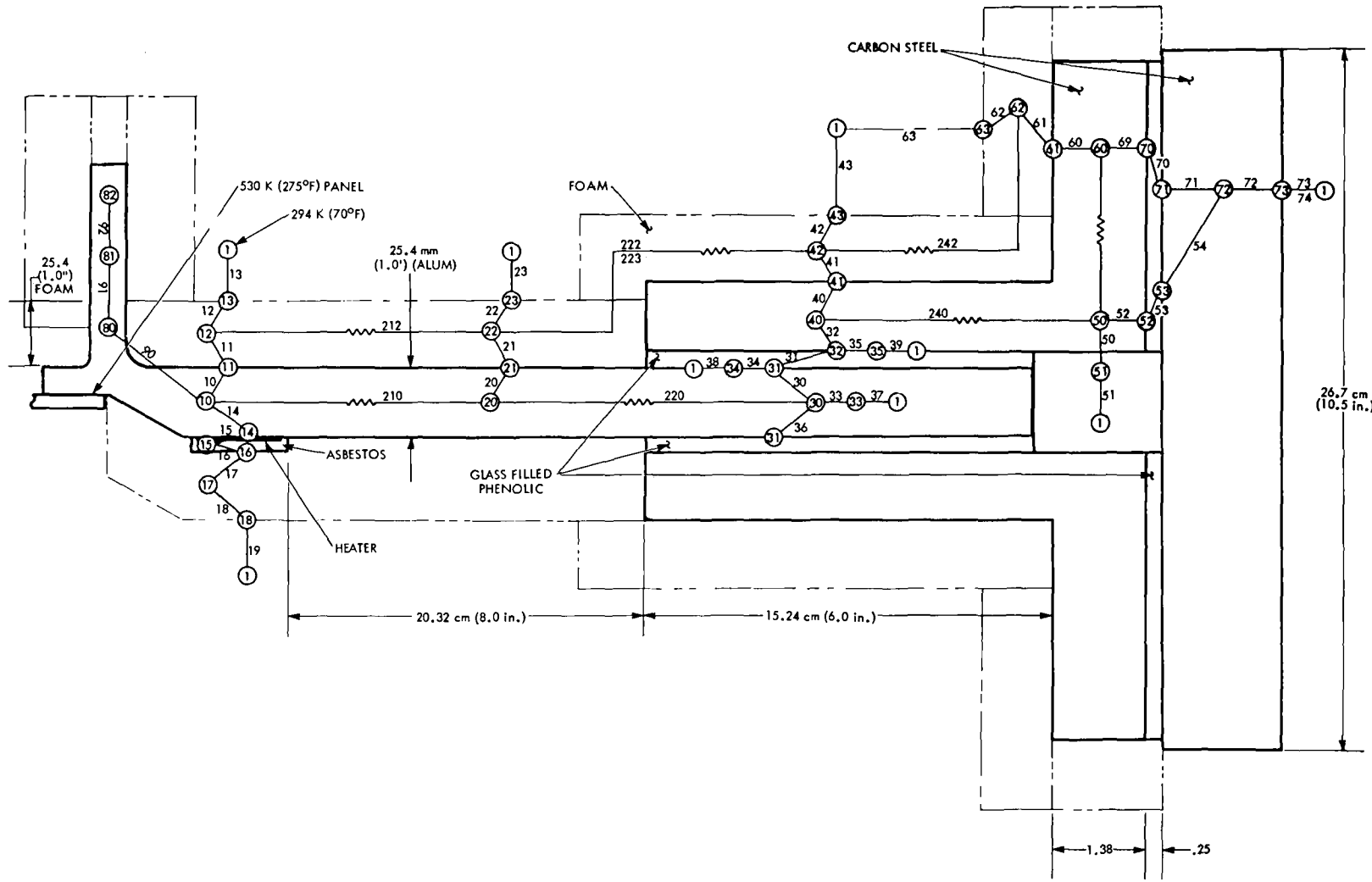

Figure 89. Load Adapter Schematic and Thermal Model

Predicted steady-state temperature distributions for load adapter, load grips, and hydraulic cylinder connector are presented in Table 14. These temperatures assume a test panel/load adapter interface temperature of 408.3 K (275°F). This interface temperature is within a few degrees of the maximum temperature predicted for the outlet end of the full-scale panel.

Table 14. Load Input System Temperature Distribution

Node	Location	Temperature K	(°F)
10	Test panel/load adapter	408.3	(275)
20	Load adapter midpoint	394.4	(250)
30	Load adapter/end	374.4	(214)
40	Load grips	342.7	(157)
50	Load grips	339.4	(151)
60	Load grips	338.9	(150)
72	Load cell connector	310.0	(98)

The strip heater power required for steady-state operation is estimated to be 430 watts. Additional power will be required to heat up the load adapter during panel warmup. This additional power requirement should be well within the capability of the two 1000-watt heat strips.

Test Panel Stress Analysis

This section of the appendix presents the structural analysis of the test panel designed to represent a shortened version of the final full-scale actively cooled structural panel configuration. The test panel less the load adapters is 0.6096 m (2 ft) wide by 1.2192 m (4 ft) long. A description of the test panel is given in Section 4.0. The stress analysis of the test panel uses the approach taken for full-scale panel (Appendix B) as a baseline employing the same analysis methods, and techniques.

Like the full-scale panel, the test panel was modeled in NASTRAN as a three-dimensional structure with 1096 degrees of freedom. This model, which was developed from the full-scale panel model, represents the entire test panel in addition to the two load adapters. Also included are the six attachments (two on each load adapter and two on the intermediate frame simulator)

to the test facility through the pillow blocks. A description of the model using a CRT plot which shows the node point numbering system is depicted in Figure 90. In the model, the sandwich panel is divided into 15.24-cm (6.0-in.) long by 7.62-cm (3.0-in.) wide elements for which sandwich plate bending elements are used. Beam elements are used to represent the single intermediate frame and the stringers. The load adapters are represented by a combination of plate-bending elements and offset beam elements. These are connected to the appropriate panel and adapter node points. This model was used to determine the internal load and stress distributions, nodal forces, and nodal deflections for the applied mechanical load and thermal test conditions in order to assure that the test conditions duplicate the full-scale panel structural design conditions, and to provide predicted data which can be compared to the test data.

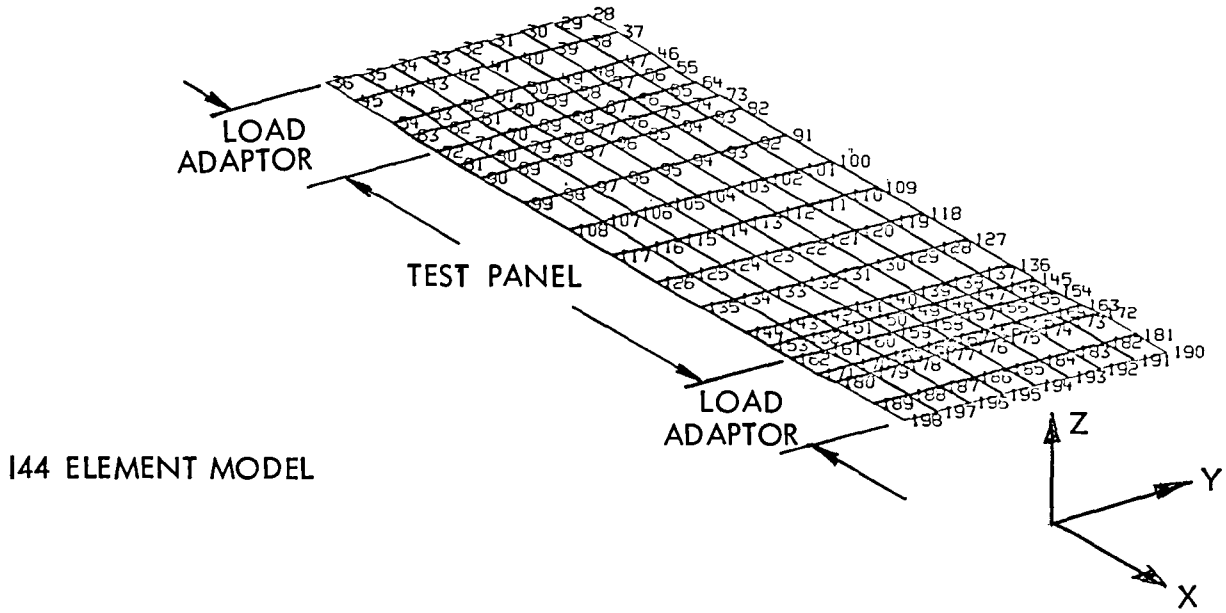

Figure 90. Test Panel and Load Adapter NASTRAN Model

A major part of the test panel structural analysis was the design development of the load adapters. This involved the same iterative procedure of initial sizing, modeling, analysis, model revision, and rerunning the analysis as described for the full-scale panel design development and stress analysis in Appendix B. The objective of the load adapter design development was to

provide a load interface at the test panel/adapter attachment which would duplicate the boundary conditions of adjacent full-scale panels attached end-to-end across a large hypersonic aircraft main frame. Specifically, the test machine applied concentrated load must be distributed at the panel interface in such a manner as to match the panel axial stiffness and neutral axis profiles. In addition, the adapter design must incorporate the aircraft main frame design considerations and stiffness parameters that were selected for the full-scale panel design. The results of the test panel structural analysis showed that the load adapter design objective was achieved.

With the load adapter design firmed up, the next step was to predict test panel stresses and deflections resulting from the application of a 210.15 kN/m (1200 lbf/in.) axial load and a heat flux of 136.19 kW/m^2 (12 Btu/ft^2•s). This duplicates the full-scale design environment with the exception that the lateral load of ±6.9 kPa (±1 psi) is ignored.

The predicted thermal distribution for the test panel/load adapter is shown in Figure 91. This distribution was developed by combining results of the thermal analyses conducted for the test panel and load adapters, as discussed earlier in this appendix.

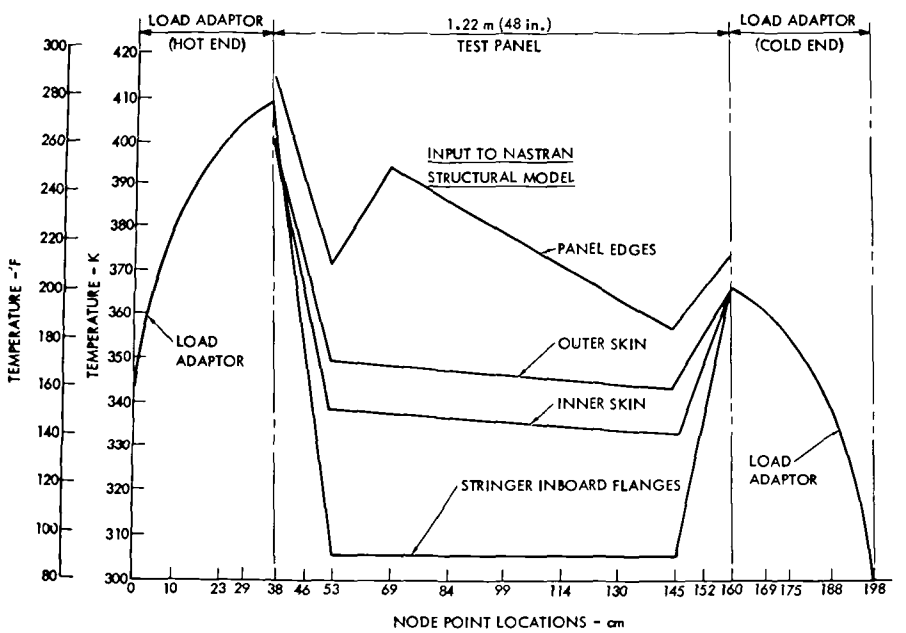

Figure 91. Test Panel Temperature Distribution used for Structural Analysis

The computerized stress analysis predicts thermal and mechanical stresses separately. The results are plotted in Figures 92 through 94. Figure 92 presents the test panel brazed sandwich maximum predicted stress levels across the panel width at selected locations down the panel length. These selected

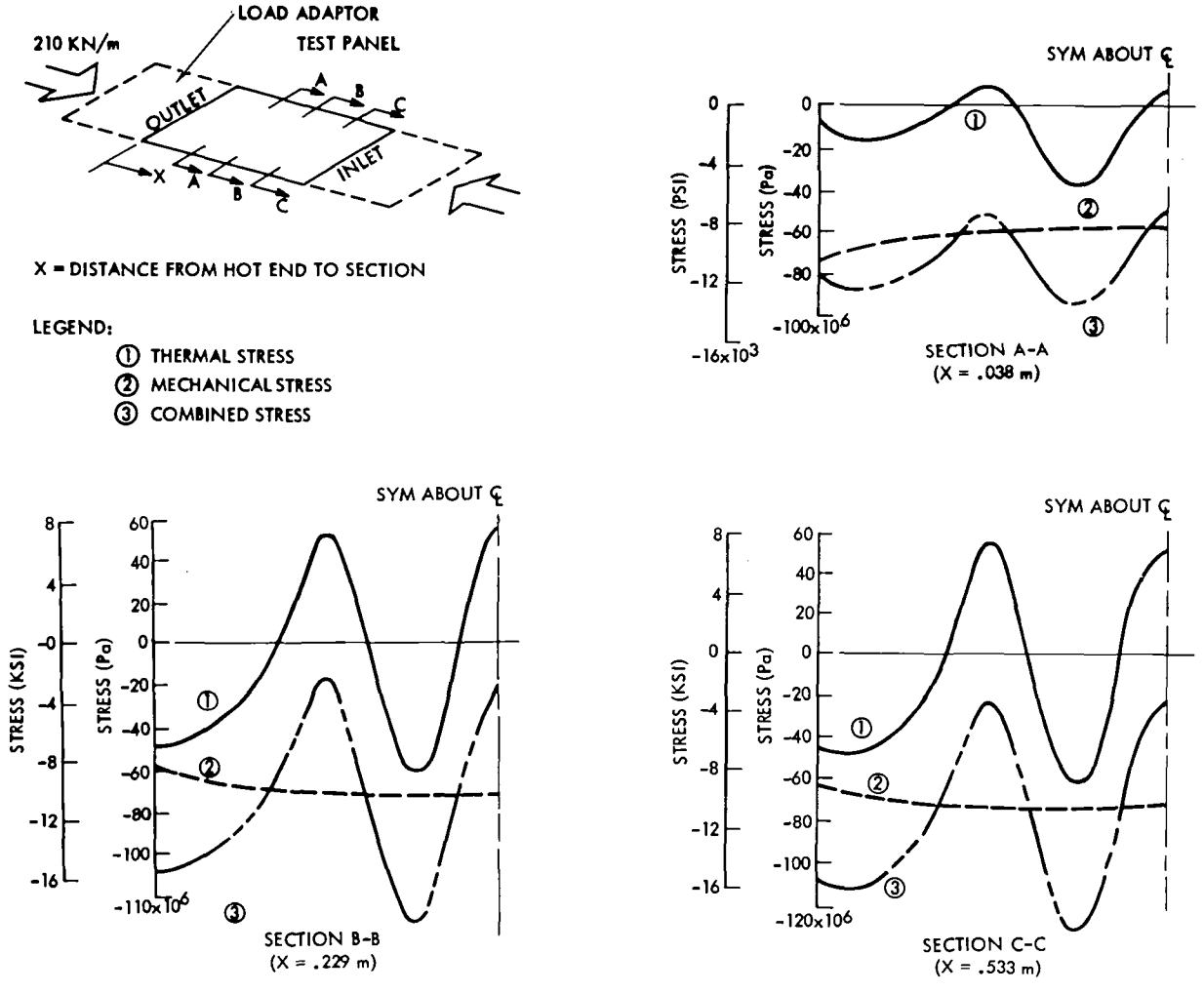

Figure 92. Test Panel Brazed Sandwich Stresses

locations are where the stress levels are maximum. Figure 93 plots stringer flange (inboard and outboard) stresses as a function of stringer length. Figure 94 plots predicted test panel lateral deflection under the influence of the test environment. Combining the mechanical and thermal stresses or deflections at any given panel location results in the predicted strain gauge or deflectometer values to be encountered during test.

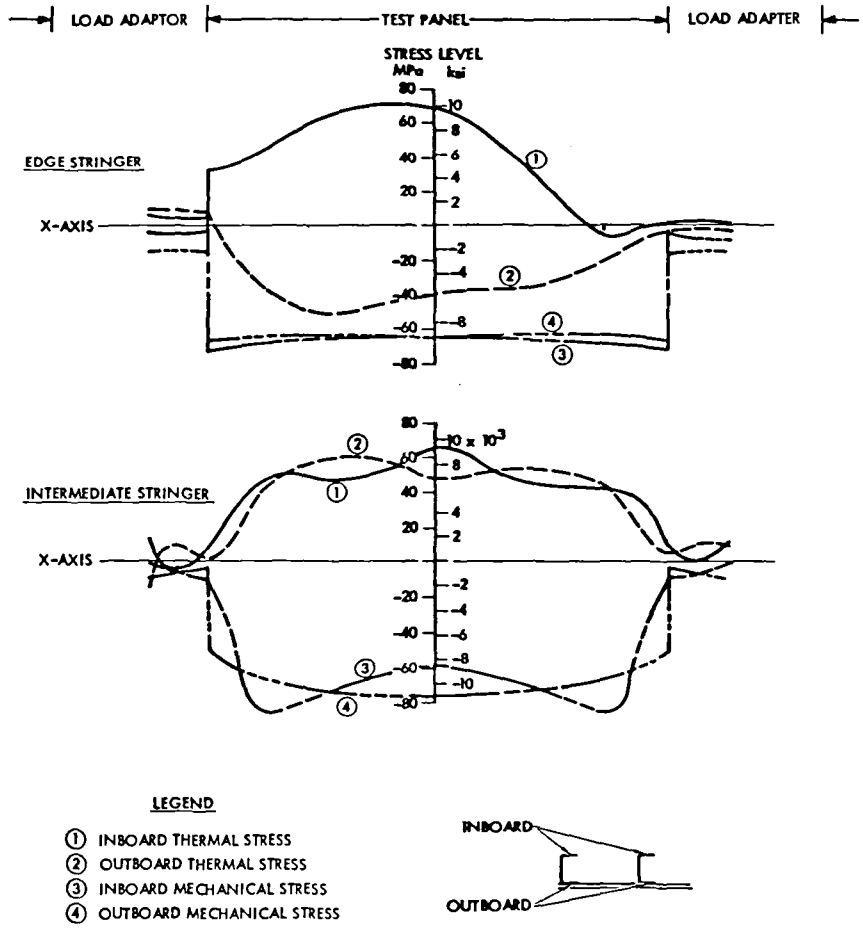

Figure 93. Test Panel Stringer Stresses

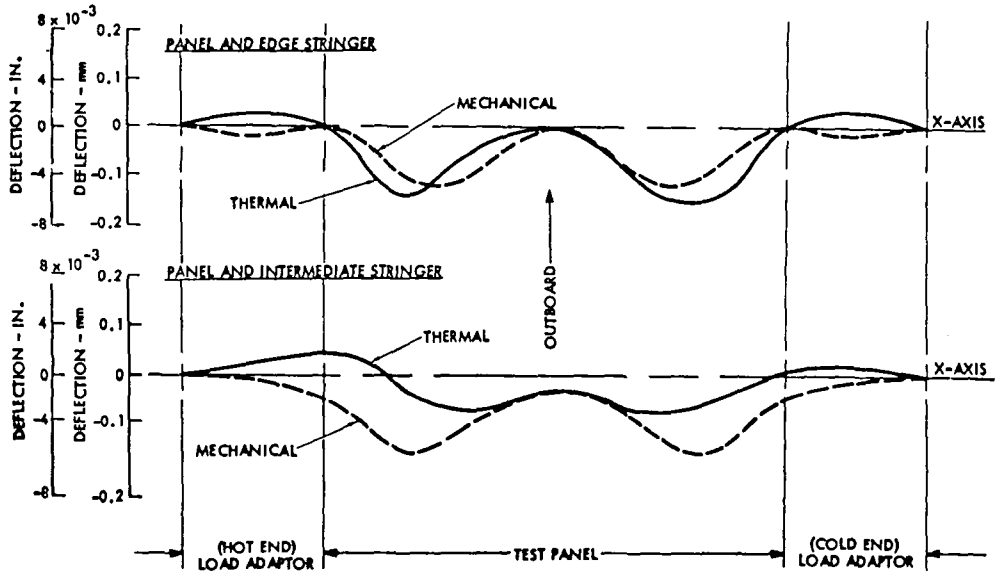

Figure 94. Test Panel Deflection Predictions

An important assumption applied to the full-scale panel analysis and carried into the test panel analysis was the small effect of imperfect fabrication with respect to panel flatness (Ref. Appendix B). Therefore, the completed test panel was inspected for flatness. The resulting inspection record with appropriate notes is shown in Figure 95. The positive measurements are outboard from the theoretical moldline, and the negative or minus measurements are inboard. These data indicate a maximum longitudinal flatness tolerance between transverse frames of approximately ±0.30 mm (0.012 in.), which is well below the 0.79 mm (0.031 in.) assumed for the full-scale and test panel analyses.

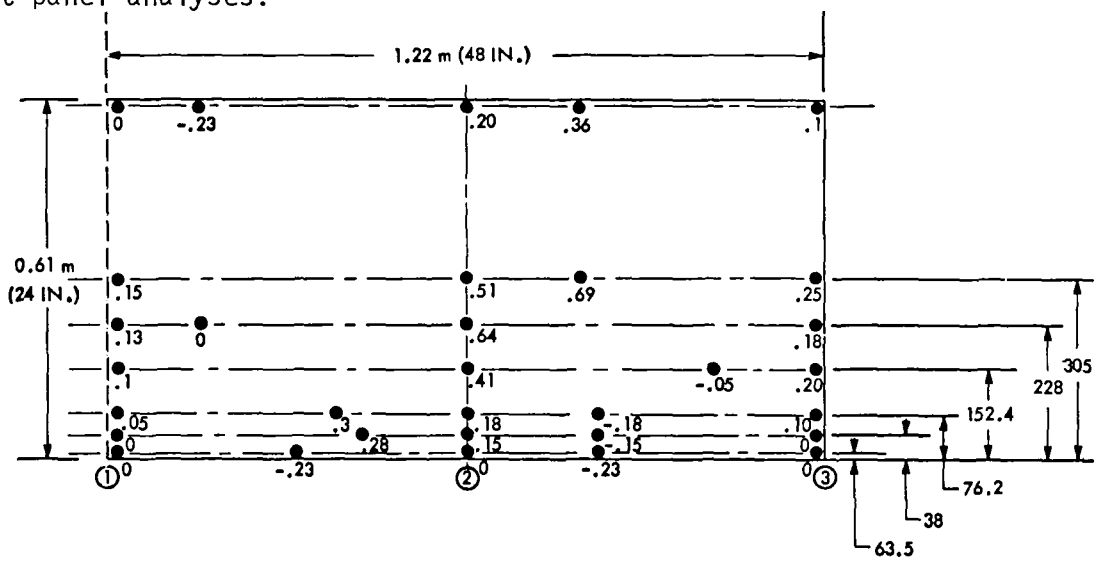

NOTES:

1) MEASUREMENTS IN mm TAKEN FROM OUTER MOLD LINE SURFACE
2) POINTS ① ② AND ③ SET AT ZERO INITIALLY
3) LOAD ADAPTORS AND INTERMEDIATE FRAME INSTALLED
4) MEASUREMENTS TAKEN AT ENDS, MIDPOINTS AND WHERE PEAKS/VALLEYS OCCUR
5) DIMENSIONS IN mm UNLESS OTHERWISE NOTED

Figure 95. Test Panel Out-Of-Flatness Inspection Results

Because of the achievement of the load adapter design objective, the stresses and deflections computed for the test panel are almost identical to those computed for the full-scale panel. Therefore, the summary of minimum margins of safety presented in Appendix B (Table 7) for the full-scale panel is applicable to the test panel. Three additional minimum margins that are of particular interest to the test panel are shown in Table 15.

Table 15. Test Panel Supplementary Structural Margins of Safety

	FAILURE MODE	APPLIED STRESS	ALLOWABLE STRESS	M.S.
1	STRINGER CAP (ULT TENS.)	175.8 MPa (25,500 PSI)	455 MPa (66,000 PSI)	1.58
2	STRINGER BOND (ULT SHR)	4.3 MPa (624 PSI)	6.9 MPa (< 1,000 PSI)	.60
3	PANEL (COMP YIELD)	117.2 MPa (17,000 PSI)	190.3 MPa (27,600 PSI)	.62

Test Panel Fabrication Details

The final piece of hardware fabricated in this program was the 0.61-m by 1.22-m (2- by 4-ft) actively cooled structural test panel with load adapters. This panel contained all three of the critical areas tested as fatigue specimens and was representative of the 0.61-m by 6.1-m (2- by 20-ft) full-scale panel in all respects except length.

The 0.61-m by 1.22-m (2- by 4-ft) test article contained one panel with associated support structures and two end-load adapters. The inlet and outlet manifolds of the panel were raised from the flat plane and were welded-cap assemblies approximately 0.5 m (20 in.) long running transverse to the panel length. Figure 96 is a composite sketch of the lay-up of all components comprising the 2- by 4-foot brazed sandwich structure. Details were assembled as shown in the sketch and all joints were brazed simultaneously during a single brazing operation. This panel consisted of a flat frame which contained two edge filler plates and two end filler plates. The frame was a fabricated

detail with fusion welds at the four corners. These welds were radiographed to assure that the joint areas were free of voids and cracks. Because of the length of the panel, four sections of corrugated core were contained within the frame. The core sections at the inlet and outlet ends of the panel were machined to conform to the configuration of the frame fingers and inserts. The core contained three hardspots in the center section of the panel for subsequent attachment to the intermediate frame. Filler bars were placed in convolutions of the core to provide support and to maintain alignment of convolutions at butting edges of the core sections. Face sheets (utilizing clad brazing material) on each side of the frame closed out the sandwich structure. Two conduction plates are placed on the inboard face sheet over the edge filler plates. Manifold bases are located on the inboard face sheets over the frame "fingers" with two-sided braze sheets placed between the skin and manifolds to effect the braze joints. The face sheets and conduction plates contain braze alloy clad to the joint faying surfaces.

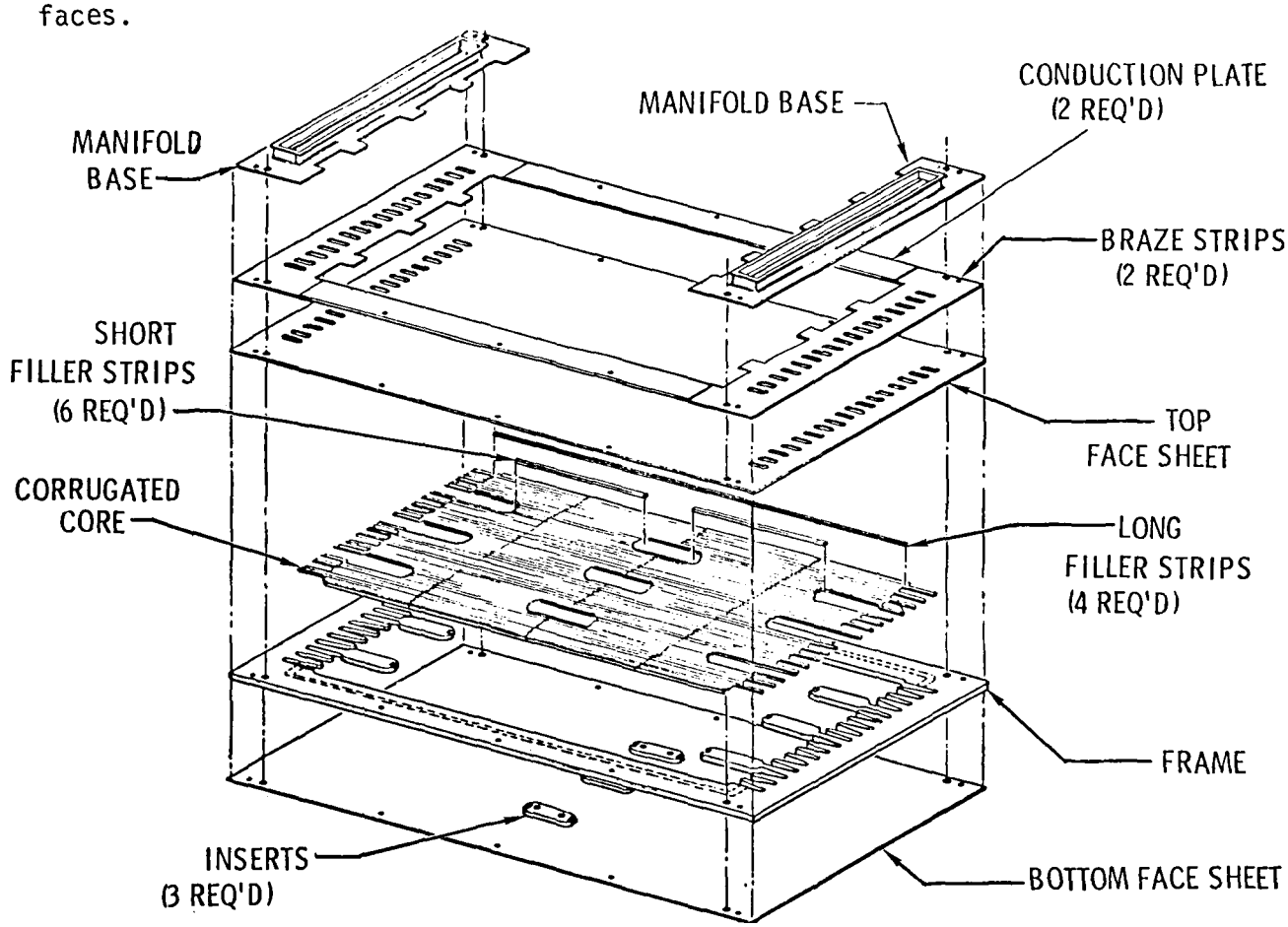

Figure 96. Brazed Sandwich Structure Component Lay-Up

Judicial use of tooling materials and their dimensional tolerances are critical in heated platen press retort brazing of assemblies of which this test panel is typical. Figure 97 is a composite sketch of the tooling lay-up used

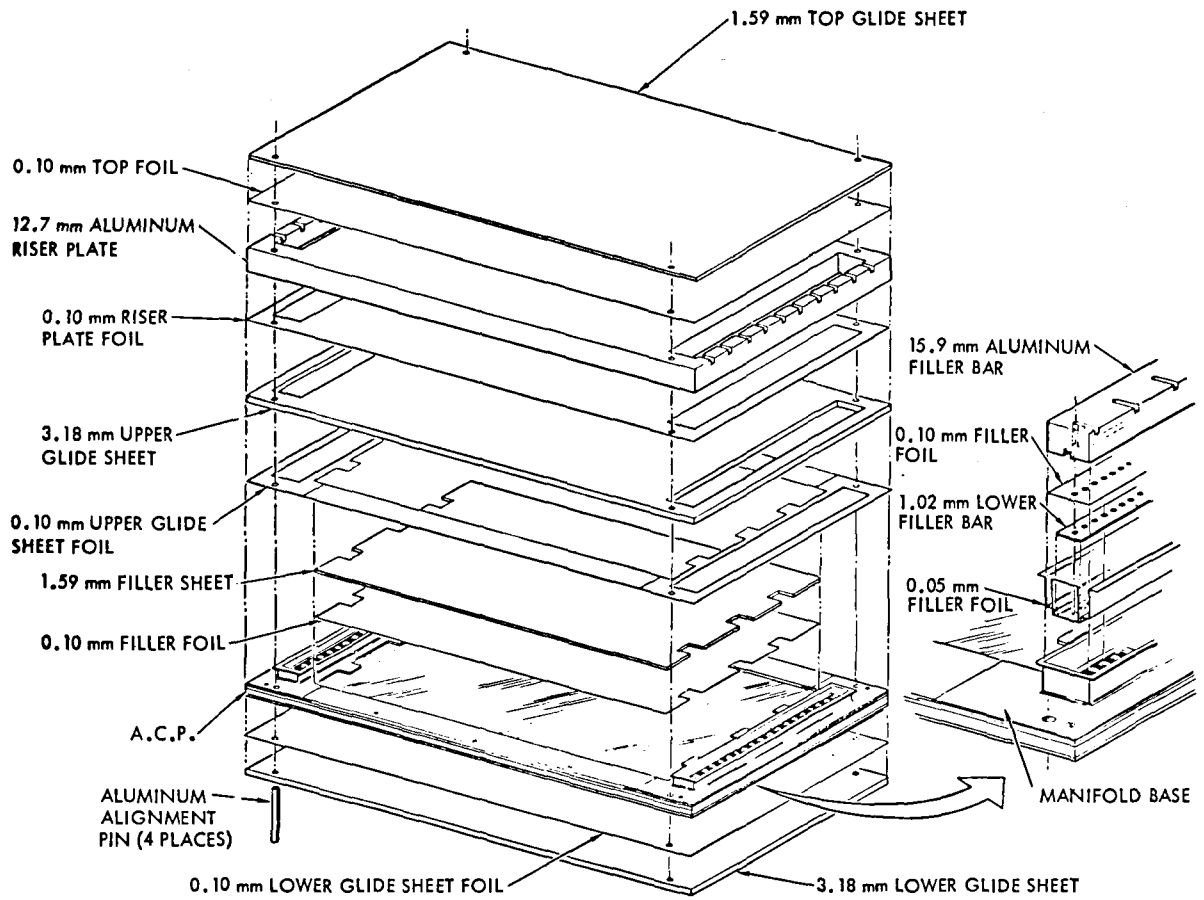

NOTE: ALL TOOLING IS STAINLESS STEEL EXCEPT AS NOTED

Figure 97. Brazed Sandwich Tooling Lay-Up

for brazing the panel sandwich structure. The stainless-steel foil was oxidized and used as a barrier between all aluminum and stainless-steel components to prevent inadvertent brazing and facilitate tooling removal after brazing. The dimensions and tolerances of tooling details were carefully monitored and modified, as necessary, during the lay-up sequence to assure uniform panel pressure during the brazing cycle. Over-pressurization of any single area could cause crushing of the core and lack of contact or pressure could cause void areas in the braze joints. In either instance, panel quality or dimensions could be affected. The grooves machined in the riser plate assure both evacuation and pressurization of the panel internal sections.

Brazing of the panel was performed in a retort using the inert gas pressure technique. After brazing, all tooling details were removed from the panel with no sticking or adhesion problems. Solution-heat-treating of the panel and manifold cap assemblies was performed without the use of fixtures. The parts were quenched in the "UCON-A"/water quenching solution. The quenching solution was rinsed off with tap water. However, to assure that no residue of either UCON-A or tap water remained on the panel and manifold assemblies, the parts were rinsed with deionized water, isopropyl alcohol, and Freon TF (Type I). When the panel was quenched, minor warpage did occur as expected. Of course, the warpage resulting from quenching this panel was more than that of the much smaller fatigue specimens. The warpage, however, was far less than would be expected if pure water quenching had been used. The panel was carefully hand-straightened to eliminate the warpage. Since fixturing was not used, no marking or damage to the skins had occurred. The panel and manifold details were kept below freezing temperature to retard the natural aging process until manifold base/cap welding was initiated. During welding, heated argon gas was passed through the inside of the panel to prevent condensation. The ends of the panel over the manifold bas were bowed 2.54 mm (0.1 in.) from their normal flat plane by clamping the moldline surface to specially formed tooling bars having a convex curvature. This pre-formed bow was introduced into the panel to offset the bow expected to result from welding the manifold cap to the manifold base. This calculated amount of pre-forming was apparently adequate since, after welding and clamp removal, the panel was flat with essentially no bowing as a result of the welding operation. After heat-aging the panel to the T-6 temper, the panel and three internal

stringers were chromic-acid anodized and then adhesively bonded together. After final machining, the panel successfully passed the internal pressure test of 1.24 MPa (180 psi) and the helium leak test. No leaks were evident. Radiographs revealed no internal defects.

The load adapters and all support structures were sulphuric-acid anodized. The panel was fastened to the load adapter/frame assembly, using Taper-Loc fasteners. The six NASA-provided pillow blocks were first fastened to their respective titanium and aluminum attach fittings and subsequently to the panel frame assembly. These were purposely fastened in this fashion to facilitate subsequent removal and replacement whenever required, while still maintaining perfect alignment. Alignment of the pillow blocks is critical with respect to the neutral axis of the panel and load adapters. After alignment and securing the pillow blocks, a dimensional check showed that alignment of all six pillow blocks was within 0.05 mm (0.002 in.) of the neutral axis of the panel and adapters. Completion of fabrication included adhesive bonding of the heater strips to the load adapters and fabrication of foam insulation blocks, matching the contours of the load adapters. The foam blocks were made in sections to facilitate installation and removal at the test site.

The mass of the completed test article including the panel, load adapters, all support details, fasteners, and pillow blocks was 57.49 kg (126.75 lbm).

Figures 98 through100 show the 2-ft by 4-ft test article during various stages of fabrication. Figure 98 shows the welded-up panel perimeter frame with the edge fluid channel side exposed. The fusion-welds are at the four corners at the ends of each "comb." The "hardspots" for subsequent mechanical attachment to structural details are part of the frame assembly. Figure 99 shows the frame, core, filler bars, and interior hardspots layed-up on the external face sheet. Attempts to spot-tack the core to the face sheet were not successful. The filler bars do help to maintain alignment of the core convolutions; however, capability to tack the core in place would aid greatly in the assembly process.

Figure100 shows all the details of the braze panel assembled and pinned together as a unit. The conduction plates and manifold bases are assembled on the inboard skin. The coolant slots in the face sheet are seen in the manifolds.

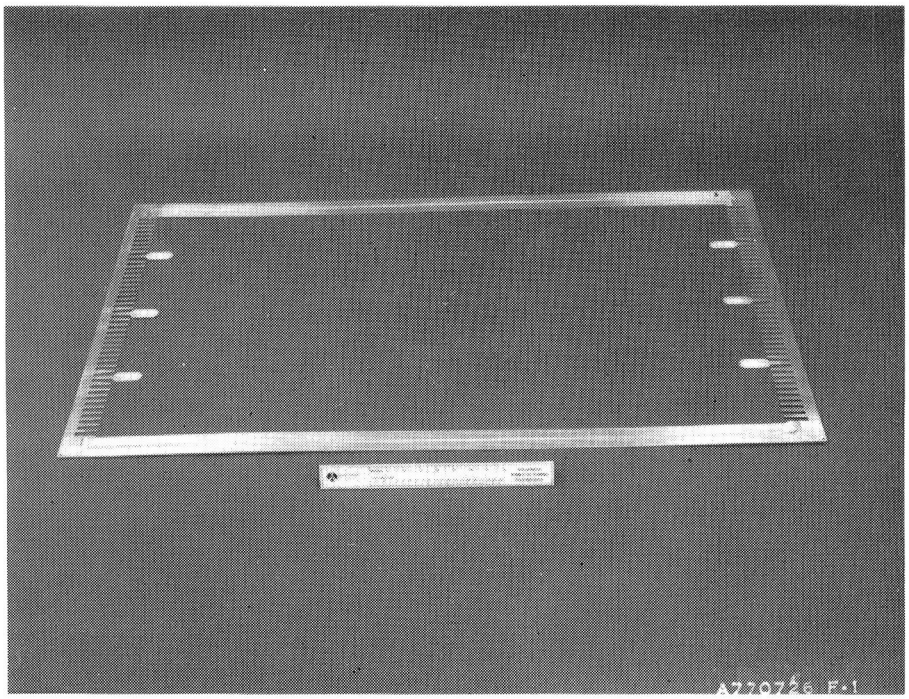

Figure 98. Test Article (TA) Brazed Sandwich Perimeter Frame

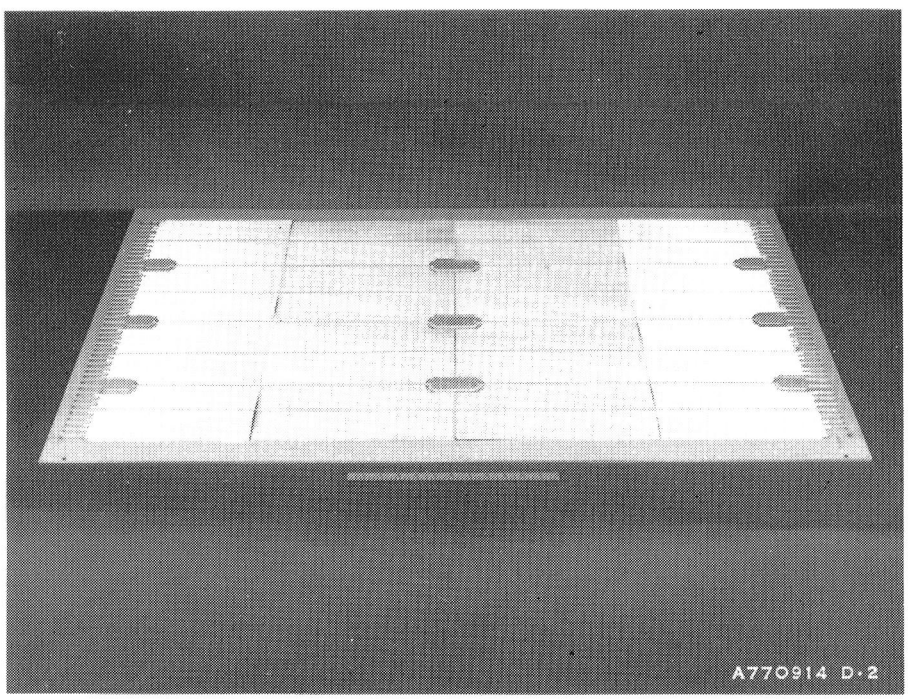

Figure 99. TA Sandwich Internal Details Assembled Prior To Closure

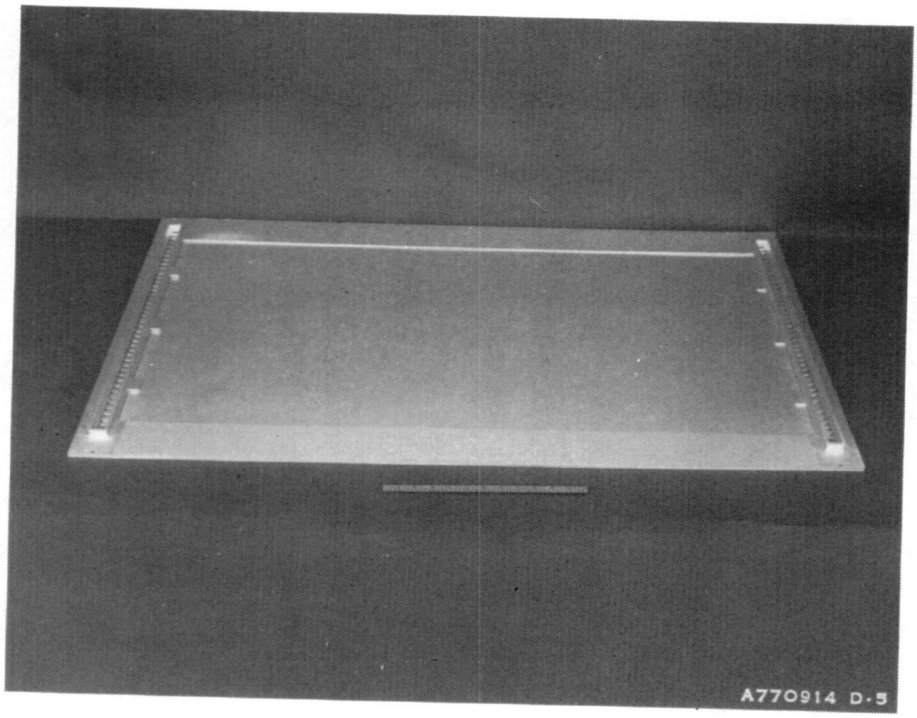

Figure 100. TA Sandwich Structure Assembled for Brazing

Figure 101 shows oxidized foil placed on the aluminum panel details as a barrier or separator to prevent inadvertent brazing or bonding of the panel to tooling details. Figure 102 illustrates the tooling riser plate in place to bring all pressure areas (with the exception of the manifold area) in one plane. Manifold filler bars, located within the manifold base, are shown in Figure 103. These bars permit uniform pressure to be exerted on the skin-to-finger joint areas. The evacuation grooves are seen on both the riser plate and filler bars.

Figure 104 depicts the complete braze assembly, which includes the panel assembly to be brazed and all the braze tooling, positioned in the stainless-steel retort. During brazing, part temperatures are monitored with the thermocouples shown in this photo. After fluxless brazing, the panel is removed from the retort. Figures 105 and 106 show both sides of the brazed panel immediately after removal from the brazing retort. The panel, as removed, was very flat. The stains on the panel are from the oxidized foil and are subsequently cleaned. The inboard side of the panel exposing the brazed manifolds is displayed in Figure 105 while the moldline side is shown in Figure 106. The impressions of

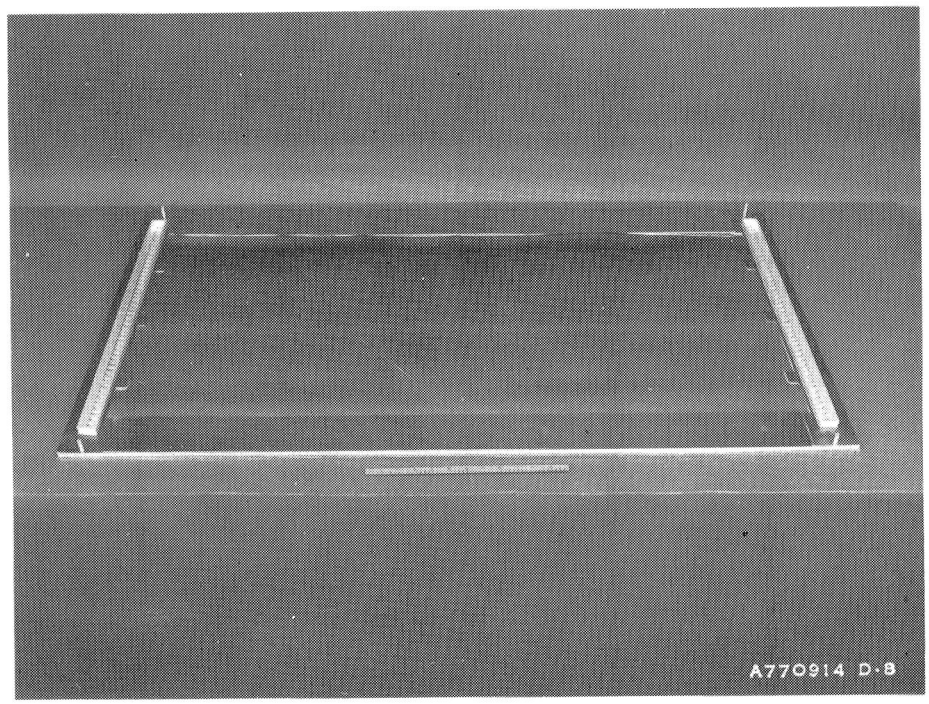

Figure 101. TA Sandwich with Oxidized Foil In Place

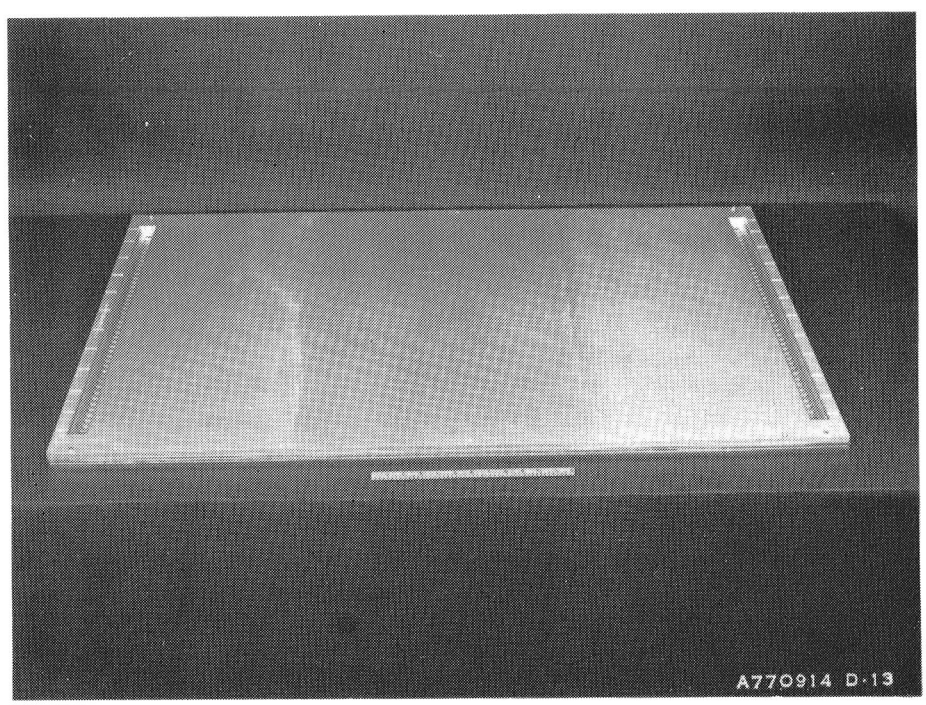

Figure 102. TA Sandwich with Tooling Riser Plate In Place

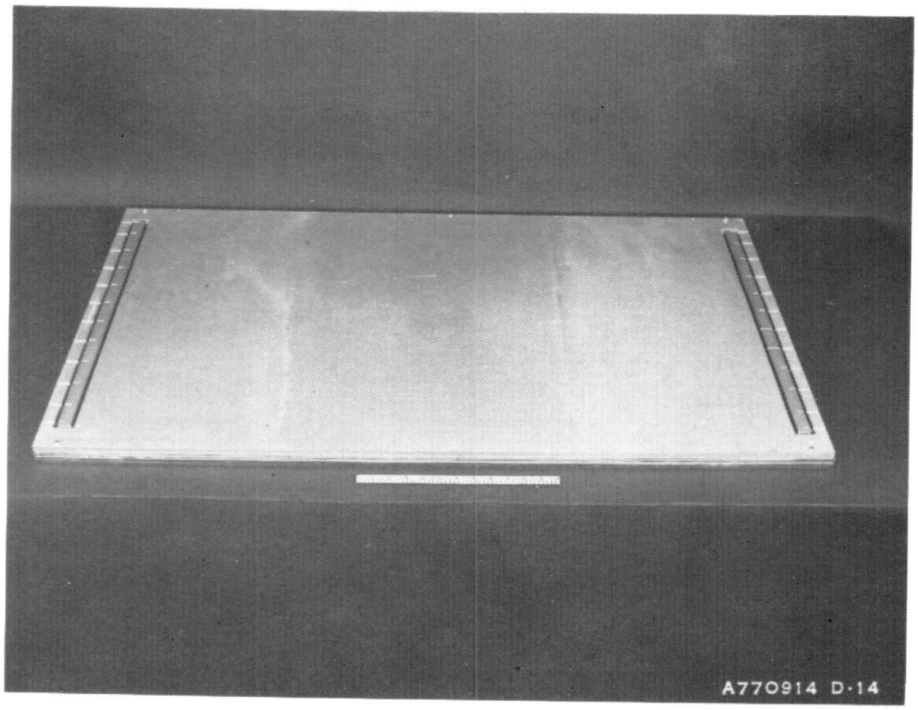

Figure 103. TA Sandwich with Manifold Filler Bar In Place

Figure 104. TA Braze Assembly being Installed in Retort

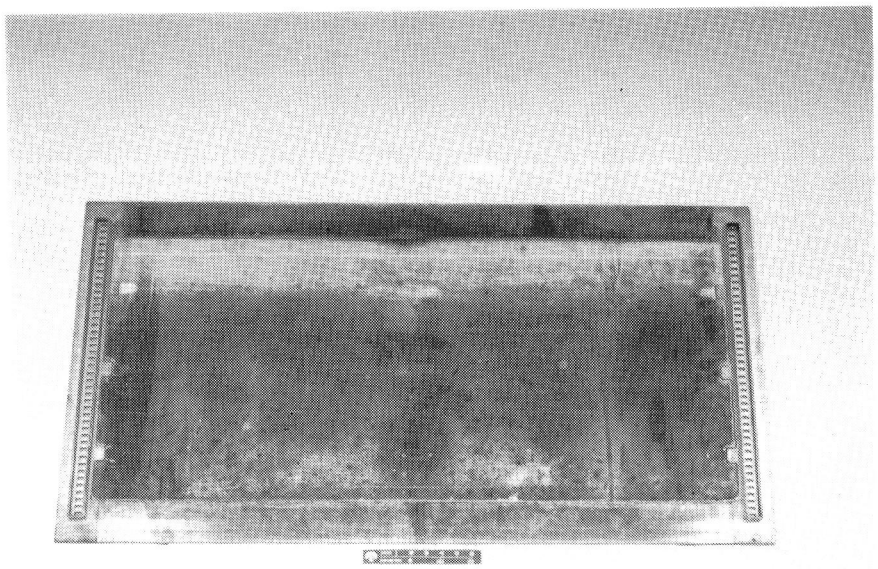

Figure 105. TA Panel Inboard Side after Brazing

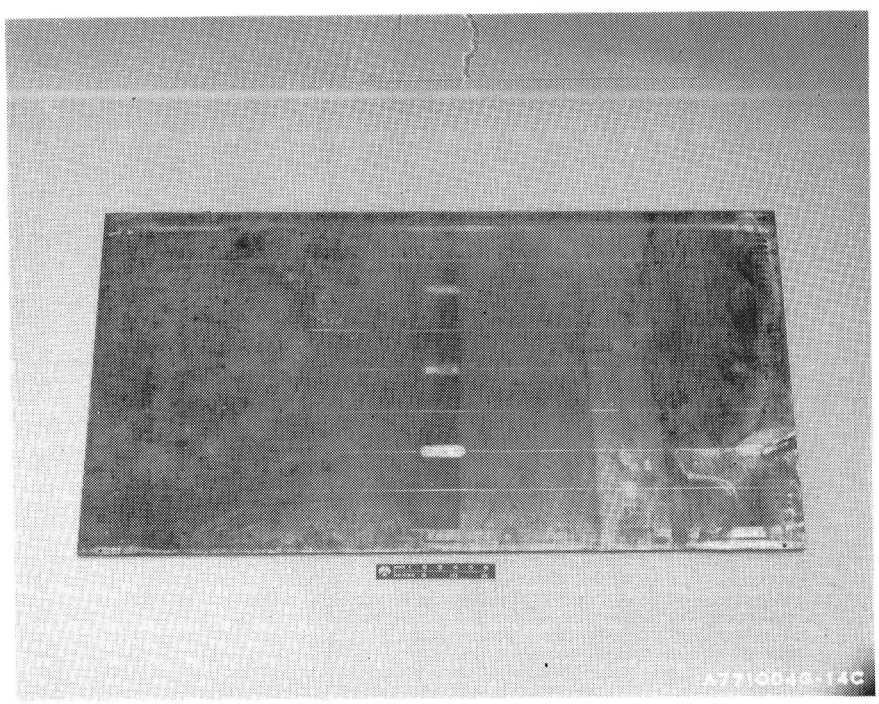

Figure 106. TA Panel Outer Moldline Side after Brazing

the manifold fingers, hardspots, and support rods are clear in these photos. Special manifold fixtures were made to clamp over the manifold bases and perform the helium leak tests and internal pressure tests before subsequent thermal treatment. Figure107 shows the test fixtures in place on the manifold during helium leak testing.

Figure 107. TA Panel in Preparation for Proof Pressure and Helium Leak Test

Figure 108 shows the inboard side of the panel after solution heat treating, welding the manifold caps onto the manifold bases, and heat-aging to the T-6 temper. The panel still contains excess material along the edges, which was subsequently machined off.

After chromic-acid anodizing the panel and center stringers, they were adhesive-bonded together on the inboard side of the panel. Figure 109 shows the panel after the adhesive bonding and curing operation.

Fabrication of the load adapter/frame assembly was a critical element in the overall test specimen. Dimensions and tolerances were extremely important

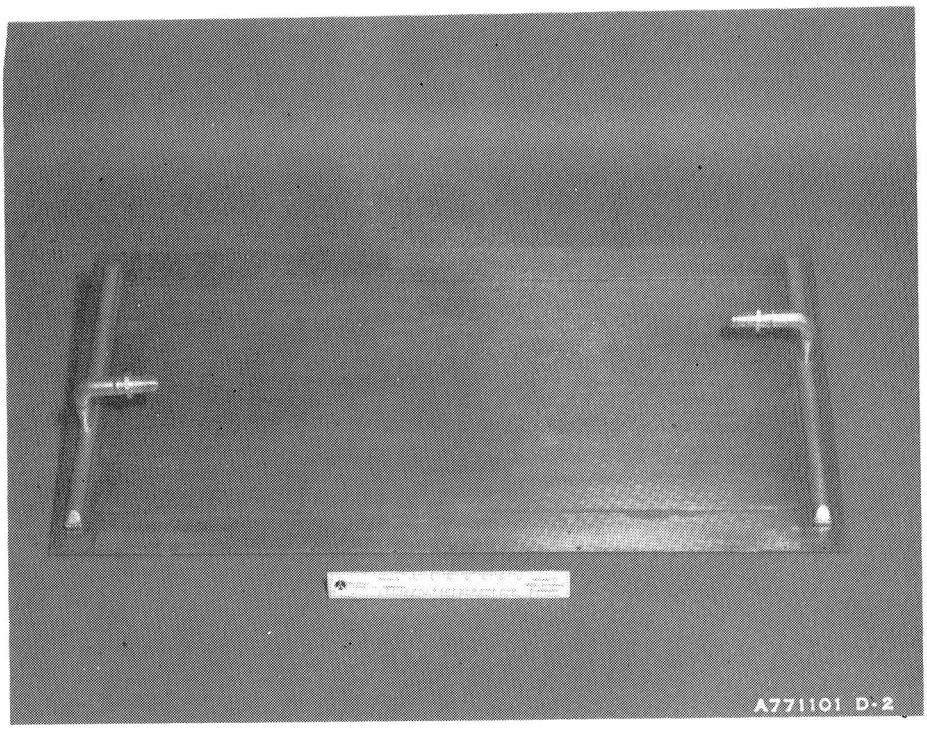

Figure 108. TA Panel with Manifold Caps Welded In Place

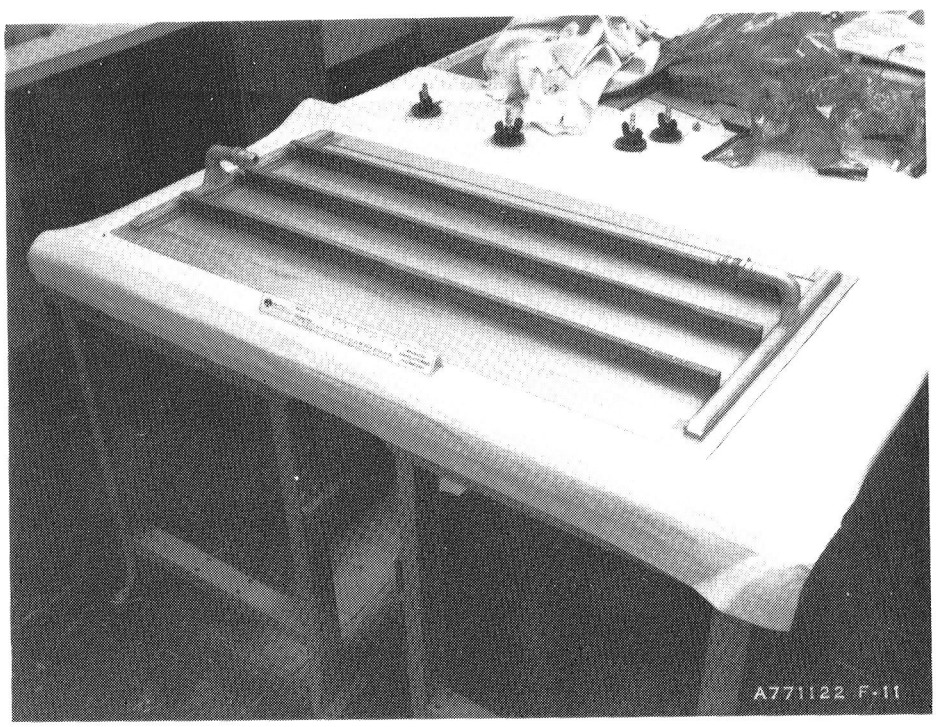

Figure 109. TA Panel After Internal Stringer Installation

to the final panel installation. Figures 110 through 112 show the load adapter/frame assembly prior to installation of the panel itself. Figure 110 is an overall view of the load adapter edge stringer and bathtub fitting assembly. The I-beam frame on the bottom of the assembly and the flat plate in the center were made specifically to maintain dimensional alignment of this assembly during installation of the panel and were subsequently used as a shipping fixture to eliminate torqueing of the panel during handling and shipping. The clamps shown were to be used during the Taper-Loc fastener drilling sequence.

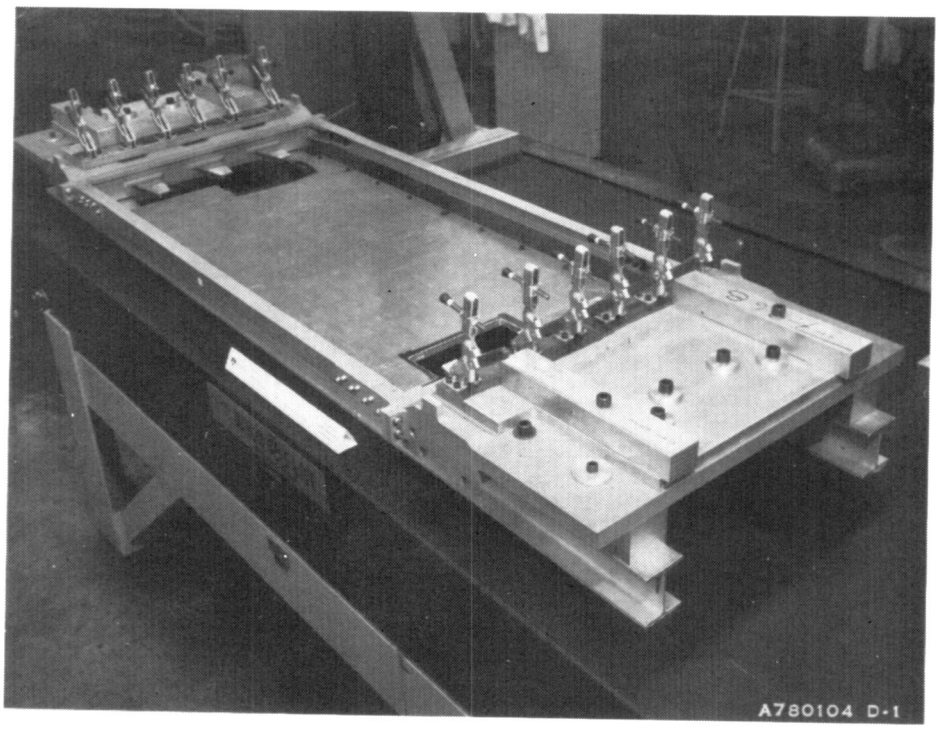

Figure 110. TA with Load Adapters Clamped In Place Supported by I-Beam Frame

Figure 111 shows the load adapter/main frame simulator. The brackets that protrude from the simulator frame pick up the inboard flanges of the internal stringers on the panel assembly. These brackets contain machined aluminum shims which are bonded to the brackets. These shims take up the tolerance between the brackets and the internal stringers on the panel.

Figure 112 shows the dummy bathtub fitting which attaches to the load adapter and to the edge stringer; the barrel-nut located in the load adapter

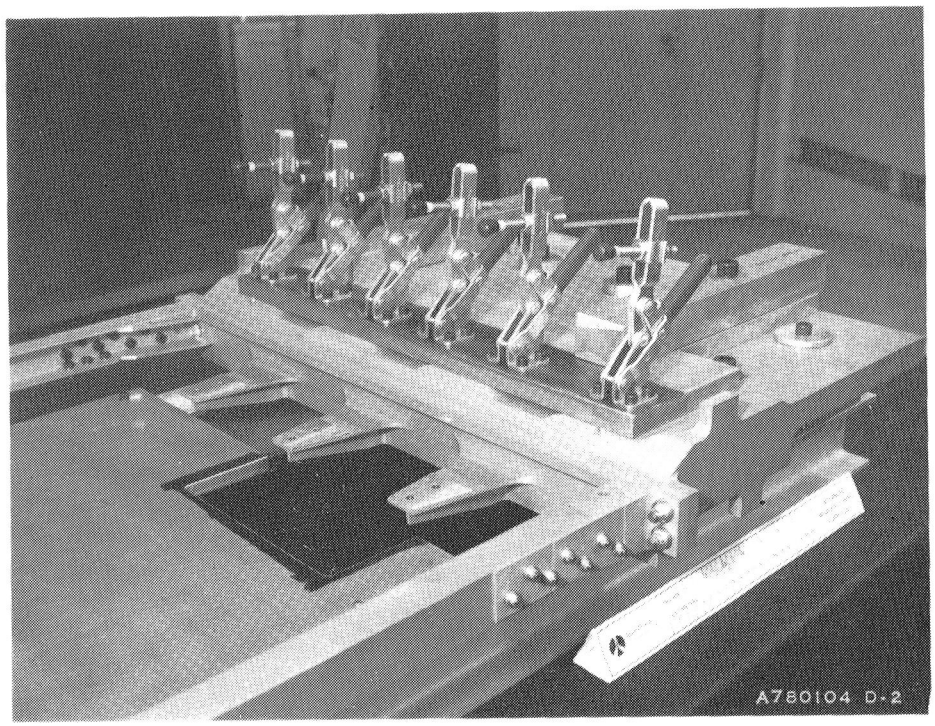

Figure 111. Load Adapter/Main Frame Simulator

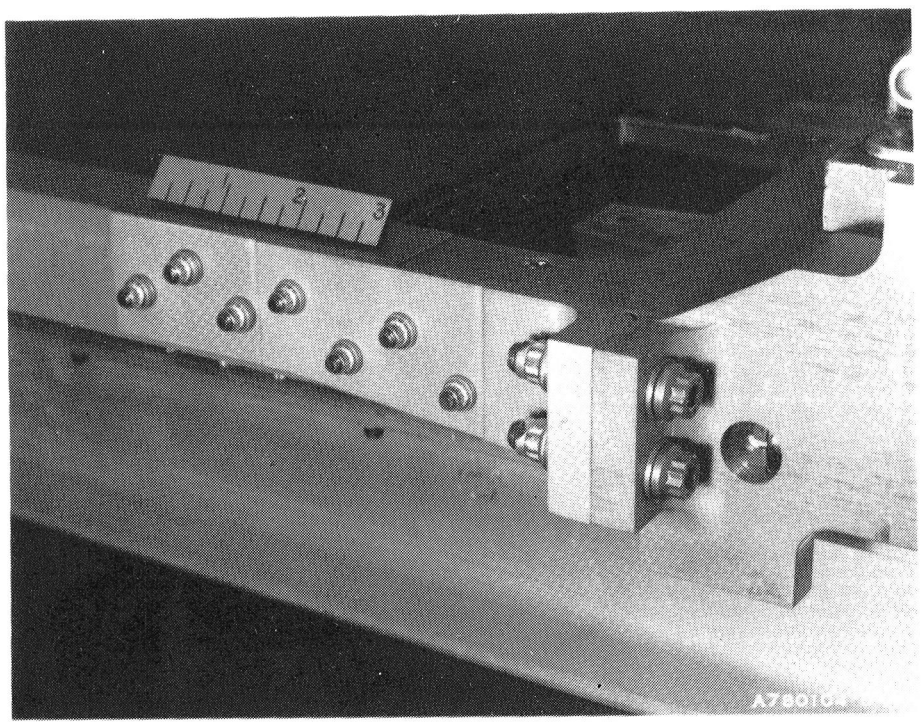

Figure 112. Dummy Bathtub Fitting

is also shown. The bolt going through this barrel-nut is seen in the previous figure (Figure111) and attaches the load adapter to the bathtub fitting.

The panel was attached to the load adapters and the edge stringers using Taper-Loc fasteners. Figures113 through120 show the test panel/load adapter assembly in various stages of completion.

Figure 113 illustrates the panel, load adapters, transverse intermediate frame, pillow blocks, manifold plumbing with support brackets, and all fasteners comprising the test article; the photo shows the inboard side.

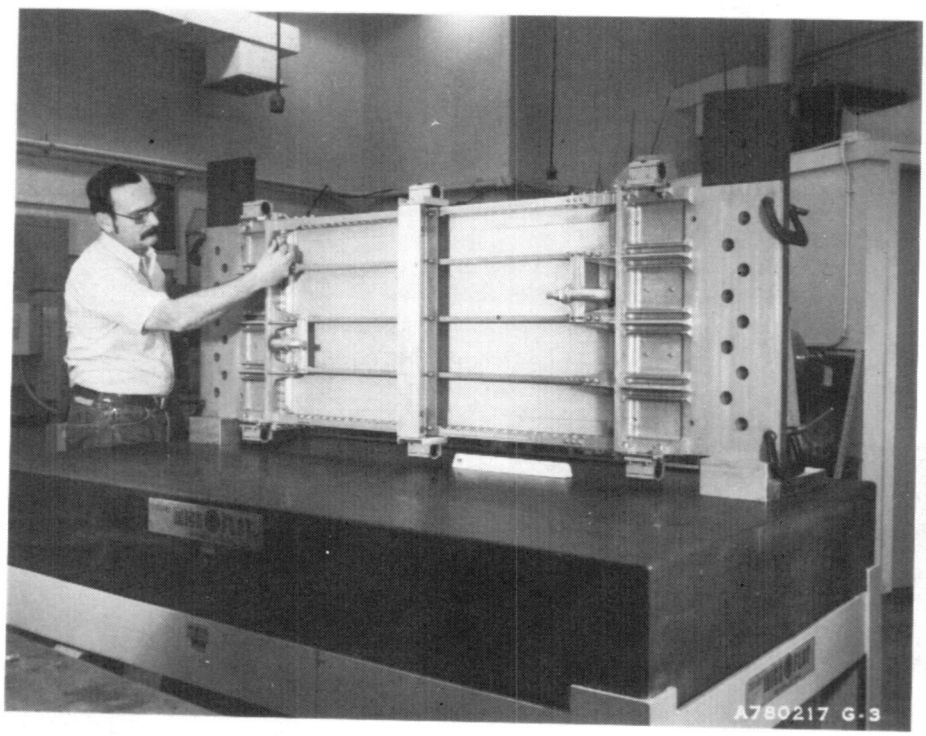

Figure 113. Inboard Side of Assembled Test Article

Figure114, taken from the outlet manifold end of the test article, shows the bolt attachment for the transverse intermediate frame simulator to the stringers bonded to the sandwich structure. The bolts are inserted from the moldline side of the sandwich structure. Figure115 is taken toward the outlet manifold. The Taper-Loc fasteners along the panel edges and adjacent to the outlet manifold through the load adapter are clearly visible.

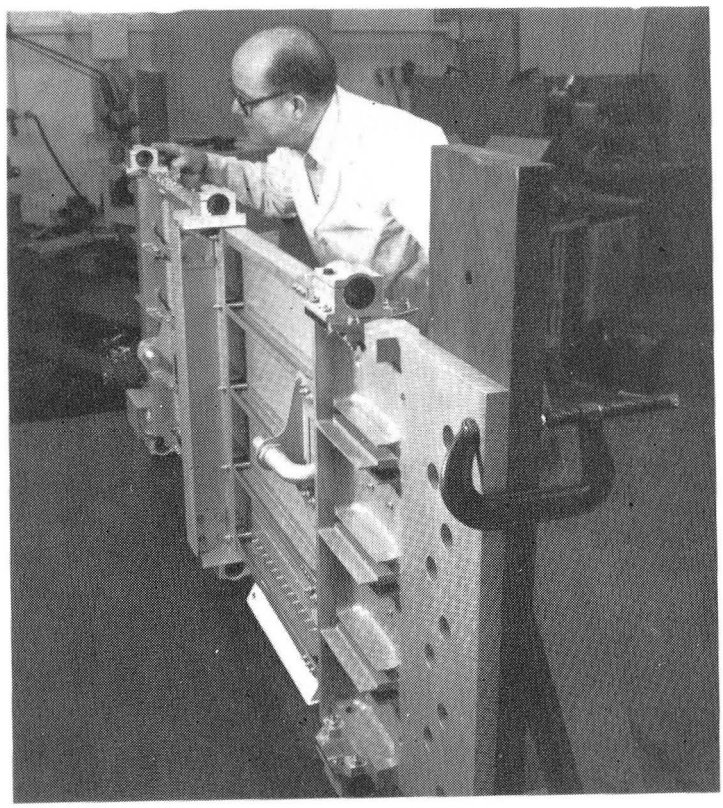

Figure 114. Panel/Intermediate Frame Simulator Attachment Hardware

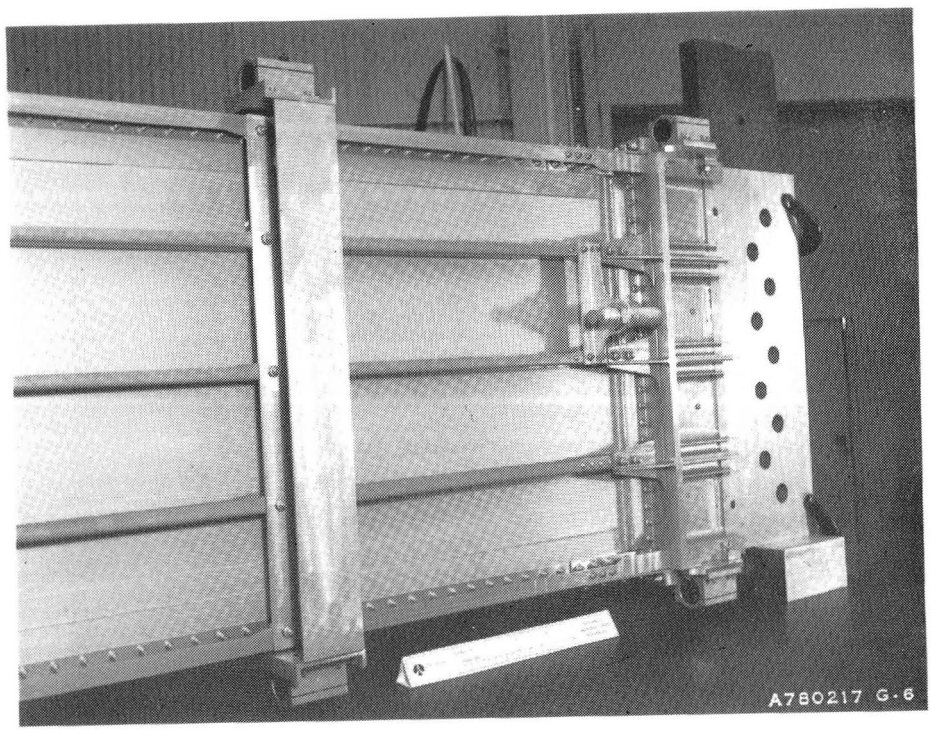

Figure 115. Panel/Load Adapter Taper-Lok Attachment

Figure 116 is an over-all view of the entire test article as seen from the moldline side. The bright bands on the load adapters are areas where sulphuric-acid anodizing has been removed in preparation for heat strip installation and bonding.

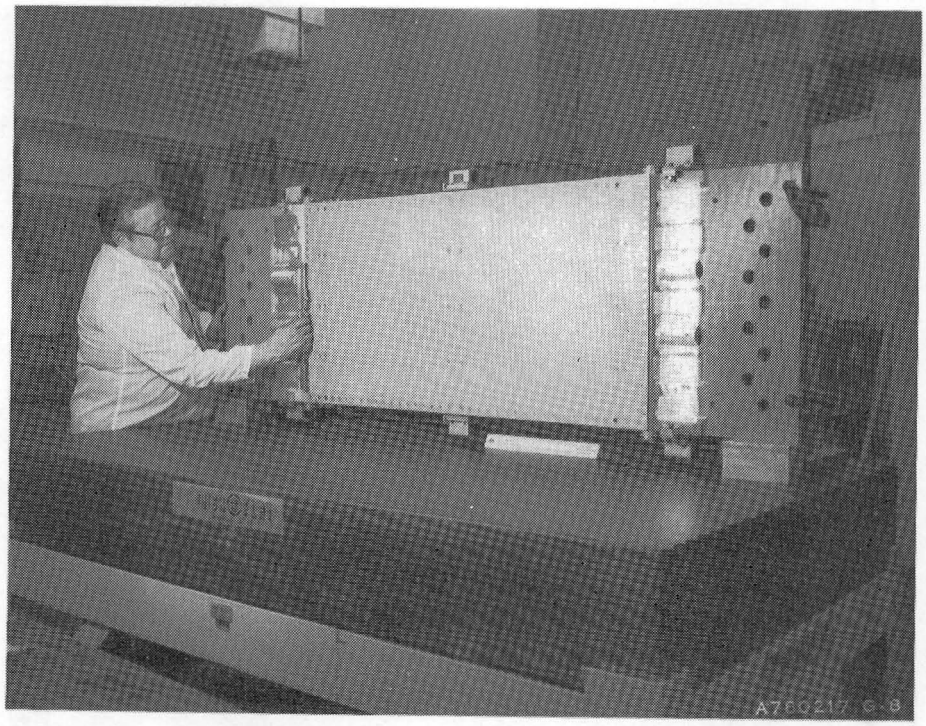

Figure 116. TA Moldline Side Prepped for Heat Strip Installation

Figure117 is a close-up of the moldline side of the panel and load adapter and shows the flush head installation of all fasteners.

Figure118 shows the moldline side of the test article with the heater strips bonded to the load adapters. Figure119 shows the inboard side of the test article during final installation of the fiberfax insulation. This insulation is packed into the fin areas of the load adapters and covered with aluminum tape. Figure120 is a close-up of the inlet manifold end. The insulation is carefully cut around the manifolds and load adapter fins, packed in, and held in place with aluminum tape. The round bars through the pillow blocks are part of the alignment tooling and are not part of the test article as delivered.

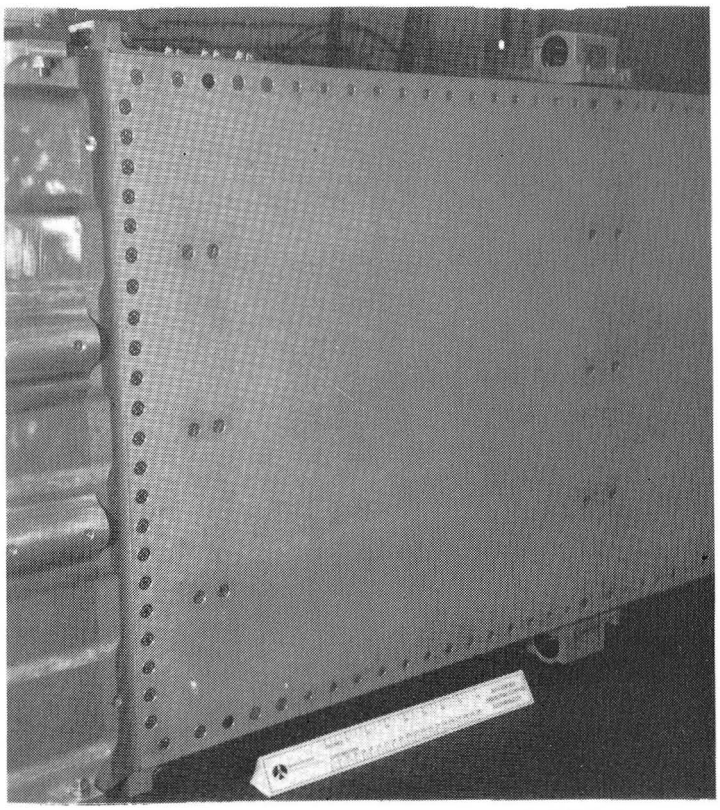

Figure 117. TA Moldline Side, Highlights Taper-Lok Fastener Head

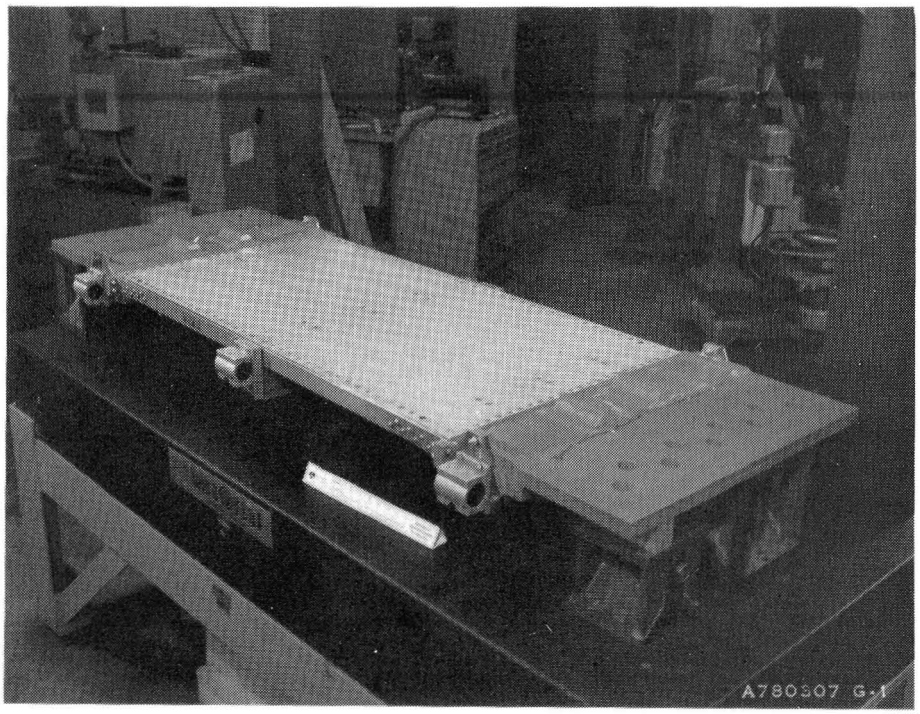

Figure 118. TA Moldline Side with Heat Strips Installed

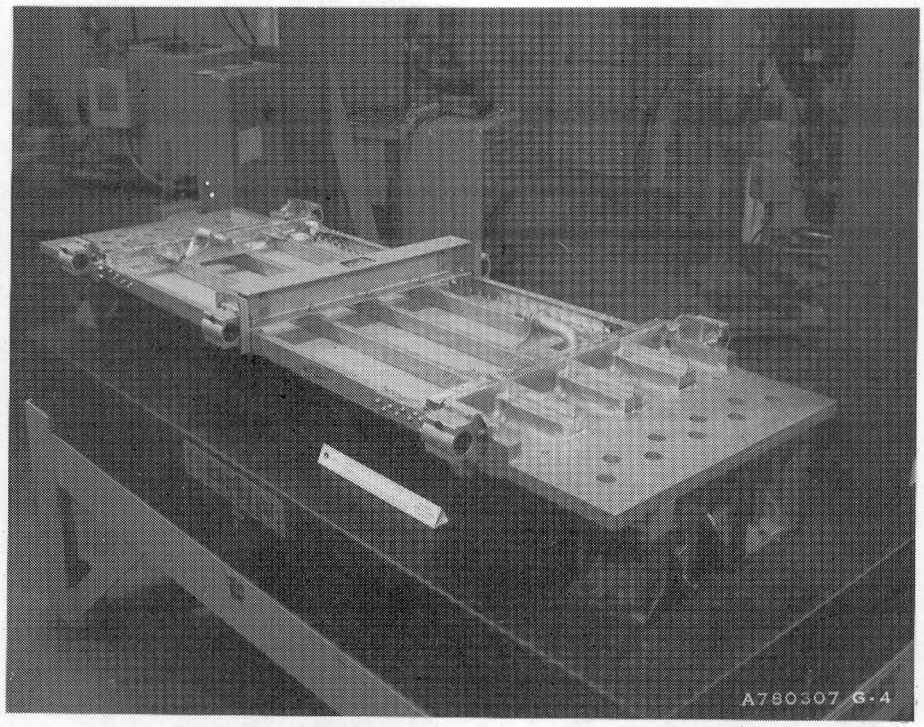

Figure 119. TA Inboard Side Showing Fiberfax Insulation Installed

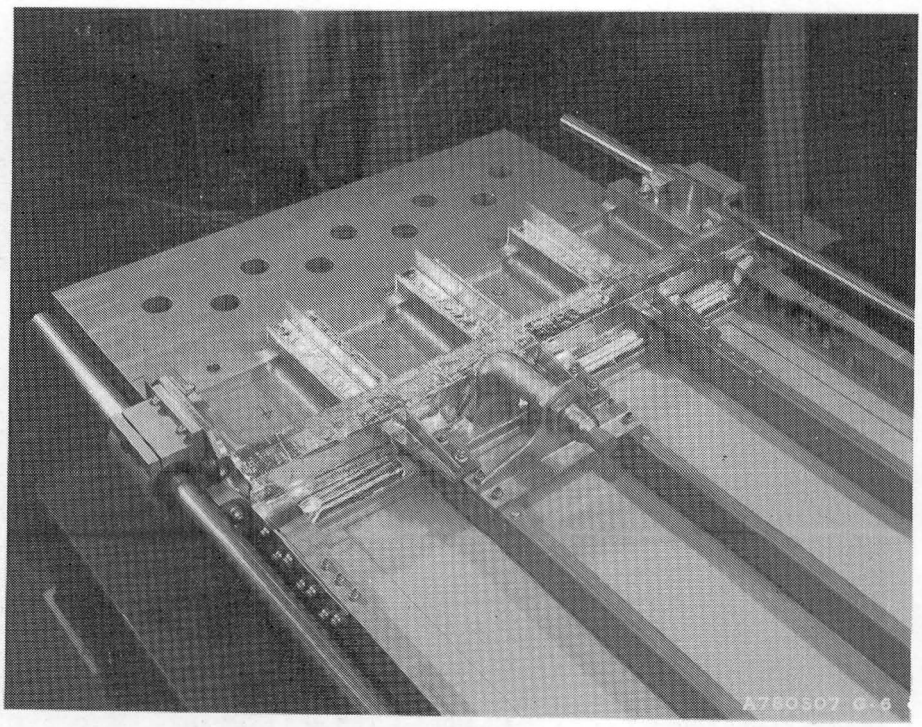

Figure 120. Closeup of Fiberfax Insulation Installation

Figures 121 and 122 respectively show both the inboard side and outer moldline side of the 0.61-m by 6.1-m (2- by 4-ft) test article as completed for delivery with all polyurethane insulation blocks in place. This is the configuration of the panel that will be tested by NASA.

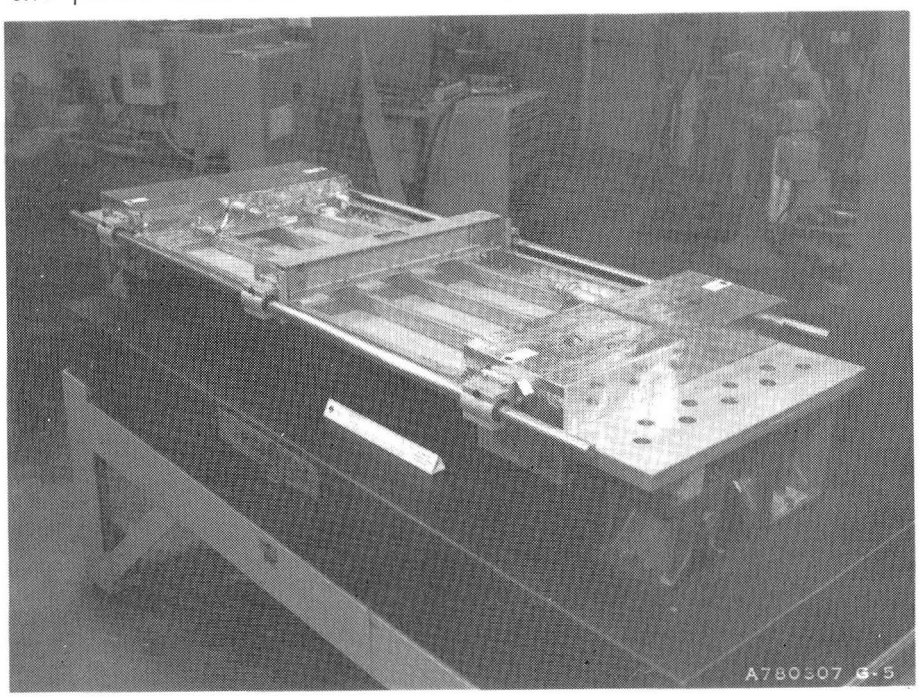

Figure 121. Completed TA Inboard Side

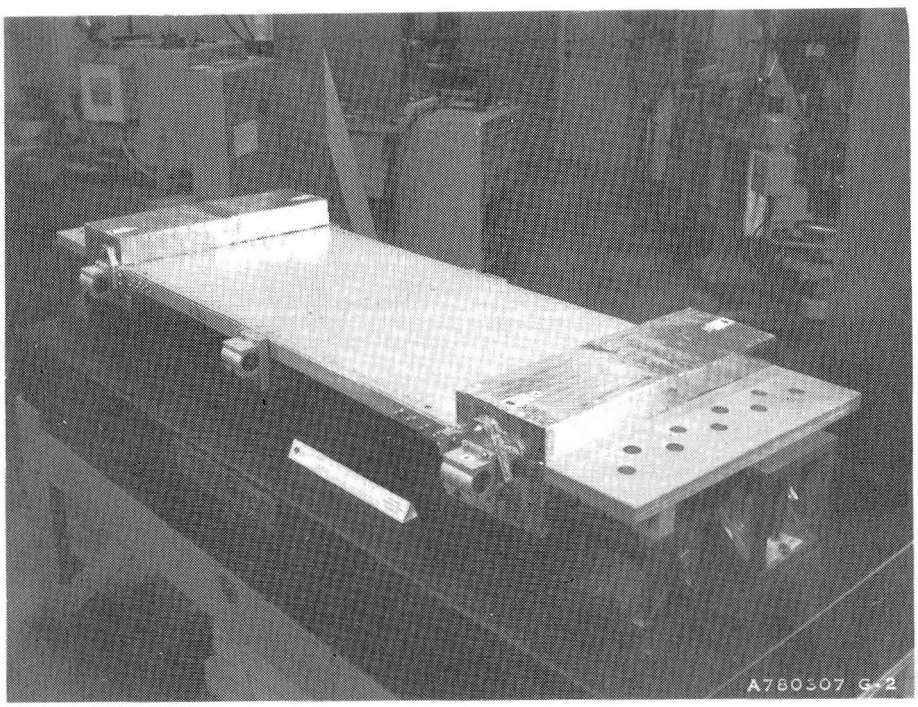

Figure 122. Completed TA Outer Moldline

REFERENCES

(1) McConarty, W. A. and Anthony, F. M., *Design and Evaluation of Active Cooling Systems for Mach 6 Cruise Vehicle Wings*, CR-1916, 1971, NASA.

(2) Helenbrook, R. G., McConarty, W. A., and Anthony, F. M., *Evaluation of Active Cooling Systems for a Mach 6 Hypersonic Transport Airframe*, CR-1917, 1971, NASA.

(3) Helenbrook, R. G., and Anthony, F. M., *Design of a Convective Cooling System for a Mach 6 Hypersonic Transport Airframe*, CR-1918, 1971, NASA.

(4) Federal Aviation Regulations, Volume III, *Part 25—Airworthiness Standards: Transport Category Airplanes*.

(5) *Metallic Materials and Elements for Aerospace Vehicle Structures*, Department of Defense, MIL-HDBK-5B, September, 1971.

(6) *Fabrication of Test Articles for Actively Cooled Structural Panels; Task 1, Small Test Specimens*. SD 74-CE-0010, Rockwell International, 1974.

(7) Garcia, E. E., et al., *Thermal Hydraulic Analyzer Program*, SD 72-SH-0053, Rockwell International, Space Division, June 1972.

(8) Shuford, C. L. and LeBlanc, L. P., *Aerodynamic and Structural Heat Transfer Thermal Analyzer Program No. YF 0012*, SD 70-148, Rockwell International, Space Division, May, 1970.

(9) Giles, G. L., and Anderson, M. S., *Effects of Eccentricities and Lateral Pressure on the Design of Stiffened Compression Panels*. NASA TN D-6484, June, 1972.

(10) *NARFEM Finite Element Model*, SD 71-302, Rockwell International, Space Division, December, 1970.

(11) *The NASTRAN User's Manual*, NASA SP-222 (01), National Aeronautics and Space Administration, Washington, D.C., June, 1972.

(12) Aluminum Company of America, *Brazing Alcoa Aluminum*, 1967.

(13) *Materials Properties Manual*, Rockwell International, Space Division, Publication 2543-W, January, 1978.

(14) Koch, L. C. and Pagel, L. L., *High Heat Flux Actively Cooled Honeycomb Sandwich Structural Panel for a Hypersonic Aircraft*, NASA CR-2959, 1978.

(15) *Adhesive, Tape, Cryogenic & Heat Resistant*, Specification No. MB0120-048, Rockwell International Space Division, November 1966.

(16) Streeter, V., *Fluid Mechanics*, 4th Edition, McGraw Hill, N.Y., 1966.

(17) Mead, Daniel R., *Taper-Lok Reference Manual*, Third Edition. The Mead Company, 1972.

(18) Ford, C. C. and Garcia, E. E., *General Thermal Analyzer Program User's Guide (Program No. XF0014)*, Rockwell International, Space Division, November, 1973.

1. Report No.	2. Government Accession No.	3. Recipient's Catalog No.
NASA CR-3159	--	--

4. Title and Subtitle	5. Report Date
Actively Cooled Plate Fin Sandwich Structural Panels for Hypersonic Aircraft	August 1979
	6. Performing Organization Code: --

7. Author(s)	8. Performing Organization Report No.
L. M. Smith C. S. Beuyukian	SD 78-AP-0074
	10. Work Unit No.: --

9. Performing Organization Name and Address	11. Contract or Grant No.
Rockwell International 12214 Lakewood Blvd. Downey, California 90241	NAS1-13382
	13. Type of Report and Period Covered: Contractor Report

12. Sponsoring Agency Name and Address	14. Sponsoring Agency Code
National Aeronautics and Space Administration Washington, D.C., 20546	

15. Supplementary Notes

Langley Research Center Technical Monitor: Robert J. Nowak
Final Report

16. Abstract

This report presents results of a program conducted to design and fabricate an unshielded actively cooled structural panel for application to a hypersonic aircraft. The design is an all-aluminum stringer-stiffened platefin sandwich structure which uses a 60/40 mixture of ethylene glycol/water as the coolant.

The panel was designed to sustain 20,000 cycles (5000 times a scatter factor of 4) of ±210 kN/m (±1200 lbf/in.) axial inplane loading combined with a ±6.89 kPa (±1.0 psi) uniform pressure while subjected to a 136 kW/m^2 (12 Btu/ft^2-sec) uniform heat flux. Eight small test specimens of the basic plate fin sandwich concept and three fatigue specimens from critical areas of the panel design were fabricated by Rockwell and tested (at room temperature) by NASA. A test panel representative of all features of the panel design was fabricated by Rockwell and delivered to NASA for testing to determine the combined thermal/mechanical performance and structural integrity of the system.

The overall findings are that (1) the stringer-stiffened platefin sandwich actively cooling concept results in a low mass design that is an excellent contender for application to a hypersonic vehicle, and (2) the fabrication processes are state of the art but new or modified facilities are required to support full-scale panel fabrication. Results of the program are summarized in the body of the report and supporting details are presented in the appendices.

17. Key Words (Suggested by Author(s))	18. Distribution Statement
Actively Cooled Structure High Heat Flux Hypersonic Vehicle Fluxless Brazing Fatigue Specimens	Unclassified—Unlimited Subject Category 39

19. Security Classif. (of this report)	20. Security Classif. (of this page)	21. No. of Pages	22. Price*
Unclassified	Unclassified	172	$8.00

* For sale by the National Technical Information Service, Springfield, Virginia 22161

NASA-Langley, 1979

National Aeronautics and Space Administration

Washington, D.C.
20546

Official Business
Penalty for Private Use, $300

THIRD-CLASS BULK RATE

Postage and Fees Paid
National Aeronautics and
Space Administration
NASA-451

NASA

POSTMASTER: If Undeliverable (Section 158 Postal Manual) Do Not Return